

Distribution Agreement

In presenting this thesis or dissertation as a partial fulfillment of the requirements for an advanced degree from Emory University, I hereby grant to Emory University and its agents the non-exclusive license to archive, make accessible, and display my thesis or dissertation in whole or in part in all forms of media, now or hereafter known, including display on the world wide web. I understand that I may select some access restrictions as part of the online submission of this thesis or dissertation. I retain all ownership rights to the copyright of the thesis or dissertation. I also retain the right to use in future works (such as articles or books) all or part of this thesis or dissertation.

Signature:

Amber L. Caldara

Date

Desmosome Assembly and Disassembly: Lessons from Studying Dermatological Diseases

By

Amber L. Caldara
Doctor of Philosophy

Graduate Division of Biological and Biomedical Sciences
Cancer Biology

Andrew P. Kowalczyk, Ph.D.
Advisor

Victor Faundez, M.D., Ph.D.
Committee Member

Adam I. Marcus, Ph.D.
Committee Member

Brian G. Petrich, Ph.D.
Committee Member

George R. Beck, Ph.D.
Committee Member

Accepted:

Lisa A. Tedesco, Ph.D.
Dean of the James T. Laney School of Graduate Studies

Date

**Desmosome Assembly and Disassembly: Lessons from Studying
Dermatological Diseases**

By

Amber L. Caldara
B.S. Kennesaw State University 2015
A.A.S State University of New York Rockland 2010

Advisor: Andrew P. Kowalczyk, Ph.D.

An abstract of
A dissertation submitted to the Faculty of the
James T. Laney School of Graduate Studies of Emory University
In partial fulfillment of the requirements for the degree of Doctor of Philosophy
in the Graduate Division of Biological and Biomedical Sciences
Cancer Biology
2019

Abstract

Desmosome Assembly and Disassembly: Lessons from Studying Dermatological Diseases

By Amber L. Caldara

Cell-cell adhesion complexes mediate fundamental cellular interactions crucial in maintaining the integrity of skin, an essential protective barrier to the outside world. Desmosomes are large adhesion complexes critical for epidermal integrity and differentiation. These junctions are rigid enough to confer resistance to mechanical stress but dynamic enough to allow for processes such as wound healing and epidermal differentiation. Altered desmosomal adhesion results in the formation and progression of several genetic and acquired skin disorders. Additionally, desmosome stability is compromised during the process of epithelial to mesenchymal transition, a necessary step for tumors to metastasize. Thus, understanding the complex dynamics of desmosomal components and how desmosomes assemble and disassemble is essential for developing novel treatments for a variety of skin diseases.

Lipid rafts are sphingolipid and cholesterol rich membrane domains that introduce membrane heterogeneity and act as platforms for protein aggregation and signaling. All desmosomal proteins have been shown to associate with lipid rafts, however the biological significance of this association is unknown. We investigate the mechanism by which desmoglein (Dsg) associates with lipid rafts and uncover that the length of the transmembrane domain (TMD) is a key regulator of raft association. Additionally, we identify a patient with severe dermatitis multiple allergies and metabolic wasting syndrome that is caused by a point mutation within the TMD of Dsg1. This mutation abrogates lipid raft association of Dsg1, prevents Dsg1 incorporation into the desmosome, and results in Dsg1 retention in the Golgi apparatus. Additionally, we demonstrate that the bilayer within the desmosome is thicker than non-desmosome bilayer, thus identifying the desmosome as a lipid raft-like domain.

We then study the disassembly of desmosome through a pemphigus vulgaris model. Pemphigus vulgaris (PV) is an autoimmune disorder in which autoantibodies targeting Dsg3 and Dsg1 disrupt desmosome adhesion resulting in intraepidermal blisters. We determine that the sum of antibody titers against Dsg1 and Dsg3 is more correlative to disease severity than either titer on its own. We next demonstrate a relationship between Dsg3 autoantibody titers and an *in vitro* model to study the loss of cell-cell adhesion. These data demonstrate a relationship between Dsg antibody titer and disease severity and validate current methods for studying PV in cell culture. Together, these studies increase our understanding of how desmosomes assemble and disassemble, thus providing a platform for future investigation of the mechanisms regulating desmosome stability during tumorigenesis.

**Desmosome Assembly and Disassembly: Lessons from Studying
Dermatological Diseases**

By

Amber L. Caldara
B.S. Kennesaw State University 2015
A.A.S State University of New York Rockland 2010

Advisor: Andrew P. Kowalczyk, Ph.D.

A dissertation submitted to the Faculty of the
James T. Laney School of Graduate Studies of Emory University
In partial fulfillment of the requirements for the degree of Doctor of Philosophy
in the Graduate Division of Biological and Biomedical Sciences
Cancer Biology
2019

Table of Contents

Chapter 1: Focus and Impact	1
Chapter 2: The epidermis and cell-cell junctions	5
2.1 The Epidermis	5
2.2 Cell-Cell Complexes in the Epidermis.....	7
2.2.1 Tight Junctions	9
2.2.2 Gap Junctions	10
2.2.3 Anchoring Junctions	11
2.2.3.1 Adherens Junctions	12
2.2.3.2 Hemidesmosomes	14
2.2.3.3 Desmosomes	15
2.3 The Desmosome	15
2.3.1 Molecular components of the desmosome	17
2.3.1.1 Desmogleins.....	17
2.3.1.2 Desmocollin	20
2.3.1.3 Desmoplakin	21
2.3.1.4 Plakophilin	22
2.3.1.5 Plakoglobin	23
Chapter 3: Epithelial cell junctions and junctional proteins in tumorigenesis	25
3.1 Epithelial to mesenchymal transition	26
3.2 Tight junction proteins and cancer	28
3.3 Adherens junction proteins and cancer	28

3.4 Desmosome proteins and cancer	29
Chapter 4: Regulation of the desmosome	33
4.1 Factors regulating the expression of desmosomal proteins.....	33
4.2 Desmosome Stability.....	35
4.3 Desmosome Assembly	38
4.4 Desmosome regulation: Lipid rafts	39
4.4.1 Lipid rafts	39
4.4.1.1 Structure of Lipid rafts.....	40
4.4.1.2 Function of lipid rafts.....	42
4.4.3 Lipid rafts and desmosome function	46
Chapter 5: The Desmosome is a Mesoscale Lipid Raft-Like Domain.....	49
5.1 Abstract	50
5.2 Introduction	50
5.3 Results	53
5.3.1 Palmitoylation of Dsg3 is not required for lipid raft association	53
5.3.2 The transmembrane domain of desmogleins mediates lipid raft association ...	54
5.3.3 A mutation in the transmembrane domain of DSG1 causes severe dermatitis, multiple allergies, and metabolic wasting syndrome.....	56
5.3.4 Disease causing mutation abrogates lipid raft association of Dsg1	60
5.3.5 The lipid bilayer within desmosomes is thicker than non-desmosomal membranes.....	61
5.4 Discussion	63
5.5 Materials and methods	68
5.6 Acknowledgements	77

Chapter 6: Pemphigus Vulgaris	91
6.1 Pemphigus Overview	91
6.2 Clinic	93
6.2.1 Etiology	93
6.2.2 Diagnosis and Symptoms	95
6.2.3 Measure of disease severity	96
6.2.5 Enzyme Linked Immunosorbent Assays	99
6.2.6 Treatment and Patient outcomes.....	100
6.3 Bench.....	103
6.3.1 Models and techniques to study PV	103
6.3.1.1 Human Tissue	103
6.3.1.2 Mouse Models.....	104
6.3.1.3 Keratinocyte Culture	105
6.3.2 Mechanism of acantholysis	105
6.4 Outlook.....	107
Chapter 7: Pemphigus Vulgaris Dsg ELISA scores are associated with PDAI and loss of keratinocyte adhesion <i>in vitro</i>.....	108
7.1 Abstract	109
7.2 Introduction	110
7.3 Results and discussion.....	112
7.3.1 Epidemiology and clinical phenotype	112
7.3.2 Total ELISA score correlates with PDAI.....	113
7.3.3 DSG3 ELISA correlates with fragmentation assay	114
7.3.4 PDAI correlates to disassociation assay for mucosal dominant patients.....	116

7.3.5 Concluding remarks.....	116
7.4 Materials and Methods	117
7.6 Acknowledgements	121
Chapter 8: Summary and future directions	129
Section 8.1 Summary of dissertation work	129
Section 8.2 Future directions.....	130
8.2.1 Does Dsg3 endocytosis or loss of surface Dsg3 in keratinocytes after PV IgG treatment correlate to PDAI?.....	130
8.2.2 What is the mechanism behind the thickening of the epidermis in SAM patients?.....	132
8.2.3 How is DSG1(G578R) acting as a dominant negative?	135
8.2.4 What is the role of lipid raft association in Dsg3 endocytosis?.....	136
8.2.5 What are the mechanisms of Dsg3 clustering and linear array formation in Pemphigus Vulgaris?.....	138
Chapter 9: References	148

List of Figures

Figure 2.1 Structure of the epidermis	7
Figure 2.2 Cell-cell junctions in epithelial cells	8
Figure 2.3 Desmosome organization in the epidermis.....	16
Figure 2.4 Molecular components of the desmosome	19
Figure 3.1 Loss of cell junctions during epithelial to mesenchymal transition	27
Figure 4.1 Lipid raft structure	42
Figure 4.2 Model for the role of lipid rafts in desmosome function.....	47
Figure 5.1: Palmitoylation is not required for Dsg3 lipid raft association.....	78
Figure 5.2: The Dsg3 TMD is necessary for lipid raft association.....	79
Figure 5.3: The Dsg1 TMD is critical for lipid raft association	80
Figure 5.4: Desmoglein 1 (DSG1) transmembrane domain mutation causes severe dermatitis, multiple allergies, and metabolic wasting (SAM) Syndrome	82
Figure 5.5: SAM-causing DSG1 mutation causes defects in junction targeting	83
Figure 5.6: SAM-causing DSG1 mutation delays trafficking to the plasma membrane ..	85
Figure 5.7: The Dsg1(G578R) mutant is inserted into the membrane in the correct orientation and is present on the cell surface at levels similar to WT Dsg1	86
Figure 5.8: SAM-causing DSG1 mutation abolishes lipid raft association	87
Figure 5.9: The desmosome bilayer is thicker than adjacent bilayers	88
Figure 5.10: Model.....	89
Figure 6.1 Progression of pemphigus vulgaris	92
Figure 7.1 Patients have a range of PDAI and ELISA scores	123
Figure 7.2 Patients have unique symbol assigned	124

Figure 7.3 Total ELISA correlates with PDAI	125
Figure 7.4 Disassociation Index correlates with Dsg3 ELISA.	127
Figure 7.5 Disassociation Index correlates with PDAI for mucosal dominant patients.	128
Figure 8.1 Patients with high Dsg3 antibody titers correlate with endocytosis assay at 3 hours.....	142
Figure 8.2 Loss of Dsg3 surface staining weakly correlates to Dsg3 ELISA.	144
Figure 8.3 DSG1 mediates EGFR signaling.	145
Figure 8.4 The TMD of DSG3 is critical for lipid raft mediated endocytosis.....	146
Figure 8.5 A pathogenic monoclonal antibody induces linear array formation	147

List of Tables

Table 3.1 Cell junction proteins and cancer.....	32
Table 4.1 Regulation of the Desmosome	37
Table 4.2 Summary of lipid raft and desmosomes literature	48
Table 5.1 Summary of Transmembrane Domains	90
Table 6.1 Pemphigus vulgaris incidence rates	95
Table 6.2 Summary of disease severity scoring systems for pemphigus vulgaris.....	97
Table 7.1 Descriptive Statistics for Patients.	122

List of Abbreviations

In alphabetical order

ABSIS	Autoimmune Bullous Skin Disorder Identity Score
BCC	Basal cell carcinoma
Cryo-ET	Cryoelectron tomography
DP	Desmoplakin
DRM	Detergent resistant membrane
Dsc	Desmocollin
Dsg	Desmoglein
Dyn	Dynamin
EGFR	Epidermal growth factor receptor
ELISA	Enzyme linked immunosorbent assay
EMT	Epithelial to mesenchymal transition
Endo	endophilin
ESCC	Esophageal squamous cell carcinoma
GFP	Green fluorescent protein
HK	Human keratinocyte
HLA	human leukocyte antigen
IgG	Immunoglobulin
IL2R	Interleukin 2 receptor
JAM	Junction adhesion molecule
JMD	Juxtamembrane domain
mAb	monoclonal antibody
MET	mesenchymal to epithelial transition
NCE	non-clatherin endocytosis
NCSCLC	Non-small cell lung cancer
PAAS	Pemphigus Area and Activity Score

PDAI	Pemphigus Disease Area Index
PG	Plakoglobin
PKP	Plakophilin
PV	Pemphigus vulgaris
PVAS	Pemphigus Vulgaris Activity Score
SAM	Severe dermatitis, multiple allergies, and metabolic wasting
SB	Stratum basale
SC	Stratum corneum
SCC	Squamous cell carcinoma
SG	Stratum granulosum
SIM	Structured illumination microscopy
SS	Stratum spinosum
TMD	Transmembrane domain
WT	Wild type
TCR	T-Cell antigen receptor
ER	Endoplasmic Reticulum

Chapter 1

Focus and Impact

The epidermis is the outermost layer of the skin and a specialized epithelial tissue with critical functions in human health. In fact, disruption of this highly regulated tissue can lead to fatal dermatological diseases. Daily, the epidermis is exposed to an onslaught of mechanical forces, and yet it resists breakage and maintains tissue integrity in healthy individuals. The maintenance of the stratified epidermis is highly regulated by specialized membrane domains called cell-cell junctions. Cell junctions occur when proteins of neighboring cells directly interact in the extracellular space. These junctions contribute to the polarity, tissue integrity, and proliferative balance necessary for epithelial barrier function.

This dissertation starts by describing the structure and function of the epidermis in Chapter 2. Further, it considers the critical role of cell-cell junctions in the maintenance of the stratified epidermis through mediating epithelial cell polarization and differentiation. Additionally, adherent cell junctions create a network between adjacent cells, thereby allowing the epidermis to resist mechanical forces. Each cell junction is described individually, with particular focus on function within the epidermis. As the original research in this dissertation centers on the desmosome, an expansive description of desmosome structure, function, and molecular components is included (Section 2.3).

Cancer occurs when cell processes become disrupted, resulting in hyperproliferation and avoidance of senescence. Often, the stability of cell junctions is compromised during tumorigenesis, particularly during the process of epithelial to mesenchymal transition (EMT). EMT is one of the steps necessary for cancer cells to invade into nearby tissues as well as to distant tissues to establish metastatic sites. During EMT cell junctions are downregulated and the mechanisms governing this downregulation are poorly understood. Additionally, these junctions must be reestablished at the site of metastasis for a tumor to adhere to the foreign tissue. Currently, cancer research aims to identify novel cancer-specific therapeutics that minimize toxicity to healthy tissue while selectively killing tumor cells. Understanding the mechanisms of cell junction assembly and disassembly could provide us with targets for such therapeutics. This dissertation focuses on an adhesive cell junction, the desmosome, and **the overall goal of this dissertation is to better understand the biological mechanisms of desmosome assembly and disassembly, perhaps illuminating some of the mechanisms involved with desmosome deregulation in cancer progression.** Chapter 3 of this dissertation discusses our current understanding of cell-cell junction deregulation in the progression of cancer as well as potential tumor suppressive or tumor promoting roles of junctional proteins.

Chapter 4 discusses what is currently known about mechanisms for assembly and disassembly of the desmosome. Cancer research has shed light on transcription factors, genetic modifications, and growth factors that regulate the expression of desmosome components. This chapter also discusses our current understanding of desmosome

assembly, including protein biosynthesis and trafficking to the plasma membrane. One method cells use to compartmentalize the plasma membrane and control spatial and temporal localization of proteins is through lipid rafts. Desmosomal proteins associate with lipid rafts, and perturbation of lipid rafts prevents the desmosome assembly, however the biological significance of this association is still unresolved.

Chapter 5 presents original research in which we sought to determine the mechanisms of desmoglein association with lipid rafts and how this raft association impacts desmosome assembly. We conclude that the length of the transmembrane domain (TMD) of desmoglein is the chief mechanism by which desmogleins associate with lipid rafts. Further, we identify a point mutation within the TMD of Dsg1 that causes a fatal dermatological disorder. This point mutation causes a loss of lipid raft association and failure to incorporate into the desmosome, and to our knowledge it is the first report of a failure to associate with lipid rafts directly causing a human disease. Lastly, we present evidence demonstrating that the desmosome is a specialized type of lipid raft and present a model in which the biophysical properties of the plasma membrane contribute to the formation of this specialized membrane domain.

Pemphigus vulgaris (PV) is a human autoimmune disease in which autoantibodies target desmoglein proteins, resulting in destabilization of the desmosome and the downregulation of desmogleins. Studying this disease has allowed us to study desmoglein internalization and desmosome disassembly. Chapter 6 provides a description of the disease, including clinical measures of disease severity and current *in vitro* models to study the disease. In Chapter 7 we use purified IgG from 23 PV patients to compare the results

from an *in vitro* cell-cell adhesion assay to clinical measures of disease severity to determine if our assays have pathological relevance. In fact, we demonstrate an association between Dsg3 ELISA and the cell-cell adhesion assay, thus the results presented in this chapter validate the use of this model and demonstrate relevance to disease progression in patients. Additionally, we compare autoantibody titers to the current scoring system used for patient severity and demonstrate that the sum of Dsg3 and Dsg1 ELISA scores correlates better to disease severity than either score individually. These findings confirm the association of Dsg ELISA values with disease severity and establish a relationship between Dsg IgG titers in patients and loss of adhesion in cultured keratinocytes.

The dissertation concludes with a summary of the original research including major conclusions of the original research contained in chapters 5 and 7. Additionally chapter 8 discusses the remaining questions and future directions of this research.

Chapter 2

The epidermis and cell-cell junctions

2.1 The Epidermis

The epidermis is the outer most layer of the skin and acts as a barrier to the external world (1). This barrier protects the human body from outside pathogens, harmful chemicals, viruses, and radiation (2-5). Additionally, the epidermis protects against excessive loss of moisture (6, 7). When the epidermal barrier is compromised, human diseases such as atopic dermatitis (eczema), which is characterized by an increased allergen and pathogen penetration, can occur (8, 9). Severe cases, such as burn injury, can result be fatal as a consequence of extreme infection (10). The epidermis is a highly stratified epithelium comprised of 4 layers, each with unique structure and function; the stratum basale, the stratum spinosum, the stratum granulosum, and the stratum corneum (Fig 2.1). The basal layer harbors highly proliferative, self-renewing keratinocytes which allow for constant renewal and regeneration of the epidermis as well as effective wound healing (11). These basal keratinocytes lose the ability to attach to the basement membrane and subsequently go through a complex differentiation process (12, 13). As these cells undergo the differentiation process, they migrate from the basal cell layer to the upper granular layers prior to cornification and incorporation into the stratum corneum, which is

comprised of interlocking layers of dead keratinocytes which contain a cornified envelope just inside the plasma membrane (4, 14). The cornified envelope is a highly insoluble structure comprised of lipids, such as ceramides (15), and proteins, such as involucrin and loricrin (16, 17). This structure is thought to be critical to the barrier function and water impermeability of the human epidermis (18, 19). This highly regulated differentiation results in the keratinocytes within the epidermis to have differing morphologies and protein expression profiles dependent on degree of differentiation, which allows for the four distinct layers to be easily identified. The epidermis is a complex tissue that delicately balances barrier function while remaining dynamic enough to allow for tissue regeneration and wound healing. Several pathways such as PTEN, SMAD, and NOTCH contribute to the maintenance of a precise balance of proliferation and differentiation which is critical for efficient barrier function (20-22). The importance of this balance is highlighted by numerous human disorders, including common diseases such as psoriasis, associated with disrupted epidermal differentiation (23-25).

The epidermis also functions as a protector against mechanical damage. Daily, our skin endures an onslaught of mechanical forces and yet typically maintains tissue integrity in healthy individuals. This tissue integrity is maintained by a complex system of protein-protein interactions that integrate the cells of the epidermis to one another to prevent loss of cell adhesion (26). Unfortunately, compromised protein function within cell-cell networks result in numerous dermatological diseases characterized by loss of cell adhesion which presents clinically as blisters or lesions of the skin (27). Preserving epidermal integrity is critical for human survival, and cell-cell protein complexes, or junctions, are

critical for this maintenance. Cell-cell junctions within the epidermis contribute to all of the epidermal functions discussed above; protection from pathogens, protection from loss of moisture, proper epidermal differentiation, and resistance to mechanical forces (28-31).

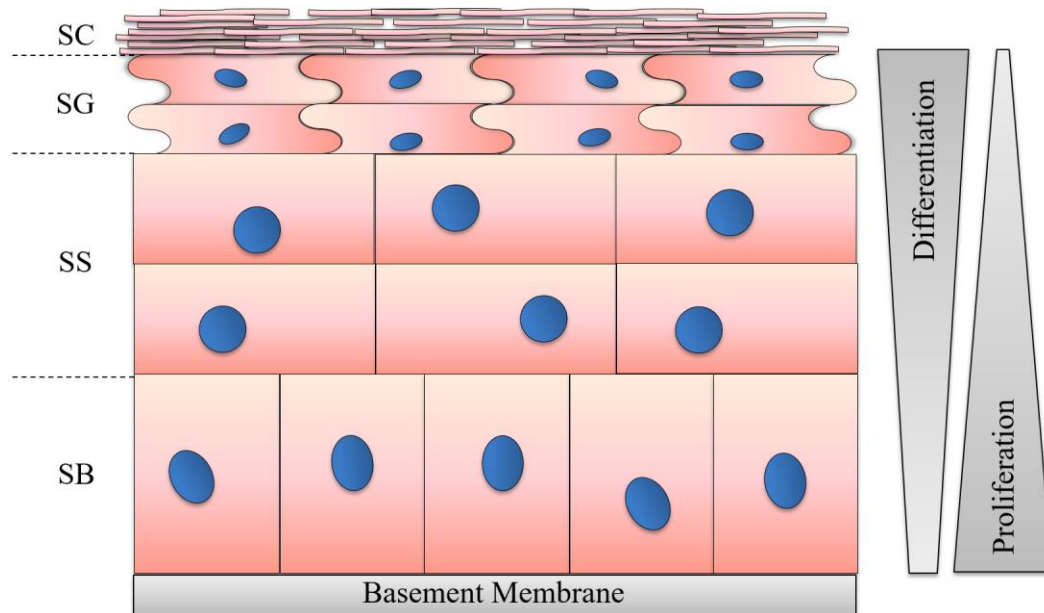


Figure 2.1 Structure of the epidermis. The stratum basale (SB) is the most proliferative layer of the epidermis. As cells detach from the basement membrane they differentiate and travel outwards through the stratum spinosum (SS) and the stratum granulosum (SG) prior to cornification and incorporation into the stratum corneum (SC).

2.2 Cell-Cell Complexes in the Epidermis

Cell-Cell junctions are protein complexes which tether neighboring cells and allow for communication through a complex network of protein-protein interactions (Fig 2.2). These unique membrane domains are formed when proteins coalesce at the plasma

membrane to form a mature junction. These complexes can be separated into three distinct types based on function; tight junctions, gap junctions, and anchoring junctions. These complexes can have many different roles including adhesion, barrier function, and cell-cell communication (28, 29, 32). In the epidermis, these cell-cell junctions are critical for maintaining proper barrier function as well as to confer the ability for this tissue to resist mechanical forces. Additionally, cell-cell contact has been found to be essential for proper keratinocyte differentiation (33). Here I will review the functions of cell-cell junctions, particularly within the epidermis.

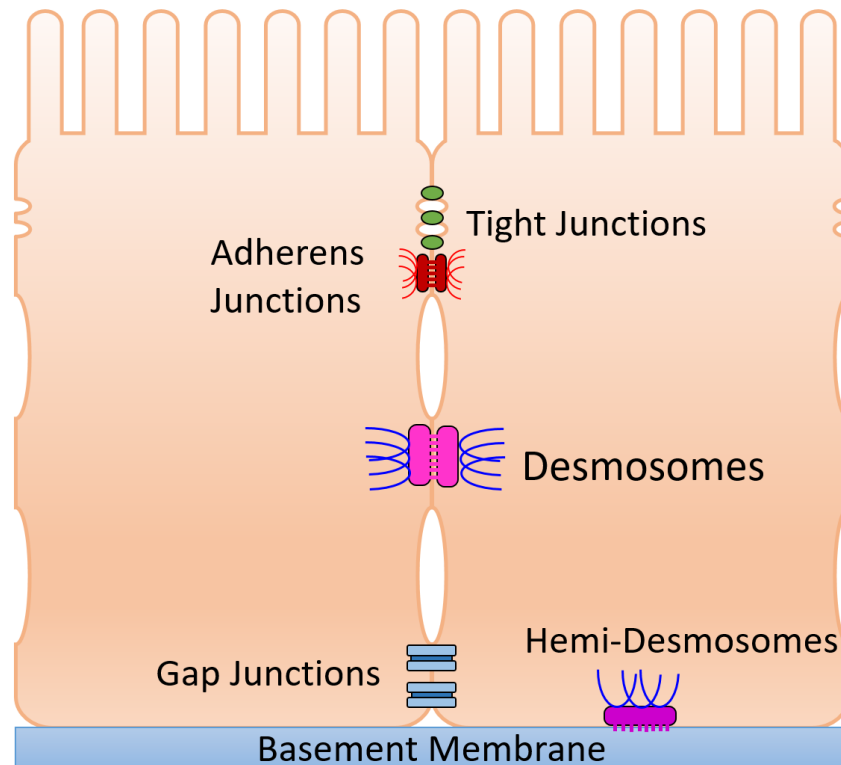


Figure 2.2 Cell-cell junctions in epithelial cells. Cell junctions within the epidermis include the tight junction (green), the adherens junction (red), the desmosome (pink), the gap junction (blue), and the hemidesmosome (purple). These junctions have critical roles in the maintenance and function of epithelial tissues.

2.2.1 Tight Junctions

The major function of tight junctions is to regulate the flow of solutes through spaces between cells (34, 35). While differentiation dependent expression patterns for tight junction proteins are observed within the epidermis, tight junctions are predominantly found within the granular layer of the epidermis (31). Though tight junctions are most notable in the granular layer, they have also been observed in other layers of the stratified epidermis (30). Claudins and occludins are the major transmembrane proteins found within tight junctions (36, 37). In humans, there are 24 known claudin genes (38), and the differing expression of these genes allow for selective permeabilities (39). Mice deficient in claudin-1 expression die within one day of birth due to severe epidermal barrier deficiencies, demonstrating the importance of claudin based tight junctions in the barrier function of the stratified epidermis (31). Conversely, occludin knockouts in mice suggest that occludin does not have an essential role in tight junction formation or function. However, phenotypes associated with these knockouts, such as postnatal growth retardation, suggest that the function of occludin extends beyond the barrier function of the tight junction (40). In addition to these two protein types, single transmembrane domain junction adhesion molecules (JAMs) have also been found to contribute to tight junction adhesion and other functions of the tight junction (37, 41). Together, the extracellular domains of these protein families form tight links between adjacent cells, which create a seal, permitting cells to regulate the flow of materials into the paracellular space (34). The intracellular domains of these proteins interact with adapter proteins such as ZO-1 and ZO-2 which then interact with actin (36). Knockouts of either ZO-1 or ZO-2 in mice results in

embryonic lethality (42, 43) and knock down experiments in epithelial cell models revealed altered localization of claudins resulting in deficient barrier function (44), demonstrating an essential role of these tight junction plaque proteins. Expression of tight junction proteins within the epidermis is highly regulated and several human skin diseases, such as psoriasis vulgaris (45-47), atopic dermatitis (48, 49), and lichen planus (46), are associated with aberrant expression and localization of TJ proteins.

2.2.2 Gap Junctions

Gap junctions have the unique function of allowing rapid diffusion of molecules between adjacent cells, allowing for quick communication within a tissue (50). This communication is essential for tissue maintenance as it allows for cells to synchronize and to correctly differentiate (50). In the human epidermis, gap junctions are found in basal, spinous, and granular layers while excluded from the stratum corneum (51). Ions, second messengers, and small metabolites are examples of solutes that can be directly exchanged from the cytoplasm of one cell to a neighboring cell through a gap junction (52-55). The connexin family is a large group of proteins and are the key components of gap junctions (56, 57). Connexin expression is tissue type and cell type dependent, with several of the connexins expressed within the epidermis (58, 59), though the implications of this tissue specificity are not yet fully understood. Six connexin proteins form a cylindrical channel, or a connexon, in the plasma membrane that is linked with a connexon on a neighboring cell, thus effectively creating a pore between the two cells (60, 61). Gap junctions are not simply open channels that allow for passive diffusion, rather they are highly selective pores

and the type of connexins in a given pore regulates the selectivity of that junction (62). The connexin protein family is highly diverse, and this diversity leads to a variety in pore size, selectivity, and function (50, 57). In the epidermis, connexins seem to play a crucial role in proper wound healing as several studies have noted an increase in connexin expression after wounding in humans and rats (63, 64), and abnormal expression of connexins delays wound healing in diabetic skin (65). Further evidence of the critical role connexins play in epidermal health lies in the upregulation of connexin expression in psoriasis and in hyperkeratosis skin conditions (63, 66). Moreover, mutations within connexin cause human dermatological disorders (67-69). Together, these studies demonstrate the importance of gap junctions and connexins in the proper maintenance and function of the human epidermis.

2.2.3 Anchoring Junctions

The fundamental purpose of anchoring junctions is to hold the tissue together and to confer resistance to mechanical forces. There are three distinct junctions with adhesive functions; adherens junctions, hemidesmosomes, and desmosomes. Adherens junctions and desmosomes are protein complexes that link the cytoskeletons of neighboring cells to one another, preventing loss of adhesion between the keratinocyte layers of the epidermis. The hemidesmosome is responsible for the epidermis maintaining anchorage to the basement membrane and underlying dermal layer (29, 70). Each of these junctions and their contributions to maintaining structural cohesion in the epidermis will be reviewed below.

2.2.3.1 Adherens Junctions

Unlike simple epithelium in which adherens junctions are located in lateral membranes, adherens junctions within the epidermis are found on the lateral and apical surface of basal cells and the entire cell surface of suprabasal cells (71). Interestingly, these adhesive junctions strengthen in response to mechanical force, thereby fortifying the tissues they support (72, 73). Adherens junctions within the epidermis are comprised of the classical cadherin E-cadherin (74, 75). E-cadherin, a calcium dependent single pass transmembrane protein and member of the cadherin family of proteins, interacts homophilically between neighboring cells through an adhesive extracellular interface (76). Deletion of E-cadherin in mouse epidermis results in embryonic lethality as a result of tight junction defects (77). Additionally, postnatal loss of E-cadherin in mouse keratinocytes leads to a loss of adherens junctions coupled with aberrant differentiation (78). Taken together these data demonstrate a critical role for E-cadherin in the maintenance of other cell-cell junctions and the function of the epidermis. The cytoplasmic tail of E-cadherin binds to plaque proteins such as β -catenin and p120 (79, 80). p120 is essential for adherens junction formation and stability. Endocytosis of classical cadherins is inhibited when p120 is bound to the juxtamembrane domain (JMD) domain of the cytoplasmic tail (81-83). A study of VE-cadherin, a classical cadherin similar to E-cadherin, revealed that p120 binds to the cytoplasmic tail to block a constitutive endocytic signal, thus promoting stability on the plasma membrane (84). Epidermis specific knockouts of p120 in mice show that deletion of p120 within the epidermis results in hyperproliferation of keratinocytes (85).

Evidence suggests that β -catenin is not an obligate member of adherens junctions, as a similar plaque protein, plakoglobin, can rescue β -catenin function, at least in part (86). However, adherens junctions containing β -catenin are capable of recruiting vinculin to adherens junctions through α -catenin after tension stress is applied while adherens junctions containing plakoglobin lose vinculin recruiting capabilities (87). However, genetic knockouts of β -catenin in mice result in embryonic lethality, likely due to the critical role β -catenin plays in Wnt signaling (87). The Wnt signaling cascade regulates cell fate both during development and in maintaining tissue homeostasis throughout the lifecycle of an organism (88). In canonical Wnt signaling, cytoplasmic β -catenin is stabilized and translocated to the nucleus, resulting in the transcription of Wnt signaling target genes (88). Furthermore, postnatal epidermis specific knock outs of β -catenin caused hair loss as a result of a failure for stem cells to differentiate into follicular keratinocytes causing keratinocytes to differentiate into interfollicular epidermis, further supporting a β -catenin function in cell fate decisions (89). Additionally, some pilomatricomas, or tumors originating from the hair follicle, are caused by mutations in β -catenin which result in stabilization and an increase in Wnt signaling (90). These data support an important role for β -catenin in balancing adhesion and cell-fate decisions. The E-cadherin/ β -catenin complex association with the actin cytoskeleton occurs through α -catenin which binds to β -catenin and actin (91, 92). As mentioned briefly above, α -catenin aids in the recruitment of vinculin to adherens junctions for force-dependent fortification of the junction (93). Additionally, a conditional knockout of α -catenin in mice caused a loss adherens junctions, resulting in hyperproliferation and a loss of polarization of epithelial cells (94). Together,

these studies provide compelling evidence that the adherens junction is crucial for proper function of the stratified epidermis.

2.2.3.2 Hemidesmosomes

Hemidesmosomes serve to connect and anchor the epithelium to components of the underlying dermal tissue and the basement membrane (70). There are two types of hemidesmosomes, type I is found within stratified epithelia while type II is found within simple epithelia (70). Early electron microscopy studies identified hemidesmosomes at the region where the basal layer of the epidermis adheres to the basal lamina (95, 96). Basal keratinocytes express transmembrane integrins $\alpha 6$ and $\beta 4$, which create a heterodimer to form the core of the hemidesmosome (97). The extracellular domains of these integrins interact with proteins of the basement membrane, such as laminin (98, 99). Plectin, a hemidesmosome plaque protein and member of the plakin protein family, directly binds to the cytoplasmic tail domain of integrin $\beta 4$ (100, 101) and with keratins 5 and 14 (102), thus providing a bridge between the transmembrane proteins of the hemidesmosome and the intermediate filament cytoskeleton. Mutations within the plectin gene have been linked to skin blistering disorders, and studies of these patients revealed that these mutations compromised the inner plaque structure of hemidesmosomes (103-107). Studies of the blistering skin disorder bullous pemphigoid uncovered an additional transmembrane domain protein of the epidermal hemidesmosome, now known as BPAG2 (108, 109). BPAG2 extends from the cytoplasm of basal keratinocytes and has a lengthy extracellular domain containing 15 collagen repeats as well as 16 noncollagenous domains (109). The

function of BPAG2 is not fully understood, however it has been observed that the ectodomain of BPAG2 is cleaved by proteases and successively incorporated into the basal lamina (110). Together, this complex of proteins tethers the cytoskeleton of keratinocytes within the epidermis to the basement membrane, and when this adhesion is disrupted separation of the epidermis from the dermis can occur, resulting in blistering skin disorders (111).

2.2.3.3 Desmosomes

While desmosomes have overlapping adhesive functions with adherens junctions, they are functionally distinct, robust junctions essential for epithelial integrity. The structure, function, and regulation of desmosomes will be reviewed extensively below as the research contained within this dissertation focuses on the desmosome.

2.3 The Desmosome

Desmosomes are large, multiprotein complexes responsible for riveting together adjacent cells in tissues. These disc-shaped complexes are crucial in tissues that experience mechanical stress, such as the skin and heart(112). In the epidermis, desmosomes exist between keratinocytes and the composition of the desmosome varies depending on layer of the stratified epidermis (Figure 2.3). Desmosomes are very protein dense with a 75:15:10 ratio of protein, carbohydrate, and lipid respectively (113). In fact, this protein density led

to the desmosome being one of the earliest structures viewed with electron microscopy (114, 115). When the desmosome is visualized via electron microscopy it can be divided into the extracellular core, the outer dense plaque, and the inner dense plaque (114). Early techniques allowed for the purification of desmosomes from bovine snout, permitting the identification of desmosomal components (116). It was studies of these isolated desmosomes that provided the first insights into the density (113) and integral membrane glycoprotein makeup of the desmosome (117, 118) as well as the presence of desmosomal plaque proteins (119).

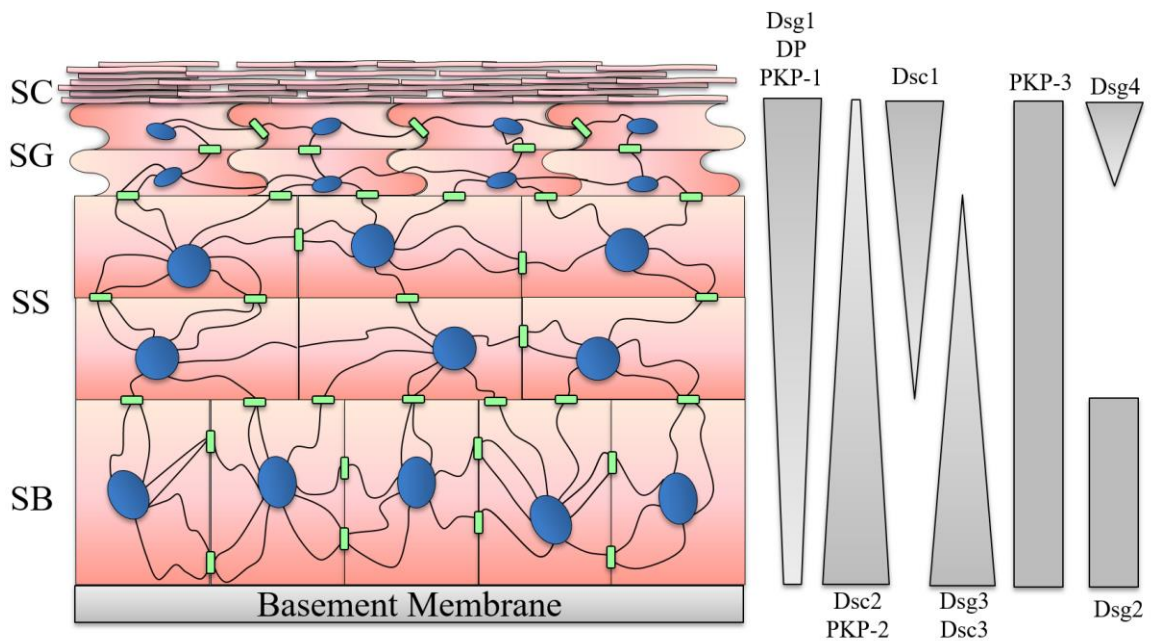


Figure 2.3 Desmosome organization in the epidermis. Desmosomes (green) interact with the keratin intermediate cytoskeleton and are found between cells in the stratum basale, stratum spinosum and the stratum granulosum. Desmosome proteins are expressed in a differentiation specific pattern as shown in the stratified epidermis.

2.3.1 Molecular components of the desmosome

The core of the desmosome is comprised of calcium-dependent members of the cadherin family, desmogleins and desmocollins (120-122). Desmosomal cadherins have adhesive extracellular domains and intracellular domains that interact with members of the armadillo protein family. Armadillo proteins then interact with the plakin family of proteins and together form the desmosomal plaque (123-127) (Fig 2.4). These proteins bind to the intermediate filament cytoskeleton, creating a dense, interconnected network of desmosomal proteins that anchor the desmosome to the cytoskeleton (128, 129). This structural arrangement confers resistance to mechanical stress in tissues such as the heart and skin (128, 129). The molecular components of the desmosome will be discussed in greater detail below.

2.3.1.1 Desmogleins

Desmogleins (Dsg) are single pass calcium-dependent adhesion proteins of the cadherin family. These proteins have four extracellular repeat domains, an extracellular anchor domain, a transmembrane domain, and a cytoplasmic tail (122). The extracellular repeat domains have a high affinity for calcium and calcium binding results in the rigid conformation required to facilitate adhesion (130, 131). Desmogleins form homophilic *trans* interactions with desmogleins to facilitate adhesion, and these interactions have isoform specificity (132, 133). Desmogleins have also been observed binding in *trans* with desmocollins (134, 135). The cytoplasmic tail of desmoglein binds to plakoglobin (136-

138), plakophilin (139, 140), and the N-terminal domain of desmoplakin (139, 141). In humans, there are four desmoglein isoforms that are expressed in a differentiation specific pattern (Figure 2.3). Dsg3 and Dsg2 are expressed mainly in the basal layer of the epidermis, Dsg1 is expressed mainly in the spinous layer and the granular layer, and Dsg4 is mainly expressed in the hair follicle (128, 142-144). Investigators used fluorescence in situ hybridization as well as other techniques to map the genes for desmoglein proteins to band q12 on the human chromosome 18, and similar studies in mice illustrated a similar location of the desmoglein genes on chromosome 18 (145-149). Several studies lead to the conclusion that the expression of desmoglein isoforms plays an active role in the differentiation process rather than as a consequence. Downregulation of Dsg1 in an organotypic epidermal culture model resulted in an immature granular layer, supporting Dsg1 function as a contributor to keratinocyte differentiation (150). Additionally, misexpression of Dsg3 in the suprabasal epidermal layers in transgenic mice lead to hyper proliferation as well as abnormal differentiation (151). Similarly, over expression of Dsg2 in the epidermis results in hyper proliferation (152). Further studies manipulating the expression of desmoglein isoforms support the conclusion that the isoforms of desmoglein have different functional roles within the epidermis (153). The precise role of this tissue specific expression pattern is not yet fully understood, however there are some indications that the desmosomes within the different layers of the epidermis remain functionally distinct.

Several human dermatological disorders resulting from loss of desmoglein function indicate that desmogleins are critical for desmosome adhesion and epidermal homeostasis.

Desmoglein 1 is a target in the autoimmune disease pemphigus foliaceus (154, 155) and in the infectious disease bullous impetigo (156, 157). Dsg1 function is compromised in both of these diseases, resulting in epidermal fragility. Furthermore, genetic diseases such as striate palmoplantar keratoderma (SPPK) or severe dermatitis multiple allergies and metabolic wasting syndrome (SAM) result from heterozygous or homozygous loss of function mutations or deletions in Dsg1 (158-161). Ablation of Dsg1 expression in mice resulted in death within 24 hours of birth due to loss of barrier function and splitting of the epidermis (162). Dsg3 is the main target in the autoimmune disorder pemphigus vulgaris, and loss of Dsg3 function results in blisters of mucosal tissues as well as the epidermis which, if left untreated, can be lethal (156, 163). Pemphigus vulgaris will be reviewed more extensively in chapter 6. The numerous skin disorders associated with desmoglein function highlights the importance of this cadherin in desmosome function.

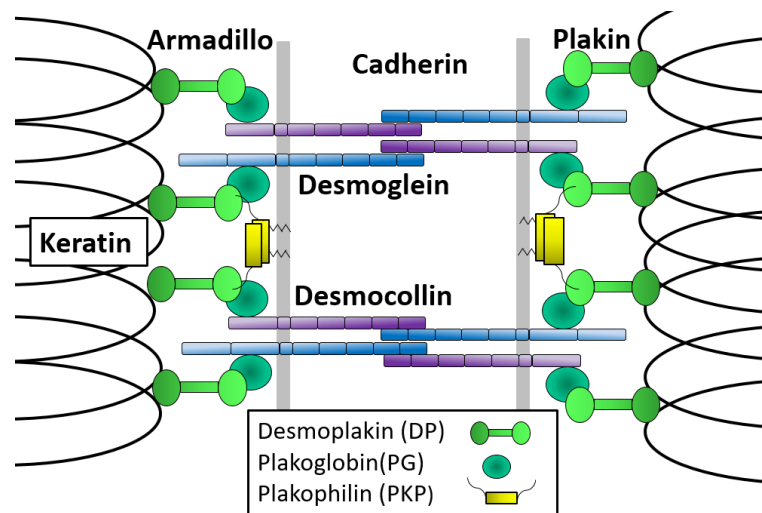


Figure 2.4 Molecular components of the desmosome. Desmogleins and desmocollins interact *in trans* in the extracellular space, span the plasma membrane, and interact with plaque proteins in the cytoplasm. Plaque proteins from the plakin and armadillo family interact with the desmosomal cadherins to form a dense plaque and a tight association to the keratin intermediate cytoskeleton (164).

2.3.1.2 Desmocollin

Desmocollins (Dsc) are the second member of the cadherin family that comprises the adhesive core of the desmosome. Similar to desmogleins, desmocollins have 4 extracellular repeat domains, an extracellular anchor domain, a single transmembrane domain, and a cytoplasmic tail that interacts with plaque proteins (122). Like desmogleins, the genes for the desmocollins are located in band q12 on chromosome 18 in humans (146, 148, 149). DNA sequencing of mouse desmocollin genes uncovered that desmocollins are more closely related to the classical cadherins, such as E-cadherin, than they are to desmogleins (165). There are three different isoforms of desmocollin (Dsc1-3), however each isoform has two splice variants resulting in a Dsc “a” form or a Dsc “b” form, the latter of which has a shorter cytoplasmic tail (121, 166). Dsc2 is expressed in all desmosome-containing tissues, while Dsc1 and Dsc3 are expressed mainly in stratified epithelia like the epidermis with Dsc3 being highly expressed in the basal layers and Dsc1 having high expression in the suprabasal layers (Figure 2.3). Desmocollins are capable of both homophillic interactions (133) and heterophyllic interactions with desmogleins (134, 135), and both types of desmosomal cadherin are required to form robust desmosomes (167). Studies of the desmocollin isoforms suggest that, like desmogleins, desmocollin isoforms are functionally distinct. Absence of Dsc1 did not result in any detectable alteration in desmosome structure, however Dsc1 null mice showed thickened epidermis, due to abnormal keratinocyte proliferation and differentiation, and epidermal fragility, demonstrating the critical role for Dsc1 in the barrier function of the epidermis (168). A dominant negative form of Dsg3 only impacted the ability for desmosome formation, while

a dominant negative form of Dsc3 resulted in a defect in both desmosome formation and adherens junction formation, suggesting a critical role for desmocollins in communication and interplay between desmosomes and adherens junctions (169). Further evidence that desmocollins are critical for epidermal health lies in the observation that all of the desmocollins have been identified as targets in rare variants of pemphigus (170, 171). Desmocollins have also been implicated in hypotrichiosis (172), SPPK (173, 174), and woolly hair syndrome (174), providing additional evidence that desmocollins have important epidermal homeostasis functions.

2.3.1.3 Desmoplakin

Desmoplakin (DP) is one of the major components of the desmosome and is a member of the plakin family of proteins. Plakins are large proteins that act as cytolinkers, proteins which cross-link adhesion complexes with the cytoskeleton (175, 176). DP forms dumbbell shaped homodimers and contains a N-terminal domain, a rod domain, and a C-terminal domain (177). Alternative splicing results in two isoforms of desmoplakin with DP_{II} having a shorter rod domain than DP_I (177). The N terminal domain of desmoplakin binds to plakoglobin (127, 140) and plakophilin (140, 178), facilitating the organization of the desmosomal plaque and the cadherins on the plasma membrane. Some studies have shown that desmoplakin can interact directly with desmogleins and desmocollins, though those interactions are weaker than those observed with plakoglobin and plakophilin (139, 140). The C-terminus of DP binds to the keratin intermediate cytoskeleton, thus DP links the adhesive desmosomal cadherins to the cytoskeleton (177, 179). Global knockout

models of DP result in embryonic lethality, however, analysis of these mouse embryos uncovered the importance of DP in intermediate filament attachment to desmosomes and in desmosome stabilization (180). Epidermis-specific ablation of DP in mice resulted in desmosomes that lacked interactions with keratin filaments resulting in a severe loss of desmosome function and subsequent susceptibility to intercellular separation (181). Loss of DP is fatal in mice and loss of DP function has been implicated in several human diseases. Some patients suffering from SPPK, SAM syndrome, and woolly have loss of function mutations in one or both copies of DP (182-185). Together, these data demonstrate a critical role for DP in desmosome structure and function.

2.3.1.4 Plakophilin

Plakophilin (PKP) is a member of the armadillo protein superfamily and has a long N-terminus domain, a central domain containing nine armadillo repeats, and a short C-terminal domain (186). The crystal structure of PKP-1 reveals that the central domain is kinked because of a long flexible insert found between the fifth and sixth armadillo repeats, which differentiates PKP from other armadillo proteins that contain straight central domains (187). There are three isoforms of PKP and all are found within the stratified epidermis. PKP-1 and PKP-2 have opposing expression patterns with PKP-3 being predominantly basal while PKP-2 has equal expression throughout the layers of the epidermis (188, 189). PKP-1 and PKP-2 have at least two splice variants (190-192). Overexpression of PKP-1 in HaCat keratinocytes resulted in enhanced recruitment of desmosomal proteins to the plasma membrane, demonstrating that PKP aids in the

organization and formation of desmosomes (193). Null mutations in the PKP-1 gene is associated with a human dermatological disorder characterized by thickened epidermis and compromised desmosome structure and adhesion (194). Additionally, PKP-3 regulates desmosome assembly, size, and stability and overexpression of PKP-3 decreases the calcium dependency for desmosomes (195). A sequence at the amino-terminus of the head domain is responsible for PKP-1 binding to desmoplakin, and this sequence is conserved between all of the plakophilins (178, 193). PKP binding to desmoplakin is required for desmoplakin to be recruited to desmosomes and for proper desmosome assembly (178). The head domain of PKP is also responsible for PKP binding to keratin and desmogleins (141, 193). The armadillo repeat domain of PKP seems to have a critical role in mediating actin dynamics as expression of a PKP-1 mutant lacking the head domain in keratinocytes resulted in PKP-1 association with actin and an increased number of filopodia and lamellipodia (193).

2.3.1.5 Plakoglobin

Plakoglobin (PG), also known as gamma-catenin, is encoded by the JUP gene and is a member of the catenin protein family in the larger armadillo repeat superfamily. While PG is capable of binding classical cadherins as well as desmosomal cadherins and has been observed in both AJs and Desmosomes, it has a higher affinity for desmosomal cadherins and preferentially localizes to the desmosome (196, 197). Plakoglobin associates with desmosomal cadherins early in the biosynthetic pathway and is required for DP association with Dsg complexes (127, 198). Additionally, deletion of the plakoglobin binding domain

in Dsg3 prevented Dsg3 incorporation into desmosomes, suggesting PG has a critical function in the clustering of desmosomal cadherins to form a mature desmosome (136). In addition to binding to desmosomal cadherins and DP, PG also binds to PKPs and keratin intermediate filaments (140, 199). Complete loss of plakoglobin in mice results in embryonic lethality due to heart defects (200), however keratinocyte specific PG ablation results in thickened epidermis and a defect in keratin association with the desmosomal plaque (25). These findings parallel the symptoms of patients suffering from SPPK as a result of mutations in plakoglobin (201, 202).

Chapter 3

Epithelial cell junctions and junctional proteins in tumorigenesis

Cancer occurs when genetic mutations cause cells to aberrantly proliferate resulting in abnormal malignant growths within tissues (203). Because cancer is derived from our normal tissues, and therefore closely resembles our healthy cells, it is a very difficult disease to understand and to treat without toxicity to healthy tissue (204). This leads to a great need to understand the mechanisms driving the malignant behaviors of cancer with the ultimate goal of identifying novel cancer-specific therapy targets to minimize toxicity to healthy organs and tissues while maximizing anti-cancer effects. There are several types of cancers associated with the skin and specifically the epidermis. The two most common types are basal cell carcinomas (BCC) and squamous cell skin carcinomas (SCC), which are derived from the stem cells that give rise to keratinocytes found in the stratified epidermis (205, 206). Both BCC and SCC have been linked to solar radiation as well as genetic predisposition and are among the most common neoplasms in white populations, with incidence rates increasing (205, 207-210). As discussed above, cell junctions are essential for the maintenance and function of the epidermis, and the role of these junctions as well as individual junctional components in tumor progression will be discussed below.

3.1 Epithelial to mesenchymal transition

During wound healing and embryogenesis, epithelial cells use a process termed epithelial to mesenchymal transition (EMT) in which epithelial cells lose their polarity to become more motile, mesenchymal-like cells (211-214) (Figure 3.1). Tumor cells hijack EMT to facilitate motility and invasiveness, particularly during metastatic progression (214, 215). On the other hand, tumor cells must revert back to an epithelial phenotype at the site of a new metastatic tumor through a process called mesenchymal to epithelial transition (MET) (216). Because of the difficulty in modeling MET, we still lack a holistic understanding of how this process work. However, it is clear that MET is an obligate step in the establishment of secondary tumor sites. As discussed above, cell-cell junctions are essential for connecting cells within a tissue as well as in maintaining epithelial polarity and the regulation and dynamics of these junctions are altered in order to allow for both EMT and MET. The first junction to be lost during the process of EMT is the tight junction, followed by the loss of adherens junction and desmosome integrity. Transforming growth factor beta (TGF β) is a secreted protein known to stimulate and induce EMT (217, 218), and the study of this pathway uncovered tight junctions as key regulators for the initial stages of EMT (219, 220). The loss of tight junctions is followed by a loss of polarity and downregulation of the adherens junction protein E-cadherin. E-cadherin is perhaps the most well studied adhesion molecule in the context of EMT, and loss of E-cadherin has been shown to occur in tumors of a variety of cancer types (221-224) . The loss of E-cadherin coupled with an increase in N-cadherin expression is so widely associated with EMT and cancer progression that it is now known as a marker for EMT (225). The

observation that E-cadherin expression is decreased in primary breast tumors but elevated in matched metastatic tumors supports the hypothesis that E-cadherin, and adherens junctions, must be downregulated to allow for cells to separate from the primary tumor to travel and invade a metastatic site, but then upregulated to establish functional junctions at the metastatic site (226).

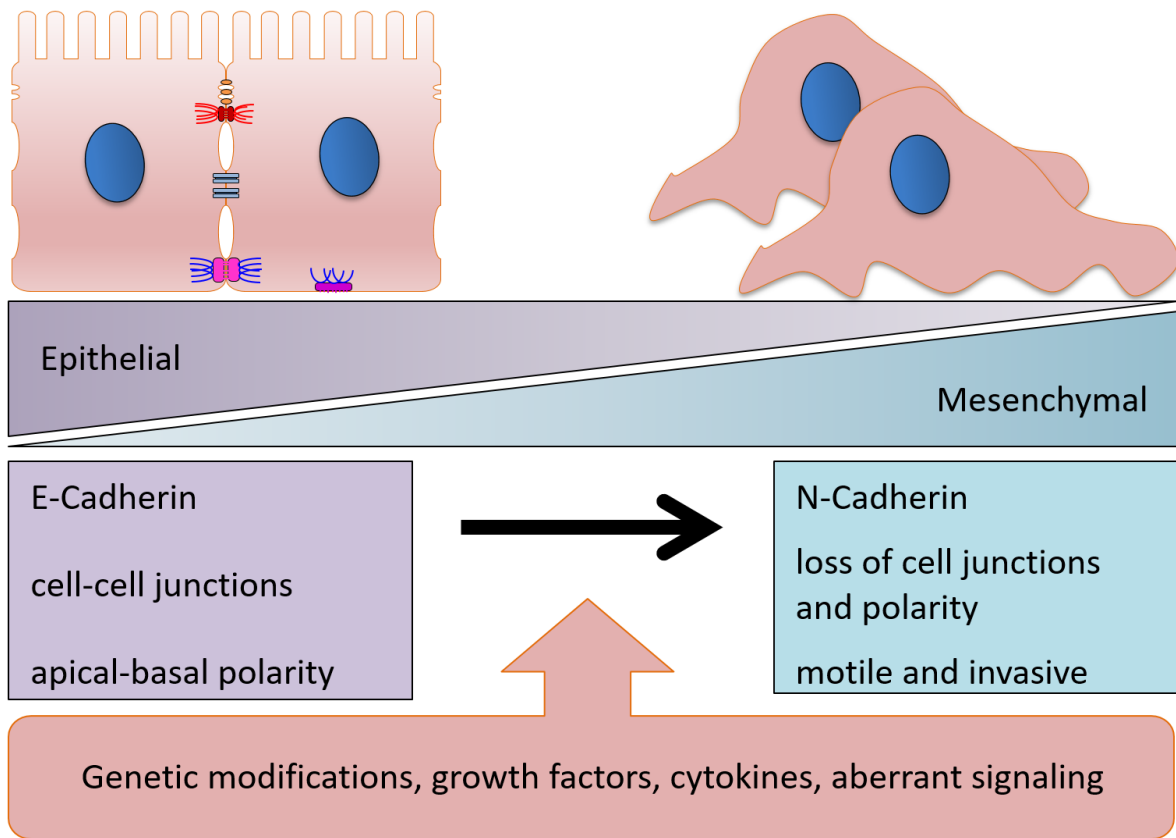


Figure 3.1 Loss of cell junctions during epithelial to mesenchymal transition. Genetic modifications, growth factors, cytokines, and aberrant signaling stimulate the process of epithelial to mesenchymal transition during tumorigenesis. Epithelial cells lose their polarity and cell-cell junctions and become more motile and invasive in the process.

3.2 Tight junction proteins and cancer

Beyond EMT, individual components of tight junctions and adherens junctions have varying roles in cancer progression (Table 3.1). Breast cancer cells showing an increased expression of claudin-2 demonstrated increased interactions with hepatocytes and subsequent preferential metastasis to the liver when compared to other common metastatic sites such as the bone or lung (227). Additionally, loss of occludin is associated with poorer patient prognosis and is also positively correlated with the establishment of bone metastatic sites (228, 229). Taken together, these data support that tight junctional proteins can interact with the microenvironment to aid in the establishment of metastatic sites. Moreover, loss of claudin-3 is associated with poor patient survival in colon cancer and results in hyper activation of the Wnt signaling cascade, facilitating tumorigenesis and suggesting a non-adhesive, signaling function for tight junction proteins in cancer progression (230).

3.3 Adherens junction proteins and cancer

As mentioned in chapter 2, the adherens junction protein, β -catenin, is an obligate member of the Wnt signaling complex and important for Wnt signal transduction. Irregular Wnt signaling has important implications in tumorigenesis and has been highly studied as targeting this signaling cascade could provide cancer therapeutics (231-233). In fact, hyperactivation of the Wnt pathway is thought to be an initiator of colon cancer (234, 235). Downregulation of E-cadherin, as seen during EMT, displaces β -catenin to the cytoplasm

allowing for increased interplay with the Wnt signaling cascade and β -catenin dependent transcriptional activity (236). Recently, a small molecule inhibitor of β -catenin interactions with Wnt pathway proteins has been developed and when colon cancer cells are treated with this inhibitor it decreases cancer cell survival by inducing apoptosis (237). Deletion of α -catenin in mouse epidermis resulted in hyper proliferation of keratinocytes, implicating anti-proliferative functions for α -catenin (94). Observations of decreased α -catenin expression in a variety of cancers coupled with the identification of α -catenin signaling functions support a tumor suppressive role of α -catenin (238-240). Collectively, studies of tight junction and adherens junction proteins demonstrate an important relationship between these junctions and cancer progression.

3.4 Desmosome proteins and cancer

Like tight junctions and adherens junctions, desmosome function is compromised during the process of EMT. Immunohistochemical staining of oral squamous cell carcinomas revealed that a loss of desmoplakin and loss of desmoglein staining correlated with a loss of differentiation and a higher degree of invasiveness (241). Additionally, desmoplakin and desmoglein were drastically reduced in patients harboring secondary metastatic tumors when compared to patients without metastatic tumors (241). Thus the downregulation of desmosomal components may be important for the progression of EMT. Further studies have confirmed that the majority of desmosomal components are downregulated in squamous cell carcinoma of the skin, head & neck, and breast (242-248) (Table 1.1). SCC cell lines in which desmosomal cadherins were overexpressed were found to have lost their

invasive potential (249). Investigators demonstrated that the ablation of Dsc3 led to an increase in skin tumors and that spontaneous loss of Dsc3 expression in skin tumor progression is a common occurrence (250). Furthermore, tumor suppressive roles of desmosomal plaque proteins have been observed as desmoplakin inhibits the Wnt signaling pathway (251) and plakoglobin expression suppresses keratinocyte motility (252). Taken together, these data support a model in which the desmosome and desmosomal proteins have tumor suppressive roles, however some studies have proposed tumorigenic functions of desmosomal proteins.

The expression of Dsg3 is upregulated in esophageal squamous cell carcinoma (ESCC), however there was no significance of this increased expression on patient survival (253). While there is clear evidence that Dsg3 acts as a tumor suppressor (243, 245), there is also data suggesting that Dsg3 promotes cancer cell migration and invasion through PKC signaling in squamous cell carcinoma (254). Similarly, Dsg2 expression has been shown to be upregulated in squamous cell carcinomas and basal cell carcinomas (242, 244, 255). This increased expression of Dsg2 has been linked to high risk SCC patients and higher expression of Dsg2 is correlated to more metastatic epithelial-derived prostate cancer cell lines when compared to a non-metastatic pre-cursor cell line. Mechanistically, it seems that Dsg2 has non-adhesive, signaling roles that facilitate cancer progression. Overexpression of Dsg2 in a mouse model promoted the development of BCC through the activation of the Stat3 pathway (256). Knockdown of Dsg2 in non-small cell lung cancer (NSCLC) results in a loss of proliferation accompanied by upregulated p27 expression and cell cycle arrest in the G1 phase (257). Furthermore, Dsg2 promotes the secretion of EGFR

and c-Src via vesicles from Dsg2 expressing cells, enhancing the proliferation of keratinocytes exposed to these vesicles and thereby altering the tumor microenvironment to one more favorable to the growth and survival of cancer (256). It is becoming increasingly clear that desmosomal cadherins may play a role in the pathogenesis of certain types of cancers, however little is understood about the mechanisms governing these associations.

Table 3.1 Cell junction proteins and cancer

Cancer(s) / Cancer Process		Reference(s)
Tight Junctions		
↑ Claudin-2	Metastasis (breast → liver)	(227)
↑ Claudin 18	Gastric cancers, non-small lung cancer	(258, 259)
↑ Occludin	Lung cancer	(260)
↑ JAM-A	Multiple Myeloma, Lung adenocarcinoma, breast cancer	(261-263)
↓ Claudin 3	Colon cancer	(230)
↓ Occludin	Metastasis (breast → bone), breast cancer, cervical cancer , lung carcinoma	(228, 229, 264)
↓ JAM-A	Gastric cancer	(265)
Adherens Junctions		
↑ β-catenin	Colon carcinoma	(240)
↓ E-cadherin	EMT, Breast cancer, gastric cancer, prostate cancer	(221-224, 266)
↓ α- catenin	Gastric cancer, breast cancer, colorectal cancers	(238, 239, 267, 268)
↓ β-catenin	oral squamous cell carcinoma	(243)
↓ p120	Colorectal carcinoma, bladder carcinoma, gastric carcinoma, breast carcinoma	(269-273)
Desmosomes		
↑ Dsg2	Basal cell carcinoma, squamous cell carcinoma	(242, 244, 255)
↑ Dsg3	Head and neck cancers , squamous cell carcinoma (oral & lung)	(254, 274-276)
↑ Dsc1	Colorectal adenocarcinoma	(277)
↑ Dsc3	Colorectal adenocarcinoma	(277)
↓ Dsg1	Skin squamous cell carcinoma, Basal cell carcinoma, oral squamous cell carcinoma, head and neck cancer	(242, 245-248)
↓ Dsg2	Gastric carcinoma	(278, 279)
↓ Dsg3	Skin squamous cell carcinoma, oral squamous cell carcinoma	(242-245, 247)
↓ Dsc1	Skin squamous cell carcinoma	(242)
↓ Dsc2	Skin squamous cell carcinoma, colorectal adenocarcinoma, oral squamous cell carcinoma	(242, 247, 277)
↓ Dsc3	Skin squamous cell carcinoma , breast cancers , oral squamous cell carcinoma	(242, 243, 250, 280, 281)
↓ DP	Skin squamous cell carcinoma	(242)
↓ PG	Skin squamous cell carcinoma , bladder cancer cell lines , prostate cancer, Basal cell carcinoma, lung cancer	(242, 245, 246, 282-284)

*↑: Increased expression or function

↓: Decreased expression or function

Chapter 4

Regulation of the desmosome

While the desmosome is robust and provides resistance to mechanical forces, it is a dynamic structure allowing for junctional remodeling during biological processes such as cell division, cell migration, wound healing, and during development. As discussed in chapter 3, the pathways governing desmosome stability are hijacked during tumorigenesis, resulting in destabilization and downregulation of the desmosome during EMT. The main focus of this dissertation is to gain a greater understanding of the mechanisms governing the assembly and disassembly of the desmosome. The loss of desmosome function during EMT can occur either as a result of downregulation of desmosome proteins or as a result of destabilization of the desmosome. This chapter reviews what is currently known about desmosome assembly and stability including what is understood about lipid rafts in desmosome regulation. Much of what is known about desmosome disassembly has been learned through the study of the autoimmune skin disease pemphigus vulgaris and will be reviewed in chapter 6.

4.1 Factors regulating the expression of desmosomal proteins

Studies primarily focused on understanding the deregulation of desmosomes during the process of tumorigenesis provide insights as to which transcription factors and

epigenetic modifications govern the expression of desmosome components (Table 2.1). Transcription factors are proteins that when bound to DNA, regulate the expression of downstream targets. Transcription factors are often aberrantly active in cancer, and thus studying these proteins in the context of tumorigenesis can uncover potential therapeutic targets (285). Studies in cultured keratinocytes and in mouse models demonstrate that loss of p63 function reduces Dsc3, Dp, and Dsg1 levels at the transcriptional and post-translational level (286). Similarly, mutations within p53 have identified Dsc3 as a target of the transcription factor (287, 288). A study in a cell line derived from oral squamous cell carcinoma cells uncovered that the degradation of Dsg2 was dependent on activity of the transcription factor Snail (289). Several other transcription factors like Klf5, Smad4, Grainy head-like 1, Cdx1, and Lef-1 have been implicated as regulators of desmosomal protein expression (21, 266, 290-294), however, further research is required to understand the pathways responsible for these observations and the significance.

In addition to transcription factor activity, epigenetic modifications are capable of controlling gene expression. Similar to transcription factors, epigenetic alterations have a role in the progression of cancer (295). Hypermethylation of promoter regions prevent the DNA from being accessible to transcriptional machinery, thereby silencing downstream genes. A study of 32 breast cancer patients uncovered that 13 of the 32 patients demonstrated a loss of Dsc3 expression associated with hypermethylation of the promoter region, however no clear mechanism for the hypermethylation was identified (280). Similar hypermethylation of the Dsc3 promoter region and subsequent loss of expression was identified in several other cancer types including prostate cancer and esophageal

adenocarcinomas and the loss of expression correlated with worse patient prognosis (296, 297). Furthermore, hypermethylation has been associated with the downregulation of plakoglobin and plakophilin in several cancer types (283, 298-300). In addition to hypermethylation of DNA, post translational modifications to histones can affect the transcription of desmosome genes. Aberrant histone methylation and acetylation in prostate carcinoma and bladder cancer is linked to altered expression of many desmosome proteins (301, 302). While it is clear that genetic and epigenetic modifications that occur during tumorigenesis affect the expression of desmosomal proteins, the upstream effectors that lead to these modifications are still left a mystery.

4.2 Desmosome Stability

While desmosome integrity can be altered by downregulating the expression of individual desmosome components, the stability of the desmosome can also be altered post translationally through several mechanisms. Growth factors are proteins that act as signaling molecules that often regulate cell proliferation and survival. These factors exist in the extracellular space and bind to receptors on the cell surface to initiate a signaling cascade. Investigators have identified several growth factors that impact desmosome stability (Table 4.1). EGF treatment results in the phosphorylation of PG, resulting in a loss of binding between PG and DP and subsequent loss of intercellular connections (138). Plakoglobin was removed from cell borders and present in the cytoplasm in cells treated with TNF α , but when cells were treated with other cytokines PG localization was not altered (303). Thus TNF α selectively targets the localization of PG. Additionally, IGF-1

treatment resulted in the phosphorylation of PKP-1 and reduced intercellular adhesion (304). Further studies of these growth factors and downstream signaling could illuminate mechanisms for desmosome regulation, particularly in the context of tumorigenesis as growth factors are key tumor promoting factors.

In addition to growth factors, desmosome stability is affected by extracellular calcium levels. The extracellular domain of cadherins, including desmogleins and desmocollins, contain binding domains for calcium (122). Calcium binding results in a conformation change that allows for cadherins to adhere in the extracellular space. When keratinocytes are cultured in low calcium media (50uM) they are unable to form desmosomes while the addition of calcium (550uM) results in the formation of desmosomes over several hours. Similarly, when keratinocytes cultured in high calcium are switched to low calcium media, desmosomes are rapidly disassembled. However, confluent keratinocytes cultured in high calcium for six days reveal that a portion of desmosomes become calcium independent as determined by a calcium chelating assay (305). Additionally, our lab as well as others have been able to generate calcium independent desmosomes through PKC α signaling and PKP-1 overexpression (305, 306). It may be that desmosomes in unperturbed epidermis exist in both calcium dependent and calcium independent states, and that extracellular calcium is critical for desmosome stability during desmosome formation and maturation. Support for this model lies in the observation that after wounding, desmosomes switch to a calcium dependent state in a PKC dependent manner (307).

Table 4.1 Regulation of the Desmosome

Transcription factors		
<i>Transcription factor</i>	<i>Target(s)</i>	<i>Reference(s)</i>
p63	Dsc3, DP, Dsg1	(286, 308)
p53	Dsc3	(287, 288)
Snail	Dsg2	(289)
Klf5	Dsg1, DP	(249)
Smad4	Dsg4	(291)
Grainy head-like 1	Dsg1	(292, 293)
Cdx1/Cdx2	Dsc2	(294)
Lef-1	Dsc2, Dsc3	(309)
Stat3	Dsg3	(310)
Epigenetic modifications		
<i>Modification</i>	<i>Target(s)</i>	<i>Reference(s)</i>
Promoter Methylation	Dsc3, PG, PKP	(280, 288, 296-300)
Histone Methylation	Dsc 1-3, Dsg 1-4, DP	(301)
Histone Acetylation	Dsg2, Dsg1	(302, 308)
Growth factors		
<i>Growth factor</i>	<i>Target(s)</i>	<i>Reference</i>
EGF	PG, Dsg2, Dsc2	(138, 311)
TNF α	PG, Dsg2	(303, 312)
HGF	Dsg1, DP	(313, 314)
IGF-1	PKP1	(304)
IFN γ	Dsg2, Dsg3	(315)

4.3 Desmosome Assembly

Prior to the formation of a desmosome, desmosomal proteins must traffic through the biosynthetic pathway to the plasma membrane (PM). PKP and DP are the first desmosomal components to accumulate at the plasma membrane after cells are switched from a low calcium to a high calcium environment (316, 317). PKP-2 is critical for DP accumulation at the PM and subsequent desmosome assembly (318). Palmitoylation and lipid raft association of PKP is required for proper desmosome assembly (319). Additionally, whereas DP is not palmitoylated, pan inhibition of palmitoylation results in a loss of DP association with cell borders, perhaps due to a failure of unpalmitoylated PKP to associate with lipid rafts (319). Interestingly, Dsg2 and Dsc2 localize to different vesicle populations. While microtubules are essential for the transport of both of these cadherins, Dsg relies on kinesin-1 while Dsc relies on kinesin-2, further demonstrating different transport mechanisms (320). Plakoglobin associates with desmosomal cadherins early on in the biosynthetic pathway and traffics as a complex to the PM. As mentioned above, desmosomes switch from a calcium dependent to a calcium independent state when cultured for several days, thus while desmosomes form within three hours of a low to high calcium switch, it is apparent that they continue to mature.

Several studies have implicated the formation of adherens junctions as an obligate precursor to the formation of desmosomes in epithelial cells. Function blocking antibodies to the external domain the adherens junction protein E-cadherin prevent the formation of desmosomes (321) and epidermal cells lacking E-cadherin demonstrate a failure to form desmosomes (322). Recently, in collaboration with the Sivasankar lab, we demonstrated

that E-cadherin interacts *in trans* with desmosomal cadherins and is located within nascent desmosomes and excluded as desmosomes mature (323). Thus, it seems that classical cadherins are required to initiate or nucleate desmosome formation, but are excluded from mature desmosomes. One hypothesis derived from work in this dissertation for the mechanism driving the exclusion of E-cadherin from mature desmosome is that desmosomal components associate with lipid rafts while E-cadherin does not, thus E-cadherin cannot associate with mature desmosomes that associate with lipid rafts. In fact, lipid rafts are critical for desmosome assembly (324). In section 4.4, lipid rafts and their role in desmosome assembly and disassembly are defined.

4.4 Desmosome regulation: Lipid rafts

4.4.1 Lipid rafts

The plasma membrane is a biomembrane that consists of phospholipids, proteins, and sterols. As early as the 1970s, the lipid bilayer has been recognized as a dynamic structure and the *fluid mosaic model* of biomembranes was introduced (325). The phospholipids that make up the biomembrane are amphipathic and have a hydrophilic, polar head group as well as a hydrophobic region typically consisting of two acyl chains. Not all of the phospholipids within the plasma membrane are the same and can be separated into two classes, phosphoglycerides, also known as glycolipids, and sphingolipids (326). Sterols, such as cholesterol, are the third type of lipid found in the plasma membrane. The

phospholipids, proteins, and sterols of the plasma membrane are not found uniformly throughout the bilayer, rather there is heterogeneity in the membrane.

4.4.1.1 Structure of Lipid rafts

The first insights to membrane heterogeneity were born from biochemical studies in which it was realized that detergents did not result in complete solubilization of the plasma membrane and that the remnants left behind were enriched in cholesterol and sphingolipids (327-329). These observations led to the hypothesis that microdomains enriched in these two components exist on the plasma membrane. Additionally, a spin label study of enzyme dynamics within the membrane indicated a mosaic-like structure of the membrane rather than an equal distribution of membrane lipids and proteins (330). Together these studies led to the first formal hypothesis that the plasma membrane consists of separate domains in 1982 by Klausner & Karnovsky (331). Kai Simons was the first to term sphingolipid and cholesterol rich microdomains as lipid rafts, and they were originally thought to mainly contribute to protein trafficking, with a particular focus on trafficking from the Golgi (332). In 2006 a keystone symposium defined lipid rafts as a small (10-200nm), heterogeneous, highly dynamic, sterol- and sphingolipid-enriched domains that compartmentalize cellular processes (333). Furthermore, the phospholipid composition of plasma membranes, as well as the protein and sterol content, varies between cell types implicating that plasma membrane composition has a larger role in cell and even tissue function (334).

The structure of the phospholipids in a given area of the membrane as well as the relative phospholipid, protein, and sterol composition impacts the properties of the membrane (335). For example, sphingolipids with saturated acyl chains have less surface area and thus can pack more tightly to form a dense, gel-like area of the membrane. Cholesterol promotes ordered packing of phospholipids by interacting with the hydrophobic tails of phospholipids, promoting a more ordered arrangement of the hydrophobic acyl chains, and can disrupt the fluidity of the membrane thereby restricting the lateral mobility of lipids and proteins in the membrane (336-338). Because of the high density and order of proteins and lipids in rafts, they are resistant to solubilization using detergents such as Triton X-100. When cells are lysed in the presence of Triton X-100 followed by a sucrose gradient fractionation, lipid raft fractions can be identified in a western blot by probing for known resident proteins such as flotillins and proteins known to be excluded from rafts such as calnexin (339). Thus, sucrose gradient fractionations have become a powerful technique in identifying proteins that associate with lipid rafts. In model membranes, sphingolipids spontaneously coalesce to form rafts and promote membrane heterogeneity (340). However, the addition of physiological levels of cholesterol to model membranes containing a mixture of lipids greatly promoted phase separation, indicating a clear role for cholesterol in promoting membrane heterogeneity (340). Studies in model membranes have concluded that lipid rafts are thicker than other areas of the plasma membrane, however this has yet to be confirmed in living cells (341-343) (Figure 4.1). In fact, several studies have concluded that the addition of cholesterol to membranes increases the thickness of the membrane and that this thickness is related to the relative order of the

membrane (344-347). Understanding the properties and compartmentalization of the plasma membrane is fundamental to our understanding of integral membrane proteins.

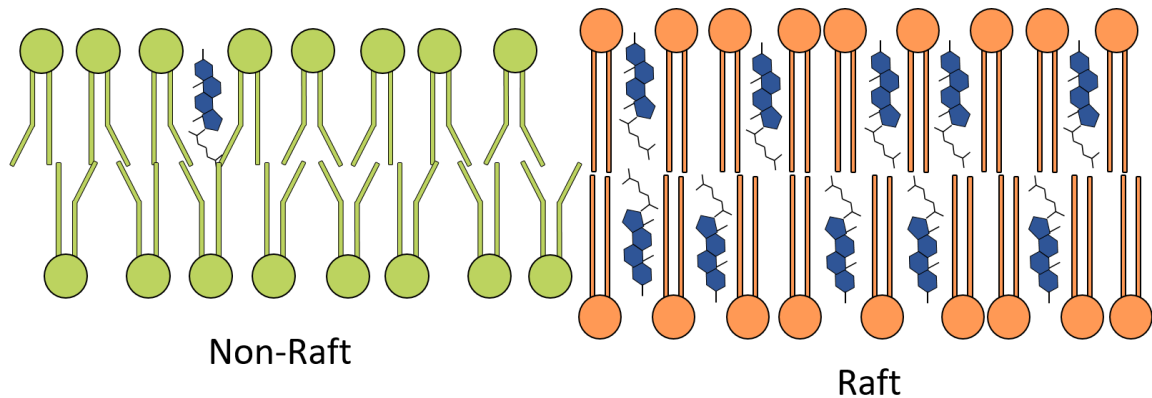


Figure 4.1 Lipid raft structure. Lipid rafts are enriched in sphingolipids and cholesterol. Both the cholesterol content and the saturated tails of the sphingolipids contribute to a thickening of the lipid raft bilayer when compared to non-raft areas of the plasma membrane. Additionally, lipid rafts are more ordered and denser than other areas of the plasma membrane.

4.4.1.2 Function of lipid rafts

Lipid rafts compartmentalize the plasma membrane and act as platforms to control the spatial and temporal association of proteins. Components of a signaling cascade must have access to one another in order to properly transduce a signal. This became apparent through studies of the immune synapse where T cell antigen receptors (TCR) were shown to cluster and colocalize with downstream signaling components, and that this clustering was necessary for effective TCR signaling (348). It is intuitive that the compartmentalization of the plasma membrane allows for the spatial regulation of proteins.

Association with lipid rafts is one way for cells to increase the probability of desirable protein interactions on the plasma membrane as only a subset of membrane proteins seem to associate with rafts. For example, the IGF-IR receptor localizes to lipid rafts and perturbation of lipid rafts prevents signaling despite no changes in the activation of the receptor itself (349, 350). Downstream effectors have also demonstrated lipid raft association (351), thus the loss of signaling after the loss of lipid raft integrity is likely due to a lack of proximity between the receptor and downstream signaling molecules. Lipid rafts have been studied in additional signaling cascades such as TCR (352-354), glial-cell-derived neurotrophic factor (355), and Ras signaling (356). Several reviews discuss the importance of lipid rafts in cellular signaling (357-360).

In addition to important functions in regulating cellular signaling at the plasma membrane, lipid rafts are found in the membranes of other organelles and cellular compartments and are critical in the biosynthetic trafficking of proteins. Cholesterol is synthesized in the endoplasmic reticulum while sphingolipid synthesis and modifications occur in the Golgi (361). Sphingolipids are found in very low concentrations in the ER, meaning that the first membrane-enriched for cholesterol-sphingolipid rich domains are found is the Golgi (361-363). Vesicles enriched for COPI have low amounts of sphingomyelin and cholesterol, supporting the notion that lipid raft components are not transferred to the ER in high quantities (364). Recent studies demonstrate that some ER resident proteins localize to lipid raft domains, suggesting that the low levels of sphingolipids and cholesterol within the ER form raft domains (365, 366). Nonetheless, forced accumulation of cholesterol in the ER inhibited protein transport and secretion,

highlighting the importance of maintaining low levels of cholesterol in the ER (367). The Golgi is responsible for sorting cargo, including proteins, into vesicles destined for cellular organelles and the plasma membrane (368). There is a cholesterol gradient in the Golgi with higher levels on the *trans* side of the Golgi, indicating that cholesterol, and thereby lipid rafts, travels outwards through the biosynthetic pathway (363, 369). Depletion of cellular cholesterol inhibits vesicle budding from the Golgi, while high cholesterol levels stimulated vesicle formation, indicating a critical role for cholesterol in trafficking from the Golgi (370). Collectively, these data support a model in which raft components, including associated proteins, traffic outward towards the plasma membrane during biosynthesis.

As previously mentioned, the incorporation of cholesterol and sphingolipids result in a thicker bilayer, thus it is intuitive that the ER with a lower concentrations of these components would retain proteins with shorter hydrophobic transmembrane segments while the plasma membrane, which should be comparatively thicker, is enriched for proteins harboring longer transmembrane domain segments. If the hydrophobic transmembrane domain is longer or shorter than the hydrophobic span of the raft membrane there is a hydrophobic mismatch between the TMD and the bilayer (371). If the mismatch is due to a slightly shorter TMD, the bilayer can deform or the TMD can be surrounded locally by favorable lipids. If the mismatch occurs as a result of a TMD that is too long, the TMD can tilt in the membrane so that it remains in a favorable environment. However, if the mismatch is too great, it becomes energetically unfavorable for the protein to associate with a lipid raft and thus will be excluded (371). This was shown experimentally

and the length of the TMD was proposed as one of potentially many mechanisms for regulating protein association with specific organelles, including retention in the Golgi apparatus (369).

In addition to facilitating trafficking to the plasma membrane, lipid rafts mediate endocytosis. Initially, endocytosis was thought to depend exclusively on clathrin, a coat protein known to facilitate PM invagination, however it is now widely accepted that several clathrin independent mechanisms for endocytosis exist. Caveolae were first identified in the 1950s via electron microscopy and are specialized lipid raft-enriched, clathrin-deficient invaginations of the plasma membrane that mediate endocytosis (372, 373). The major protein associated with caveolae is caveolin 1 (Cav1), which forms the coat of these invaginations and vesicles (374, 375). Fourteen to sixteen Cav1 molecules oligomerize to facilitate the formation of caveolin (376, 377). However, both Cav1 and cholesterol must be present to form caveolae demonstrating the importance of lipid rafts in this method of endocytosis (374). While caveolae endocytosis is the most well studied lipid raft dependent endocytosis mechanism, others do exist. For example, cholera toxin-B is internalized in a raft dependent manner independent of caveolae (378). Similarly, interleukin 2 receptors are internalized in a raft dependent, clathrin-independent, caveolin-independent mechanism (379). As these lipid raft mediated endocytic pathways are studied, new mechanisms are continuously emerging, however much work still needs to be done for us to fully understand these mechanisms.

4.4.3 Lipid rafts and desmosome function

Prior to the understanding of plasma membrane microdomains and the concept of lipid rafts emerged, there was evidence that desmosomes were enriched for cholesterol and sphingolipids. Desmosomes purified from bovine snouts were subsequently tested for lipid composition and found to have a high sphingolipid and cholesterol content (113). This was later confirmed using spectrometry and gas chromatography a few years later (380). Sucrose gradient fractionations have confirmed that most desmosomal proteins associate with lipid raft fractions of the plasma membrane (319, 324, 381-384) and Table 4.2. Additionally, perturbation of lipid rafts using cholesterol chelating agents, such as methyl- β -cyclodextrin, have demonstrated that lipid rafts are necessary for proper assembly (324, 382) and disassembly (382, 385) of desmosomes. Recent studies of Dsg2 highlight the importance of raft association in non-adhesive, signaling functions of desmogleins. Lipid rafts are necessary for Dsg2 mediated EGFR signaling and the release of extracellular vesicles in cancer cells (384, 386). Palmitoylation is one mechanism by which proteins associate with lipid rafts (387, 388). As mentioned above, several desmosomal proteins have been shown to be palmitoylated and PKP mutants that could not be palmitoylated demonstrated a reduction in lipid raft association (319). Furthermore, the expression of these PKP palmitoylation mutants in cells prevented desmosome assembly and resulted in a loss of cell-cell adhesion (319). Collectively, these studies lead to the formation of the hypothesis that the molecular components of the desmosome associate with lipid rafts and that this association is necessary for proper protein function and maintenance of the desmosome (Figure 4.2). Additional studies are necessary to fully understand the

regulation of the desmosome by lipid rafts. Chapter 5 of this dissertation focuses on understanding the mechanism by which desmogleins associate with lipid rafts and further discusses the implications this association has on desmosome biology.

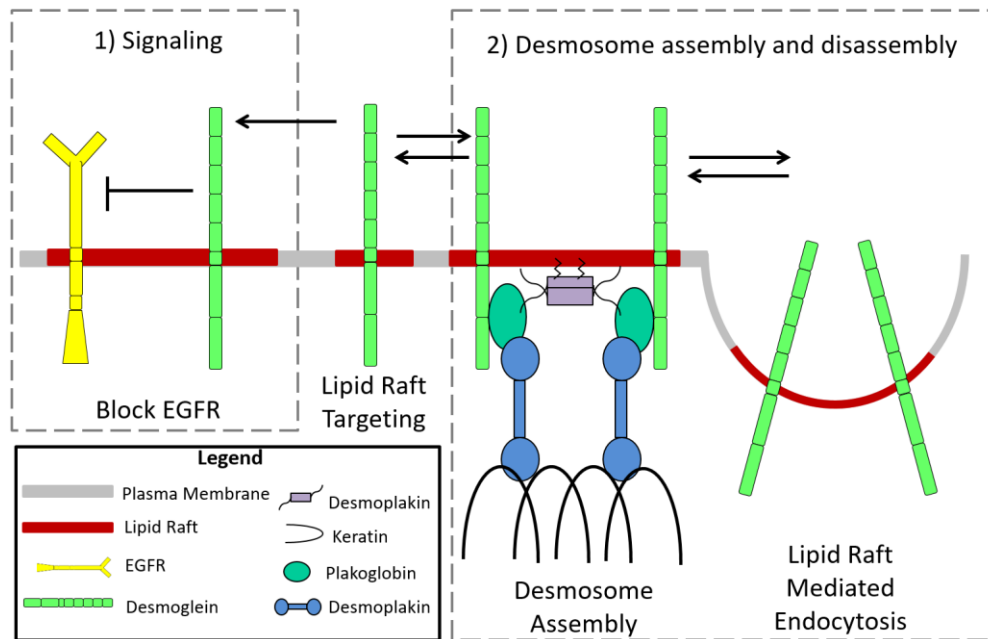


Figure 4.2 Model for the role of lipid rafts in desmosome function. 1) Molecular components of the desmosome associate with lipid rafts to mediate signaling cascades (discussed in future directions). 2) Molecular components of the desmosome associate with lipid rafts and this association is critical for proper assembly and disassembly dynamics of the desmosome.

<i>Year</i>	<i>Method</i>	<i>Observation(s)</i>	<i>Reference</i>
1974	Lipid extraction and thin layer chromatography on purified desmosomes	Desmosomes have high sphingolipid and cholesterol content	(113)
1977	Gas chromatography and spectrometry	Desmosomes have high sphingolipid and cholesterol content	(380)
2008	Sucrose gradient fractionations	PG and DP associate with lipid rafts	(381)
2008	PV IgG treatment and clathrin inhibitor	Dsg3 endocytosis is clathrin independent	(385)
	PV IgG treatment and Filipin or Nystatin	Dsg3 internalization is cholesterol dependent	
2011	Sucrose gradient fractionation Methyl- β -cyclodextrin	Dsc2 associates with lipid rafts	(324)
		Desmosome assembly is cholesterol dependent	
2012	GST pulldowns Immunofluorescence Sucrose gradient fractionation	Dsg2 associates with Caveolin 1 Dsg2 colocalizes with Caveolin 1 Dsg2 and PG associate with lipid rafts	(389)
2014	Sucrose gradient fractionation Methyl- β -cyclodextrin Immunofluorescence PV IgG treatment	Dsg3 associates with lipid rafts Desmosome assembly is cholesterol dependent Dsg3 colocalizes with raft markers Dsg3 colocalizes with raft markers in linear arrays	(382)
2014	Sucrose gradient fractionation Palmitoylation null mutation	PKP2 and Dsg2 associate with lipid rafts Palmitoylation regulates PKP association with lipid rafts	(319)
2016	Sucrose gradient fractionation Palmitoylation null mutants	Dsg2 and Dsg3 associate with lipid rafts Palmitoylation of Dsg2 and Dsg3 does not regulate raft association	(383)
2016	Sucrose gradient fractionation Methyl- β -cyclodextrin	Dsg2 associates with lipid rafts	(384)
		Dsg2 mediated EGFR signaling is cholesterol dependent	
2017	Cholera toxin B labeling and FACS	Dsg2 containing vesicles are enriched for lipid rafts	(386)

Table 4.2 Summary of lipid raft and desmosomes literature

Chapter 5

The Desmosome is a Mesoscale Lipid Raft-Like Domain

This chapter is adapted from

Joshua D Lewis^{1,2*}, **Amber L Caldara**^{1,3*}, Stephanie E Zimmer^{1,2}, Sara N Stahley^{1,2}, Anna Seybold^{4,5}, Nicole L Strong¹, Achilleas S Frangakis^{4,5}, Ilya Levental⁶, James K Wahl III⁷, Alexa L Mattheyses⁸, Takashi Sasaki⁹, Kazuhiko Nakabayashi¹⁰, Kenichiro Hata¹⁰, Yoichi Matsubara¹⁰, Akemi Ishida-Yamamoto¹¹, Masayuki Amagai¹², Akiharu Kubo¹² and Andrew P Kowalczyk^{1,2,13}

¹ Department of Cell Department of Cell Biology, Emory University School of Medicine, Atlanta, Georgia, USA ²Graduate program in Biochemistry, Cell and Developmental Biology, Emory University School of Medicine, Atlanta, Georgia, USA ³Graduate program in Cancer Biology, Emory University School of Medicine, Atlanta, Georgia, USA ⁴Buchmann Institute for Molecular Life Sciences, Goethe University Frankfurt, Frankfurt, Germany ⁵Institute for Biophysics, Goethe University Frankfurt, Frankfurt, Germany ⁶Department of Integrative Biology and Pharmacology, University of Texas Health Science Center at Houston, Houston, Texas, USA ⁷Department of Oral Biology, College of Dentistry, University of Nebraska Medical Center, Lincoln, Nebraska, USA ⁸Department of Cell, Developmental, and Integrative Biology, University of Alabama, Birmingham, Alabama, USA ⁹Center for Supercentenarian Medical Research, Keio University School of Medicine, Tokyo, Japan ¹⁰National Research Institute for Child Health and Development, Tokyo, Japan ¹¹Department of Dermatology, Asahikawa Medical University, Asahikawa, Japan ¹²Department of Dermatology, Keio University School of Medicine, Tokyo, Japan ¹³Department of Dermatology, Emory University School of Medicine, Atlanta, Georgia, USA

*** Authors contributed equally to this work**

Molecular Biology of the Cell

5.1 Abstract

Desmogleins are cadherin family adhesion molecules essential for epidermal integrity. Previous studies have shown that desmogleins associate with lipid rafts, but the significance of this association was not clear. Here, we report that the desmoglein transmembrane domain (TMD) is the primary determinant of raft association. Further, we identify a novel mutation in the DSG1 TMD (G562R) that causes severe dermatitis, multiple allergies, and metabolic wasting (SAM) syndrome. Molecular modeling predicts that this G to R mutation shortens the DSG1 TMD, and experiments directly demonstrate that this mutation compromises both lipid raft association and desmosome incorporation. Finally, cryo-electron tomography (cryo-ET) indicates that the lipid bilayer within the desmosome is ~10% thicker than adjacent regions of the plasma membrane. These findings suggest that differences in bilayer thickness influence the organization of adhesion molecules within the epithelial plasma membrane, with cadherin TMDs recruited to the desmosome via establishment of a specialized mesoscale lipid raft-like membrane domain.

5.2 Introduction

A characteristic feature of epithelial cells is the assembly of specialized plasma membrane domains that mediate cell adhesion, communication, and barrier function (28, 390). Among these structures, adherens junctions and desmosomes play overlapping but distinct roles in cell adhesion, signaling, and morphogenesis (390). Desmosomes are particularly abundant in tissues exposed to mechanical stress, including the skin and heart

(112, 391, 392). These adhesive complexes are characterized by highly organized and dense arrangements of desmosomal proteins that can be visualized by electron microscopy (142, 393, 394). Considerable progress has been made in identifying protein interactions that mediate adhesion in both adherens junctions and desmosomes, as well as the associations that anchor these adhesive structures to the cytoskeleton (395-398). However, the physical constraints imposed by the epithelial plasma membrane that contribute to the segregation of adherens junctions and desmosomal complexes into morphologically, biochemically, and functionally distinct structures are poorly understood.

The adhesive core of the desmosome is comprised of single pass transmembrane desmosomal cadherins termed desmogleins and desmocollins that mediate adhesion between adjacent cells (122, 123, 394). In humans, there are four desmoglein genes (*DSG1-4*), along with three desmocollins (*DSCI-3*) (1). The desmosomal cadherins are coupled to the intermediate filament cytoskeleton through adaptor proteins such as plakoglobin, plakophilins, and the cytolinker protein desmoplakin (142, 399, 400). These interactions form an electron dense plaque that couples the adhesive interactions of the desmosomal cadherins to the intermediate filament cytoskeleton of adjacent cells, thus conferring tissue resilience to mechanical stress (128, 392). Loss of desmosome function results in skin (156, 392) and heart (112, 401) diseases characterized by tissue fragility. In the skin, loss of desmosomal adhesion manifests clinically as epidermal blisters and erosions (156, 402), and in some disorders, aberrant thickening of the epidermis (159, 403). One example of such a disease is severe dermatitis, multiple allergies, and metabolic wasting (SAM)

syndrome (160). This disease is typically caused by null mutations in DSG1, leading to epidermal fragility and barrier defects (158, 161).

We and others have previously demonstrated that desmosomal proteins associate with lipid rafts (324, 382, 385, 389, 404). Lipid rafts are sphingolipid- and cholesterol-enriched membrane microdomains that introduce spatial heterogeneity into lipid bilayers (333, 405-407). These domains are critical for protein trafficking, membrane organization, and signaling (408-412). The sphingolipids present in rafts feature long saturated acyl chains that, along with cholesterol, contribute to the more ordered, densely packed, and thicker membrane environment characteristic of lipid rafts (335, 407, 408). Desmogleins and other desmosomal proteins have been shown to associate with lipid raft membrane domains as determined by detergent resistance and buoyancy on sucrose gradients (324, 382, 389, 404). In addition, disruption of lipid rafts by removal of cholesterol from cellular membranes results in weakened desmosomal adhesion, suggesting that lipid rafts play a role in desmosome homeostasis (324, 382). However, we do not know how desmosomal cadherins target to raft domains or how incorporation into raft domains impacts desmosomal cadherin function.

In the present study, we sought to determine the mechanisms by which raft association governs desmosome assembly, and to identify the determinants of desmoglein partitioning to rafts. Our results indicate that the transmembrane domain (TMD) of the desmogleins is critical for raft association, and that the E-cadherin TMD does not support raft targeting. Raft association appears to be essential for desmoglein function, as a novel mutation that shortens the TMD of human DSG1 abrogates lipid raft targeting, impairs

desmosome association, and causes the human skin disease SAM syndrome. Cryo-electron tomography and sub-tomogram averaging demonstrates that the lipid bilayer within the desmosome is thicker than the adjacent plasma membrane, consistent with predictions that the lipid bilayer is thicker at raft domains compared to non-raft membranes. Thus, our results support a model in which the desmosome is a specialized type of lipid raft membrane microdomain, and the lengthy desmoglein TMD enables efficient desmosome incorporation by facilitating desmoglein partitioning into the thicker desmosomal lipid bilayer. These findings suggest that epithelial junctional complexes achieve plasma membrane domain specification not only through selective protein interactions, but also through constraints imposed by the biophysical characteristics of the plasma membrane.

5.3 Results

5.3.1 Palmitoylation of Dsg3 is not required for lipid raft association

Desmogleins and other desmosomal components associate with lipid raft membrane microdomains (324, 382, 385, 404). A number of raft associating proteins, including plakophilins, utilize palmitoylation as a membrane raft targeting mechanism (319, 387, 388). Palmitoylation is a reversible post-translational modification that occurs when palmitoyltransferases add a 16-carbon fatty acid (palmitate) to cysteine residues (413, 414). Sequence alignments (Figure 5.1A) reveal that desmosomal cadherins contain conserved cysteine residues at the cytoplasmic face of the transmembrane domain, and our previous studies have shown that these residues are critical for desmoglein palmitoylation

(383). We hypothesized that palmitoylation of desmogleins would mediate lipid raft association. Therefore, we mutated cysteines 640 and 642 to alanine residues in murine DSG3 and used a lentiviral expression system to generate stable A431 cell lines expressing FLAG tagged wild type or mutant Dsg3(CC). A431 cells are an epidermal carcinoma cell line that has been used extensively for desmosome studies due to their human origin, relatively flat morphology and assembly of robust desmosomes (125, 383, 415-418). Mass tag labeling confirmed that the mutation of these conserved membrane proximal cysteines eliminated Dsg3 palmitoylation (Figure 5.1B). Interestingly, the loss of Dsg3 palmitoylation had no discernable effect on lipid raft association as determined by Dsg3 incorporation into buoyant and detergent resistant membranes (DRM) (339) (Figure 5.1C). In addition, both WT Dsg3 and Dsg3(CC) localized to cell-cell borders as assessed by widefield immunofluorescence (Figure 5.1D). Furthermore, Dsg3 and Dsg3(CC) exhibited similar Triton-X 100 solubility, suggesting no defect in the desmosome or cytoskeletal association of Dsg3(CC) (Figure 5.1, E-G). Collectively, these results indicate that palmitoylation is not required for lipid raft association of desmogleins or for normal Dsg3 subcellular distribution in quiescent A431 monolayers.

5.3.2 The transmembrane domain of desmogleins mediates lipid raft association

In addition to palmitoylation, emerging evidence indicates that lipid raft association of membrane spanning proteins is also regulated by the physiochemical properties of the transmembrane domain (TMD) (419). In particular, TMD length is a critical determinant for targeting to lipid rafts (419-422). Sequence alignments (Figure 5.1A) indicate that the

TMDs of the desmogleins, which associate with rafts, are considerably longer (24 amino acids) than the corresponding TMDs of classical cadherins, such as E-cadherin (21 amino acids) and VE-cadherin (20 amino acids), which exhibit minimal raft association (382). Recent studies indicate that the free energy of raft association can be calculated based on TMD length, surface area, and palmitoylation (419). These parameters predict efficient WT Dsg1 raft partitioning ($\Delta G_{\text{raft}}=0.17$), with markedly lower raft affinity for the TMD of E-cadherin ($\Delta G_{\text{raft}}=0.30$) (Table I). To directly test if the TMD is the principal motif conferring lipid raft association on the desmoglein family of proteins, we generated a chimeric cadherin in which the Dsg3 TMD was replaced with the E-cadherin TMD (Dsg3(EcadTMD)). Lentiviral transduction was used to generate stable A431 cell lines expressing either wild type Dsg3-FLAG or Dsg3(EcadTMD)-FLAG. Sucrose gradient fractionations demonstrated that the Dsg3(EcadTMD) chimera was virtually excluded from DRM fractions when compared to wild type Dsg3 (Figure 5.2A and B). Immunofluorescence localization indicated that Dsg3(EcadTMD) localized to cell-cell contact sites. However, Triton X-100 extraction showed decreased insoluble pool partitioning as assessed by both immunofluorescence (Figure 5.2C) and western blot analysis (Figure 5.2, D-F), suggesting decreased Dsg3(EcadTMD) association with cytoskeletal elements relative to wild type Dsg3. Expression of the Dsg3(EcadTMD) mutant caused no apparent changes in endogenous E-cadherin distribution (Figure 5.2, A and D-F). To determine if the Dsg3 TMD is sufficient to confer lipid raft targeting, we constructed interleukin 2 receptor (IL2R) α chain-Dsg3 chimeric proteins comprising the IL2R extracellular domain coupled to the Dsg3 cytoplasmic tail with either the IL2R TMD or the Dsg3 TMD (Figure 5.2G and reference (423)). The IL2R-Dsg3 chimera harboring

the Dsg3 TMD partitioned to DRM fractions, whereas the chimera containing the IL2R TMD did not partition with DRM fractions. Collectively, these studies indicate that the Dsg3 TMD is the primary determinant of Dsg3 raft association.

To test if the TMD of other desmoglein family members also functions in raft association, similar experiments were conducted in the context of Dsg1. Dsg1 WT and a Dsg1(EcadTMD) chimera were generated. Both proteins were tagged with a carboxyl terminal green fluorescent protein (GFP) and stably expressed in A431 cell lines as described above. Similar to the Dsg3(EcadTMD) chimera, the Dsg1(EcadTMD) chimera showed a marked decrease in association with DRM fractions as determined by sucrose gradient fractionation (Figure 5, A and B). Additionally, Dsg1(EcadTMD) was partially excluded from Triton insoluble fractions of cell lysates (Figure 5, C-E), similar to the results seen with Dsg3(EcadTMD) (Figure 5.2, D-F). Lastly, both the WT Dsg1 and Dsg1(EcadTMD) demonstrated border staining characteristic of desmogleins (Figure 5.3F). Together, these results demonstrate a central role for the TMDs of the desmoglein family in lipid raft association.

5.3.3 A mutation in the transmembrane domain of DSG1 causes severe dermatitis, multiple allergies, and metabolic wasting syndrome

Loss of DSG1 function is associated with a number of autoimmune, infectious, and genetic diseases (156, 401, 403). One recently discovered desmosome-associated disease is severe dermatitis, multiple allergies, and metabolic wasting (SAM) syndrome (160).

Most instances of SAM syndrome are caused by homozygous functional null mutations in the desmosomal cadherin desmoglein 1 (*DSG1*) (158, 161). Here, we report a novel and dominantly inherited heterozygous *DSG1* missense mutation within the *DSG1* TMD (Figure 5.4). The probands presented with ichthyosiform erythrokeratoderma, diffuse palmoplantar keratosis and multiple allergies (Figure 5.4A). Proband III-2 suffered metabolic wasting and died of status asthmaticus and recurrent infections. Hemotoxylin and eosin staining of skin biopsied from the proband revealed compact hyperkeratosis with parakeratosis, frequent detachment of the entire stratum corneum, and dissociation of individual corneocytes (Figure 5.4B). Although these findings indicate an adhesion defect, we observed minimal alterations in desmosome ultrastructure when patient epidermis was examined by electron microscopy (Figure 5.4C). These clinical and genetic observations led us to diagnose the patient with SAM syndrome. Unlike previously reported instances of *DSG1* mutations in SAM syndrome (158, 160, 161, 424), this patient harbored a novel missense mutation in *DSG1* which introduces a hydrophilic arginine residue (p.G562R) into the otherwise hydrophobic transmembrane domain of *DSG1* (Figure 5.4, D-F). Subsequent to our characterization of this initial family, a second unrelated individual was identified with a G562R heterozygous mutation previously reported as a case of erythrokeratoderma variabilis (425). The parents of this patient lacked this mutation and were disease free. Together, these observations demonstrate that a heterozygous G562R mutation in the *DSG1* TMD causes a human skin disease best characterized clinically as SAM syndrome.

To determine how the G562R mutation impacted DSG1 organization in patient skin, biopsies from the proband were processed for immunofluorescence microscopy. DSG1 levels were markedly reduced (~40%) in the spinous and granular layers of patient epidermis (Figure 5.4, G and H), and DSG1 localized in cytoplasmic puncta and aberrant clusters at cell-cell borders. Interestingly, DSG1 staining in patient stratum corneum was markedly increased, perhaps reflecting increased antibody penetration. Desmoplakin levels were slightly reduced in patient epidermis, whereas DSG3 levels were markedly increased (Figure 5.4 I-K). To further investigate alterations in DSG1 distribution, we performed structured illumination microscopy (SIM) on patient and control epidermis. DSG1 fluorescence intensity within patient and control desmosomes was comparable in basal keratinocytes, where DSG1 expression is low and other DSG isoforms (DSG2, DSG3) are expressed. However, DSG1 fluorescence intensity in patient desmosomes was significantly reduced (Figure 5.4, L and M) in the spinous and granular layers where DSG1 is prominently expressed. Thus, although morphologically normal desmosomes could be observed by electron microscopy (Figure 5.4C), these desmosomes apparently lack sufficient DSG1 levels to support normal epidermal cohesion.

To investigate the mechanism by which the DSG1(G562R) mutation causes SAM syndrome, GFP-tagged murine wild type Dsg1 α and a mutant harboring the equivalent G-to-R substitution, Dsg1(G578R), were expressed in A431 epithelial cells. Widefield fluorescence imaging revealed that both WT Dsg1 and Dsg1(G578R) were present at cell-to-cell borders (Fig 5.5A). Interestingly, the Dsg1(G578R) mutant also exhibited a prominent perinuclear staining pattern. There were no obvious differences in desmoplakin

localization in the two cell lines (Figure 5.5A), and plakoglobin generally co-localized with both cell-cell border and perinuclear pools of WT Dsg1 and Dsg1(G578R) (Figure 5.5B). To determine if the Dsg1(G578R) mutant was defective in desmosome targeting, SIM was performed and Dsg1 fluorescence intensity was measured at cell borders both within and outside of individual desmosomes to control for possible variations in Dsg1 levels at different cell-cell contact sites. We observed that Dsg1(G578R) displayed a decreased association with desmosomes when compared to WT Dsg1 (Figure 5.5, C and D). Furthermore, parallel bands of GFP fluorescence signal overlapping with DP were routinely observed for WT Dsg1-GFP but not for Dsg1(G578R)-GFP (Figure 5.5, C and E). Lastly, WT Dsg1 efficiently entered a detergent-resistant pool, consistent with incorporation into insoluble desmosome and cytoskeletal-associated complexes, whereas mutated Dsg1(G578R) remained predominantly soluble (Figure 5.5, F-H). Together, these findings indicate that the G-to-R TMD mutation reduces DSG1 incorporation into desmosomes in both cultured cells and in patient epidermis.

In addition to being deficient in desmosome targeting, we also observed that DSG1 was present in cytoplasmic puncta in SAM patient epidermis (Figure 5.4G) and that Dsg1(G578R) was concentrated in perinuclear compartments in A431 cell lines (Figure 5.5, A and B). To determine if the Dsg1(G578R) mutant exhibited membrane trafficking defects, cell surface proteins were biotinylated and pulse chase experiments conducted to measure Dsg1 turnover rates. These experiments revealed no difference in the rate of Dsg1(G578R) turnover from the plasma membrane compared to WT Dsg1 (Figure 5.6, A and B). We also confirmed that Dsg1(G578R) is inserted into the plasma membrane in the

correct orientation by demonstrating that the c-terminal GFP tag is accessible to antibody detection only after cells have been permeabilized with Triton X-100 (Figure 5.7A). Furthermore, biotinylation experiments detected no significant difference in the ratio of surface to total Dsg for WT Dsg1 or Dsg1(G578R) at steady state (Figure 5.7, B and C).

To measure rates of delivery to the plasma membrane, cell surface proteins were cleaved using trypsin and the rate of Dsg1 recovery at the cell surface was monitored by biotinylation (Figure 5.6, C and D). Prior to trypsinization, Dsg1(G578R) cell surface levels were similar to WT Dsg1 (Figure 5.6E), again indicating that steady state cell surface levels of the mutant were comparable to WT Dsg1. However, while the surface pool of WT Dsg1 recovered within 3-6 hours after trypsinization, Dsg1(G578R) exhibited delayed plasma membrane recovery (Figure 5.6D). To determine if Dsg1(G578R) was being retained in secretory compartments, A431 cell lines were grown in low calcium medium overnight to internalize all cadherins, and subsequently switched to high calcium medium to allow Dsg1 to traffic out to cell-cell borders. These experiments revealed that Dsg1(G578R) was retained in GM130-labeled compartments (Figure 5.6, F and G), indicating that the G-to-R mutation causes retention of Dsg1 in the Golgi apparatus, delaying its trafficking through the secretory pathway.

5.3.4 Disease causing mutation abrogates lipid raft association of Dsg1

Based on our findings that the TMD of the desmogleins is critical for lipid raft association, we hypothesized that the G-to-R mutation observed in SAM patients would

prevent Dsg1 from partitioning to lipid rafts. Calculations based on parameters which predict free energy of raft association from TMD sequences (419) revealed that introduction of the SAM-causing G-to-R mutation into the DSG1 TMD dramatically alters the energetics of raft association (Table I). Consistent with these calculations, sucrose gradient fractionations revealed that Dsg1(G578R) was virtually absent from lipid raft (DRM) fractions (Figure 5.8, A and B). Interestingly, we observed a notable reduction in plakoglobin association with DRM in cell lines expressing Dsg1(G578R), suggesting that the DSG1 mutant also recruited plakoglobin out of raft domains. To further test the ability of WT Dsg1 and Dsg1(G578R) to associate with lipid rafts, these proteins were transiently expressed in rat basophilic leukemia cells and giant plasma membrane vesicles (GPMV) were chemically isolated (426, 427). Non-raft plasma membrane domains were labelled with F-DiO, a dialkylcarbocyanine dye. WT Dsg1 efficiently partitioned into areas of plasma membrane vesicles lacking F-DiO, indicating partitioning to the liquid-ordered raft domain (Figure 5.8, C and D). In contrast, Dsg1(G578R) was almost entirely co-segregated with F-DiO and excluded from the liquid ordered plasma membrane domain, indicating minimal raft affinity. Together, these findings reveal that the G-to-R TMD mutation reduces cell surface DSG1 association with lipid rafts.

5.3.5 The lipid bilayer within desmosomes is thicker than non-desmosomal membranes

The results above illustrate a critical role for the desmoglein TMD in the association of this family of cadherins with lipid raft membrane microdomains and for its crucial role in epidermal homeostasis. To understand how the physiochemical properties of the

desmoglein TMD confer raft and desmosome targeting, structural models of the TMDs of wild type Dsg1, the Dsg1(G578R) SAM mutant, and E-cadherin were generated by the Robetta structure prediction server (428). The modeling predicts that the SAM-causing G-to-R mutation interrupts the Dsg1 TMD helix and significantly shortens the run of helical hydrophobic residues (Table I and Figure 5.9A), potentially deforming the lipid bilayer as phospholipids position to maintain energetically favorable interactions between hydrophilic and hydrophobic amino acid residues (341, 371). These findings are consistent with the notion that the SAM-causing mutant disrupts lipid raft association by shortening the DSG1 TMD, thereby increasing the energy cost of entering the thicker lipid bilayer characteristic of lipid raft domains (419).

Experiments in model membranes suggest that the high cholesterol content (341, 344) and long, saturated acyl chains (429, 430) present in lipid raft domains contribute to significant thickening of raft phospholipid bilayers relative to non-raft regions of the membrane. A prediction derived from such observations, and from the experimentally demonstrated presence of desmosomal proteins in rafts, is that the lipid bilayer within desmosomes in cells or tissues would be thicker than non-desmosomal regions of the plasma membrane, thereby accommodating the lengthy desmoglein TMD. To test this possibility, cryo-electron tomography and sub-tomogram averaging were performed on mouse liver samples enriched in the plasma membrane fraction (Figure 5.9B). The thickness of lipid bilayers measured in the sub-tomogram averages within desmosomal and non-desmosomal regions of the plasma membrane was then determined. This analysis revealed that desmosomal bilayers were 10% thicker (4.5 ± 0.4 nm) than regions

immediately adjacent to the desmosome (4.0 ± 0.3 nm, $p = 2.2E-122$) or at arbitrary regions of membrane visible within the tomograms (4.0 ± 0.3 nm, $p = 6.4E-104$) (Figure 3.9C). Together, these findings suggest that desmosomes represent a highly specialized plasma membrane domain that is characterized by lipid raft associated proteins and a thickened phospholipid bilayer characteristic of lipid raft-like model membranes.

5.4 Discussion

Lipid rafts have emerged as important membrane microdomains that regulate membrane organization, endocytosis, and signaling (333, 407-410). Desmosomal proteins have been shown to associate with lipid rafts in a variety of epithelial cell types (324, 382, 385, 389, 404), but the mechanisms and physiological relevance of this association are poorly understood. Here, we report that the transmembrane domains of the desmogleins are the key determinants for targeting these cadherins to lipid rafts. A mutation within the DSG1 TMD that shortens this domain abrogates both lipid raft partitioning and desmosome association, and leads to the human skin disease SAM syndrome. Cryo-electron tomography reveals that the lipid bilayer within the desmosome is markedly thicker than the adjacent lipid bilayer, thereby favoring incorporation of the longer desmoglein TMDs into this plasma membrane domain. Collectively, our results suggest that desmosomes are a specialized mesoscale lipid raft-like membrane domain.

Essential functions for desmogleins have been exposed by human diseases in which desmogleins are targeted by autoantibodies, infectious agents, or genetic mutation (391,

403). DSG1 is the primary desmoglein expressed in the outermost layers of the epidermis, and DSG1 loss of function mutations lead to at least two different types of epidermal disorders. Haploinsufficiency of DSG1 causes palmoplantar keratoderma (431), whereas complete loss of DSG1 leads to SAM syndrome (158, 160, 161). Most individuals afflicted with SAM syndrome succumb to chronic infection in early childhood (160). Here, we report two separate instances of SAM syndrome, one inherited and one sporadic, caused by a glycine to arginine substitution (G562) within the hydrophobic transmembrane domain (Figure 3.4). Arginine residues play an important role in terminating TMDs and establishing TMD orientation within the lipid bilayer (432, 433), consistent with molecular modeling indicating that the disease-causing glycine to arginine substitution shortens the DSG1 TMD (Figure 3.9).

Our data indicate that shortening of the DSG1 TMD by insertion of an arginine residue disrupts DSG1 function in SAM syndrome patients by preventing lipid raft association. TMD length correlates positively with raft association (419), and our structural predictions and molecular modeling predict that desmoglein TMDs confer raft association (Table I and Figure 5.9A). This notion is consistent with our findings using both classical DRM fractionation experiments (Figures 5.3 and 5.4) and direct observations of partitioning of cell surface Dsg1 into liquid ordered plasma membrane domains (Figure 5.8). In addition to shortening the Dsg1 TMD, insertion of an arginine residue into the TMD could also impact local protein and lipid packing within the desmosomal membrane domain. This could occur as polar residues, such as arginine, are thought to “snorkel” out of the hydrophobic bilayer to interact with the hydrophilic, aqueous environment, while

hydrophobic TMD residues retain contact with the acyl chains of the lipids (434). Such an arrangement within the bilayer could increase the effective surface area of the TMD and decrease packing of lipids and proteins, thereby altering Dsg1 association with lipid raft and desmosomal components.

Interestingly, we observed defects in the rate of mutant Dsg1 delivery to the plasma membrane after trypsinization (Figure 5.6). In addition, plakoglobin co-localized with DSG1(G578R) pools that were retained in the Golgi apparatus (Figure 5.5B), and we observed a reduction in plakoglobin association with DRM fractions in cells expressing the DSG1(G578R) mutant (Figure 5.8). Nonetheless, Dsg1(G578R) is inserted into membranes in the correct orientation and steady state plasma membrane levels of the mutant are similar to WT Dsg1 (Figure 5.7). Surprisingly, palmitoylation does not appear to be required for desmoglein raft association (Figure 3.1 and reference (383), although it does impact desmoglein dynamics at the plasma membrane (383). Recently, the desmosomal component plakophilin also was shown to be palmitoylated (319), further demonstrating an important role for this reversible post-translational modification in regulating desmosome assembly dynamics. Further studies will be needed to assess how palmitoylation is utilized in combination with other physiochemical properties of the desmoglein TMD to modulate the trafficking and adhesive properties of these unique cadherins.

A prediction based on our finding that the desmoglein TMD is responsible for partitioning to lipid rafts is that the lipid bilayer within desmosomes should be thicker than surrounding non-desmosomal membrane. Indeed, cryo-electron tomography revealed that

the lipid bilayer within the desmosome is substantially thicker than non-desmosomal regions of the plasma membrane (Figure 5.9, B-D). These observations indicate that it would be energetically costly for the DSG1 G-to-R SAM mutant to enter the thicker bilayer present in desmosomes due to hydrophobic mismatch between phospholipids and Dsg1 TMD amino-acid residues (371, 435). Therefore, it is likely that shortening of the TMD in the SAM mutant and failure to enter the thicker lipid bilayer domain of the desmosome represents a central pathophysiological mechanism of this disease-causing mutation. Indeed, we observed that the DSG1 G-to-R mutant is deficient in entering desmosomes both in patient epidermis (Figure 5.4) and when expressed in cultured epithelial cell lines (Figure 5.5). We also find that Dsg3 and Dsg1 polypeptides harboring the shorter E-cad TMD are unable to associate with lipid rafts and behave similarly to full length E-cadherin (Figures 5.2 and 5.3). The predicted E-cadherin TMD is 21 amino acids, compared to the 24 amino acid TMD of desmogleins (Table I). Although these chimeras do not effectively enter lipid rafts as assessed by DRM fractionation assays, we do find that these Dsg(EcadTMD) chimeras can associate with desmosomes as assessed by SIM (not shown). It is likely that for these chimeras, protein-protein interactions mediated by the desmoglein cytoplasmic and extracellular domains can partially overcome the energy cost of incorporating into the thicker bilayers present in the desmosome. In addition, mismatch of TMD length and hydrophobic thickness of the bilayer can be accommodated by changes in TMD tilt within the membrane and by local bilayer deformation (341, 371). In contrast, the predicted 16 amino acid TMD of the Dsg1(G578R) mutant is significantly shorter than the TMD of both desmogleins and E-cadherin, and therefore its entry into desmosomal membranes is apparently energetically prohibitive.

Together, our observations support a model in which adherens junctions and desmosomes assemble into distinct plasma membrane microdomains based not only on protein interactions, but also due to the biophysical nature of the epithelial plasma membrane and the TMD characteristics of different cadherin subfamilies (Figure 5.10, A and B). Interestingly, early studies of desmosomal composition found that these junctions are enriched in sphingolipids and cholesterol, key components of what are now referred to as lipid rafts (113, 380). In addition, most of the major desmosomal proteins are palmitoylated, including the desmosomal cadherins and plakophilins, whereas adherens junction components lack this modification (319, 383). Given the key role for palmitoylation in lipid raft association, these findings further suggest that affinities for different lipid domains of the plasma membrane are central features that distinguish adherens junction and desmosomal proteins. Further studies will be needed to determine the precise structural and functional characteristics of different cadherin TMDs and how they selectively dictate lipid raft association. In addition, it will be important to discern how TMD characteristics are used in conjunction with lipid modifications such as palmitoylation to sort desmosome and adherens junction components into distinct plasma membrane domains with unique morphologies and functions. These features appear to be of fundamental importance for skin physiology, as our findings reveal that a mutation altering the structure of the desmoglein transmembrane domain is a novel pathomechanism of a desmosomal disease. This work also raises the possibility that other human disorders may result from alterations in lipid raft association or raft homeostasis. Indeed, loss of lipid raft targeting may be an under-appreciated pathomechanism in human diseases which were previously conceived as generalized protein trafficking defects.

5.5 Materials and methods

Subjects. All affected and healthy family members or their legal guardians provided written and informed consent in accordance with the guidelines of the Institutional Review Board of Keio University and Emory University School of Medicine in adherence to the Helsinki guidelines. The investigators were not blinded to the allocation during experiments and outcome assessment.

Mutation analysis. Whole-exome sequencing was performed using genomic DNA isolated from the probands (II-2 and III-2) and their parents (I-1, I-2 and II-1). Whole exome sequencing libraries were constructed using SureSelect Human All Exon V5 (Agilent) and sequenced by HiSeq2500 (Illumina). Sequencing reads were mapped to a human reference genome sequence (hs37d5) by BWA software (0.7.12-r1039). The mapped reads were realigned and variation sites were detected by GATK-3.30 software. The detected variation sites were annotated by SnpEff/SnpSift 4.1d software. Since the phenotype appeared in the proband II-2 (delivered from healthy parents) and transmitted to the proband III-2 (Figure 5.4D), we searched for genetic variations that de novo mutated in the proband II-2 and transmitted to the proband III-2. Only one variation was identified to fulfill the criteria, which was c.1684G>A (p.G562R) of *DSG1*, coding for the desmosomal cadherin desmoglein 1. Sanger sequencing confirmed the mutation was identified in the probands but not from other healthy family members (Figure 5.4, D and E). The mutation had not been identified in cohort studies (436-439). The whole exome

sequencing of the probands II-2 and III-2 revealed no other variations in the exons and exon-intron boundaries of *DSG1*.

Immunohistochemistry and electron microscopy of patient samples. Biopsies were embedded in optimum cutting temperature (OCT) solution and stored at -80°C. Prior to immunostaining, 5 µm cryosections were prepared on glass microscope slides. Primary and secondary antibodies are described below. Sections were sealed using mounting medium (ProLong Gold by ThermoFisher Scientific) and a coverslip. For electron microscopic studies, the biopsied sample was fixed in an ice-cold 2% glutaraldehyde/60 mM Hepes (pH 7.4) buffer followed by fixation with 1% osmium tetroxide, staining with 1% uranyl acetate, and embedding in Epon812. Ultrathin sections were stained with 1.5% uranyl acetate and Reynolds lead citrate and examined with an electron microscope (JEM-1010, JEOL) at the accelerating voltage of 80 kV.

Construction of mutants. Constructs were cloned using PCR and mutagenesis by the Cloning Division within Emory Integrated Genomics Core or purchased through Cyagen vectorbuilder services.

Structural Predictions. Sequences for transmembrane domains were analyzed using the Robetta structure prediction server (428)

Cell line generation, culture, and reagents. A431 cells were cultured in DMEM (Corning 10-013-CV) with 10% fetal bovine serum (Hyclone SH30071.03) and 1% penicillin/streptomycin (Corning 30-004-CI). Cells were stably infected with lentiviruses expressing the various murine desmoglein constructs. 5 μ g/mL blasticidin was used to select for infected cells. No clonal isolation was performed. Cell lines expressing wild type and mutant DSG1-GFP were subjected to fluorescence activated cell sorting in order to obtain populations with roughly equal DSG1-GFP expression levels. For experiments utilizing a calcium switch, low calcium medium was prepared as described previously (440): no calcium DMEM (Gibco/Molecular Probes 21068028), 10% fetal bovine serum, calcium chelating BT Chelex 100 resin (Biorad 143-2832), and 1% penicillin/streptomycin.

Immunofluorescence. A431 cells were cultured to ~70% confluence on glass coverslips. In experiments in which pre-extraction is explicitly used, cells were treated with PBS+ containing 0.2% Triton X-100 and 300 mM sucrose on ice for 1 min prior to fixation. Cells were fixed in 3.7% paraformaldehyde in PBS+ on ice for 10 min. Cells were permeabilized in PBS+ containing 0.1% Triton X-100 and 3% bovine serum albumin for 10 min. Non-specific antibody binding was prevented with a blocking step in PBS+ containing 3% bovine serum albumin and 0.05% Triton X-100. Primary and secondary antibodies (listed below) were diluted into blocking solution. For rinse buffer, we used PBS+ containing 0.2% bovine serum albumin and 0.05% Triton X-100. Cells were mounted to glass microscope slides using prolong gold mounting medium (described above).

Antibodies. Mouse anti-DSG3 AK15 was described previously (441). Rabbit anti-calnexin (Enzo Life Sciences ADI-SPA-860). Mouse anti-desmoplakin1/2 (Fitzgerald 10R-D108AX). Rabbit anti-desmoplakin NW6 was a kind gift from Dr. Kathleen Green (Northwestern University). Mouse anti-Dsg1-P124 (Progen 651111). Mouse anti-plakoglobin (gamma catenin) (BD TransLabs 610253). Mouse anti-E-cadherin (BD Biosciences 610252). Mouse anti-flotillin 1 (BD 610820). Mouse anti-flotillin 2 (BD 610383). Rabbit anti-Green Fluorescent Protein Life A11122). Rabbit anti-FLAG (Bethyl A190-102A). Secondary antibodies conjugated to Alexa Fluors were purchased from Invitrogen. Horseradish peroxidase-conjugated secondary antibodies were purchased from Biorad.

Image acquisition and processing. Widefield fluorescence microscopy was performed using a DMRXA2 microscope (Leica, Wetzlar, Germany) equipped with a 100X/1.40 NA oil immersion objective and narrow band pass filters. Images were acquired with an ORCA digital camera (Hamamatsu Photonics, Bridgewater, NJ) and processed using Fiji ImageJ. Super-resolution microscopy was performed using a Nikon N-SIM system on an Eclipse Ti-E microscope system equipped with a 100X/1.49 NA oil immersion objective, 488- and 561-nm solid-state lasers in 3D structured illumination microscopy mode. Images were captured using an EM charge-coupled device camera (DU-897, Andor Technology) and reconstructed using NIS-Elements software with the N-SIM module (version 3.22, Nikon). All microscopy was performed at room temperature. Widefield microscopy results are

representative of 2 independent replicates with at least 10 cells each while SIM results are representative of at least 50 desmosomes per condition.

Desmosome targeting analysis using SIM. To quantify desmosome targeting in cultured cells, Dsg1.GFP fluorescence was measured within regions of interest (ROI) drawn around desmoplakin railroad track staining at cell-cell borders. Desmoplakin was detected using the Fitzgerald antibody as described above. This Dsg1.GFP fluorescence intensity was compared to adjacent ROI at regions of cell borders lacking desmosomes. For both wild type and mutant Dsg1, targeting to desmosomes was measured as a fold-enrichment of Dsg1.GFP fluorescence in desmosomes compared to non-desmosomal regions. For SAM patient and control tissue, desmosomal ROIs were defined using desmoplakin (via NW6 antibody labeling, see above) railroad tracks and DSG1 fluorescence was measured therein.

Triton solubility/insolubility. A431 cells were cultured until confluent in 6 well tissue culture plates. Cells were washed twice with ice cold phosphate buffered saline. The triton soluble pool was isolated by incubating cells with triton buffer (1% Triton X-100, 10 mM Tris, pH 7.5, 140 mM NaCl, 5 mM EDTA, 2 mM EGTA, with protease inhibitor) for 10 min on ice. Lysate was then centrifuged at 16,000 x g for 10 min at 4°C to pellet triton insoluble fraction. Triton-soluble supernatant was collected and mixed 1:1 with 2x laemmli sample buffer containing 5% B-mercaptoethanol. The triton-insoluble pellet was resuspended in 2X laemmli sample buffer (Biorad 161-0737) sample buffer containing 5%

β -mercaptoethanol. All samples were heated to 95°C for 10 minutes, vortexed for 30s half way through, prior to being run on a gel for western blotting.

Isolation of detergent resistant membranes. Detergent resistant membranes were isolated as described previously (339). Briefly, cells were cultured in 25 cm² flasks (two per gradient) and washed with PBS+. Cells were collected by scraping in TNE buffer supplemented with protease inhibitors (Roche) and pelleted by centrifugation at 0.4 x g at 4°C for 5 min (5415R, Eppendorf). Cells were re-suspended in TNE buffer and homogenized using a 25-gauge needle. TNE buffer containing Triton X-100 was added (final concentration of 1%) and cells were incubated on ice for 30 min. 400 μ L of detergent extract was mixed with 800 μ L of 56% sucrose in TNE and placed at the bottom of a centrifuge tube. 1.9 mL volumes of 35% and 5% sucrose were layered on top of the sample. Following an 18 hour centrifugation at 4°C (44,000 rpm, SW55 rotor, Beckman Optima LE-80 K Ultracentrifuge), 420 μ L fractions (1–11, remaining volume combined to make up fraction 12) were removed from top to bottom of the gradient and stored at –20°C until processed for western blot analysis. Flotillin-1 and Flotillin-2 were used as raft markers while calnexin was used as a non-raft marker. Unless otherwise stated, all films shown are representative for at least three independent experiments.

Giant plasma membrane vesicle (GPMV) isolation and partitioning measurements. GPMVs were isolated and imaged as described (442, 443). Before GPMV isolation, cell

membranes were stained with 5 $\mu\text{g}/\text{mL}$ of FAST-DiO (Invitrogen), a fluorescent lipidic dye that strongly partitions to disordered phases because of double bonds in its fatty anchors (444).

Biotin labeling in pulse-chase experiments. For Dsg1 cleavage and recovery experiments, cells were grown to confluence in 35 mm cell culture plates (Corning 430165). Cells were trypsinized using TrypLE (Gibco 12605-010) for ~8 min and suspended. After the indicated refractory period, surface proteins were biotinylated. For experiments monitoring protein turnover from the plasma membrane, surface proteins were biotinylated before the indicated period. Biotinylation was achieved using PBS+ containing 0.5 mg/ml EX-Link sulfo NHS SS Biotin (Thermo Scientific 21331) for 30 min at 37°C. Unbound biotin was quenched in PBS+ containing 50 mM NH_4Cl for 1 min. Cells were lysed in RIPA (PBS+ containing 1% Triton X-100, 0.1% sodium dodecyl sulfate, 0.1% sodium deoxycholate, 10 mM Tris-HCl, 140 mM NaCl, 1 mM EDTA, 0.5 mM EGTA, and protease inhibitor cocktail (Roche 11836170001)), scraped to transfer from culture plate to an Eppendorf tube, and incubated for 10 min on ice. Lysate was cleared via centrifugation at 16,000 x *g* at 4°C for 10 min. Biotinylated protein was captured on streptavidin-coated beads during overnight incubation at 4°C. Beads were collected via centrifugation at 2,500 x *g* at 4°C for 1 min. Protein was released from beads using Laemmli buffer containing 5% β -mercaptoethanol for 5 minutes at 95 degrees.

Mass-tagging of palmitoylated proteins. For mass-tag labeling, we followed the procedure described by (445). Lysates from A431 cells expressing the indicated constructs were prepared in TEA buffer (50 mM triethanolamine; pH7.3, 150 mM NaCl, and 5 mM EDTA) containing 4% SDS. 200 µg of total cellular protein was treated with a final concentration of 10 mM neutralized TCEP for 30 min with end over end rotation. NEM was added to a final concentration of 25 mM and rocking continued for 2 hours. NEM was removed by 3 rounds of chloroform/methanol/H₂O precipitation. The final pellet was resuspended in TEA buffer containing 0.2% Triton X-100. Samples are treated with 0.75 M NH₂OH (+HA) or without hydroxylamine (-HA) and incubated at room temperature for 1 hour. Excess hydroxylamine was removed with one round of chloroform/methanol/H₂O precipitation and the pellet was resuspended in TEA buffer containing 0.2% Triton X-100 supplemented with 1 mM mPEG-Mal (10 kDa; Sigma). Samples were incubated with rocking for 2 hours and reactions were terminated by 1 round of chloroform/methanol/H₂O precipitation. The final pellet was suspended in 1x Laemmli sample buffer and resolved by SDS-PAGE.

Isolation, freezing, and imaging of desmosomes. To isolate desmosomes from mouse liver, a method based on the protocol of Tsukita and Tsukita (1989) was used, in which a desmosomal fraction was obtained by sucrose density gradient centrifugation, followed by NP-40 detergent treatment. The fraction should contain only bile canaliculi derived plasma-membranes, as the homogenization and centrifugation steps are designed to free the preparation from contaminating cell fragments and nuclear membranes due to their

higher densities (446-448). The desmosomal fraction was immediately plunge-frozen on holey carbon grids, which were subsequently inserted into the column of a FEI Titan Krios at liquid nitrogen temperatures. Tilt series of the sample (+60 to -60°) were recorded and subsequently reconstructed into 3D tomograms. Subtomogram averaging was performed as described by Forster and Hegerl in *Methods in Cell biology* in 2007 (449).

Membrane thickness measurements. For the thickness of the desmosomal membranes, 1768 selected positions (derived from 3 desmosomes in 2 tomograms) with visible cadherins were selected. As a comparison (control), 668 randomly selected positions at membranes adjacent to desmosomes (derived from 3 membranes in 3 tomograms) and 515 randomly selected positions from arbitrary membranes in the tomograms (derived from 2 membranes in 1 tomogram) were selected. Each position was cross-correlated with multiple references of a simplified membrane model of the two leaflets (dark lines representing phospholipid head groups and are included in the measurements) with varying bilayer distance (3.08, 3.52, 3.96, 4.4, 4.84 and 5.28 nm spacing) using sub-tomogram averaging routines with limited rotational freedom ($\pm 30^\circ$ in 5° steps for all three Euler-angles) after rough pre-alignment using the overall membrane orientation. The reference with the highest cross-correlation score then provides the bilayer spacing of each single sub-volume.

Statistics. Error bars represent standard error of the mean. Significance was determined using a student's t-test (two tailed, heteroscedastic) and p-values have been indicated. Statistical analysis of immunofluorescence results was conducted on at least two independent experiments with ten images per condition per replicate. Statistical analysis of western blotting was conducted on results from three independent experiments.

5.6 Acknowledgements

The authors would like to thank Dr. Kathleen Green and members of the Kowalczyk lab for comments and insights during the preparation of this manuscript. We would also like to thank Joseph Lorent for help generating the transmembrane domain models. This work was supported by grants (R01AR048266, R01AR048266-13S1, and R01AR050501 to A.P.K.), (LOEWE Dynamem to A.S.F) and fellowships (F31AR066476 and T32GM008367 to J.D.L.) from the National Institutes of Health, and by the Practical Research Project for Rare/Intractable Diseases (16ek0109067h0003 to Y.M. and 16ek0109151h0002 to A.K.) from the Japan Agency for Medical Research and Development. Additional support was provided by core facilities at Emory University, including the Integrated Cellular Imaging Core, the Emory Flow Cytometry Core, and the Cloning Division within Emory Integrated Genomics Core.

The authors declare no competing financial interests.

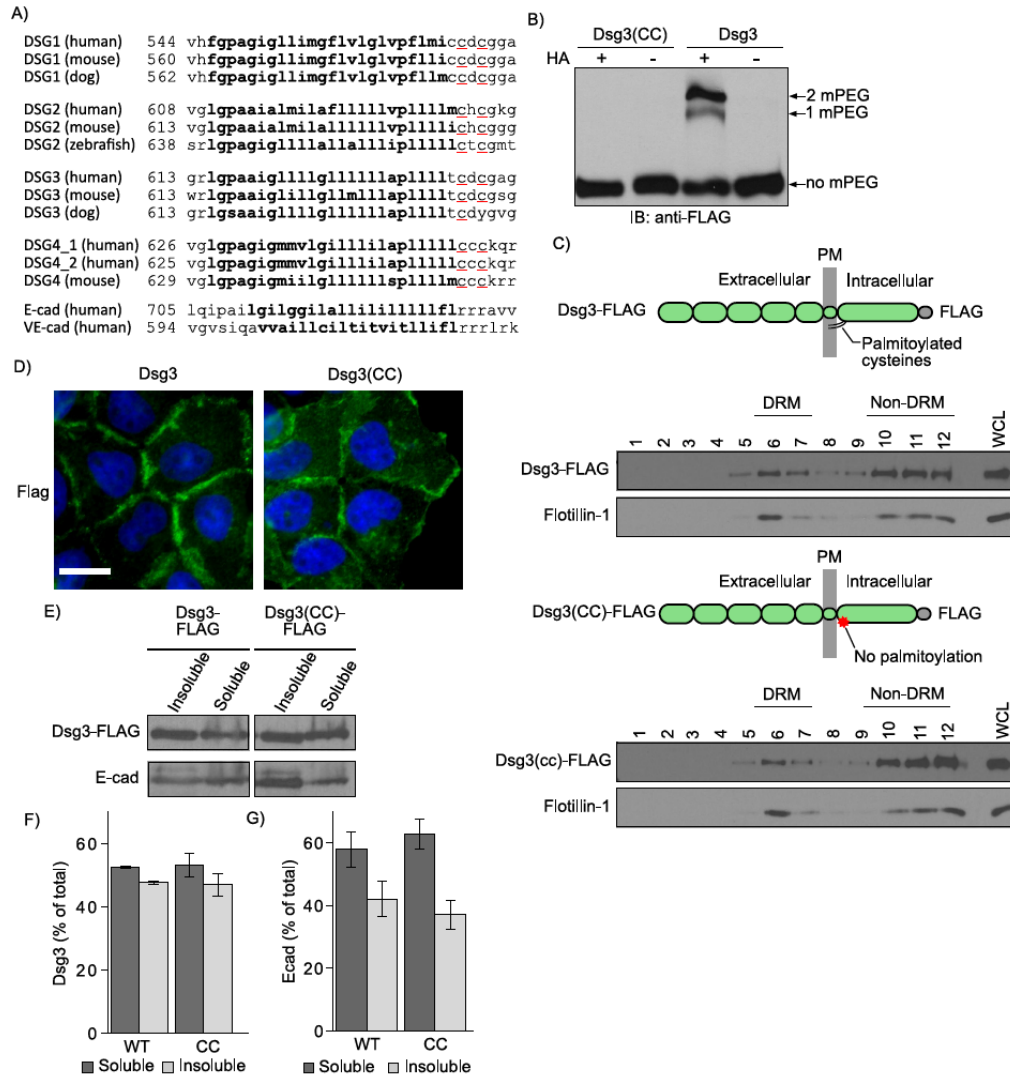


Figure 5.1: Palmitoylation is not required for Dsg3 lipid raft association. A) Sequence alignment of the desmogleins reveals a pair of highly conserved cysteine residues (red underline) at the interface between the transmembrane domain (bolded text) and the cytoplasmic domain. B) Mass-tag labeling replaces palmitoyl moieties on cysteine residues with mPEG, causing a size shift detectable by western blot analysis. Dsg3 is doubly palmitoylated and mutation of the membrane-proximal cysteine residues to alanine abolishes palmitoylation. C) Lipid raft fractionation of HeLa cells expressing Dsg3-FLAG from adenoviruses reveals no defect in lipid raft targeting of the palmitoylation-null mutant. D) Widefield images of A431 cell lines stably harboring flag tagged constructs. Scale bar = 20µm. E) Western blot of Triton-X 100 soluble pools and insoluble pools from A431 cell lines stably expressing either Dsg3 or Dsg3(EcadTMD). F) Densitometry quantification of Dsg3 in triton soluble and insoluble pools from Panel E. Loss of palmitoylation has no detectable effect on the solubility of Dsg3 in Triton X-100, a classic measure of desmosome and cytoskeletal association. G) Densitometry quantification of E-cadherin distribution between Triton soluble and insoluble pools.

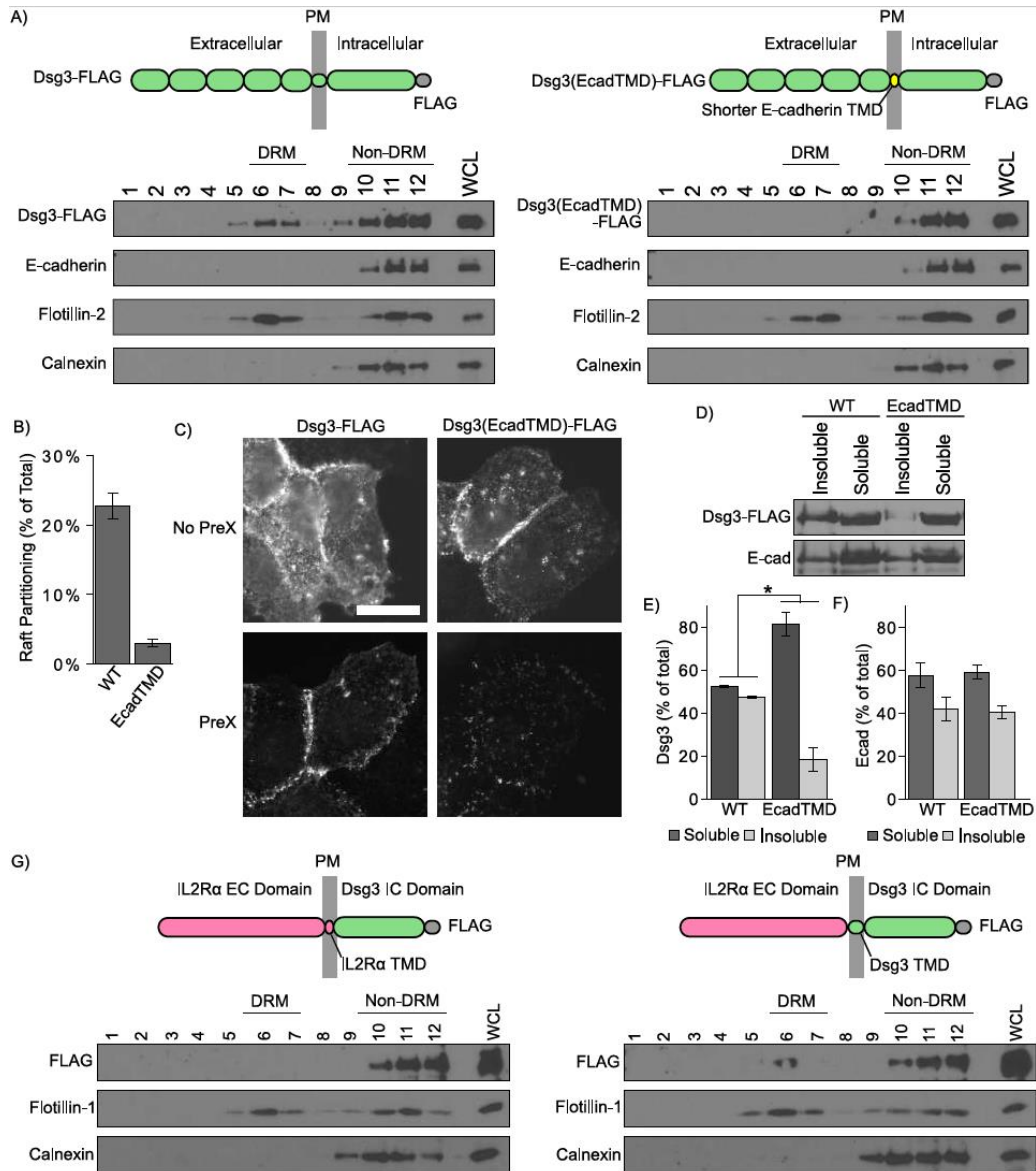


Figure 5.2: The Dsg3 TMD is necessary for lipid raft association. A) Sucrose gradient fractionation of A431 cells stably expressing murine Dsg3 (wild-type or EcadTMD mutant). Replacing the Dsg3 TMD with the shorter E-cadherin TMD (bolded text) abolishes lipid raft targeting. B) Densitometry quantification of WT Dsg3 and Dsg3(EcadTMD) in detergent resistant membrane (DRM) fractions shown in Panel A. C) Dsg3(EcadTMD) is more susceptible than Dsg3 WT to pre-extraction in Triton X-100 prior to fixation and immunofluorescence localization. Scale bar = 20 μm. D) Western blot analysis indicates Dsg3(EcadTMD) is more soluble in Triton X-100 than Dsg3 WT. E) Quantification of Dsg3 in Triton soluble or insoluble pools from Panel D. F) Quantification of E-cadherin in Triton soluble and insoluble pools in cells expressing either WT Dsg3 or the Dsg3(EcadTMD) mutant G) Lipid raft fractionation of FLAG-tagged IL2R-Dsg3 chimeras expressed in HeLa cells using an adenoviral delivery system. Inclusion of the lengthy Dsg3 TMD in the chimera (right panel) confers lipid raft targeting. * $p < 0.05$

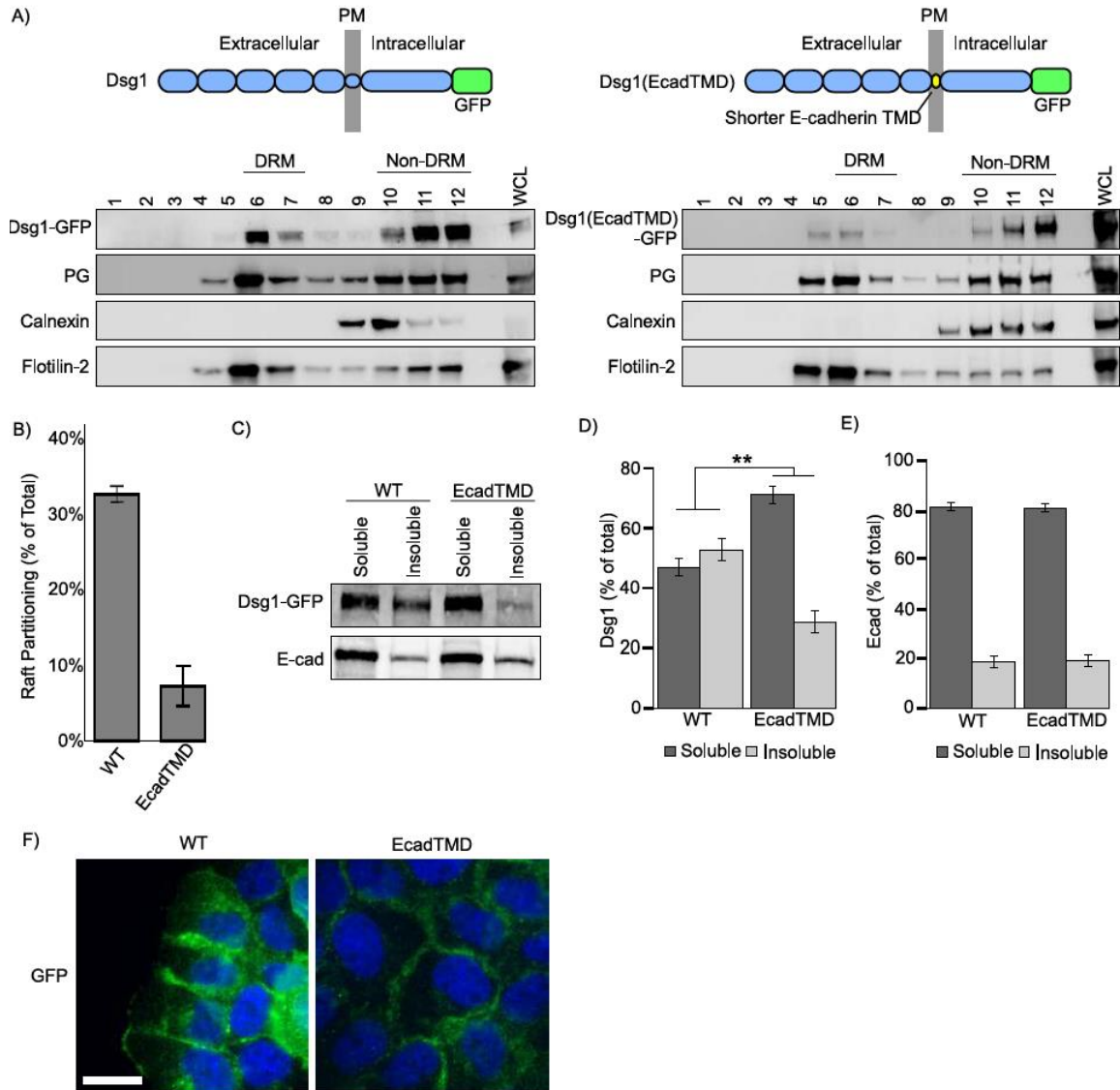


Figure 5.3: The Dsg1 TMD is critical for lipid raft association. A) Western blot of Triton-X 100 extracts and sucrose gradient fractionations of A431 cells stably expressing murine WT Dsg1 (Dsg1(EcadTMD) chimera). B) Quantification from densitometry analysis of the percentage of total Dsg1 in the detergent resistant membrane (DRM) fractions of sucrose gradient fractionations. C) Differential detergent extraction and western blot analysis indicates that Dsg1(EcadTMD) is more soluble in Triton X-100 than wild type Dsg1. D) Quantification of Dsg1 western blots shown in panel C. E) Quantification of E-cadherin western blots shown in panel C. F) Widefield images of A431 cells expressing either GFP tagged WT Dsg1 or Dsg1(EcadTMD). Both constructs localized to cell-cell borders and no abnormal localization was seen. Scale bar = 20µm. **p<0.001

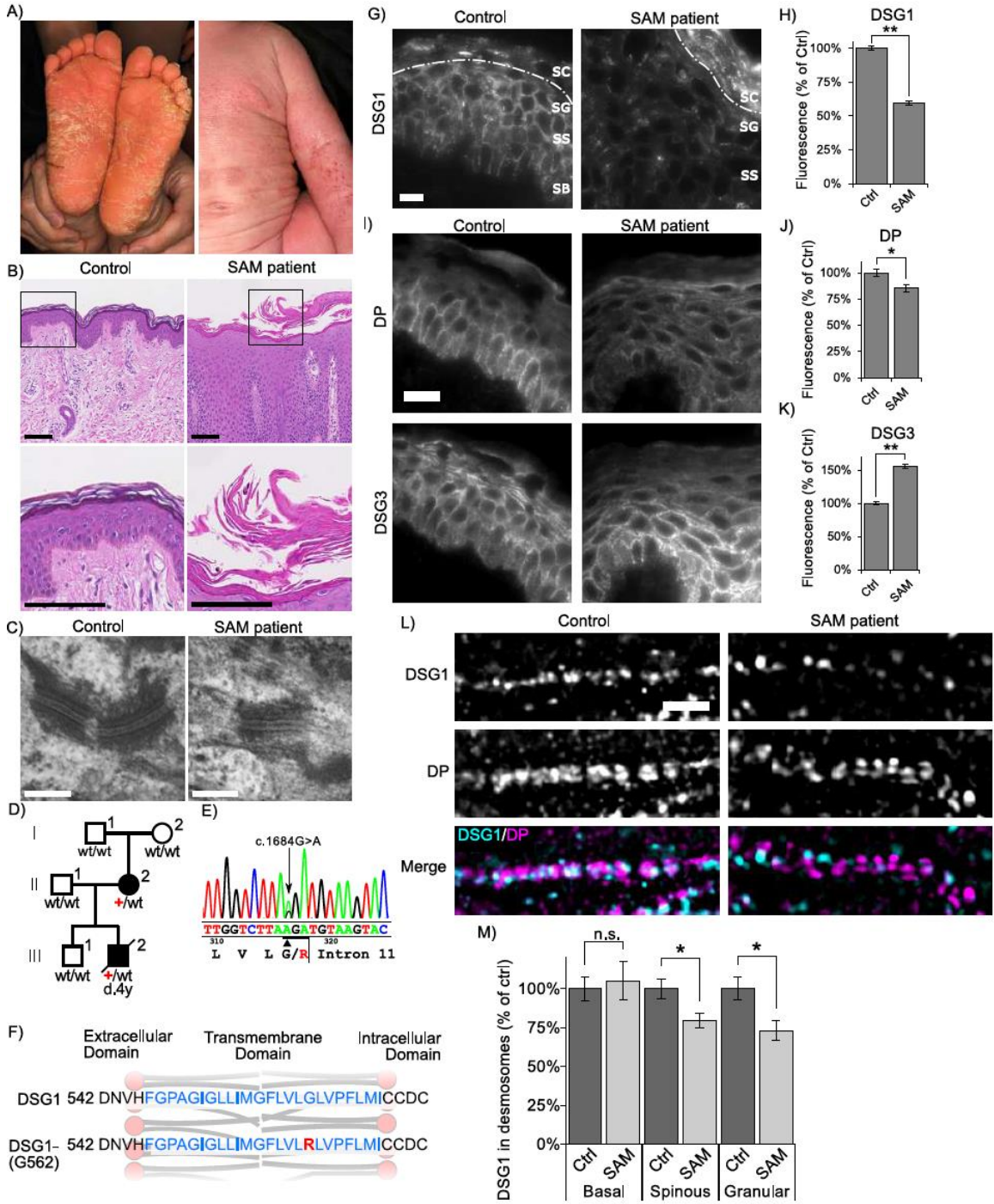


Figure 5.4: Desmoglein 1 (DSG1) transmembrane domain mutation causes severe dermatitis, multiple allergies, and metabolic wasting (SAM) Syndrome. A) Individual III-2 displays feet covered with hyperkeratotic yellowish papules and plaques, and ichthyosiform erythroderma with severe itch occur over much of his body. B) Hematoxylin and eosin staining of III-2's skin biopsy reveals acantholytic lesions in the upper layers of the epidermis. Scale bar = 100 μ m. C) Electron micrographs of epidermal sections from the proband indicate relatively normal desmosome morphology. Scale bar = 200 nm. D) Pedigree of affected individuals and near relatives. Inheritance determined by genomic DNA sequencing. E) Genomic DNA sequencing of white blood cells reveals these SAM patients have a heterozygous point mutation, c.1684G>A (black arrow) in DSG1. The adjacent splice site is unaffected. F) Schematic showing the location of the SAM-causing G-to-R substitution (red) within the transmembrane domain (blue). G-H) Widefield microscopy of DSG1 immunofluorescence in human skin biopsies reveals both DSG1 downregulation and inappropriate clustering at cell borders in SAM patient epidermis. SC = stratum corneum, SG = stratum granulosum, SS = stratum spinosum, SB = stratum basale. SC/SG boundary demarcated by dashed line. Downregulation of DSG1 is observed in the SG and SS. I-K) Desmoplakin (DP) is slightly downregulated in patient skin, and DSG3 is upregulated. Scale bar = 20 μ m. L-M) Structured Illumination Microscopy (SIM) indicates reduced desmosomal DSG1 in SAM patient tissue in the stratum spinosum and granulosum. Scale bar = 5 μ m. *p<0.01, **p<0.001

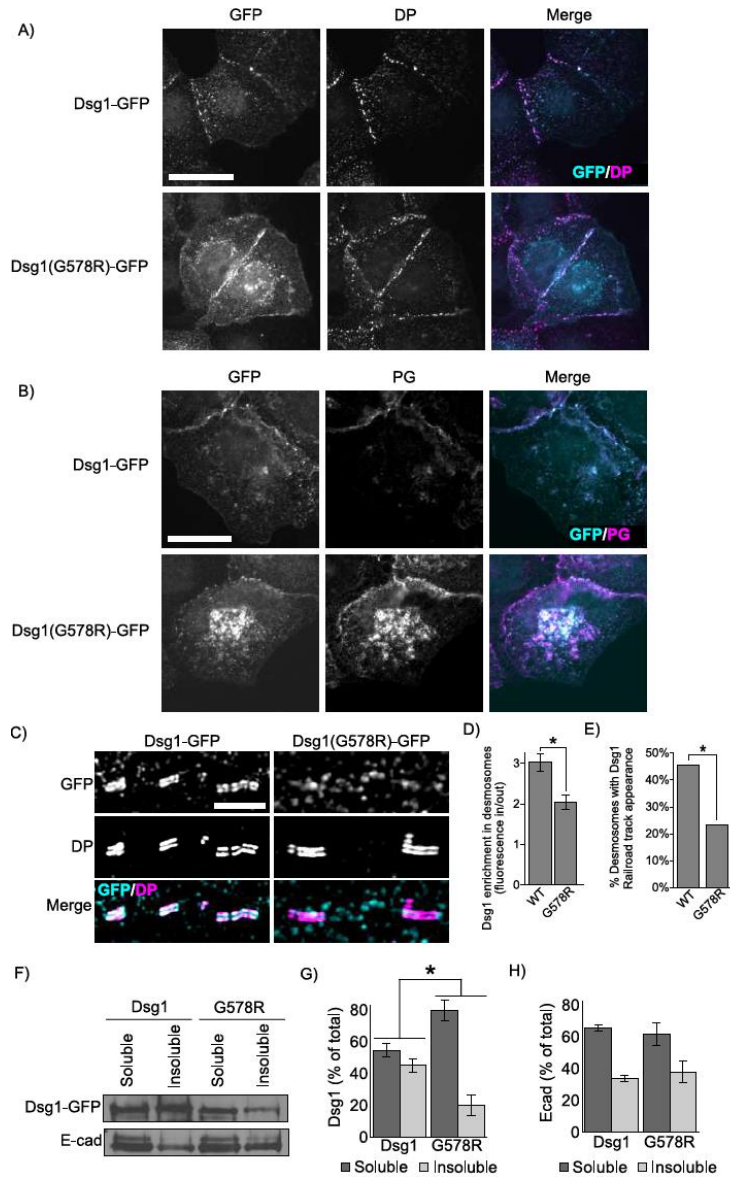


Figure 5.5: SAM-causing DSG1 mutation causes defects in junction targeting. A) Widefield immunofluorescence micrographs of A431 cell lines stably expressing either wild type Dsg1-GFP or Dsg1(G578R)-GFP reveal broadly similar distribution of desmoplakin (DP) and B) colocalization between DSG1 and plakoglobin (PG). Scale bar = 20 μ m. C) Super-resolution micrographs of A431 stable cell lines acquired using structured illumination microscopy (SIM) reveal defects in Dsg1(G578R) desmosome targeting. Scale bar = 5 μ m. D) Desmosomes are identified by SIM imaging as regions of parallel desmoplakin immunofluorescence staining resembling railroad tracks. Quantification of Dsg1 found within DP railroad tracks compared to border Dsg1 outside of railroad tracks. E) Quantification of railroad track appearance observed for WT or mutant Dsg1.GFP. F-H) The G578R mutation increases solubility of the mutant in Triton X-100 as determined by western blot analysis. E-cadherin distribution in Triton soluble and insoluble pools is not altered in A431 cell lines expressing the Dsg1 mutant. * $p < 0.05$

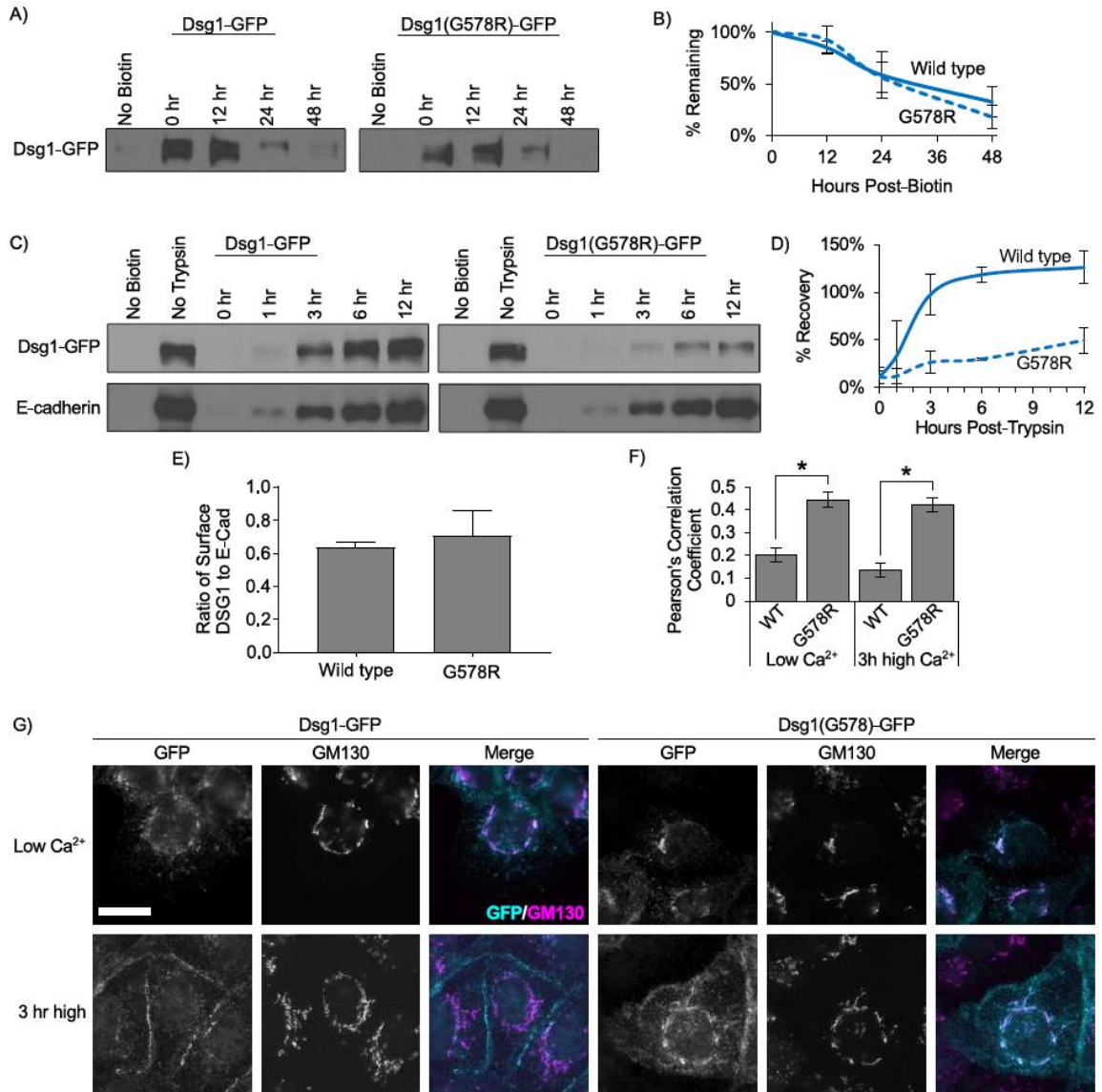


Figure 5.6: SAM-causing DSG1 mutation delays trafficking to the plasma membrane.

A) Pulse chase experiments were performed to determine the rate of turnover of Dsg1 from the plasma membrane in A431 cells expressing murine Dsg1-GFP. Cell surface proteins were biotinylated at t=0, washed and incubated at 37 degrees for various amounts of time. Cell lysates were collected after the indicated times. Biotinylated proteins were captured using streptavidin beads and processed for western blot analysis B) Quantification using densitometry revealed no significant differences in the rate of turnover of Dsg1 versus Dsg1(G578R) C) Dsg1(G578R) is trafficked to the plasma membrane substantially more slowly than wild-type. Cell surface proteins were cleaved using trypsin at t=0. Trypsin was removed and cells were then incubated for the indicated times. The amount of newly delivered surface Dsg1 was assayed via biotin labeling followed by capture using streptavidin beads and subsequent western blot analysis. D) Quantification using densitometry indicates Dsg1(G578R) recovers more slowly than WT-Dsg1. E) Densitometry analysis of the Dsg1 no-trypsin condition in panel C as a ratio to densitometry analysis of the E-cadherin no-trypsin condition in panel C reveals comparable surface levels of WT Dsg1 and Dsg1(G578R). F) Cells were cultured in low calcium medium to cause cadherin removal from cell-cell borders and accumulation in intracellular compartments (Panel E, Low Ca²⁺). Some cells were then switched back to normal calcium to allow for junction assembly (Panel E, 3 hr high). Dsg1(G578R) displays increased colocalization with the Golgi apparatus protein GM130 under both conditions. Scale bar = 20µm. G) Quantification of colocalization of Dsg1 and GM130. *p<0.001

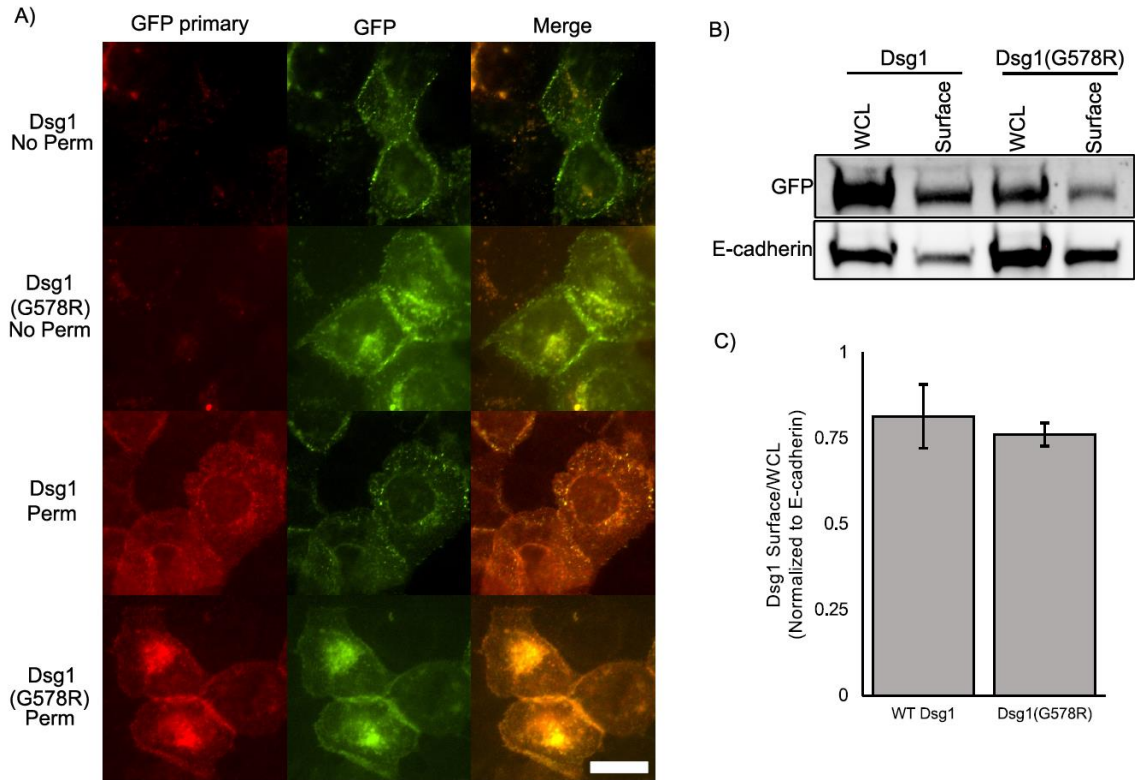


Figure 5.7: The Dsg1(G578R) mutant is inserted into the membrane in the correct orientation and is present on the cell surface at levels similar to WT Dsg1. A) Immunofluorescence localization of WT Dsg1.GFP and Dsg1(G578R).GFP in cells fixed with or without Triton-X 100 permeabilization using antibodies directed against the cytoplasmic GFP tag. The c-terminal GFP tag for both the Dsg1 WT and the Dsg1(G578R) SAM mutant is accessible only in cells permeabilized with Triton X-100, indicating that the Dsg carboxyl terminus is intracellular for both WT and mutant Dsg1. Scale bar = 20µm. B) A431 cell surface proteins were biotinylated and captured using streptavidin beads followed by western blot analysis for Dsg1 WT or Dsg1(G578R) SAM mutant. Whole cell lysates (WCL) represent total Dsg1 protein levels in unbiotinylated cells. Dsg1 WT and mutant were detected using the cytoplasmic GFP tag. C) Dsg1 WT and mutant levels at the cell surface (biotinylated) were normalized to E-cadherin cell surface levels and the ratio of surface protein to whole cell lysate was calculated. Quantification represents three independent experiments.

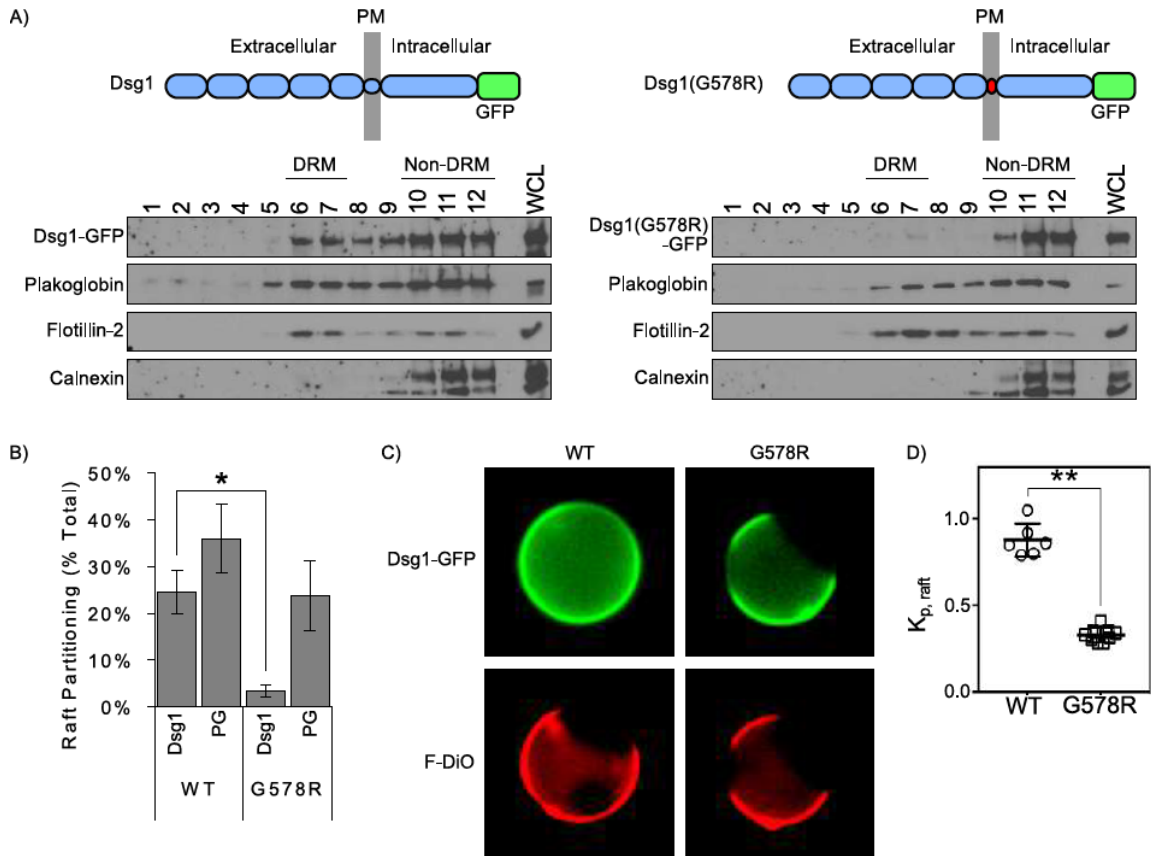


Figure 5.8: SAM-causing DSG1 mutation abolishes lipid raft association. A) Sucrose gradient fractionation and western blot analysis of A431 cell lines stably expressing WT and mutant Dsg1. B) Quantification of results in Panel A indicates SAM-causing mutation abolishes Dsg1 partitioning to DRM (lipid raft fractions). C) Representative images of giant plasma membrane vesicles isolated from rat basophilic leukemia cells expressing GFP-tagged WT Dsg1 or Dsg1(G578R). Unsaturated lipid marker FAST-DiO (F-DiO) to visualize the non-raft phase. D) Normalized line scans of Dsg1 fluorescence intensity were measured through peaks corresponding to Dsg1 intensity in raft and nonraft membrane, respectively. Background-subtracted ratios of these two intensities yield raft partition coefficients, $K_{p,raft}$. Data are shown as mean \pm SEM from three independent experiments. * $p < 0.05$, ** $p < 0.001$

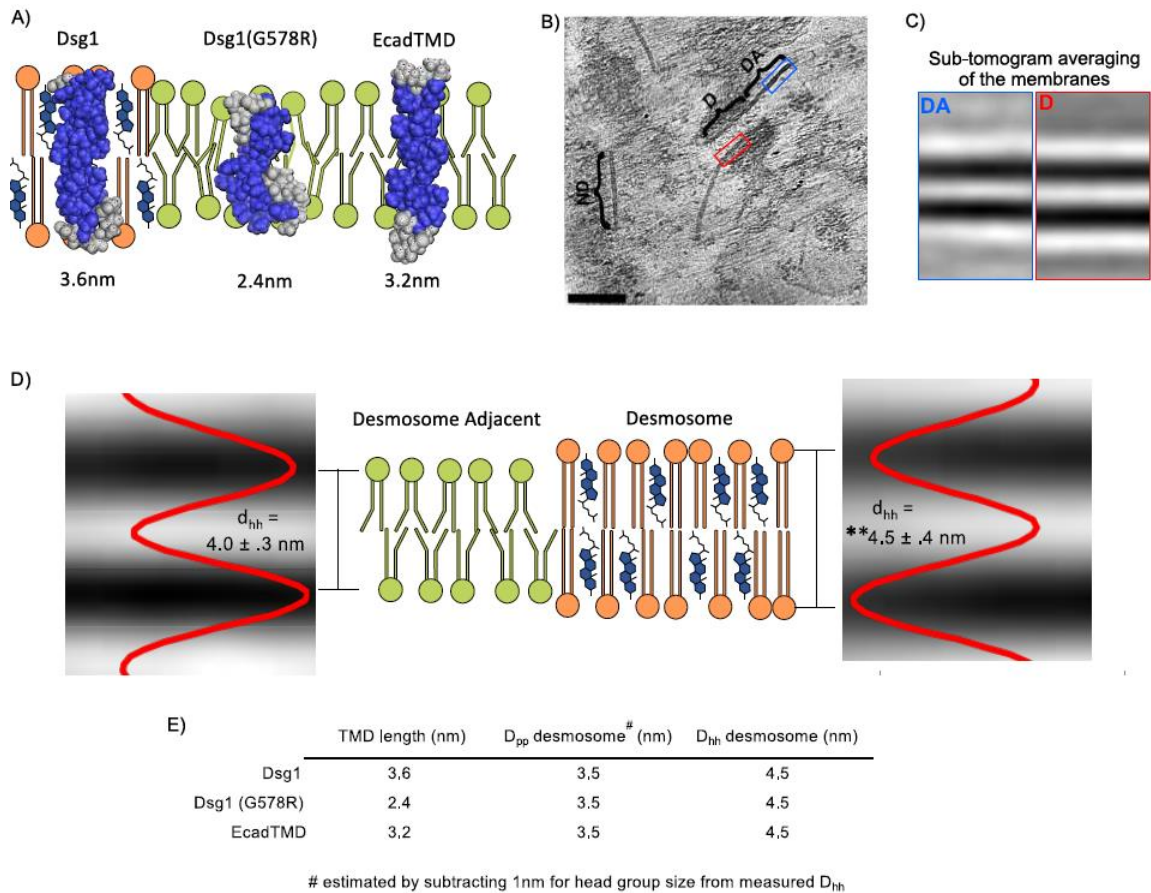
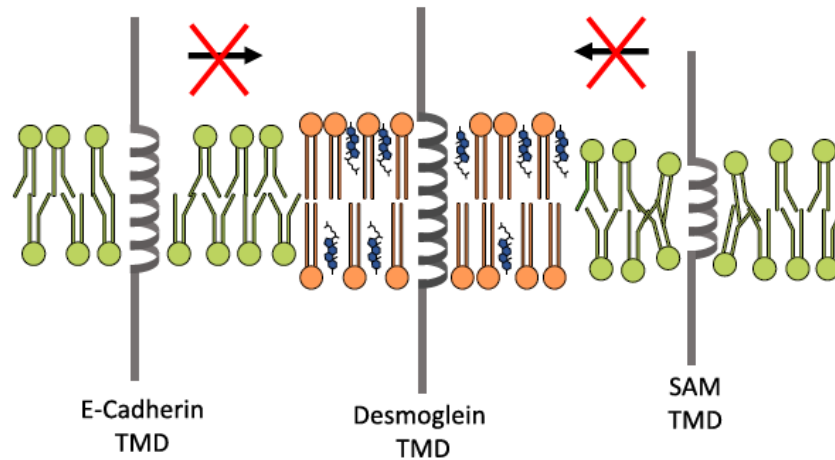


Figure 5.9: The desmosome bilayer is thicker than adjacent bilayers. A) Structural models of the DSG1 WT, DSG1 SAM mutant and E-cadherin TMDs acquired using the Robetta prediction server and depicted in schematized lipid bilayers. The length of each TMD is shown in nm and is based on TMD amino-acid number. B) Representative slice from a cryo-electron tomogram showing a desmosome (D) with characteristic intracellular plaque attached to intermediate filaments. Directly adjacent to the desmosome, membrane remnants can be seen (DA). Other non-desmosomal (ND) regions of the plasma membrane embedded in a thin layer of ice are also visible. Insets are projections of the average of all sub-volumes from the most significant class. Scale bar = 100nm. C) Schematic showing the thickness of the desmosome bilayer compared to desmosome adjacent bilayers. The lipid bilayer within desmosomal membranes is thicker ($4.5 \pm 0.4 \text{ nm}$) when compared to membranes adjacent to desmosomes ($4.0 \pm 0.3 \text{ nm}$) or from non-desmosomal membranes ($4.0 \pm 0.3 \text{ nm}$) $**p < .001$. Intensity plots are shown superimposed to sub-tomogram average projections for desmosome and desmosome adjacent membranes. D) Summary table depicting the TMD lengths and the measured phospho-head group to head group distance (D_{hh}) as shown in Panel C. Also shown is the estimated distance between phosphate residues (D_{pp}) which corresponds to the hydrophobic interior of the bilayer. This hydrophobic region of the bilayer was estimated by subtracting the predicted polar head group size (1nm) (429) from the measured D_{hh} shown in Panel C.

A) Desmoglein Transmembrane Domains Mediate Lipid Raft Association



B) Lipid Bilayer Architecture Contributes to Adhesive Junction Organization

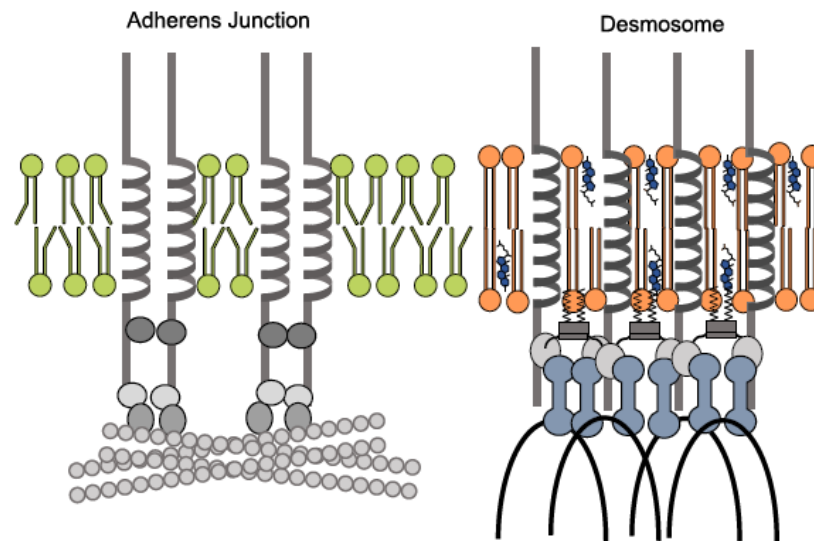


Figure 5.10: Model. A) The extended desmoglein transmembrane domain facilitates lipid raft association. In contrast, the entry of E-cadherin and the Dsg1 SAM mutant into lipid rafts is unfavorable due to hydrophobic mismatch between the cadherin TMD and the phospholipid headgroups of the lipid bilayer. B) Desmosomal proteins enter lipid raft domains through TMD affinities for raft-like membrane domains and palmitoylation of desmosomal cadherins and plaque proteins. In contrast, adherens junction components lack these raft-targeting features, resulting in exclusion of adherens junction components from lipid raft membrane domains. Thus, the biophysical properties of the bilayer associated with the desmosome promote spatial segregation of adherens junctions and desmosomes

Table 1. Summary of Transmembrane domains

Construct	TMD Sequence	Amino Acid Number	Length (nm)	ΔG_{raft}
WT Dsg1	FGPAGIGLLIMGFLVLGLVLPFLMI	24	3.6	0.166
Dsg1 (G578R)	FGPAGIGLLIMGFLVLR	16	2.4	0.387
E-cadherin	LGILGGILALLILLLLLLFL	21	3.15	0.304

Table 5.1 Summary of Transmembrane Domains

Chapter 6

Pemphigus Vulgaris

6.1 Pemphigus Overview

Derived from the Greek word “pemphix”, meaning to bubble or blister, pemphigus is a group of skin blistering disorders, and Pemphigus vulgaris (PV) is the most common variant (450). PV occurs when the body starts to generate autoantibodies targeting the extracellular domain of the desmosomal cadherin, Dsg3. Many patients suffering from PV also harbor autoantibodies targeting another isoform of desmoglein, Dsg1. These autoantibodies compromise desmosome structure and stability, thereby leading to a loss of keratinocyte adhesion and the development of acantholysis (Figure 6.1). Acantholysis is the loss of cell-cell adhesion between keratinocytes. Typically, patients harboring only anti Dsg3 antibodies have mucosal dominant disease, where lesions are found only on mucosal tissues, while patients with anti Dsg1 antibodies as well as anti Dsg3 antibodies have mucutaneous disease that has spread to the stratified epidermis of the skin. This difference in disease presentation can be explained by the differentiation specific expression patterns of desmogleins. Desmoglein 3 is the predominant desmoglein expressed in mucosal tissues, while it is only present in the basal layers of the stratified epidermis, however in the stratified epidermis Dsg1 at a high enough level to protect the skin when only Dsg3 autoantibodies are present. Thus for PV to affect the stratified epidermis, both Dsg1 and Dsg3 antibodies must be present (155, 451). For more than half of PV patients the first sign

of disease is the development of oral lesions, and many of these patients develop cutaneous disease (452). The acquisition of anti Dsg1 antibodies, as well as the switch from mucosal dominant to mucocutaneous, is viewed as a mechanism of disease progression. While this disease is relatively rare, if left untreated it is almost always fatal. This chapter provides a description of our current understanding of PV clinically, such as diagnosis and treatment, and experimentally, such as experimental models and known mechanisms of disease.

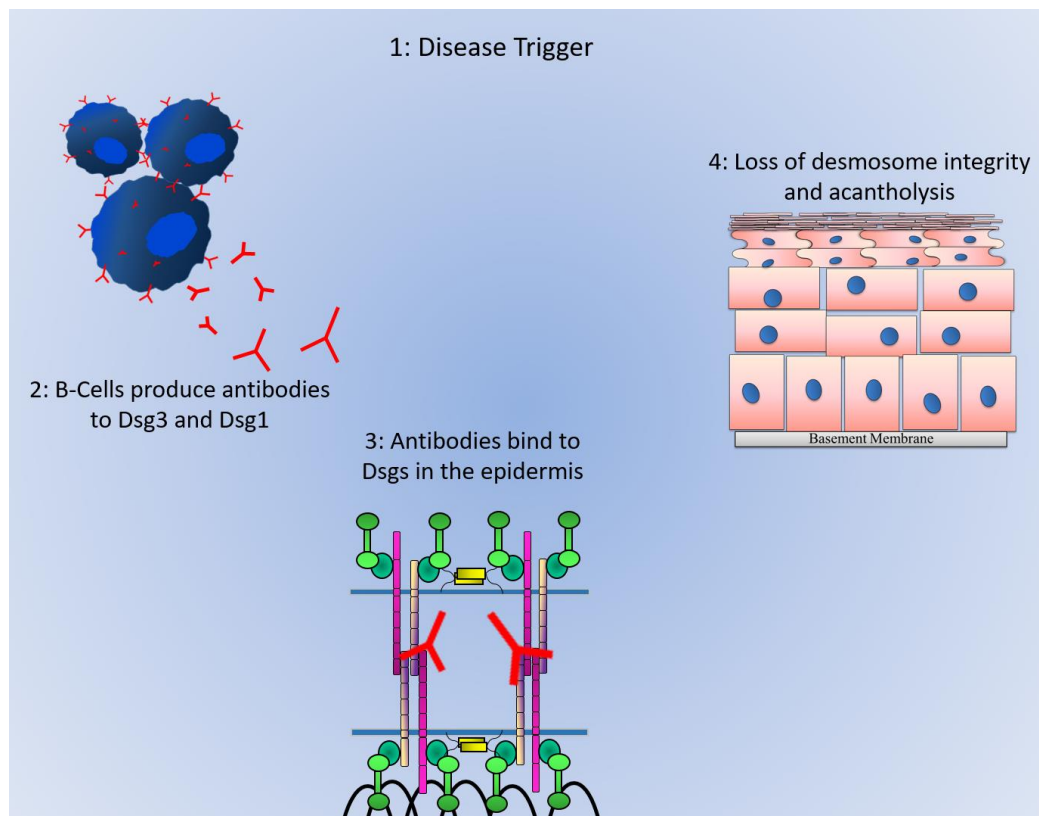


Figure 6.1 Progression of pemphigus vulgaris. 1) A variety of factors can contribute to the onset of disease 2) B-cells produce autoantibodies targeting desmogleins 1 and 3. 3) Autoantibodies bind to extracellular domains of desmogleins resulting in the disruption of desmosomes and a loss of desmosome integrity. 4) The loss of desmosome integrity results in loss of adhesion, or acantholysis, and subsequent blistering of patient epidermis.

6.2 Clinic

6.2.1 Etiology

Unfortunately, little is understood about what causes a patient to develop PV. This is likely because not all PV cases are caused by the same element. While no single genetic factor has been linked to all PV cases, several studies suggest alleles of the of the human leukocyte antigen (HLA) gene are associated with an increased risk of PV (453-458). Of note, versions of the HLA gene are linked to a predisposition to autoimmune disorders as a whole and not specific to PV (459). Supporting evidence for genetic causes lies in the observation that certain ethnic groups are more susceptible to the development of this disorder (Table 6.1). Incidence rates vary by country, however an Israel wide study demonstrated that the Jewish population was at a 3.5 times higher risk for developing pemphigus vulgaris when compared to the Arab population (460). A genome-wide association study identified a variant of the pro-apoptotic transcription factor ST18 to be highly associated with the development of PV in people of Jewish decent. The same study showed a similar association with the ST18 variant in the Egyptian population, but surprisingly there was no association with this gene and the development of PV in the German population, suggesting that the ST18 variant leads to a population specific predisposition to the development of PV (461).

While there is currently no identifiable genetic cause to PV, the literature suggests many different events could trigger the disease in patients. Drugs containing thiols or phenols seem to be the most common inducers of pemphigus. Thiols cause loss of adhesion by provoking the activation of enzymes such as papain and elastase that induce

acantholysis, while inhibiting enzymes like keratinocyte transglutaminase, an important factor for keratogenesis (462). Phenols stimulate the secretion of cytokines from keratinocytes, such as tumor necrosis factor- α , that potentially trigger cutaneous inflammation and promote acantholysis (463, 464). When skin explants were cultured in the presence of thiols and phenols in vitro they promoted acantholysis, supporting the hypothesis that they may initiate the formation of pemphigus vulgaris (465-467). While it is clear that there is an association with these drugs and acantholysis, we have no understanding of how these events trigger the autoantibody production characteristic of pemphigus vulgaris. Additionally, several studies report that women are at a higher risk of developing PV (468-470). It is still unclear whether women are at a greater risk due to genetic factors or environmental factors, however pregnancy is known to trigger the development of PV (471, 472). Lastly, other factors have been implicated as initiators of pemphigus such as stress (473-475) and radiation (476-478), however it is increasingly clear that there is no one factor that causes all cases of PV

Country	Incidence rate*	Reference
Germany	0.5	(479)
Saudi Arabia	1.6	(480)
France	1.7	(468)
Korea	2.06	(470)
Poland	2.44	(481)
Turkey	4.7	(469)
Bulgaria	4.7	(482)
Tunisia	6.7	(468)
U.K.	6.8	(483)
Greece	8.0	(484)
Israel	16.1	(485)
Iran	50	(486)
Ethnicity	Incidence rate*	Reference
Jewish	8.8	(460)
Arabic	2.5	(460)

*per 1 million per year

Table 6.1 Pemphigus vulgaris incidence rates. Incidence rates of pemphigus vulgaris vary between countries and ethnic populations. Studies included in this table were specific for pemphigus vulgaris and do not include numbers for pemphigus foliaceus.

6.2.2 Diagnosis and Symptoms

Because pemphigus is a rare condition, it requires a dermatologist with experience in treating blistering disorders to make a diagnosis. The diagnosis of PV is typically based on the following criteria: clinical presentation, histopathology, direct immunofluorescence microscopy, indirect immunofluorescence microscopy or ELISA (487). At a minimum, patient symptoms must align with what is typical for PV and Dsg3 antibodies must be detected in patient sera. PV patients display intraepidermal breaks thought to be caused by autoantibody binding to Dsg3 and the subsequent loss of desmosomal adhesive function. The immunopathology of pemphigus vulgaris consists of autoantibodies targeting Dsg3 or

Dsg3 and Dsg1. Skin biopsies coupled with direct immunofluorescence, serum samples used with indirect immunofluorescence, and autoantibody ELISA scores are all methods used in the diagnosis of PV (reviewed below).

6.2.3 Measure of disease severity

Potentially due to the rarity of PV, there are very few unbiased random clinical trials assessing patient treatment and outcomes. Additionally, it has been difficult to compare results from these studies because different measurements of patient outcome and different methods of measuring disease progression were used in each study, thus it has become apparent that there is a great need for a reliable and universal scoring systems for clinicians to use in the treatment and study of pemphigus vulgaris patients (488). Several different methods of tracking the severity and progression of PV have been developed throughout the world (Table 6.2). Though there are many scoring systems, The Autoimmune Bullous Skin Disorder Identity Score (ABSIS) (489) and Pemphigus Disease Area Index (PDAI) (490), emerged as the two main scoring systems used by dermatologists to monitor PV progression. Several studies have validated the use of these scoring systems and PDAI has emerged as the most reliable scoring system to track disease severity among pemphigus vulgaris patients (491). This scoring system was developed by the international pemphigus definitions committee from 2006-2008 and the intra-rater reliability was found to be found to be 0.98, much higher when compared to the intra-rater reliability of ABSIS, 0.80. To obtain a PDAI score, clinicians separate the body and give each section a score based off of the area covered by lesions, rather than number of lesions or average size of

lesions, which are methods used in previous scoring systems. While PDAI scores have been reported to be more reliable than previous measures of disease severity, there is still a need to better understand and track disease progression within these patients.

	Year Developed	Region developed	Reference(s)
The Ikeda Index/ The Japanese severity index for pemphigus	1993 revised in 2003	Japan	(492, 493)
Pemphigus Area and Activity score (PAAS)	1998	India	(494)
Pemphigus Severity Scale	2000	United States	(495)
Clinical Severity Scoring	2000	England	(163)
Oral Pemphigus Symptom score	2003	India	(496)
Disease Severity Score	2005	India	(497)
Kumar's scoring system	2006	India	(498)
Autoimmune Bullous Skin Disorder Scoring System (ABSIS)	2007	Germany	(489)
Pemphigus Disease Area Index (PDAI)	2006 -2008	International Group	(490)
Pemphigus Vulgaris lesion severity score	2008	Iran	(499)
Pemphigus Vulgaris Activity Score (PVAS)	2012	Iran	(500)

Table 6.2 Summary of disease severity scoring systems for pemphigus vulgaris. Labs studying pemphigus independently derived scoring systems of PV disease severity until 2008 when the ABSIS system and PDAI system were validated.

6.2.4 Immunofluorescence in the diagnosis of PV

Often the symptoms of PV can be similar to other dermatological diseases, such as paraneoplastic pemphigus, and thus additional diagnostic factors are required for a confident diagnosis of PV. Early indirect immunofluorescence studies in the 1960s showed that antibodies in PV patient sera were directed against intercellular areas of the epithelium and that this observation was unique to PV in comparison to other skin disorders and therefore diagnostically useful (501). For a timely diagnosis, immunofluorescence is key in determining which type of pemphigus a patient has and thus which treatments are applicable (502). Two different immunofluorescence techniques can be used to diagnose pemphigus. Direct immunofluorescence, or the addition of fluorescein-conjugated anti-human antibodies to a patient tissue specimen will result in a “fishnet-like” border staining, implicating the presence of autoantibodies in the tissue (503). Additionally, indirect immunofluorescence can be useful in the diagnosis of PV. Here mammalian tissue specimens are treated with patient sera followed by fluorescein-conjugated anti-human antibodies. These techniques are useful in the diagnosis of pemphigus, however they do not allow for a clear distinction between the variants of pemphigus as a similar staining pattern can be seen. Thus, it has become accepted that the autoantibody titers and type are critical in differentiating between PV and PF.

6.2.5 Enzyme Linked Immunosorbent Assays

In the 1970s evidence from studies with skin explants emerged and revealed that these antibodies found in PV patient sera were of pathogenic significance (504). These first experiments demonstrated that loss of cell cohesion occurs in human skin explants grown in the presence of pemphigus vulgaris serum (504). Observations as early as the 1980s illustrate that autoantibody titers within patient serum, in general, parallels disease progression (505). The use of ELISAs to quantify the autoantibody titer of PV patients was introduced in 1999 by Dr. Masayuki Amagai (506). ELISA is a biochemical approach to detect and quantify the presence of a ligand within a sample. In the case of PV, ELISAs are used to quantify the titer of autoantibodies against either Dsg1 or Dsg3 in patient sera. Since the introduction of ELISA, the assay has become important for the diagnosis of PV, including differentiation between the mucosal dominant and mucocutaneous variants (451). Currently, standardized ELISA kits are used by clinicians and investigators to ensure interlab reliability. These scores have also been used in studies designed to understand the pathogenesis and progression of PV.

While in general, it is accepted that higher titers of autoantibodies in autoimmune disease correlates to a worse clinical course for patients, Dsg3 titers have not been found to be a good predictor of patient prognosis (507). High Dsg3 titers at the time of diagnosis prior to treatment have been associated with a worse clinical course (508). However, studies have reported that Dsg3 antibody levels are related to worse disease for mucosal dominant patients only (163, 509), while other labs have reported that the titer of Dsg3 autoantibodies does not correlate with mucosal dominant patients (507). In contrast to Dsg3

antibody titers, anti Dsg1 antibody titers are reported to correlate best with disease progression, particularly in patients with cutaneous lesions (163, 507, 510). Some patients have positive antibody titers despite being in remission, perhaps because when patients undergo treatment with corticosteroids skin lesions can clear up without preventing the development of autoantibodies. In fact, presence of Dsg antibodies in patients with clinical remission can be a predictor of relapse (511). While ELISA scores are important as a diagnostic tool, further investigation is required to understand autoantibody titer changes as they relate to disease severity and progression.

6.2.6 Treatment and Patient outcomes

Unfortunately, untreated pemphigus vulgaris is considered to be fatal with a mortality rate of 90%. After the introduction of corticosteroids as a treatment option in the 1950s, this mortality rate dropped to approximately 30% (512, 513). As newer steroids were developed and subsequently used in the treatment of PV, the mortality rate has hovered around 5% since the 1980s (512, 514). The goal of treatment for PV is to increase quality of life and to induce remission while minimizing treatment related side effects. Corticosteroids and glucocorticoids are still the typical first line of treatment for PV and prednisone, or a derivative of it, is the steroid most likely to be prescribed to a patient at diagnosis (487). A study of 140 patients found that high initial doses of corticosteroids followed by gradual reduction in dose resulted in 98.4% of the patients in the study having

complete remission of symptoms within five years (515). While all of the patients on the study were receiving steroids, many were receiving adjuvant therapy as well, which makes it difficult to definitively conclude that the success of the study was a result of steroid treatment alone. As with any drug use, long term use of steroids is associated with side effects ranging in severity, including musculoskeletal, gastrointestinal, and cardiovascular side effects (516). One study concluded that 19 of the 21 patients enrolled had hyperglycemia the first day after steroid therapy and that 36% of those patients became diabetic after 8 weeks of treatment, however because the number of patients enrolled in the study is low further studies are required to fully understand the prevalence of treatment induced diabetes in PV patients(517). A retrospective cohort study assessed the glucocorticoid-related adverse event (GAE) rate in PV treatments and determined that the GAE rate was 0.46 events per patient-year and that a higher risk was associated with higher doses of treatment (518). Even with complete remission of symptoms and continued treatment with steroids, patients often relapse and become resistant to the steroid treatment (511). Thus, while we have seen great success using steroids as a treatment option for PV, patients can experience relapse and become resistant to further steroid treatment, thus there is a great need to improve the treatment options available for patients suffering from this disease.

Non-steroid immunotherapies have become a mainstay in PV treatment. Immunosuppressants such as azathioprine, (Aza) mycophenolate mofetil (MMF), and cyclophosphamide, are now being used to reduce the production of autoantibodies. Many of these drugs are used in combination with steroids as they are considered “steroid-

sparing”, meaning they reduce the need for steroids while simultaneously improving the symptoms of pemphigus. These drugs are now recognized as safe to use as adjuvant therapy in the treatment of PV, however there is some debate as to which drug is the most effective. One study concluded that the most effective drug used in combination with steroids was Aza when compared to cyclophosphamide and mycophenolate (519). Following this study, Aza was shown to be an effective treatment on its own in a subset of patients with mild to moderate disease in which disease is not rapidly spreading (520). Conversely, a German group published results demonstrating that MMF was as effective as Aza with less adverse side effects associated with it, however to achieve desirable results, it required a higher dose of steroid to be prescribed alongside it (521). Due to the rarity of this disease, studies of these drugs in PV patients have included small numbers of patients. Thus to fully understand which drug is the most beneficial there is a need for a larger comprehensive study of these drugs used in combination with steroids as well as on their own.

Rituximab (RTX) is a humanized antibody targeting CD20, consequently selectively targeting and depleting B cells (522). It was first tested for use in PV treatment in 2002 in a woman whose disease rapidly progressed, despite high doses of prednisone and Aza, and resulted in a dramatic reduction in symptoms (523). These results indicated that RTX may be a pivotal new therapy for PV. Currently, RTX is used to treat PV patients who have relapsed or that require high doses of steroid to suppress symptoms (524). RTX on its own does not result in complete remission or relapse potentially due to persisting memory B cells or long-living plasma cells capable of maintaining autoantibody production (524). Prednisone treatment in combination with a single Rtx treatment resulted

in the complete remission of symptoms in 18 of 21 patients within 3 months, demonstrating that a single cycle of rituximab is an effective therapy for PV (525). Additionally, a meta-analysis of 578 patients concluded that 76% of patients achieved complete, long lasting remission with one cycle of RTX, solidifying RTX as an efficacious treatment for PV (526). Therapies for PV have greatly improved since the steroids used in the 1950's accordingly, with proper treatment, the fatality of PV has greatly decreased.

6.3 Bench

6.3.1 Models and techniques to study PV

6.3.1.1 Human Tissue

As early as the 1970s acantholysis was reproduced *in vitro* by growing normal human skin in the presence of patient sera (504). Sheets of skin were placed on lens paper floating on the surface of culture medium containing sera from PV patients. Since then, investigators have continued to use this model to study the mechanisms of acantholysis, leading to key observations such as that blistering can occur without complement from the immune system (527). These tissue cultures have been used for electron microscopy studies of desmosomal structure after PV treatment (528) as well as to study the impact of drugs on PV induced acantholysis (529, 530). Recently, this model has been adapted such that the skin biopsies are submerged, allowing for multiple biopsies to be cultured in the same volume of media, conserving patient sera. While this technique can alter the expression of desmosomal proteins after prolonged culture, the expression remains

comparable to normal human skin if cultured for twenty four hours (531). The advantage of using a human skin culture model the data collected is likely highly translatable.

6.3.1.2 Mouse Models

Several mouse models have been used to study pemphigus vulgaris. Passive transfer of PV patient IgG or pathogenic monoclonal antibodies targeted to the EC domain of Dsg3 have resulted in pemphigus symptoms, such as intercellular spaces between desmosomes observable in mouse epidermis (532, 533). Additionally, a pemphigus mouse model was generated by transferring lymphocytes from a Dsg3-knockout mouse after immunization with Dsg3 into mice expressing Dsg3 (534). Immunization in Dsg3 knockout mice results in lymphocytes producing autoantibodies capable of recognizing mouse Dsg3, thus transferring these lymphocytes into mice expressing Dsg3 mimics PV (534). While mouse models can be useful in studying human disease they are not ideal because the results from experiments seen in mice might not hold true for humans. One way for investigators to mitigate this disadvantage of mouse models is to graft human skin onto mice. In fact, one study confirmed that injecting antibodies targeting Dsg1 and Dsg3 can induce blisters in human skin grafted onto mice (535), perhaps making this an underappreciated model for pemphigus research.

6.3.1.3 Keratinocyte Culture

Culturing primary keratinocytes or keratinocyte cell lines permit cost effective and convenient models to study PV. Primary keratinocytes, typically isolated from neonatal foreskin, were first isolated and used for PV research in 1978 and have since become commercially available (536). Primary cells can be cultured in low calcium to maintain a basal state or switch to high calcium (1.2mM) to induce differentiation (537). Additionally, investigators use HaCats, a non-tumorigenic cell line, or cell lines derived from squamous cell carcinoma. Each of these cell lines have been characterized so that the desmosomal protein expression and optimal culturing conditions are known (537). These cell lines can be cultured to a confluent monolayer then lifted from the substrate with dispase followed by the introduction to mechanical force to test the cell-cell adhesion of the monolayer. This dissociation assay can detect differences in pathogenic strength of PV patient sera and anti Dsg3 antibodies (538). Cell culture models also allow for immunofluorescence studies of desmosome structure and Dsg3 localization as well as biochemical approaches.

6.3.2 Mechanism of acantholysis

One hypothesis for how autoantibodies result in the loss of desmosomal adhesion is that the antibodies sterically hinder, or prevent *in trans* binding, between desmosomal cadherins of adjacent cells. Mapping of pemphigus antibodies through domain swapping experiments uncovers that pathogenic antibodies mainly bind to the EC1 domain of Dsgs, which is the domain responsible for *trans* interactions (164). When antibodies binding to

EC1 and EC2 are removed from patient sera through affinity purification, the patient sera was no longer able to cause acantholysis in the mouse epidermis (539). Furthermore, a monoclonal antibody to the EC1 domain of Dsg3 is capable of inducing lesions in a mouse model (441). Together, these data suggest that autoantibodies bind to the desmoglein epitope responsible for *trans* adhesion to physically block cadherin interactions thereby causing loss of keratinocyte adhesion.

Beyond steric hindrance, several signaling pathways have been implicated as contributors to pemphigus pathogenesis. Phosphorylation and activation of p38 occurs after PV treatment, and this has been demonstrated to occur in a dose dependent manner (540). Additionally, inhibition of p38 prevents blistering in mice treated with PV IgG (541). Furthermore, inhibition of p38 prevented loss of keratinocyte adhesion even though autoantibodies still bound to Dsg3 and disrupted Dsg3 *trans* binding (542). This suggests that steric hindrance alone is not enough to cause pemphigus. In addition to the p38 pathway, Rho, c-myc, and PKC signaling have all been implicated (543-547).

In addition to steric hindrance and the induction of signaling pathways, Dsg3 has been observed to undergo a series of events after PV IgG binding including endocytosis of non-junctional desmoglein, clustering of Dsg3, the formation of double membrane invaginations termed linear arrays, junctional Dsg3 endocytosis (548, 549). The endocytosis of Dsg3 appears to occur from the tips of linear arrays (548). Additionally, cholesterol depletion protected keratinocytes from loss of adhesion, suggesting that lipid rafts are of clinical significance to PV (382). Furthermore, the endocytosis of Dsg3 was demonstrated to be clathrin- and dynamin- independent (385). Structured illumination

microscopy of patient biopsies has uncovered that Dsg3 clustering occurs in patient epidermis, confirming observations seen in cell culture models (550). Additionally, linear arrays have been identified in patient biopsies (550). Together these studies suggest that autoantibodies against Dsg3 cause loss of cell adhesion in PV through a combination of steric hindrance, induction of signaling pathways, and the endocytosis and downregulation of Dsg3.

6.4 Outlook

Currently, our understanding of how autoantibody titer correlates to disease progression is making it difficult for clinicians to make decisions about drug administration and patient treatment. While our understanding of pemphigus has greatly improved through recent research, there is a need to link clinical data of disease progression, such as PDAI and ELISA scores, to the *in vitro* models to study the mechanisms of disease progression in a larger scale. These studies could validate certain *in vitro* models and provide new insights to pathomechanisms of PV. The next chapter of this dissertation compares ELISA and PDAI data from 23 patients to determine if autoantibody titer correlates to disease severity. Additionally, we aim to determine if observations seen *in vitro* have pathological relevance by comparing data acquired using serum from the 23 patients to PDAI and ELISA scores.

Chapter 7

Pemphigus Vulgaris Dsg ELISA scores are associated with PDAI and loss of keratinocyte adhesion *in vitro*

This chapter is adapted from

Amber L. Caldara^{1,2}, Maxine F. Warren^{1,3}, Alice Cho^{4,5}, Stephanie E. Zimmer^{1,6}, Ron J. Feldman³, Robert A. Swerlick³, Jens P. Wrämmert^{5,6}, and Andrew P. Kowalczyk^{1,7,8}

1 Department of Cell Biology, Emory University School of Medicine, Atlanta, Georgia, United States of America 2 Graduate Program in Cancer Biology, Emory University School of Medicine, Atlanta, Georgia, United States of America 3 Department of Dermatology, Emory University School of Medicine, Atlanta, Georgia, United States of America 4 Graduate Program in Immunology and Molecular Pathogenesis, Emory University School of Medicine, Atlanta, Georgia, United States of America 5 Department of Pediatrics Division of Infectious Disease, Emory School of Medicine, Atlanta, Georgia, United States of America 6 Emory Vaccine Center, Emory School of Medicine, Atlanta Georgia, United States of America 7 Graduate Program in Biochemistry, Cell and Developmental Biology, Emory University School of Medicine, Atlanta, Georgia, United States of America 8 Winship Cancer Institute, Emory University School of Medicine, Atlanta, Georgia, United States of America

In preparation

7.1 Abstract

Pemphigus vulgaris (PV) is an autoimmune bullous skin disease characterized by severe epidermal blistering and mucous membrane erosions. PV is caused by antibodies directed against the desmosomal cadherin desmoglein 3 (Dsg3), and in cases involving the skin, both Dsg3 and Dsg1. PV can be assessed clinically using the Pemphigus Disease Area Index (PDAI) and using an ELISA for Dsg IgG titers in patient sera. *In vitro*, PV IgG activity can be investigated by incubating normal human keratinocytes with PV patient IgG and monitoring changes in desmosomal protein organization and overall strength of cell-cell adhesion using a dispase-based cell-cell dissociation assay. However, the relationship between clinical PV assessments and *in vitro* activity of patient IgG have not been systematically studied. In the present study, we compared the relationship between the *in vitro* pathogenicity of PV IgG from 23 patients to their PDAI score and ELISA titers. Overall, Dsg1 ELISA values showed a stronger correlation with PDAI scores ($p < 0.01$) when compared to Dsg3 ELISA ($p < 0.02$). However, the sum of Dsg3 and Dsg1 ELISA values exhibited a highly significant correlation to PDAI ($p < 0.0005$). Interestingly, the loss of cell-cell adhesion strength as assessed using *in vitro* dispase cell dissociation assays exhibited a positive correlation with Dsg3 ELISA titers ($p < 0.005$), supporting the validity of the dispase assay as a measure of PV pathogenicity. These findings confirm the association of Dsg ELISA values with PDAI and establish a relationship between Dsg IgG titers in patients and loss of adhesion in cultured keratinocytes.

7.2 Introduction

Pemphigus vulgaris (PV) is an autoimmune bullous skin disease characterized by severe epidermal blistering and mucosal membrane erosions. Its incidence is estimated to be 0.1-0.5 cases per 100,000 people per year, with an average age of onset between 40 and 60 years (450). Although rare, PV can be a devastating diagnosis for patients, and in fact was considered almost universally fatal before the advent of immunosuppressing agents, which are currently the mainstay of treatment (512, 513). PV is caused by antibodies directed against desmosomal cadherins, a class of cell-cell adhesion proteins with critical roles in skin biology and pathophysiology. Specifically, desmogleins 1 (Dsg1) and 3 (Dsg3) are targeted. This attack on desmosomal integrity results in loss of keratinocyte cohesion, or acantholysis, which translates clinically into intraepidermal blistering that can be extensive and debilitating.

PV patients can be separated into two variants, mucosal dominant and mucocutaneous (451). Mucosal dominant patients present mucosal erosions and mainly have auto antibodies targeting Dsg3. Many of these patients progress to mucocutaneous disease in which erosions are present in both the mucosal surfaces as well as the skin. Patients who progress to the have skin blisters have antibodies targeting Dsg1 as well as antibodies to Dsg3 (451, 506). Currently, there are two measurements used to monitor disease severity: Pemphigus Disease Area Index (PDAI) score, a validated scoring system that standardizes the clinical evaluation of PV across institutions and physicians, and enzyme-linked immunosorbent assay (ELISA), which is the standard method for measuring the level of antibodies present in sera (491, 506). Some studies report that

ELISA scores for antibodies against Dsg1 correlate better with disease severity (163, 507, 510), while other reports that ELISA scores for antibodies against Dsg3 correlate better with disease severity for mucosal dominant PV patients (163, 509). A recent international study revealed that Dsg1 and Dsg3 ELISA scores correlated with PDAI at diagnosis, but that these correlations, particularly Dsg3 ELISA, were no longer significant after treatment (551). Thus, there is some uncertainty about how aggressively to treat PV patients based on either PDAI or ELISA values alone. To address this gap in knowledge, we used clinical data from 23 patients diagnosed with PV and compared ELISA scores to PDAI.

The precise mechanism by which PV IgG ultimately leads to loss of cellular cohesion in patient skin has not been fully elucidated. This is largely because our current understanding of PV pathomechanisms is derived almost exclusively from *in vitro* studies. Such experiments in the past have demonstrated that exposure of cultured keratinocytes to pathogenic PV antibodies triggers a reproducible sequence of events culminating in cell separation: clustering of cell surface Dsg3, endocytosis of these clusters, and their disassembly within the cell (385, 548, 549). Recently, we confirmed that desmosomes within patient epidermis appeared altered (550). However, much is still unknown about how the processes observed *in vitro* correlate with disease progression in patients. Thus, the literature remains incomplete regarding the mechanisms of PV-induced desmosomal breakdown in patient skin. We directly tested the pathogenicity of patient IgG using *in vitro* assays of cell-cell adhesion strength and to determine whether these quantitative assessments of desmosomal mechanical disorganization correlated with either the clinical (PDAI) or molecular (ELISA) measures of disease severity.

The overarching hypothesis underpinning these studies is that anti-desmoglein antibodies in PV patients cause alterations in desmosomal adhesion that are directly related to and are indicative of disease severity. In this paper, we utilize a combination of pemphigus patient clinical assessments and *in vitro* models of disease to yield new insights into PV pathomechanisms and form a foundation for the development of new diagnostic criteria for this devastating skin disease.

7.3 Results and discussion

7.3.1 Epidemiology and clinical phenotype

25 samples from 23 patients were included in this study. Samples from the same patient were taken at different points during their treatment and disease progression. The average age was 47.3 years with a standard deviation of 10.5 years (Table 7.1). The oldest patient was 68 years while the youngest was 25, while 9 (39.1%) were female and 14 (60.9%) were male. Interestingly, our study has a higher percentage of males than females, which is atypical as many studies report that PV afflicts more females than males. Ten (43.5%) patients and 11 (44%) samples were mucosal dominant while 14 (56.5%) patients and 15 (56%) samples were mucocutaneous. Disease severity varied by patient as determined by PDAI and ELISA scores (Figure 7.1). Each patient was given a unique symbol with mucosal dominant patients depicted as squares and mucocutaneous patients are depicted with circles (Figure 7.2).

7.3.2 Total ELISA score correlates with PDAI

While the Pemphigus Disease Severity Index (PDAI) score has been validated in a number of studies, few have compared PDAI scores to ELISA titers. It has been shown that, in general, mucosal dominant patients mainly have antibodies against Dsg3 while mucocutaneous patients have antibodies against both Dsg3 and Dsg1 (451, 506). As ELISA scores are being more widely used by clinicians in the diagnosis of PV, there is a need to fully understand how these scores correlate with disease progression as measured by PDAI. When comparing all 25 samples, both Dsg3 ($r=.4604$, $p=.0118$) and Dsg1 ELISA scores ($r=.5306$ and $p=.0034$) demonstrated a moderate positive correlation with PDAI. Consistent with previous reports, Dsg1 ELISA correlated with PDAI more strongly than Dsg3 (Figure 7.3 A & B). Interestingly, cumulative Dsg1 and Dsg3 ELISA values were strongly associated with high PDAI scores ($r=.6562$, $p=.0002$). These results suggest that total Dsg3 and Dsg1 ELISA values might have a higher clinical relevance than either the Dsg1 antibody titer or Dsg3 antibody titer alone.

We next sought to determine if these correlations hold true for the two variants of PV, mucosal dominant (mPV) and mucocutaneous (mcPV). Interestingly autoantibody titers only demonstrated weak to negligible correlations when compared to the PDAI for mPV patients (Figure 7.3 D-F). Our data suggest that for mPV patients, neither Dsg3 nor Dsg1 autoantibody titers are good predictors of disease severity. Conversely for mucocutaneous patients, Dsg1 autoantibody titers demonstrated a high correlation ($r=.8097$, $p=.0004$) and Dsg3 titers demonstrated a moderate association ($r=.5061$, $p=.0335$) with PDAI (Figure 7.3 G & H). These results confirm reports that for pemphigus

patients with cutaneous disease, Dsg1 autoantibody titer is a better predictor of disease severity. Interestingly, the comparison between PDAI and Total ELISA yielded the most highly correlative result for mucocutaneous patients ($r=.8163$, $p=.0003$, Figure 7.3 I). These results suggest that for patients suffering with cutaneous disease, clinicians could consider a total ELISA score in their diagnostic assessments and treatment plans. Recently, a large scale study demonstrated that prior to treatment mucosal dominant patients demonstrated a correlation between PDAI and Dsg3 ELISA, however this association was lost after treatment was administered (551). Thus, it may be that our study did not reveal an association of Dsg3 autoantibody titer with PDAI because the samples used in our study were collected after patients started treatment.

7.3.3 DSG3 ELISA correlates with fragmentation assay

Keratinocyte monolayer fragmentation assays have been used to study the pathogenicity of PV autoantibodies (538, 552, 553). In this assay, higher levels of keratinocyte monolayer fragmentation after treatment with an antibody or PV sera is indicative of more severe loss of cell adhesion strength. However, no studies have correlated the degree of fragmentation seen *in vitro* to clinical measures of disease progression or autoantibody titers. To determine if the *in vitro* disperse fragmentation assay correlates with PDAI scores or ELISA scores, we purified PV IgG from 25 samples and compared keratinocyte monolayer fragmentation to clinical scores. Prior to treatment with PV IgG, keratinocytes, which were cultured in low calcium media (50uM), were switched to high calcium media (550uM) for 3 hours to allow desmosome formation. Note that this

culture method results in monolayers expressing predominantly Dsg3 and low levels of Dsg1 (537). Next, we treated the keratinocytes with PV IgG for 6 hours before releasing monolayers from the substrate and subjecting samples to mechanical force by gently transferring monolayers to epindorf tubes that were then taped to an orbital shaker and allowed to shake for one minute. We then generated a disassociation index score for each sample by normalizing to normal human IgG and a known pathogenic AK23 control (Figure 7.4 A & B). AK23 is a well characterized pathogenic Dsg3 monoclonal antibody that has been demonstrated to cause loss of adhesion in disassociation assays (441). Next we compared the disassociation index scores to Dsg3 ELISA scores. We demonstrate that Dsg3 titers demonstrate a moderate but statistically significant correlation to the degree of fragmentation ($r=.5428$, $p=.0025$), validating the Dsg3 based disassociation model we and others have used to study PV (Figure 7.3 C). Interestingly, when we analyzed mPV patients alone the disassociation index demonstrated a high and significant correlation with Dsg3 ELISA ($r=.7212$, $p=.0117$, Figure 7.3 D). For mcPV patients, the statistical analysis yielded a low correlation, though this correlation was significant ($r=.4429$, $p=.0501$). It is possible that a study with more patients could uncover a moderate and statistically significant relationship. Overall, these data confirm a relationship between Dsg3 autoantibody titer and loss of cell adhesion in keratinocyte cell culture, thus validating the disassociation assay as an assessment for mPV patient disease severity.

7.3.4 PDAI correlates to disassociation assay for mucosal dominant patients

We next wanted to determine if the disassociation index yields results that relate to patient severity as measured by PDAI. The total patient pool revealed a negligible relationship between PDAI and the degree of fragmentation ($r=0.2380$, $p=0.1390$, Figure 7.5A). However, analysis of the mucosal dominant patients only revealed a moderate and statistically significant correlation ($r=.6319$, $p=.0286$, Figure 7.5B). Conversely, mucocutaneous patients revealed no correlation between PDAI and the disassociation index ($r=-.0132$, $p=.4835$, Figure 7.5 C). We previously concluded that Dsg3 autoantibody titers correlate to the disassociation assay (Figure 7.3), thus it is likely that the mucosal dominant patients reveal a correlation between PDAI and the disassociation assay because they predominantly have Dsg3 autoantibodies. These establish a relationship between disease severity for mucosal dominant PV patients and the degree of fragmentation seen in a keratinocyte disassociation assay.

7.3.5 Concluding remarks

The overarching goal for these studies is to determine if anti-desmoglein antibodies in PV patients cause alterations in desmosomal adhesion that are directly related to and are indicative of disease severity. Additionally, we sought to determine if ELISA scores directly correlate with disease severity as measured by the now validated Pemphigus Disease Area Index (PDAI). We isolated PV IgG from 25 serum samples from 23 patients and used these samples to perform in vitro experiments and compare the data to clinical

measures. Indeed we found Dsg1 ELISA to correlate better with PDAI than Dsg3 ELISA, particularly with patients suffering from cutaneous disease. Furthermore, ELISA scores did not correlate with PDAI for mucosal dominant patients. However, it is possible that correlation is lost after patients start receiving treatment as clinical symptoms can be alleviated without a decrease in autoantibody titer (551, 554). Additionally, we propose that the sum of Dsg1 ELISA and Dsg3 ELISA scores is a better predictor of disease severity. This value could be used by clinicians to better determine treatment options. Additionally, we conclude that an *in vitro* cell-cell disassociation assay correlates with Dsg3 ELISA values for the total patient pool and PDAI for mucosal dominant patients, validating the use of the assay and confirming that Dsg3 autoantibodies lead to loss of keratinocyte adhesion.

7.4 Materials and Methods

Study population

Study subjects were recruited for enrollment if they were seen at the Emory Dermatology Clinic between 2012-2018 and carried a diagnosis of pemphigus vulgaris, confirmed by both intraepidermal anti-Dsg3 staining on direct immunofluorescence and by anti-Dsg3 antibody titer of >0 by ELISA. Relevant clinical information including sex, date of birth, PDAI scores, ELISA levels of Dsg1 and Dsg3 autoantibodies, and type and duration of treatment were obtained either from chart review or at the time of enrollment and recorded.

Permission for use of all stored samples was obtained from Emory University's Institutional Review Board.

Purification of IgG.

All blood specimens were drawn in the Emory Dermatology Clinic by a certified phlebotomist. Specimens were collected from enrolled subjects into five red top vacutainer tubes and allowed to clot for 30 minutes in a vertical position. Tubes were then centrifuged for 15 minutes, and sera was pipetted off from the top into a single plastic transfer tube labeled with the patients study ID number and stored at -80°C. Samples were later thawed to room temperature, and IgG was purified using the Melon purification kit (Thermofisher 45206). Concentration of the total recovered IgG was measured using a Nano drop lite from thermofisher.

Cells and culture conditions

Primary human keratinocytes (HKs) were isolated as described by Calkins *et al* and cultured in KBM-Gold basal medium (100 µM calcium) supplemented with KGM-Gold Single-Quot Kit (Lonza, Walkersville, MD). To make low calcium media, calcium was removed from standard keratinocyte growth media using BT Chelex 100 resin (Bio-rad #143-2832) and supplemented with CaCl₂ to reach 30mM.

Surface Turnover Experiments (preliminary data discussed in chapter 8)

HKs were grown to ~70% confluence in 12 well ibidi cell culture dishes and cultured in high calcium (550uM) media overnight. Cells were labeled with 10ug/ml AK23 for a half hour at 4°C. Cells were then exposed to either 200ug/ml of PV patient IgG or normal human control (NH) IgG for three hours at 37 degrees. An anti-mouse 488 secondary was used. Border intensities were determined by drawing linescans along cell borders in Image J.

Endocytosis Assay (preliminary data discussed in chapter 8)

HKs were grown to confluence in 48 well cell culture dishes and cultured in high calcium overnight. Cells were labeled with AK23-488 at four degrees for 30 minutes. Cells were then treated with 200ug/ml PV IgG for three hours. Extracellular AK23-488 was quenched with an anti-488 antibody (Invitrogen A-11094) for an hour at four degrees. Cells were then trypsinized and stained with Live/Dead Aqua (ThermoFisher L34957). A minimum of 5,000 cells were analyzed on a BD LSRII flow cytometer and analyzed using FlowJo software. The Mean fluorescence intensity (MFI) was then normalized to a four degree quench control, in which no endocytosis occurred, to remove any remaining background from an incomplete quench.

Dispase-based fragmentation assay

HKs were cultured to 100% confluence in 24-well tissue culture plates and switched to 50 μ M calcium to prevent any junction assembly for 16-18 hrs prior to switching to 550 μ M calcium for 3 hrs to allow for junction assembly. HKs were then exposed to NH or PV IgG for 6hrs at 37°C. Monolayers were removed from the cell culture substrate using the enzyme dispase and gently washed twice with PBS+ before transfer to an epindorf tube. Monolayers were exposed to mechanical force by being taped to an orbital shaker to for 1-2 minutes to induce fragmentation. Fragments were fixed in paraformaldehyde and stained with Methylene blue prior to imaging using (CTL, cellular technologies). The number of monolayer fragments was then counted. The following formula was used to normalize fragments between replicates and generate the dissociation index score with AK23 as the positive control and Normal Human (NH) treatment as then negative control

$$\frac{\#Fragments_{sample} - \#Fragments_{negative\ control}}{\#Fragments_{positive\ control} - \#Fragments_{negative\ control}}$$

Data Analysis and Statistical Methods:

One tailed, Non-parametric Spearman tests were used to identify correlations between parameters. A spearman correlation coefficient (r) of +1 is a perfect positive correlation while -1 is a perfect negative correlation. The chart below describes our interpretation of the correlation coefficient (555).

r value	Interpretation
± 0.90-1.0	Very high correlation
± 0.70-0.90	High correlation
± 0.50-0.70	Moderate correlation
± 0.30-0.50	Low correlation
± 0.00-0.30	negligible or no correlation

Low p-values indicate that the observed correlation is real while a high p-value indicates that the correlation is likely random. All statistical tests were performed using GraphPad Prism 7.03 Software. We next consulted with Dr. Subir Goyal in the Biostatistics and Bioninformatics core at Emory University to confirm our statistical analysis prior to submission.

CONFLICT OF INTEREST

The authors declare no competing financial interests

7.6 Acknowledgements

The authors would like to thank Sue Manos and Bridget Bradley for collecting samples from patients. This work was supported by grants (R01AR048266, R01AR048266-13S1, and R01AR050501 to A.P.K.) and a Gilliam fellowship from the Howard Hughes Medical Institute (awarded to A.L.C). Additional support was provided by the Emory Flow Cytometry Core.

Descriptive Statistics for Patients

Mean age \pm SD ¹	47.26 \pm 10.51
Age Range (years)	25-68
Sex n(%)	
Male	14 (60.9%)
Female	9 (39.1%)
Clinical Characterization n(%)	
Mucosal Dominant	9 (39.1%)
Mucocutaneous	14 (60.9%)
Severity ² n(%)	
Mild <12	8 (34.8%)
Moderate 12<x<25	5 (21.7%)
Severe >25	9 (39.1%)
Unknown	1 (4.3%)

1) SD: Standard Deviation, 2) PDAI scores

Table 7.1 Descriptive Statistics for Patients.

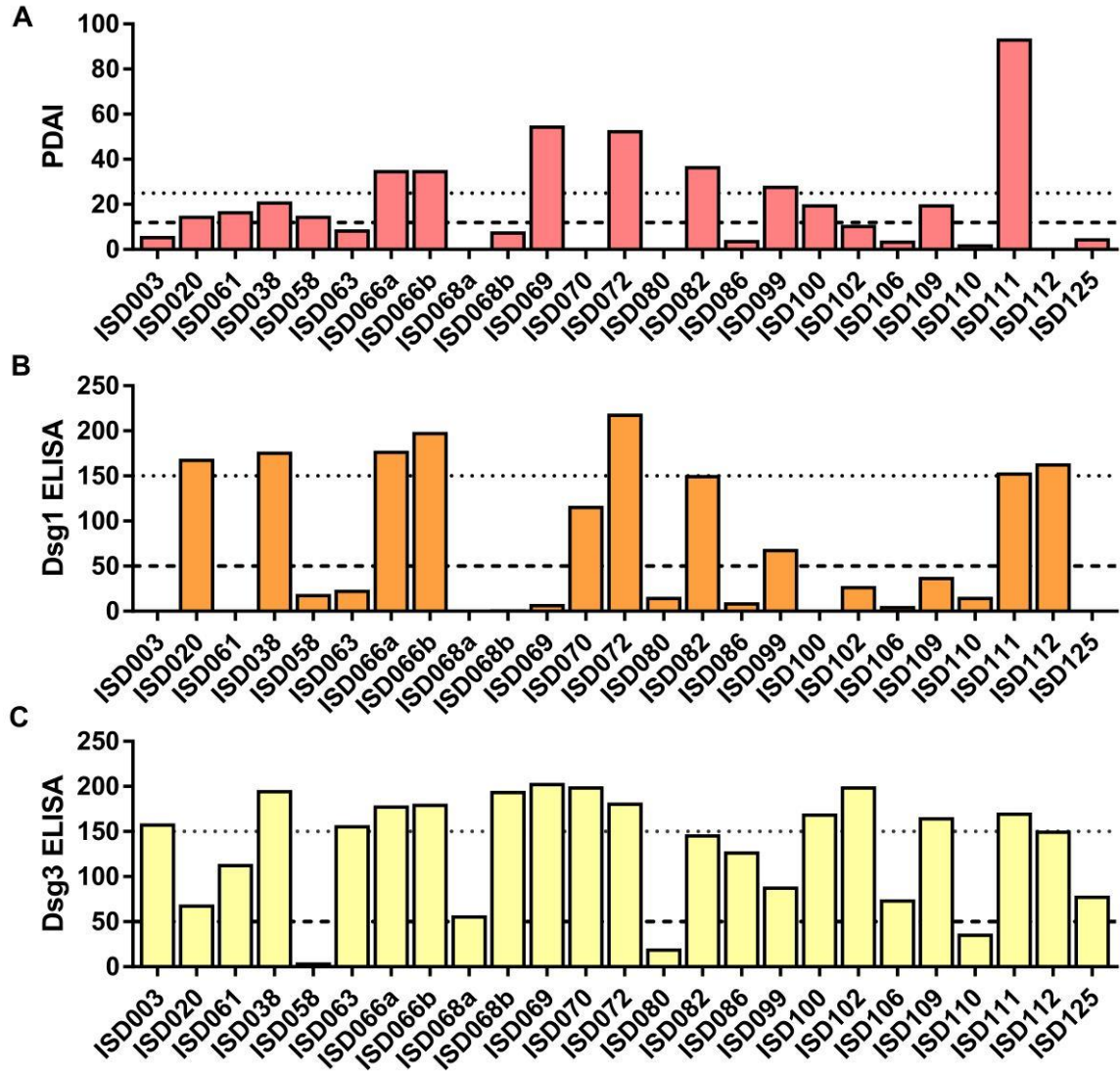


Figure 7.1 Patients have a range of PDAI and ELISA scores. A) Patient PDAI scores range from 0 to 93.6. Patient ISD112 has no recorded PDAI. B) Dsg1 ELISA scores range from 0 to 219. C) Dsg3 ELISA scores range from 5 to 204. Below the dashed line represents mild or low scores, between the two lines represents moderate scores, and above the dotted line represents high or severe scores.


























Sample	Mucosal Dominant	Shape
ISD003	Yes	
ISD020	No	
ISD025	Yes	
ISD038	No	
ISD058	Yes	
ISD063	No	
ISD066a	No	
ISD066b	No	
ISD068a	Yes	
ISD068b	Yes	
ISD069	Yes	
ISD070	Yes	
ISD072	No	
ISD080	Yes	
ISD082	No	
ISD086	No	
ISD099	No	
ISD100	Yes	
ISD102	No	
ISD106	No	
ISD109	No	
ISD110	No	
ISD111	No	
ISD112	No	
ISD125	Yes	

Figure 7.2 Patients have unique symbol assigned. 25 samples were used throughout this study. Mucosal dominant patients are coded as squares of varying colors and patterns while mucocutaneous patients are circles with varying colors and patterns. This allows a single patient to be tracked throughout the figures.

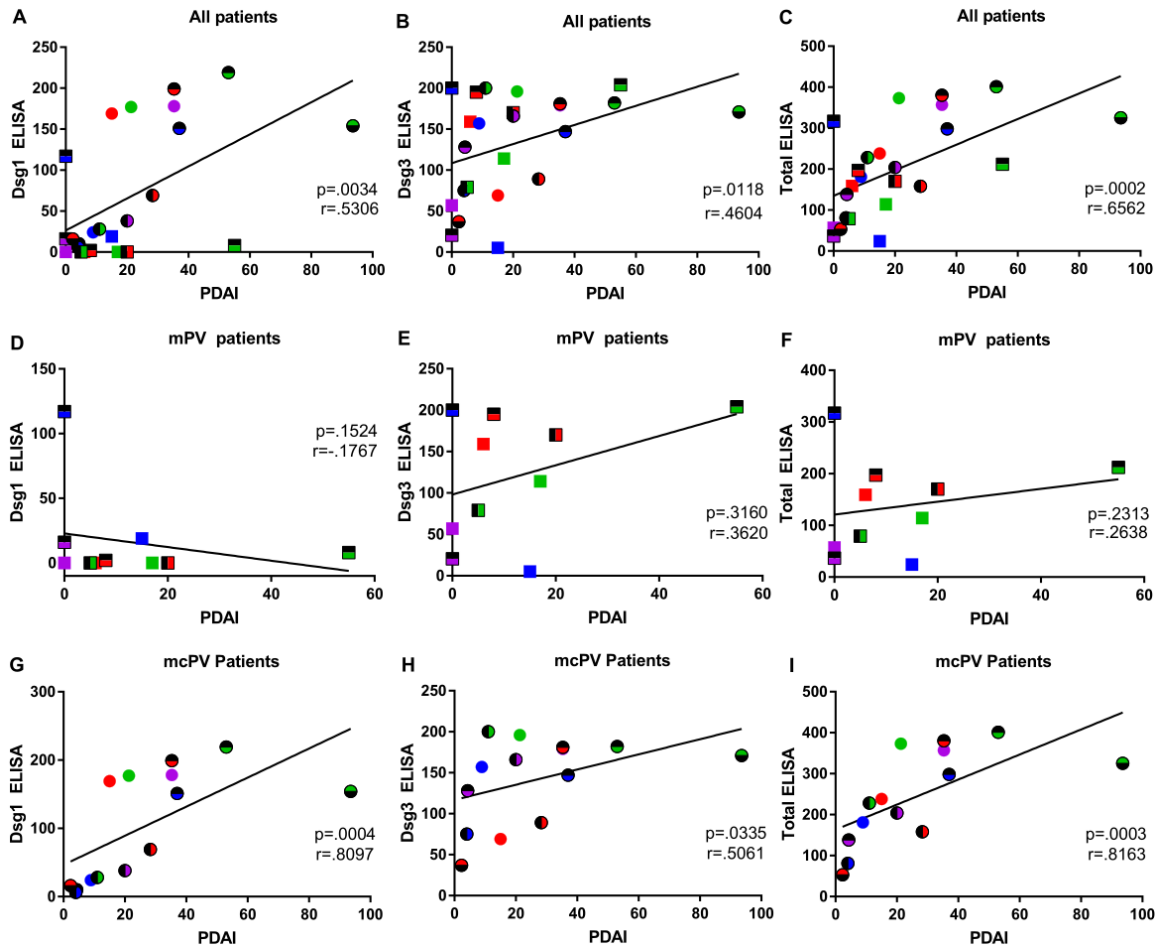


Figure 7.3 Total ELISA correlates with PDAI. Both Dsg1 ELISA (A) and Dsg3 ELISA (B) showed a significant correlation with PDAI for all patients. C) The sum of Dsg3 and Dsg1 ELISA scores to generate a Total ELISA score yielded the most significant correlation with PDAI. D) Dsg1 ELISA does not correlate with PDAI for mPV patients. E) Dsg3 ELISA does not correlate with mPV PDAI. F) Total ELISA does not correlate with mPV PDAI. G) PDAI shows a statistically significant correlation to Dsg1 ELISA for mcPV patients. H) Dsg3 ELISA does not correlate with PDAI for mcPV patients. I) The sum of Dsg3 and Dsg1 ELISA scores correlates with PDAI for mcPV samples.

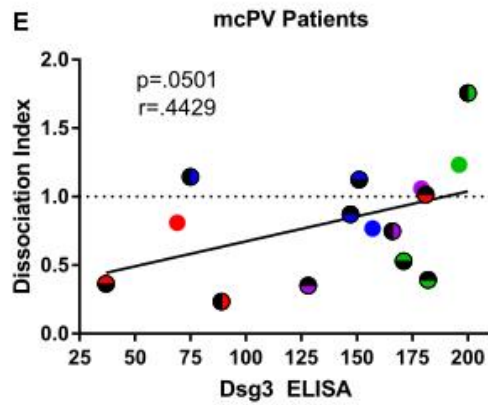
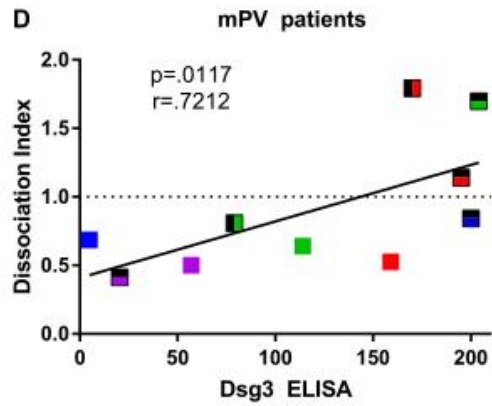
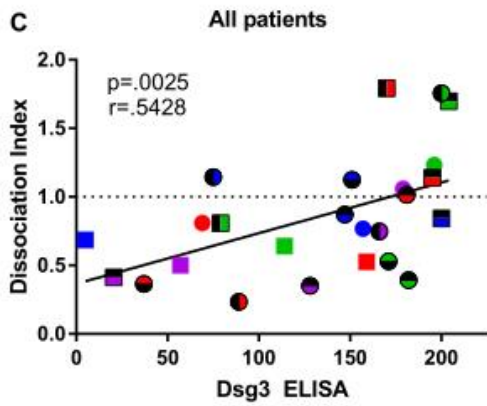
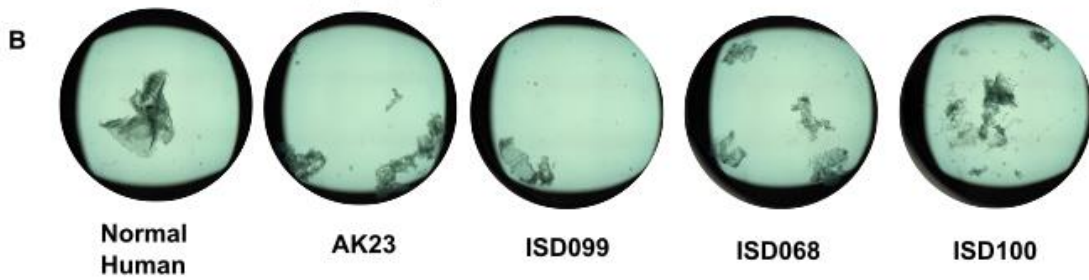
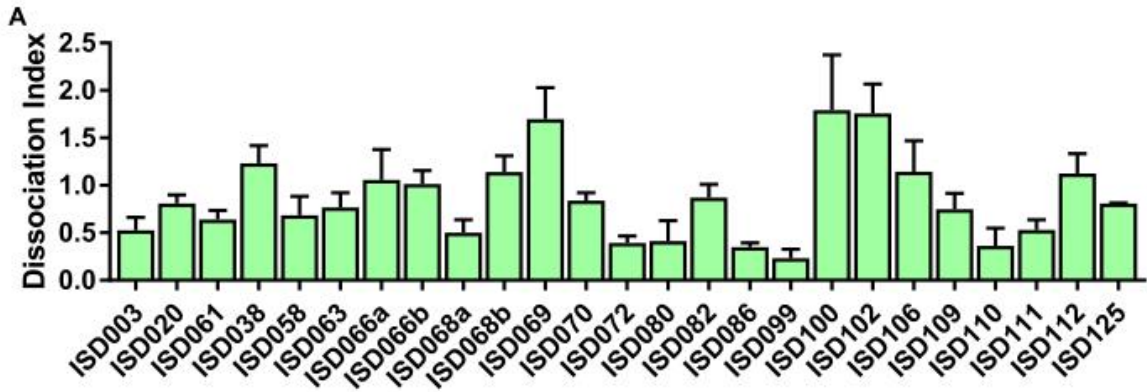


Figure 7.4 Disassociation Index correlates with Dsg3 ELISA. A) The 25 patients demonstrate a range of pathogenicity as determined by the disassociation index. Four replicates are represented and SEM is shown. B) Representative images of monolayers after the application of mechanical force. Monolayers treated with normal human serum remain largely intact while monolayers treated with AK23 (positive control) or Patient IgG fragment. C) Dsg3 ELISA correlates with disassociation index score. D) Mucosal dominant patients demonstrate a correlation between Dsg3 ELISA and disassociation index score. E) Mucocutaneous patients do not demonstrate a correlation between Dsg3 ELISA and disassociation index score

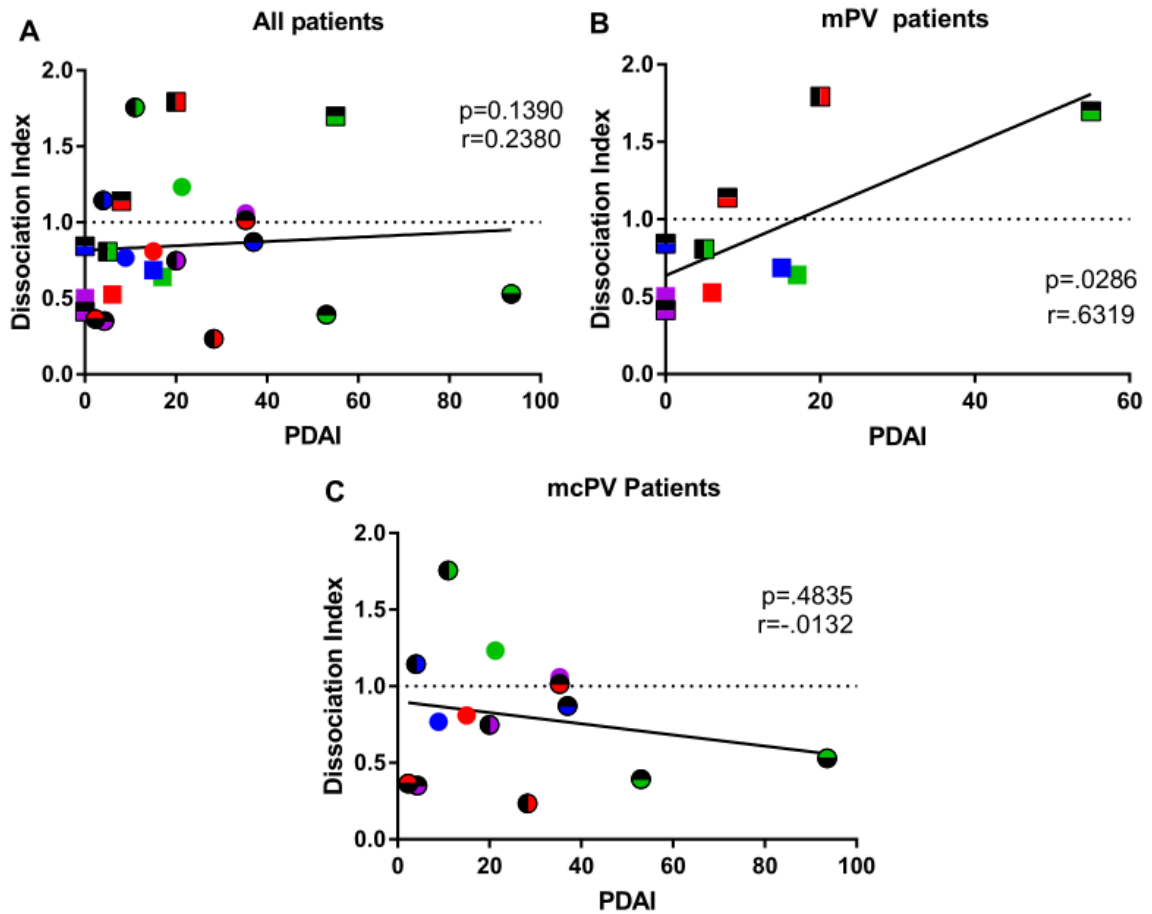


Figure 7.5 Disassociation Index correlates with PDAI for mucosal dominant patients. A) The total patient pool demonstrates no correlation between PDAI and disassociation index. B) Mucosal dominant patients demonstrate a high and statistically significant correlation between PDAI and disassociation index. C) Mucocutaneous patients show no relationship between PDAI and disassociation index.

Chapter 8

Summary and future directions

Section 8.1 Summary of dissertation work

This dissertation started by studying mechanisms of desmosome assembly. In chapter 3 we presented findings that demonstrated that the transmembrane domain of desmogleins is critical for lipid raft association while palmitoylation is not. Furthermore we uncover the importance of the lipid raft association of Dsg1 in desmosome formation, as failure to associate with lipid rafts results in a loss of Dsg1 association with the desmosome and the development of SAM syndrome. Prior to the research conducted in this dissertation, several labs had shown that all of the major desmosomal proteins associate with lipid rafts, however we had no understanding of the importance of this association in desmosome structure or function. Additionally, these findings uncovered important pathomechanisms for the human disease SAM syndrome. Additionally, the work presented in chapter 5 greatly increase our understanding of how desmogleins coalesce with other desmosomal proteins and lipids to form a mature, robust desmosome.

The work presented in this dissertation then focused on understanding mechanisms of desmosome disassembly, particularly in the context of a severe desmosome associated skin disorder, pemphigus vulgaris. In a study of 23 pemphigus vulgaris patients, we

compared the now validated Pemphigus Disease Area Index system of determining disease severity to Dsg ELISA scores. We found that Dsg1 ELISA scores better correlated with PDAI, confirming results other labs have seen. Additionally, we propose that the sum of Dsg1 and Dsg3 ELISA scores is a better measure of disease severity than either score alone. Lastly, we conclude that the Dsg3 ELISA score of a patient is correlated to the loss of adhesion in keratinocytes as measured by a Dsg3 based disassociation assay, validating the use of the assay in studying PV pathogenicity. These conclusions act as a platform on which further studies can build. Below I will outline some future avenues for this research and key gaps in our knowledge that were revealed by this work.

Section 8.2 Future directions

8.2.1 Does Dsg3 endocytosis or loss of surface Dsg3 in keratinocytes after PV IgG treatment correlate to PDAI?

When cultured keratinocytes are exposed to PV IgG, Dsg3 undergoes endocytosis and subsequent degradation, resulting in a loss of surface Dsg3 after PV IgG treatment (548, 549). To determine if Dsg3 endocytosis correlates with PDAI or Dsg3 ELISA scores of patients we performed a flow based endocytosis assay with the 25 samples used in chapter 7. Keratinocytes were labeled with a 488 conjugated monoclonal antibody against Dsg3 prior to PV IgG treatment for three hours. Prior to trypsinization, extracellular 488 was quenched using an antibody against Alexa Fluor 488. Cells were analyzed using flow cytometry and the mean fluorescence intensity (MFI) represents the amount of Dsg3

internalized. The MFI did not correlate with any of the clinical parameters and this held true when mPV and mcPV patients were analyzed separately (not shown). We hypothesized that the observed lack of correlation between MFI and Dsg3 endocytosis was due to a combination of the absence of endocytosis in samples with low pathogenicity and degradation of the labeled IgG tracer in highly pathogenic samples. In fact, when viewed by immunofluorescence some of the patients with low MFI scores (ISD112) lost all border staining, indicating severe desmosome disruption, but no internalized Dsg3 could be viewed after a three hour treatment with patient IgG (Figure 8.1 A&B). However, other patients (ISD068a) demonstrated a low MFI and maintained border staining, meaning that they Dsg3 had not undergone endocytosis for these patients after 3 hours (Figure 8.1 A & B). We predicted that patients with high Dsg3 autoantibodies, greater than an ELISA score of 150, would demonstrate a correlation with the endocytosis assay while patients with low Dsg3 autoantibodies would not. In fact, patients with high Dsg3 ELISA scores correlated with the endocytosis assay ($r=.5963$, $p=.0134$, Figure 8.1). Interestingly, some of the patients with low Dsg3 ELISA scores demonstrated high levels of Dsg3 endocytosis, perhaps indicating that those patient seras contain highly pathogenic antibodies capable of inducing endocytosis. Prior to drawing final conclusions, this assay needs to be repeated a minimum of 2 more times. Additionally, we predict that a longer treatment with PV IgG would result in a significant correlation for patients with low Dsg3 titers, and thus the experiment should be repeated with varying incubation times with PV IgG.

In addition to endocytosis, the loss of Dsg3 at the cell membrane and cell borders has been observed after keratinocytes are treated with PV IgG (548, 549). To determine if

the loss of Dsg3 at cell-cell borders is indicative of patient disease severity, we labeled keratinocytes with a monoclonal antibody to Dsg3 followed by a three hour treatment with patient IgG. After fixation, we used an anti-mouse 488 secondary to stain for the Dsg3 remaining on the cell surface. ROIs were drawn along the cell-cell borders and the average fluorescence intensity was then used for subsequent statistical analysis. We would predict that a lower fluorescence intensity would correlate with more pathogenic patient samples. However, the comparison of PDAI, Dsg1 ELISA, and total ELISA scores for all the patients were compared to border intensity yielded no statistically significant results (8.2 A-C & E). However, Dsg3 ELISA demonstrated a weak correlation ($r=.3478$, $p=.1038$, Figure 8.2D) to border intensity. Furthermore, the border intensity yielded no significant association with the disassociation index or the endocytosis assay (Figure 8.2 F & G). Similar to the endocytosis assay, these results are derived from a single replicate. Additionally, it is possible to introduce bias during the step in which ROIs are drawn. To combat this, the experiment will be modified such that the keratinocytes will be cultured to confluence and the fluorescence of the whole field of view will be used. Since the cells are not permeabilized at any point, the secondary will only interact with Dsg3 on the cell membrane, ensuring that all observed fluorescence is on the cell surface.

8.2.2 What is the mechanism behind the thickening of the epidermis in SAM patients?

Severe Dermatitis, Multiple Allergies, and Metabolic wasting (SAM) syndrome is a newly uncovered human disease typically caused by a complete loss of DSG1 function. Patients suffering from SAM syndrome display skin fragility that results in epidermal

erosions as well as thickening of the epidermis, suggesting a critical Dsg1 function in keratinocyte differentiation and barrier formation. Additionally, DSG1 haploinsufficiency causes epidermal thickening in the autosomal dominant skin disease striate palmoplantar keratoderma (556, 557). Moreover, downregulation of Dsg1 in an organotypic epidermal culture model resulted in an immature granular layer, supporting Dsg1 function as a contributor to keratinocyte differentiation (150). Additionally, the downregulation of Dsg1 is associated with more proliferative tumors and a worse prognosis in patients with epidermal derived cancers such as SCC and BCC (242, 245-248). Together, these data implicate Dsg1 as a key regulator of keratinocyte differentiation within the epidermis. Understanding the mechanisms behind this regulation would increase our understanding of the progression of several human diseases, including cancer, and provide potential targets for future therapeutics.

As seen in Chapter 5 we found that a patient harboring a single point mutation within the TMD of Dsg1, rather than the typical complete loss of function of Dsg1, presented with SAM syndrome including the thickened epidermis characteristic of this disease. We illustrated that this mutation causes the abrogation of lipid raft targeting and subsequent loss of Dsg1 association with desmosomes. Emerging studies report that desmogleins have functions outside of cell-cell adhesion and act as nodes in signaling pathways that regulate cellular function. Importantly, previous studies have shown that expression of DSG1 in cultured keratinocytes drives precocious differentiation (150, 558).

The mechanisms governing the activity of DSG1 in mediating differentiation are not yet fully understood. Interestingly, recent studies have shown that DSG1 suppresses

EGFR signaling to promote keratinocyte differentiation (150, 558, 559). Dsg1 binds to the protein Erbin which in turn sequesters SHOC2, an important scaffolding protein within the canonical EGFR pathway (Figure 8.3). EGFR is a receptor tyrosine kinase in the ErbB family that promotes proliferation and suppresses differentiation of epidermal cells (560). Suppression of EGFR by DSG1 results in a decline of keratinocyte proliferation and subsequent differentiation.

EGFR signaling is upregulated in numerous cancer types and these elevated levels are associated with a decrease in survival rates (561). In fact, the EGFR pathway is currently a target in some cancer therapies (562). One of the most common side effects for EGFR-targeted therapies is the development of dermatological complications. Patients can develop rashes, dry and itchy skin, or become more susceptible to infection (560). These dermatological issues are a result of abnormal keratinocyte proliferation and differentiation upon EGFR suppression (560). This highlights the importance of the EGFR pathway in proper epidermal function as well as in the development of epidermal tumors.

Lipid raft domains enhance cellular signaling by bringing individual components of a pathway together spatially and temporally (563, 564). Additionally, lipid raft association of signaling molecules such as EGFR has been shown to be critical to maintain proper cellular signaling (563, 565). Various studies report 40-70% of EGFR localizes to lipid rafts, and depletion of cholesterol results in altered EGFR signaling, further illustrating the importance of lipid rafts in the EGFR pathway (563, 565-568). These findings raise the possibility that Dsg and EGFR signaling activities may be spatially and temporally coordinated by raft association. Given that the loss of lipid raft association of

Dsg1 results in SAM syndrome, including thickened epidermis, we postulate that the epidermal-thickening phenotype found in the SAM syndrome patients from Chapter 5 may be caused by the inability of DSG1 to suppress EGFR signaling.

8.2.3 How is DSG1(G578R) acting as a dominant negative?

Typically, complete loss of function of DSG1 results in SAM syndrome while the loss of function of one copy of DSG1 is associated with comparatively less severe palmoplantar keratododerma. The patients discussed in chapter 5, however, have a single point mutation in one allele of Dsg1, and yet have developed the more severe SAM syndrome despite having one unaltered copy of the protein. Additionally, this disorder is inherited in an autosomal dominant fashion. Together, these data imply that the mutant copy of Dsg1 is acting as a dominant negative and affecting the functional ability of the wild type copy present in patient epidermis.

In figure 5.4G, immunofluorescence staining of patient epidermis reveals that Dsg1 is downregulated and mislocalized in patient epidermi and exhibits aberrant clustering on the cell borders as well as what appears to be intracellular staining. Additionally, our cell model demonstrates that the mutation found in the SAM patient results in a retention of Dsg1 in the Golgi Apparatus (Figure 5.6 G). This finding suggests that the mutant Dsg1 is acting as a dominant negative mutant by preventing proper localization of the wild type copy of Dsg1. Figure 5.4H uncovers that this SAM patient has lost about half of his Dsg1

expression, meaning that the presence of this mutation could also be altering the expression of the wild type Dsg1.

Preliminary experiments in primary keratinocytes in which Dsg1 WT or Dsg1(G578R) were expressed with adenovirus did not show any altered localization other than desmosomal proteins such as Dsg2 (data not shown). To better determine if Dsg1(G578R) acts in a dominant negative fashion by mislocalizing endogenous Dsg1 or other desmosomal proteins, both Dsg1 WT and Dsg1(G578R) must be expressed in the same cell. It would be necessary to tag each construct with a different colored fluor in order to differentiate between the constructs. We can also study the results of co-expressing these constructs on desmosome adhesion using the dispase based disassociation assay. Additionally, we now have access to Dsg null A431s and can study these constructs in a null background. We predict that Dsg1WT will rescue desmosome function while Dsg1(G578R) will not. Furthermore, if Dsg1(G578R) results in the mislocalization of Dsg1(WT) then coexpression of these constructs would allow us to observe this in the null background and we would observe less restoration to desmosome function than when Dsg1 WT is expressed on its own.

8.2.4 What is the role of lipid raft association in Dsg3 endocytosis?

In chapter 5 we concluded that lipid raft association of Dsg1 is critical for proper desmosome assembly, however we have yet to explore how this association affects desmosome disassembly and subsequent Dsg endocytosis. We are able to study Dsg3

endocytosis using a Pemphigus Vulgaris model. Shortly after treatment with PV IgG, non-junctional Dsg3 undergoes endocytosis through a lipid raft associated, clathrin and dynamin independent mechanism (385). Longer treatment of PV IgG results in Dsg3 endocytosis through large double membraned invaginations called linear arrays (548). Work from our lab as well as others have illustrated that lipid rafts are critical for this endocytosis event and that in fact, perturbing lipid rafts affects the formation of these arrays and prevents Dsg3 endocytosis.

In our initial studies we generated two Dsg3 constructs, Dsg3(ETMD) and Dsg3(CC). We found that Dsg3(ETMD) did not partition to lipid rafts, however the Dsg3(CC), a palmitoylation null mutant, still partitioned to lipid rafts as seen in Figures 5.1 and 5.2. Preliminary data in which A431s expressing these constructs were treated with PV IgG uncovered some interesting results. PV treatment of cells expressing Dsg3(Ecad) TMD resulted in disorganized linear arrays and a protection from endocytosis as determined by higher surface levels of Dsg3 when compared to cells expressing wild type (Figure 8.4). While we were unable to uncover any raft targeting defects for Dsg3(CC) in steady state cells (Chapter 5), after treatment with PV, A431 cells expressing this construct were protected from the loss of surface Dsg3. Additionally, linear arrays seen in these cells were often larger and more globular in appearance when compared to the typical linear arrays seen in cells expressing WT Dsg3. These results further highlight the importance of Dsg3 raft association for proper endocytosis of Dsg3. Further PV studies using these constructs could illuminate the specific endocytosis mechanisms by which Dsg3 is internalized.

8.2.5 What are the mechanisms of Dsg3 clustering and linear array formation in Pemphigus Vulgaris?

Domain swapping experiments unveiled that the dominant epitope for PV antibodies is in the calcium-sensitive conformational N-terminal region from amino acids 25-88 (164). Removal of antibodies targeting the EC1 domain of DSG1 in pemphigus foliaceus from patient sera prevented the loss of adhesion when injected into mice, implicating antibodies targeting the EC1 domain of desmogleins to be key in the pathogenesis of pemphigus (539). Additionally, dispase based fragmentation assays as well as mouse models have revealed that mouse monoclonal antibodies against the EC1 domain of Dsg3 can cause a loss of cell-cell adhesion and cause PV phenotypes when injected into mice (441). Furthermore, injection of AK23, a pathogenic monoclonal antibody, into skin explants causes acantholysis. Because these antibodies typically target epitopes in the EC1 domain, the adhesive interface of desmogleins, they are thought to directly inhibit desmoglein *trans* interactions (steric hinderance) and thus cause a loss of desmosomal adhesion. Interestingly, not all of these monoclonal antibodies are pathogenic, perhaps related to the epitope or domain of the desmoglein that is targeted. While there is an abundance of evidence that steric hinderance is caused by antibodies targeting the adhesive EC1 and EC2 domains, little is known about the role of antibodies targeting non-adhesive epitopes or are found to be non-pathogenic.

In Vitro studies have revealed that PV IgG causes Dsg3 clustering on the cell-cell borders both *in vitro* and in patient skin (548, 550). Interestingly, when cells were treated

with a polyclonal mixture of non-pathogenic mouse monoclonal antibodies against Dsg3, clustering of Dsg3 was induced. It has also been illustrated that direct disruption of the adhesive interface with antibodies against the EC1 domain is not required for clustering to occur (423). Additionally, when AK15 and AK19, two non-pathogenic antibodies were added together with AK23, a pathogenic antibody, border staining of Dsg3 became more punctate and more closely resembled cells treated with PV sera than AK23 alone(423). These observations imply that antibodies to multiple epitopes on Dsg3 are necessary for Dsg3 to cluster. While these studies have been informative, they have been limited in several ways. The monoclonal antibodies used in these studies were derived from a mouse model, and thus may act differently than human IgG and not accurately depict what is happening in PV patients. Second, there has been a relatively limited panel of mouse monoclonal antibodies to use for these experiments with only 2 non-pathogenic antibodies and 1 pathogenic antibody used.

Through working with collaborators Drs. Jens Wrämmert and Alice Cho, we have gained access to a large panel of monoclonal antibodies cloned from PV patients. Through testing over 50 human monoclonal antibodies using the disperse based fragmentation assay, we were able to determine that there were 7 monoclonal antibodies with no pathogenicity that still bound to Dsg3 with high affinity. A polyclonal mixture of these 7 antibodies was not able to induce Dsg3 clustering that was seen in a similar experiment using AK19, AK15, and AK23 mouse monoclonal antibodies. Interestingly, one of our pathogenic monoclonal antibodies (P3F3) was able to induce the formation of linear arrays, seemingly without Dsg3 clustering (Figure 8.5). This observation challenges our current model in

which a polyclonal mixture of antibodies causes the cross linking of Dsg3 on the cell surface resulting in the clustering and subsequent endocytosis of Dsg3 through linear arrays. Additionally, the lack of clustering coupled with the formation of linear arrays when keratinocytes are treated with a pathogenic monoclonal antibody indicates that clustering of Dsg3 is not an obligate precursor step to the formation of linear arrays.

These data support the notion that the clustering of Dsg3 is in response to a signaling cascade rather than a result of the physical cross linking properties of a polyclonal antibody mixture drives Dsg3 clustering. Several different signaling pathways have been implicated in the loss of cell adhesion in PV, however little is known about what is causing the activation of these signaling pathways. It is possible that PV IgG binding to certain epitopes of Dsg3 is important for the induction of these signaling pathways, some of which result in linear array formation. We now have over 50 characterized antibodies which can be used to further understand the role of Dsg3 epitopes in the pathogenesis of PV. Here we have only tested 7 of the 50 antibodies, and it is possible that these additional monoclonal antibodies result in a variety of morphological changes.

8.3 Concluding remarks

Cell-cell adhesion complexes mediate fundamental cellular interactions necessary for tissue maintenance and integrity. Desmosomes are large adhesion complexes critical in tissues that are exposed to high levels of mechanical stress. Desmosome stability is altered during the process of epithelial to mesenchymal transition, a necessary step for tumors to

metastasize. Thus, understanding the complex dynamics of desmosomal components and how desmosomes assemble and disassemble is necessary for developing novel treatments for a variety of skin diseases, including cancer. The original work in this dissertation focuses on mechanisms of desmosome assembly and disassembly through two dermatological diseases. We investigate the mechanism by which desmoglein (Dsg) associates with lipid rafts and uncover that the length of the transmembrane domain (TMD) is a key regulator of raft association. Importantly, we demonstrate that the bilayer within the desmosome is thicker than non-desmosome bilayer, thus identifying the desmosome as a lipid raft-like domain. We then study the disassembly of the desmosome through a pemphigus vulgaris model. Pemphigus vulgaris (PV) is an autoimmune disorder in which autoantibodies targeting Dsg3 and Dsg1 disrupt desmosome adhesion resulting in intraepidermal blisters. Here we validate observations that have been seen in *in vitro* models to study the progression of PV by correlating *in vitro* data to clinical measures of disease severity. We also determine that the sum of antibody titers against Dsg1 and Dsg3 is more correlative to disease severity than either titer on its own. These data demonstrate a relationship between Dsg antibody titer and disease severity, validate current methods for studying PV in cell culture, and confirm that results seen in cell culture models are relevant to the pathogenesis of pemphigus vulgaris. Together, these studies increase our understanding of how desmosomes assemble and disassemble, thus providing a platform for future investigation of the mechanisms regulating desmosome stability during tumorigenesis.

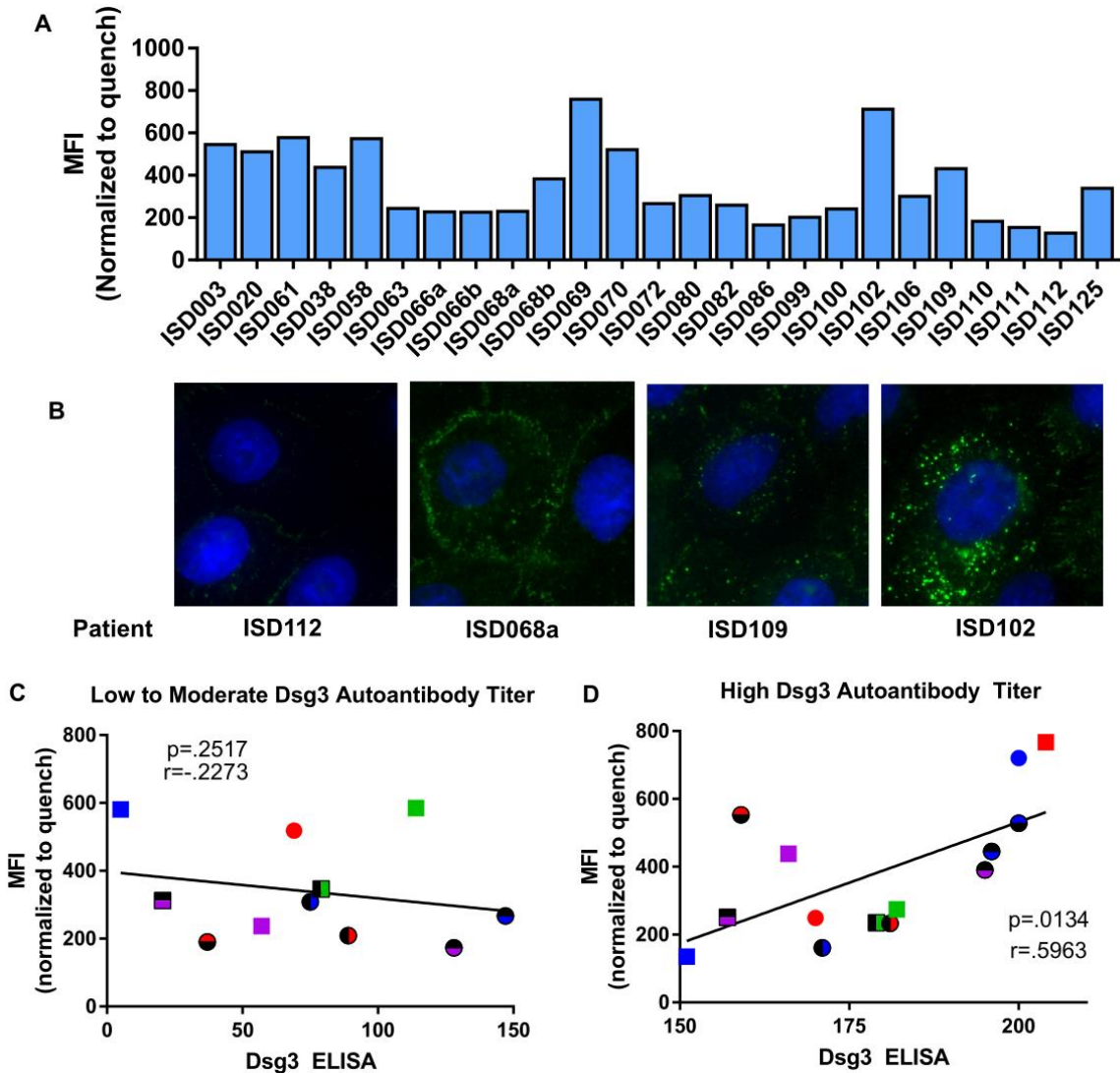


Figure 8.1 Patients with high Dsg3 antibody titers correlate with endocytosis assay at 3 hours. A) The 25 samples were found to have a range of Dsg3 internalization as determined by the mean fluorescence intensity (MFI). B) Representative images of patients with varying MFI scores. C) Patients with mild to moderate Dsg3 ELISA scores did not correlate with an endocytosis assay after PV IgG treatment for 3 hours while patients with high Dsg3 autoantibodies (D) showed a positive correlation.

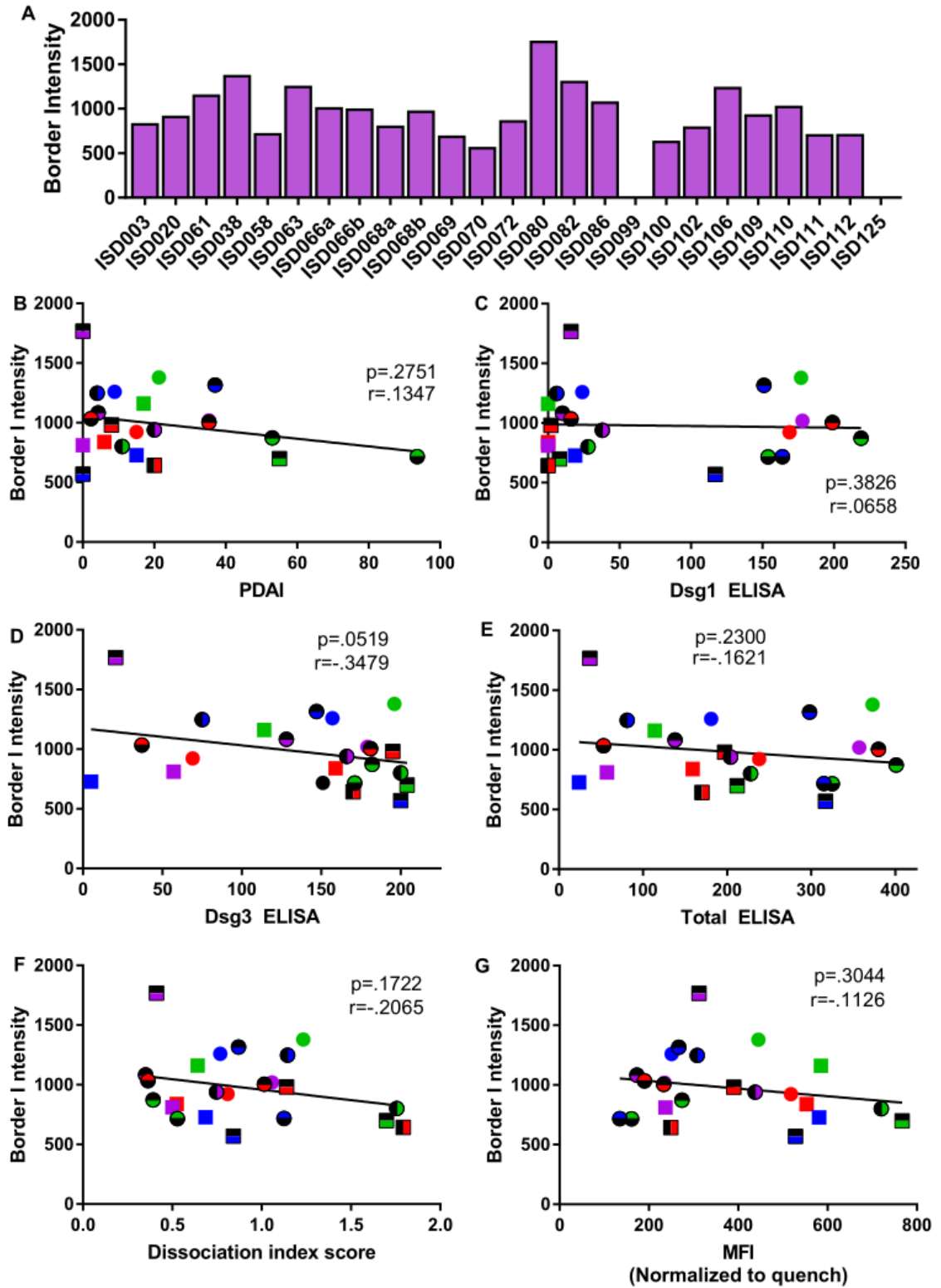


Figure 8.2 Loss of Dsg3 surface staining weakly correlates to Dsg3 ELISA. Keratinocytes were live labeled with a monoclonal antibody to Dsg3 and subsequently treated with PV IgG for three hours. A) 25 samples demonstrated a range of surface Dsg3 remaining after PV IgG treatment. Data for ISD099 and ISD125 were not collected. B-E) The loss of surface staining, or border intensity, did not significantly correlate with clinical measures of disease severity, however a weak correlation between Dsg3 ELISA was shown. F) The border intensity of Dsg3 did not correlate with the fragmentation assay. G) The border intensity of Dsg3 did not correlate with the endocytosis assay

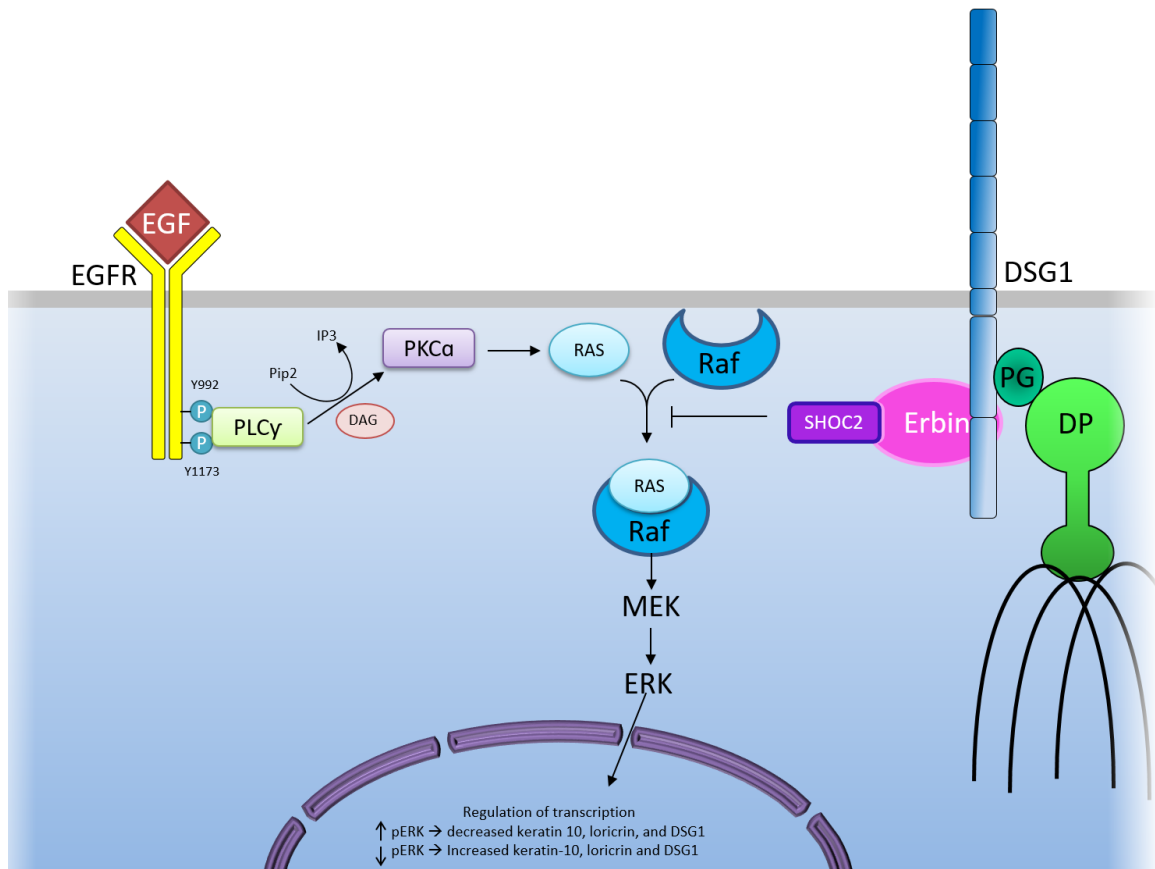


Figure 8.3 DSG1 mediates EGFR signaling. The EGFR signaling cascade is activated by a variety of ligands, such as EGF, that bind to the extracellular portion of the EGFR receptor. Dimerization and autophosphorylation then occurs which allows for downstream signaling to occur. SHOC2 is a scaffolding protein that accelerates the formation of Ras/Raf complexes and subsequent downstream signaling. Erbin binds to the cytoplasmic tail of Dsg1 and sequesters SHOC2, inhibiting EGFR signaling.

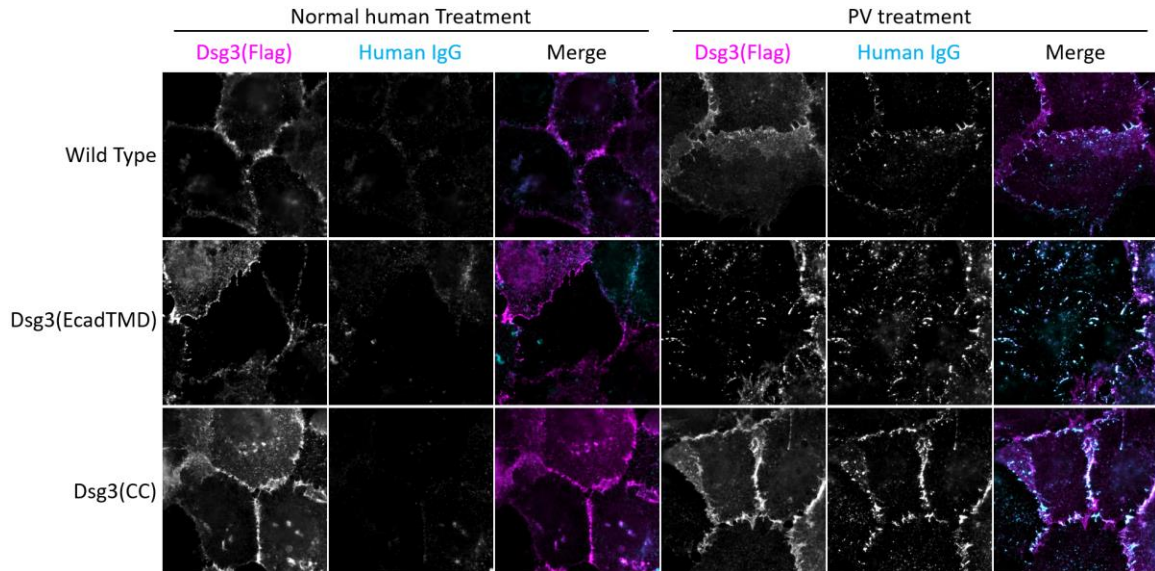


Figure 8.4 The TMD of DSG3 is critical for lipid raft mediated endocytosis. A431s expressing flag tagged DSG3 constructs were exposed to PV IgG or normal human sera for 3 hours prior to being fixed and stained for Dsg3 and Human IgG. PV IgG induced the formation of linear arrays in cells expressing WT Dsg3, however the Dsg3(EcadTMD) construct is incapable of forming the arrays typically seen while the Dsg3(CC) construct is protected from endocytosis.

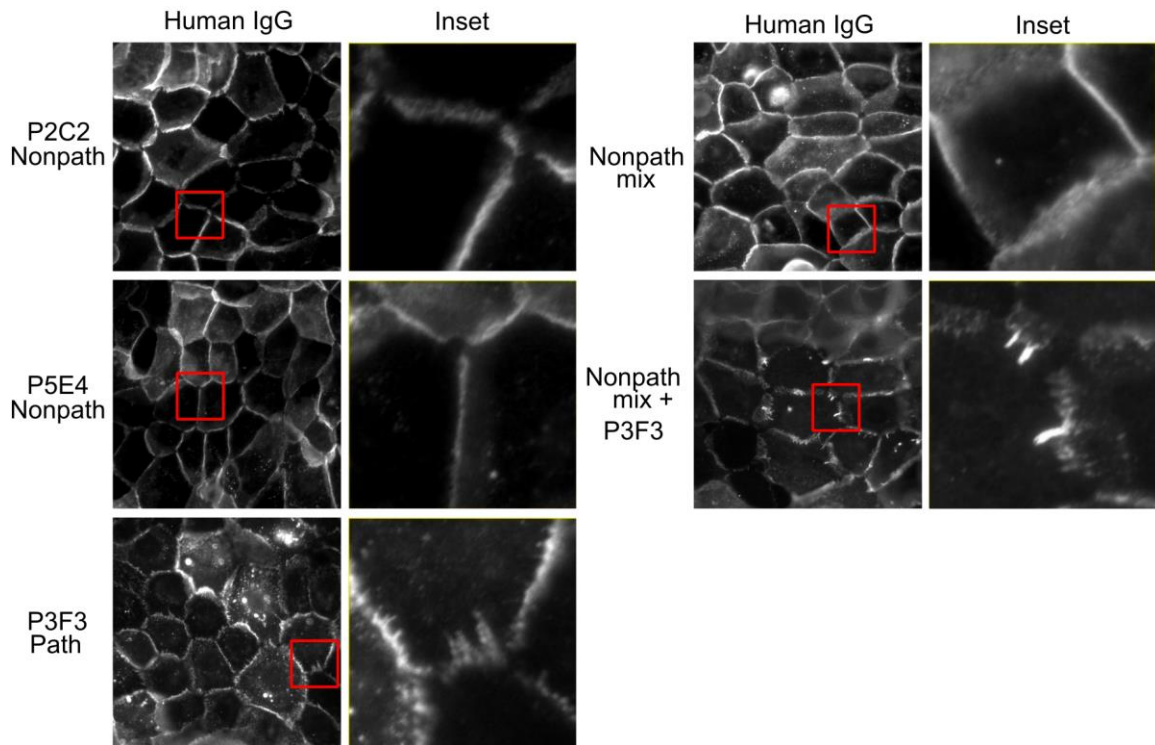


Figure 8.5 A pathogenic monoclonal antibody induces linear array formation. Primary human keratinocytes were treated with either monoclonal antibodies against DSG3 or a polyclonal mixture for 6 hours. 7 nonpathogenic (nonpath) antibodies were combined in the nonpathogenic mix and no clustering or array formation was observed. P2C2 and P5E4 panels are included to demonstrate that the nonpathogenic antibodies did not alter border staining. P3F3, a pathogenic (path) monoclonal antibody induced linear array formation on its own and with the mixture of non-pathogenic antibodies.

Chapter 9

References

1. Simpson CL, Patel DM, Green KJ. Deconstructing the skin: cytoarchitectural determinants of epidermal morphogenesis. *Nat Rev Mol Cell Biol.* 2011;12(9):565-80. Epub 2011/08/24. doi: 10.1038/nrm3175. PubMed PMID: 21860392; PMCID: PMC3280198.
2. D'Orazio J, Jarrett S, Amaro-Ortiz A, Scott T. UV radiation and the skin. *Int J Mol Sci.* 2013;14(6):12222-48. Epub 2013/06/12. doi: 10.3390/ijms140612222. PubMed PMID: 23749111; PMCID: PMC3709783.
3. Mohania D, Chandel S, Kumar P, Verma V, Digvijay K, Tripathi D, Choudhury K, Mitten SK, Shah D. Ultraviolet Radiations: Skin Defense-Damage Mechanism. *Adv Exp Med Biol.* 2017;996:71-87. Epub 2017/11/11. doi: 10.1007/978-3-319-56017-5_7. PubMed PMID: 29124692.
4. Matsui T, Amagai M. Dissecting the formation, structure and barrier function of the stratum corneum. *Int Immunol.* 2015;27(6):269-80. Epub 2015/03/31. doi: 10.1093/intimm/dxv013. PubMed PMID: 25813515.
5. Baroni A, Buommino E, De Gregorio V, Ruocco E, Ruocco V, Wolf R. Structure and function of the epidermis related to barrier properties. *Clin Dermatol.* 2012;30(3):257-62. Epub 2012/04/18. doi: 10.1016/j.clindermatol.2011.08.007. PubMed PMID: 22507037.
6. Thune P, Nilsen T, Hanstad IK, Gustavsen T, Lovig Dahl H. The water barrier function of the skin in relation to the water content of stratum corneum, pH and skin lipids. The effect of alkaline soap and syndet on dry skin in elderly, non-atopic patients. *Acta Derm Venereol.* 1988;68(4):277-83. Epub 1988/01/01. PubMed PMID: 2459871.
7. Akdeniz M, Gabriel S, Lichterfeld-Kottner A, Blume-Peytavi U, Kottner J. Transepidermal water loss in healthy adults: a systematic review and meta-analysis update. *Br J Dermatol.* 2018;179(5):1049-55. Epub 2018/07/20. doi: 10.1111/bjd.17025. PubMed PMID: 30022486.
8. Taieb A, Hanifin J, Cooper K, Bos JD, Imokawa G, David TJ, Ring J, Gelmetti C, Kapp A, Furue M, de Prost Y, Darsow U, Werfel T, Atherton D, Oranje AP. Proceedings of the 4th Georg Rajka International Symposium on Atopic Dermatitis, Arcachon, France, September 15-17, 2005. *J Allergy Clin Immunol.* 2006;117(2):378-90. Epub 2006/03/07. PubMed PMID: 16514773.
9. Roudit C, Frei R, Depner M, Karvonen AM, Renz H, Braun-Fahrländer C, Schmausser-Hechfellner E, Pekkanen J, Riedler J, Dalphin JC, von Mutius E, Lauener RP, and the Psg, Hyvarinen A, Kirjavainen P, Remes S, Roponen M, Dalphin ML, Kaulek V, Ege M, Genuneit J, Illi S, Kabesch M, Schaub B, Pfefferle PI, Doekes G. Phenotypes of Atopic Dermatitis Depending on the Timing of

Onset and Progression in Childhood. *JAMA Pediatr.* 2017;171(7):655-62. Epub 2017/05/23. doi: 10.1001/jamapediatrics.2017.0556. PubMed PMID: 28531273; PMCID: PMC5710337.

10. Williams FN, Herndon DN, Hawkins HK, Lee JO, Cox RA, Kulp GA, Finnerty CC, Chinkes DL, Jeschke MG. The leading causes of death after burn injury in a single pediatric burn center. *Crit Care.* 2009;13(6):R183. Epub 2009/11/19. doi: 10.1186/cc8170. PubMed PMID: 19919684; PMCID: PMC2811947.

11. Arwert EN, Hoste E, Watt FM. Epithelial stem cells, wound healing and cancer. *Nat Rev Cancer.* 2012;12(3):170-80. Epub 2012/03/01. doi: 10.1038/nrc3217. PubMed PMID: 22362215.

12. Allombert-Blaise C, Tamiji S, Mortier L, Fauvel H, Tual M, Delaporte E, Piette F, DeLassale EM, Formstecher P, Marchetti P, Polakowska R. Terminal differentiation of human epidermal keratinocytes involves mitochondria- and caspase-dependent cell death pathway. *Cell Death Differ.* 2003;10(7):850-2. Epub 2003/06/20. doi: 10.1038/sj.cdd.4401245. PubMed PMID: 12815468.

13. Gandarillas A. Epidermal differentiation, apoptosis, and senescence: common pathways? *Exp Gerontol.* 2000;35(1):53-62. Epub 2000/03/08. PubMed PMID: 10705039.

14. Eckhart L, Lippens S, Tschachler E, Declercq W. Cell death by cornification. *Biochim Biophys Acta.* 2013;1833(12):3471-80. Epub 2013/06/25. doi: 10.1016/j.bbamcr.2013.06.010. PubMed PMID: 23792051.

15. Marekov LN, Steinert PM. Ceramides are bound to structural proteins of the human foreskin epidermal cornified cell envelope. *The Journal of biological chemistry.* 1998;273(28):17763-70. Epub 1998/07/04. PubMed PMID: 9651377.

16. Ekanayake-Mudiyanselage S, Aschauer H, Schmook FP, Jensen JM, Meingassner JG, Proksch E. Expression of epidermal keratins and the cornified envelope protein involucrin is influenced by permeability barrier disruption. *J Invest Dermatol.* 1998;111(3):517-23. Epub 1998/09/18. doi: 10.1046/j.1523-1747.1998.00318.x. PubMed PMID: 9740250.

17. Steinert PM, Marekov LN. The proteins elafin, filaggrin, keratin intermediate filaments, loricrin, and small proline-rich proteins 1 and 2 are isodi-peptide cross-linked components of the human epidermal cornified cell envelope. *The Journal of biological chemistry.* 1995;270(30):17702-11. Epub 1995/07/28. PubMed PMID: 7543090.

18. Nemes Z, Steinert PM. Bricks and mortar of the epidermal barrier. *Exp Mol Med.* 1999;31(1):5-19. Epub 1999/05/07. doi: 10.1038/emm.1999.2. PubMed PMID: 10231017.

19. Candi E, Schmidt R, Melino G. The cornified envelope: a model of cell death in the skin. *Nat Rev Mol Cell Biol.* 2005;6(4):328-40. Epub 2005/04/02. doi: 10.1038/nrm1619. PubMed PMID: 15803139.

20. Suzuki A, Itami S, Ohishi M, Hamada K, Inoue T, Komazawa N, Senoo H, Sasaki T, Takeda J, Manabe M, Mak TW, Nakano T. Keratinocyte-specific Pten deficiency results in epidermal

hyperplasia, accelerated hair follicle morphogenesis and tumor formation. *Cancer Res.* 2003;63(3):674-81. Epub 2003/02/05. PubMed PMID: 12566313.

21. Hoot KE, Lighthall J, Han G, Lu SL, Li A, Ju W, Kulesz-Martin M, Bottinger E, Wang XJ. Keratinocyte-specific Smad2 ablation results in increased epithelial-mesenchymal transition during skin cancer formation and progression. *J Clin Invest.* 2008;118(8):2722-32. Epub 2008/07/12. doi: 10.1172/JCI33713. PubMed PMID: 18618014; PMCID: PMC2447925.

22. Demehri S, Turkoz A, Kopan R. Epidermal Notch1 loss promotes skin tumorigenesis by impacting the stromal microenvironment. *Cancer Cell.* 2009;16(1):55-66. Epub 2009/07/04. doi: 10.1016/j.ccr.2009.05.016. PubMed PMID: 19573812; PMCID: PMC2705757.

23. Greb JE, Goldminz AM, Elder JT, Lebwohl MG, Gladman DD, Wu JJ, Mehta NN, Finlay AY, Gottlieb AB. Psoriasis. *Nat Rev Dis Primers.* 2016;2:16082. Epub 2016/11/25. doi: 10.1038/nrdp.2016.82. PubMed PMID: 27883001.

24. Stojadinovic O, Pastar I, Vukelic S, Mahoney MG, Brennan D, Krzyzanowska A, Golinko M, Brem H, Tomic-Canic M. Deregulation of keratinocyte differentiation and activation: a hallmark of venous ulcers. *J Cell Mol Med.* 2008;12(6B):2675-90. Epub 2008/04/01. doi: 10.1111/j.1582-4934.2008.00321.x. PubMed PMID: 18373736; PMCID: PMC3828883.

25. Li D, Zhang W, Liu Y, Haneline LS, Shou W. Lack of plakoglobin in epidermis leads to keratoderma. *The Journal of biological chemistry.* 2012;287(13):10435-43. Epub 2012/02/09. doi: 10.1074/jbc.M111.299669. PubMed PMID: 22315228; PMCID: PMC3322998.

26. Seshadri D, Kumaran MS, Kanwar AJ. Acantholysis revisited: back to basics. *Indian J Dermatol Venereol Leprol.* 2013;79(1):120-6. Epub 2012/12/21. doi: 10.4103/0378-6323.104688. PubMed PMID: 23254748.

27. Sticherling M, Erfurt-Berge C. Autoimmune blistering diseases of the skin. *Autoimmun Rev.* 2012;11(3):226-30. Epub 2011/06/07. doi: 10.1016/j.autrev.2011.05.017. PubMed PMID: 21640850.

28. Sumigray KD, Lechler T. Cell adhesion in epidermal development and barrier formation. *Curr Top Dev Biol.* 2015;112:383-414. Epub 2015/03/04. doi: 10.1016/bs.ctdb.2014.11.027. PubMed PMID: 25733147; PMCID: PMC4737682.

29. Rubsam M, Broussard JA, Wickstrom SA, Nekrasova O, Green KJ, Niessen CM. Adherens Junctions and Desmosomes Coordinate Mechanics and Signaling to Orchestrate Tissue Morphogenesis and Function: An Evolutionary Perspective. *Cold Spring Harb Perspect Biol.* 2018;10(11). Epub 2017/09/13. doi: 10.1101/cshperspect.a029207. PubMed PMID: 28893859.

30. Schluter H, Wepf R, Moll I, Franke WW. Sealing the live part of the skin: the integrated meshwork of desmosomes, tight junctions and curvilinear ridge structures in the cells of the uppermost granular layer of the human epidermis. *Eur J Cell Biol.* 2004;83(11-12):655-65. Epub 2005/02/01. doi: 10.1078/0171-9335-00434. PubMed PMID: 15679110.

31. Furuse M, Hata M, Furuse K, Yoshida Y, Haratake A, Sugitani Y, Noda T, Kubo A, Tsukita S. Claudin-based tight junctions are crucial for the mammalian epidermal barrier: a lesson from claudin-1-deficient mice. *J Cell Biol.* 2002;156(6):1099-111. Epub 2002/03/13. doi: 10.1083/jcb.200110122. PubMed PMID: 11889141; PMCID: PMC2173463.
32. Chiasson-MacKenzie C, McClatchey AI. Cell-Cell Contact and Receptor Tyrosine Kinase Signaling. *Cold Spring Harb Perspect Biol.* 2018;10(6). Epub 2017/07/19. doi: 10.1101/cshperspect.a029215. PubMed PMID: 28716887.
33. Charest JL, Jennings JM, King WP, Kowalczyk AP, Garcia AJ. Cadherin-mediated cell-cell contact regulates keratinocyte differentiation. *J Invest Dermatol.* 2009;129(3):564-72. Epub 2008/08/30. doi: 10.1038/jid.2008.265. PubMed PMID: 18754040; PMCID: PMC2693873.
34. Balda MS, Matter K. Tight junctions at a glance. *J Cell Sci.* 2008;121(Pt 22):3677-82. Epub 2008/11/07. doi: 10.1242/jcs.023887. PubMed PMID: 18987354.
35. Zihni C, Mills C, Matter K, Balda MS. Tight junctions: from simple barriers to multifunctional molecular gates. *Nat Rev Mol Cell Biol.* 2016;17(9):564-80. Epub 2016/06/30. doi: 10.1038/nrm.2016.80. PubMed PMID: 27353478.
36. Van Itallie CM, Anderson JM. Architecture of tight junctions and principles of molecular composition. *Semin Cell Dev Biol.* 2014;36:157-65. Epub 2014/08/31. doi: 10.1016/j.semcdb.2014.08.011. PubMed PMID: 25171873; PMCID: PMC4254347.
37. Balda MS, Matter K. Transmembrane proteins of tight junctions. *Semin Cell Dev Biol.* 2000;11(4):281-9. Epub 2000/09/01. doi: 10.1006/scdb.2000.0177. PubMed PMID: 10966862.
38. Mineta K, Yamamoto Y, Yamazaki Y, Tanaka H, Tada Y, Saito K, Tamura A, Igarashi M, Endo T, Takeuchi K, Tsukita S. Predicted expansion of the claudin multigene family. *FEBS Lett.* 2011;585(4):606-12. Epub 2011/02/01. doi: 10.1016/j.febslet.2011.01.028. PubMed PMID: 21276448.
39. Van Itallie CM, Fanning AS, Anderson JM. Reversal of charge selectivity in cation or anion-selective epithelial lines by expression of different claudins. *Am J Physiol Renal Physiol.* 2003;285(6):F1078-84. Epub 2003/09/18. doi: 10.1152/ajprenal.00116.2003. PubMed PMID: 13129853.
40. Saitou M, Furuse M, Sasaki H, Schulzke JD, Fromm M, Takano H, Noda T, Tsukita S. Complex phenotype of mice lacking occludin, a component of tight junction strands. *Mol Biol Cell.* 2000;11(12):4131-42. Epub 2000/12/05. doi: 10.1091/mbc.11.12.4131. PubMed PMID: 11102513; PMCID: PMC15062.
41. Ebnet K. Junctional Adhesion Molecules (JAMs): Cell Adhesion Receptors With Pleiotropic Functions in Cell Physiology and Development. *Physiol Rev.* 2017;97(4):1529-54. Epub 2017/09/22. doi: 10.1152/physrev.00004.2017. PubMed PMID: 28931565.
42. Xu J, Kausalya PJ, Phua DC, Ali SM, Hossain Z, Hunziker W. Early embryonic lethality of mice lacking ZO-2, but Not ZO-3, reveals critical and nonredundant roles for individual zonula

occludens proteins in mammalian development. *Mol Cell Biol.* 2008;28(5):1669-78. Epub 2008/01/04. doi: 10.1128/MCB.00891-07. PubMed PMID: 18172007; PMCID: PMC2258782.

43. Tsukita S, Katsuno T, Yamazaki Y, Umeda K, Tamura A, Tsukita S. Roles of ZO-1 and ZO-2 in establishment of the belt-like adherens and tight junctions with paracellular permselective barrier function. *Ann N Y Acad Sci.* 2009;1165:44-52. Epub 2009/06/23. doi: 10.1111/j.1749-6632.2009.04056.x. PubMed PMID: 19538286.

44. Umeda K, Ikenouchi J, Katahira-Tayama S, Furuse K, Sasaki H, Nakayama M, Matsui T, Tsukita S, Furuse M, Tsukita S. ZO-1 and ZO-2 independently determine where claudins are polymerized in tight-junction strand formation. *Cell.* 2006;126(4):741-54. Epub 2006/08/23. doi: 10.1016/j.cell.2006.06.043. PubMed PMID: 16923393.

45. Kirschner N, Poetzel C, von den Driesch P, Wladykowski E, Moll I, Behne MJ, Brandner JM. Alteration of tight junction proteins is an early event in psoriasis: putative involvement of proinflammatory cytokines. *Am J Pathol.* 2009;175(3):1095-106. Epub 2009/08/08. doi: 10.2353/ajpath.2009.080973. PubMed PMID: 19661441; PMCID: PMC2731128.

46. Pummi K, Malminen M, Aho H, Karvonen SL, Peltonen J, Peltonen S. Epidermal tight junctions: ZO-1 and occludin are expressed in mature, developing, and affected skin and in vitro differentiating keratinocytes. *J Invest Dermatol.* 2001;117(5):1050-8. Epub 2001/11/17. doi: 10.1046/j.0022-202x.2001.01493.x. PubMed PMID: 11710912.

47. Yoshida Y, Morita K, Mizoguchi A, Ide C, Miyachi Y. Altered expression of occludin and tight junction formation in psoriasis. *Arch Dermatol Res.* 2001;293(5):239-44. Epub 2001/06/21. PubMed PMID: 11409568.

48. Yuki T, Tobiishi M, Kusaka-Kikushima A, Ota Y, Tokura Y. Impaired Tight Junctions in Atopic Dermatitis Skin and in a Skin-Equivalent Model Treated with Interleukin-17. *PloS one.* 2016;11(9):e0161759. Epub 2016/09/03. doi: 10.1371/journal.pone.0161759. PubMed PMID: 27588419; PMCID: PMC5010286 Kao Corporation, a commercial company, during this study. There are no patents, products in development or marketed products to declare.

49. De Benedetto A, Rafaels NM, McGirt LY, Ivanov AI, Georas SN, Cheadle C, Berger AE, Zhang K, Vidyasagar S, Yoshida T, Boguniewicz M, Hata T, Schneider LC, Hanifin JM, Gallo RL, Novak N, Weidinger S, Beaty TH, Leung DY, Barnes KC, Beck LA. Tight junction defects in patients with atopic dermatitis. *J Allergy Clin Immunol.* 2011;127(3):773-86 e1-7. Epub 2010/12/18. doi: 10.1016/j.jaci.2010.10.018. PubMed PMID: 21163515; PMCID: PMC3049863.

50. Mese G, Richard G, White TW. Gap junctions: basic structure and function. *J Invest Dermatol.* 2007;127(11):2516-24. Epub 2007/10/16. doi: 10.1038/sj.jid.5700770. PubMed PMID: 17934503.

51. Caputo R, Peluchetti D. The junctions of normal human epidermis. A freeze-fracture study. *J Ultrastruct Res.* 1977;61(1):44-61. Epub 1977/10/01. PubMed PMID: 915975.

52. Finbow ME, Pitts JD. Permeability of junctions between animal cells. Intercellular exchange of various metabolites and a vitamin-derived cofactor. *Exp Cell Res.* 1981;131(1):1-13. Epub 1981/01/01. PubMed PMID: 7447983.
53. Pitts JD, Simms JW. Permeability of junctions between animal cells. Intercellular transfer of nucleotides but not of macromolecules. *Exp Cell Res.* 1977;104(1):153-63. Epub 1977/01/01. PubMed PMID: 836400.
54. Murray SA, Fletcher WH. Hormone-induced intercellular signal transfer dissociates cyclic AMP-dependent protein kinase. *J Cell Biol.* 1984;98(5):1710-9. Epub 1984/05/01. PubMed PMID: 6327720; PMCID: PMC2113167.
55. Saez JC, Connor JA, Spray DC, Bennett MV. Hepatocyte gap junctions are permeable to the second messenger, inositol 1,4,5-trisphosphate, and to calcium ions. *Proc Natl Acad Sci U S A.* 1989;86(8):2708-12. Epub 1989/04/01. PubMed PMID: 2784857; PMCID: PMC286987.
56. Sohl G, Willecke K. Gap junctions and the connexin protein family. *Cardiovasc Res.* 2004;62(2):228-32. Epub 2004/04/20. doi: 10.1016/j.cardiores.2003.11.013. PubMed PMID: 15094343.
57. Dbouk HA, Mroue RM, El-Sabban ME, Talhouk RS. Connexins: a myriad of functions extending beyond assembly of gap junction channels. *Cell Commun Signal.* 2009;7:4. Epub 2009/03/17. doi: 10.1186/1478-811X-7-4. PubMed PMID: 19284610; PMCID: PMC2660342.
58. Oyamada M, Oyamada Y, Takamatsu T. Regulation of connexin expression. *Biochim Biophys Acta.* 2005;1719(1-2):6-23. Epub 2005/12/20. doi: 10.1016/j.bbamem.2005.11.002. PubMed PMID: 16359940.
59. Di WL, Rugg EL, Leigh IM, Kelsell DP. Multiple epidermal connexins are expressed in different keratinocyte subpopulations including connexin 31. *J Invest Dermatol.* 2001;117(4):958-64. Epub 2001/10/26. doi: 10.1046/j.0022-202x.2001.01468.x. PubMed PMID: 11676838.
60. Makowski L, Caspar DL, Phillips WC, Goodenough DA. Gap junction structures. II. Analysis of the x-ray diffraction data. *J Cell Biol.* 1977;74(2):629-45. Epub 1977/08/01. PubMed PMID: 889612; PMCID: PMC2110084.
61. Revel JP, Karnovsky MJ. Hexagonal array of subunits in intercellular junctions of the mouse heart and liver. *J Cell Biol.* 1967;33(3):C7-C12. Epub 1967/06/01. PubMed PMID: 6036535; PMCID: PMC2107199.
62. Goldberg GS, Lampe PD, Nicholson BJ. Selective transfer of endogenous metabolites through gap junctions composed of different connexins. *Nat Cell Biol.* 1999;1(7):457-9. Epub 1999/11/24. doi: 10.1038/15693. PubMed PMID: 10559992.
63. Lucke T, Choudhry R, Thom R, Selmer IS, Burden AD, Hodgins MB. Upregulation of connexin 26 is a feature of keratinocyte differentiation in hyperproliferative epidermis, vaginal epithelium, and buccal epithelium. *J Invest Dermatol.* 1999;112(3):354-61. Epub 1999/03/20. doi: 10.1046/j.1523-1747.1999.00512.x. PubMed PMID: 10084314.

64. Goliger JA, Paul DL. Wounding alters epidermal connexin expression and gap junction-mediated intercellular communication. *Mol Biol Cell*. 1995;6(11):1491-501. Epub 1995/11/01. PubMed PMID: 8589451; PMCID: PMC301306.
65. Wang CM, Lincoln J, Cook JE, Becker DL. Abnormal connexin expression underlies delayed wound healing in diabetic skin. *Diabetes*. 2007;56(11):2809-17. Epub 2007/08/25. doi: 10.2337/db07-0613. PubMed PMID: 17717278.
66. Labarthe MP, Bosco D, Saurat JH, Meda P, Salomon D. Upregulation of connexin 26 between keratinocytes of psoriatic lesions. *J Invest Dermatol*. 1998;111(1):72-6. Epub 1998/07/17. doi: 10.1046/j.1523-1747.1998.00248.x. PubMed PMID: 9665389.
67. Morley SM, White MI, Rogers M, Wasserman D, Ratajczak P, McLean WH, Richard G. A new, recurrent mutation of GJB3 (Cx31) in erythrokeratoderma variabilis. *Br J Dermatol*. 2005;152(6):1143-8. Epub 2005/06/14. doi: 10.1111/j.1365-2133.2005.06610.x. PubMed PMID: 15948974.
68. Richard G, Smith LE, Bailey RA, Itin P, Hohl D, Epstein EH, Jr., DiGiovanna JJ, Compton JG, Bale SJ. Mutations in the human connexin gene GJB3 cause erythrokeratoderma variabilis. *Nat Genet*. 1998;20(4):366-9. Epub 1998/12/08. doi: 10.1038/3840. PubMed PMID: 9843209.
69. Richard G, White TW, Smith LE, Bailey RA, Compton JG, Paul DL, Bale SJ. Functional defects of Cx26 resulting from a heterozygous missense mutation in a family with dominant deaf-mutism and palmoplantar keratoderma. *Hum Genet*. 1998;103(4):393-9. Epub 1998/12/18. PubMed PMID: 9856479.
70. Walko G, Castanon MJ, Wiche G. Molecular architecture and function of the hemidesmosome. *Cell Tissue Res*. 2015;360(3):529-44. Epub 2015/05/29. doi: 10.1007/s00441-015-2216-6. PubMed PMID: 26017636; PMCID: PMC4452579.
71. Kaiser HW, Ness W, Jungblut I, Briggaman RA, Kreysel HW, O'Keefe EJ. Adherens junctions: demonstration in human epidermis. *J Invest Dermatol*. 1993;100(2):180-5. Epub 1993/02/01. PubMed PMID: 8429240.
72. le Duc Q, Shi Q, Blonk I, Sonnenberg A, Wang N, Leckband D, de Rooij J. Vinculin potentiates E-cadherin mechanosensing and is recruited to actin-anchored sites within adherens junctions in a myosin II-dependent manner. *J Cell Biol*. 2010;189(7):1107-15. Epub 2010/06/30. doi: 10.1083/jcb.201001149. PubMed PMID: 20584916; PMCID: PMC2894457.
73. Liu Z, Tan JL, Cohen DM, Yang MT, Sniadecki NJ, Ruiz SA, Nelson CM, Chen CS. Mechanical tugging force regulates the size of cell-cell junctions. *Proc Natl Acad Sci U S A*. 2010;107(22):9944-9. Epub 2010/05/14. doi: 10.1073/pnas.0914547107. PubMed PMID: 20463286; PMCID: PMC2890446.
74. Ishiko A, Matsunaga Y, Masunaga T, Aiso S, Nishikawa T, Shimizu H. Immunomolecular mapping of adherens junction and desmosomal components in normal human epidermis. *Exp Dermatol*. 2003;12(6):747-54. Epub 2004/01/13. PubMed PMID: 14714553.

75. Haftek M, Hansen MU, Kaiser HW, Kreysel HW, Schmitt D. Interkeratinocyte adherens junctions: immunocytochemical visualization of cell-cell junctional structures, distinct from desmosomes, in human epidermis. *J Invest Dermatol.* 1996;106(3):498-504. Epub 1996/03/01. PubMed PMID: 8648183.
76. van Roy F, Berx G. The cell-cell adhesion molecule E-cadherin. *Cell Mol Life Sci.* 2008;65(23):3756-88. Epub 2008/08/30. doi: 10.1007/s00018-008-8281-1. PubMed PMID: 18726070.
77. Tunggal JA, Helfrich I, Schmitz A, Schwarz H, Gunzel D, Fromm M, Kemler R, Krieg T, Niessen CM. E-cadherin is essential for in vivo epidermal barrier function by regulating tight junctions. *EMBO J.* 2005;24(6):1146-56. Epub 2005/03/19. doi: 10.1038/sj.emboj.7600605. PubMed PMID: 15775979; PMCID: PMC556407.
78. Young P, Boussadia O, Halfter H, Grose R, Berger P, Leone DP, Robenek H, Charnay P, Kemler R, Suter U. E-cadherin controls adherens junctions in the epidermis and the renewal of hair follicles. *EMBO J.* 2003;22(21):5723-33. Epub 2003/11/01. doi: 10.1093/emboj/cdg560. PubMed PMID: 14592971; PMCID: PMC275417.
79. Ishiyama N, Lee SH, Liu S, Li GY, Smith MJ, Reichardt LF, Ikura M. Dynamic and static interactions between p120 catenin and E-cadherin regulate the stability of cell-cell adhesion. *Cell.* 2010;141(1):117-28. Epub 2010/04/08. doi: 10.1016/j.cell.2010.01.017. PubMed PMID: 20371349.
80. Huber AH, Weis WI. The structure of the beta-catenin/E-cadherin complex and the molecular basis of diverse ligand recognition by beta-catenin. *Cell.* 2001;105(3):391-402. Epub 2001/05/12. PubMed PMID: 11348595.
81. Miyashita Y, Ozawa M. Increased internalization of p120-uncoupled E-cadherin and a requirement for a dileucine motif in the cytoplasmic domain for endocytosis of the protein. *The Journal of biological chemistry.* 2007;282(15):11540-8. Epub 2007/02/15. doi: 10.1074/jbc.M608351200. PubMed PMID: 17298950.
82. Xiao K, Allison DF, Buckley KM, Kottke MD, Vincent PA, Faundez V, Kowalczyk AP. Cellular levels of p120 catenin function as a set point for cadherin expression levels in microvascular endothelial cells. *J Cell Biol.* 2003;163(3):535-45. Epub 2003/11/12. doi: 10.1083/jcb.200306001. PubMed PMID: 14610056; PMCID: PMC2173638.
83. Davis MA, Ireton RC, Reynolds AB. A core function for p120-catenin in cadherin turnover. *J Cell Biol.* 2003;163(3):525-34. Epub 2003/11/12. doi: 10.1083/jcb.200307111. PubMed PMID: 14610055; PMCID: PMC2173649.
84. Nanes BA, Chiasson-MacKenzie C, Lowery AM, Ishiyama N, Faundez V, Ikura M, Vincent PA, Kowalczyk AP. p120-catenin binding masks an endocytic signal conserved in classical cadherins. *J Cell Biol.* 2012;199(2):365-80. Epub 2012/10/17. doi: 10.1083/jcb.201205029. PubMed PMID: 23071156; PMCID: PMC3471230.

85. Perez-Moreno M, Davis MA, Wong E, Pasolli HA, Reynolds AB, Fuchs E. p120-catenin mediates inflammatory responses in the skin. *Cell*. 2006;124(3):631-44. Epub 2006/02/14. doi: 10.1016/j.cell.2005.11.043. PubMed PMID: 16469707; PMCID: PMC2443688.
86. Posthaus H, Williamson L, Baumann D, Kemler R, Caldelari R, Suter MM, Schwarz H, Muller E. beta-Catenin is not required for proliferation and differentiation of epidermal mouse keratinocytes. *J Cell Sci*. 2002;115(Pt 23):4587-95. Epub 2002/11/05. PubMed PMID: 12415003.
87. Ray S, Foote HP, Lechler T. beta-Catenin protects the epidermis from mechanical stresses. *J Cell Biol*. 2013;202(1):45-52. Epub 2013/07/03. doi: 10.1083/jcb.201212140. PubMed PMID: 23816618; PMCID: PMC3704987.
88. Clevers H. Wnt/beta-catenin signaling in development and disease. *Cell*. 2006;127(3):469-80. Epub 2006/11/04. doi: 10.1016/j.cell.2006.10.018. PubMed PMID: 17081971.
89. Huelsken J, Vogel R, Erdmann B, Cotsarelis G, Birchmeier W. beta-Catenin controls hair follicle morphogenesis and stem cell differentiation in the skin. *Cell*. 2001;105(4):533-45. Epub 2001/05/24. PubMed PMID: 11371349.
90. Kajino Y, Yamaguchi A, Hashimoto N, Matsuura A, Sato N, Kikuchi K. beta-Catenin gene mutation in human hair follicle-related tumors. *Pathol Int*. 2001;51(7):543-8. Epub 2001/07/27. PubMed PMID: 11472567.
91. Wickline ED, Dale IW, Merkel CD, Heier JA, Stolz DB, Kwiatkowski AV. alphaT-Catenin Is a Constitutive Actin-binding alpha-Catenin That Directly Couples the Cadherin.Catenin Complex to Actin Filaments. *The Journal of biological chemistry*. 2016;291(30):15687-99. Epub 2016/05/28. doi: 10.1074/jbc.M116.735423. PubMed PMID: 27231342; PMCID: PMC4957052.
92. Knudsen KA, Soler AP, Johnson KR, Wheelock MJ. Interaction of alpha-actinin with the cadherin/catenin cell-cell adhesion complex via alpha-catenin. *J Cell Biol*. 1995;130(1):67-77. Epub 1995/07/01. PubMed PMID: 7790378; PMCID: PMC2120515.
93. Yonemura S, Wada Y, Watanabe T, Nagafuchi A, Shibata M. alpha-Catenin as a tension transducer that induces adherens junction development. *Nat Cell Biol*. 2010;12(6):533-42. Epub 2010/05/11. doi: 10.1038/ncb2055. PubMed PMID: 20453849.
94. Vasioukhin V, Bauer C, Degenstein L, Wise B, Fuchs E. Hyperproliferation and defects in epithelial polarity upon conditional ablation of alpha-catenin in skin. *Cell*. 2001;104(4):605-17. Epub 2001/03/10. PubMed PMID: 11239416.
95. Tidman MJ, Eady RA. Ultrastructural morphometry of normal human dermal-epidermal junction. The influence of age, sex, and body region on laminar and nonlaminar components. *J Invest Dermatol*. 1984;83(6):448-53. Epub 1984/12/01. PubMed PMID: 6209345.
96. Tidman MJ, Eady RA. Hemidesmosome heterogeneity in junctional epidermolysis bullosa revealed by morphometric analysis. *J Invest Dermatol*. 1986;86(1):51-6. Epub 1986/01/01. PubMed PMID: 3745934.

97. Sonnenberg A, Calafat J, Janssen H, Daams H, van der Raaij-Helmer LM, Falcioni R, Kennel SJ, Aplin JD, Baker J, Loizidou M, et al. Integrin alpha 6/beta 4 complex is located in hemidesmosomes, suggesting a major role in epidermal cell-basement membrane adhesion. *J Cell Biol.* 1991;113(4):907-17. Epub 1991/05/01. PubMed PMID: 2026654; PMCID: PMC2288991.
98. Niessen CM, Hogervorst F, Jaspars LH, de Melker AA, Delwel GO, Hulsman EH, Kuikman I, Sonnenberg A. The alpha 6 beta 4 integrin is a receptor for both laminin and kalinin. *Exp Cell Res.* 1994;211(2):360-7. Epub 1994/04/01. doi: 10.1006/excr.1994.1099. PubMed PMID: 8143784.
99. Spinardi L, Einheber S, Cullen T, Milner TA, Giancotti FG. A recombinant tail-less integrin beta 4 subunit disrupts hemidesmosomes, but does not suppress alpha 6 beta 4-mediated cell adhesion to laminins. *J Cell Biol.* 1995;129(2):473-87. Epub 1995/04/01. PubMed PMID: 7721947; PMCID: PMC2199916.
100. Rezniczek GA, de Pereda JM, Reipert S, Wiche G. Linking integrin alpha6beta4-based cell adhesion to the intermediate filament cytoskeleton: direct interaction between the beta4 subunit and plectin at multiple molecular sites. *J Cell Biol.* 1998;141(1):209-25. Epub 1998/05/16. PubMed PMID: 9531560; PMCID: PMC2132717.
101. Geerts D, Fontao L, Nievers MG, Schaapveld RQ, Purkis PE, Wheeler GN, Lane EB, Leigh IM, Sonnenberg A. Binding of integrin alpha6beta4 to plectin prevents plectin association with F-actin but does not interfere with intermediate filament binding. *J Cell Biol.* 1999;147(2):417-34. Epub 1999/10/20. PubMed PMID: 10525545; PMCID: PMC2174221.
102. Steinbock FA, Nikolic B, Coulombe PA, Fuchs E, Traub P, Wiche G. Dose-dependent linkage, assembly inhibition and disassembly of vimentin and cytokeratin 5/14 filaments through plectin's intermediate filament-binding domain. *J Cell Sci.* 2000;113 (Pt 3):483-91. Epub 2000/01/20. PubMed PMID: 10639335.
103. Rezniczek GA, Walko G, Wiche G. Plectin gene defects lead to various forms of epidermolysis bullosa simplex. *Dermatol Clin.* 2010;28(1):33-41. Epub 2009/12/01. doi: 10.1016/j.det.2009.10.004. PubMed PMID: 19945614.
104. Gache Y, Chavanas S, Lacour JP, Wiche G, Owaribe K, Meneguzzi G, Ortonne JP. Defective expression of plectin/HD1 in epidermolysis bullosa simplex with muscular dystrophy. *J Clin Invest.* 1996;97(10):2289-98. Epub 1996/05/15. doi: 10.1172/JCI118671. PubMed PMID: 8636409; PMCID: PMC507309.
105. Bolling MC, Jongbloed JDH, Boven LG, Diercks GFH, Smith FJD, Irwin McLean WH, Jonkman MF. Plectin mutations underlie epidermolysis bullosa simplex in 8% of patients. *J Invest Dermatol.* 2014;134(1):273-6. Epub 2013/06/19. doi: 10.1038/jid.2013.277. PubMed PMID: 23774525.
106. Smith FJ, Eady RA, Leigh IM, McMillan JR, Rugg EL, Kelsell DP, Bryant SP, Spurr NK, Geddes JF, Kirtschig G, Milana G, de Bono AG, Owaribe K, Wiche G, Pulkkinen L, Uitto J, McLean WH, Lane EB. Plectin deficiency results in muscular dystrophy with epidermolysis bullosa. *Nat Genet.* 1996;13(4):450-7. Epub 1996/08/01. doi: 10.1038/ng0896-450. PubMed PMID: 8696340.

107. Koss-Harnes D, Hoyheim B, Anton-Lamprecht I, Gjesti A, Jorgensen RS, Jahnsen FL, Olaisen B, Wiche G, Gedde-Dahl T, Jr. A site-specific plectin mutation causes dominant epidermolysis bullosa simplex Ogna: two identical de novo mutations. *J Invest Dermatol.* 2002;118(1):87-93. Epub 2002/02/20. doi: 10.1046/j.0022-202x.2001.01591.x. PubMed PMID: 11851880.
108. Stanley JR, Tanaka T, Mueller S, Klaus-Kovtun V, Roop D. Isolation of complementary DNA for bullous pemphigoid antigen by use of patients' autoantibodies. *J Clin Invest.* 1988;82(6):1864-70. Epub 1988/12/01. doi: 10.1172/JCI113803. PubMed PMID: 2461961; PMCID: PMC442765.
109. Li K, Guidice GJ, Tamai K, Do HC, Sawamura D, Diaz LA, Uitto J. Cloning of partial cDNA for mouse 180-kDa bullous pemphigoid antigen (BPAG2), a highly conserved collagenous protein of the cutaneous basement membrane zone. *J Invest Dermatol.* 1992;99(3):258-63. Epub 1992/09/01. PubMed PMID: 1512460.
110. Franzke CW, Tasanen K, Schacke H, Zhou Z, Tryggvason K, Mauch C, Zigrino P, Sunnarborg S, Lee DC, Fahrenholz F, Bruckner-Tuderman L. Transmembrane collagen XVII, an epithelial adhesion protein, is shed from the cell surface by ADAMs. *EMBO J.* 2002;21(19):5026-35. Epub 2002/10/03. PubMed PMID: 12356719; PMCID: PMC129053.
111. Zillikens D. Acquired skin disease of hemidesmosomes. *J Dermatol Sci.* 1999;20(2):134-54. Epub 1999/06/24. PubMed PMID: 10379705.
112. Delmar M, McKenna WJ. The cardiac desmosome and arrhythmogenic cardiomyopathies: from gene to disease. *Circ Res.* 2010;107(6):700-14. Epub 2010/09/18. doi: 10.1161/CIRCRESAHA.110.223412. PubMed PMID: 20847325.
113. Skerrow CJ, Matoltsy AG. Chemical characterization of isolated epidermal desmosomes. *J Cell Biol.* 1974;63(2 Pt 1):524-30. Epub 1974/11/01. PubMed PMID: 4421013; PMCID: PMC2110930.
114. Hibbs RG, Clark WH, Jr. Electron microscope studies of the human epidermis; the cell boundaries and topography of the stratum malpighii. *J Biophys Biochem Cytol.* 1959;6(1):71-6. Epub 1959/08/01. PubMed PMID: 13673050; PMCID: PMC2229778.
115. Selby CC. An electron microscope study of thin sections of human skin. II. Superficial cell layers of footpad epidermis. *J Invest Dermatol.* 1957;29(2):131-49. Epub 1957/08/01. PubMed PMID: 13475953.
116. Skerrow CJ, Matoltsy AG. Isolation of epidermal desmosomes. *J Cell Biol.* 1974;63(2 Pt 1):515-23. Epub 1974/11/01. PubMed PMID: 4138144; PMCID: PMC2110933.
117. Skerrow CJ, Hunter I, Skerrow D. Dissection of the bovine epidermal desmosome into cytoplasmic protein and membrane glycoprotein domains. *J Cell Sci.* 1987;87 (Pt 3):411-21. Epub 1987/04/01. PubMed PMID: 3429491.
118. Gorbsky G, Steinberg MS. Isolation of the intercellular glycoproteins of desmosomes. *J Cell Biol.* 1981;90(1):243-8. Epub 1981/07/01. PubMed PMID: 6166625; PMCID: PMC2111822.

119. Gorbsky G, Cohen SM, Shida H, Giudice GJ, Steinberg MS. Isolation of the non-glycosylated proteins of desmosomes and immunolocalization of a third plaque protein: desmoplakin III. *Proc Natl Acad Sci U S A*. 1985;82(3):810-4. Epub 1985/02/01. PubMed PMID: 3883348; PMCID: PMC397136.
120. Steinberg MS, Shida H, Giudice GJ, Shida M, Patel NH, Blaschuk OW. On the molecular organization, diversity and functions of desmosomal proteins. *Ciba Found Symp*. 1987;125:3-25. PubMed PMID: 2435471.
121. Cheng X, Mihindikulasuriya K, Den Z, Kowalczyk AP, Calkins CC, Ishiko A, Shimizu A, Koch PJ. Assessment of splice variant-specific functions of desmocollin 1 in the skin. *Mol Cell Biol*. 2004;24(1):154-63. Epub 2003/12/16. PubMed PMID: 14673151; PMCID: PMC303333.
122. Harrison OJ, Brasch J, Lasso G, Katsamba PS, Ahlsen G, Honig B, Shapiro L. Structural basis of adhesive binding by desmocollins and desmogleins. *Proc Natl Acad Sci U S A*. 2016;113(26):7160-5. Epub 2016/06/15. doi: 10.1073/pnas.1606272113. PubMed PMID: 27298358; PMCID: PMC4932976.
123. Saito M, Tucker DK, Kohlhorst D, Niessen CM, Kowalczyk AP. Classical and desmosomal cadherins at a glance. *J Cell Sci*. 2012;125(Pt 11):2547-52. Epub 2012/07/27. doi: 10.1242/jcs.066654. PubMed PMID: 22833291; PMCID: PMC3403229.
124. Kowalczyk AP, Stappenbeck TS, Parry DA, Palka HL, Virata ML, Bornslaeger EA, Nilles LA, Green KJ. Structure and function of desmosomal transmembrane core and plaque molecules. *Biophys Chem*. 1994;50(1-2):97-112. PubMed PMID: 8011944.
125. Palka HL, Green KJ. Roles of plakoglobin end domains in desmosome assembly. *J Cell Sci*. 1997;110 (Pt 19):2359-71. PubMed PMID: 9410875.
126. Kowalczyk AP, Borgwardt JE, Green KJ. Analysis of desmosomal cadherin-adhesive function and stoichiometry of desmosomal cadherin-plakoglobin complexes. *J Invest Dermatol*. 1996;107(3):293-300. PubMed PMID: 8751959.
127. Kowalczyk AP, Bornslaeger EA, Borgwardt JE, Palka HL, Dhaliwal AS, Corcoran CM, Denning MF, Green KJ. The amino-terminal domain of desmoplakin binds to plakoglobin and clusters desmosomal cadherin-plakoglobin complexes. *J Cell Biol*. 1997;139(3):773-84. Epub 1997/11/14. PubMed PMID: 9348293; PMCID: PMC2141713.
128. Thomason HA, Scothern A, McHarg S, Garrod DR. Desmosomes: adhesive strength and signalling in health and disease. *Biochem J*. 2010;429(3):419-33. Epub 2010/07/16. doi: 10.1042/BJ20100567. PubMed PMID: 20626351.
129. Kowalczyk AP, Green KJ. Structure, function, and regulation of desmosomes. *Prog Mol Biol Transl Sci*. 2013;116:95-118. doi: 10.1016/B978-0-12-394311-8.00005-4. PubMed PMID: 23481192; PMCID: PMC4336551.

130. Pokutta S, Herrenknecht K, Kemler R, Engel J. Conformational changes of the recombinant extracellular domain of E-cadherin upon calcium binding. *Eur J Biochem.* 1994;223(3):1019-26. Epub 1994/08/01. PubMed PMID: 8055942.
131. Haussinger D, Ahrens T, Sass HJ, Pertz O, Engel J, Grzesiek S. Calcium-dependent homoassociation of E-cadherin by NMR spectroscopy: changes in mobility, conformation and mapping of contact regions. *J Mol Biol.* 2002;324(4):823-39. Epub 2002/12/04. PubMed PMID: 12460580.
132. Waschke J, Menendez-Castro C, Bruggeman P, Koob R, Amagai M, Gruber HJ, Drenckhahn D, Baumgartner W. Imaging and force spectroscopy on desmoglein 1 using atomic force microscopy reveal multivalent Ca²⁺-dependent, low-affinity trans-interaction. *J Membr Biol.* 2007;216(2-3):83-92. Epub 2007/07/28. doi: 10.1007/s00232-007-9037-9. PubMed PMID: 17657525.
133. Nie Z, Merritt A, Rouhi-Parkouhi M, Tabernero L, Garrod D. Membrane-impermeable cross-linking provides evidence for homophilic, isoform-specific binding of desmosomal cadherins in epithelial cells. *The Journal of biological chemistry.* 2011;286(3):2143-54. Epub 2010/11/26. doi: 10.1074/jbc.M110.192245. PubMed PMID: 21098030; PMCID: PMC3023511.
134. Chitaev NA, Troyanovsky SM. Direct Ca²⁺-dependent heterophilic interaction between desmosomal cadherins, desmoglein and desmocollin, contributes to cell-cell adhesion. *J Cell Biol.* 1997;138(1):193-201. Epub 1997/07/14. PubMed PMID: 9214392; PMCID: PMC2139935.
135. Aoyama Y, Yamamoto Y, Yamaguchi F, Kitajima Y. Low to high Ca²⁺ -switch causes phosphorylation and association of desmocollin 3 with plakoglobin and desmoglein 3 in cultured keratinocytes. *Exp Dermatol.* 2009;18(4):404-8. Epub 2009/04/07. PubMed PMID: 19348003.
136. Andl CD, Stanley JR. Central role of the plakoglobin-binding domain for desmoglein 3 incorporation into desmosomes. *J Invest Dermatol.* 2001;117(5):1068-74. Epub 2001/11/17. doi: 10.1046/j.0022-202x.2001.01528.x. PubMed PMID: 11710914.
137. Choi HJ, Gross JC, Pokutta S, Weis WI. Interactions of plakoglobin and beta-catenin with desmosomal cadherins: basis of selective exclusion of alpha- and beta-catenin from desmosomes. *The Journal of biological chemistry.* 2009;284(46):31776-88. Epub 2009/09/18. doi: 10.1074/jbc.M109.047928. PubMed PMID: 19759396; PMCID: PMC2797248.
138. Gaudry CA, Palka HL, Dusek RL, Huen AC, Khandekar MJ, Hudson LG, Green KJ. Tyrosine-phosphorylated plakoglobin is associated with desmogleins but not desmoplakin after epidermal growth factor receptor activation. *The Journal of biological chemistry.* 2001;276(27):24871-80. Epub 2001/05/04. doi: 10.1074/jbc.M102731200. PubMed PMID: 11335725.
139. Kami K, Chidgey M, Dafforn T, Overduin M. The desmoglein-specific cytoplasmic region is intrinsically disordered in solution and interacts with multiple desmosomal protein partners. *J Mol Biol.* 2009;386(2):531-43. Epub 2009/01/13. doi: 10.1016/j.jmb.2008.12.054. PubMed PMID: 19136012.

140. Smith EA, Fuchs E. Defining the interactions between intermediate filaments and desmosomes. *J Cell Biol.* 1998;141(5):1229-41. Epub 1998/06/12. PubMed PMID: 9606214; PMCID: PMC2137181.
141. Bornslaeger EA, Godsel LM, Corcoran CM, Park JK, Hatzfeld M, Kowalczyk AP, Green KJ. Plakophilin 1 interferes with plakoglobin binding to desmoplakin, yet together with plakoglobin promotes clustering of desmosomal plaque complexes at cell-cell borders. *J Cell Sci.* 2001;114(Pt 4):727-38. Epub 2001/02/15. PubMed PMID: 11171378.
142. Delva E, Tucker DK, Kowalczyk AP. The desmosome. *Cold Spring Harb Perspect Biol.* 2009;1(2):a002543. Epub 2010/01/13. doi: 10.1101/cshperspect.a002543. PubMed PMID: 20066089; PMCID: PMC2742091.
143. Kowalczyk AP, Rubenstein DS, Garrod DR, Green KJ, Stanley JR. Milestones in Investigative Dermatology: The Desmosome. *J Invest Dermatol.* 2007;127 Suppl 3:E1. Epub 2007/01/01. doi: 10.1038/sj.skinbio.6250007. PubMed PMID: 26879533.
144. Kottke MD, Delva E, Kowalczyk AP. The desmosome: cell science lessons from human diseases. *J Cell Sci.* 2006;119(Pt 5):797-806. Epub 2006/02/24. doi: 10.1242/jcs.02888. PubMed PMID: 16495480.
145. Buxton RS, Wheeler GN, Pidsley SC, Marsden MD, Adams MJ, Jenkins NA, Gilbert DJ, Copeland NG. Mouse desmocollin (Dsc3) and desmoglein (Dsg1) genes are closely linked in the proximal region of chromosome 18. *Genomics.* 1994;21(3):510-6. Epub 1994/06/01. doi: 10.1006/geno.1994.1309. PubMed PMID: 7959727.
146. Wang Y, Amagai M, Minoshima S, Sakai K, Green KJ, Nishikawa T, Shimizu N. The human genes for desmogleins (DSG1 and DSG3) are located in a small region on chromosome 18q12. *Genomics.* 1994;20(3):492-5. Epub 1994/04/01. doi: 10.1006/geno.1994.1207. PubMed PMID: 8034325.
147. Simrak D, Cowley CM, Buxton RS, Arnemann J. Tandem arrangement of the closely linked desmoglein genes on human chromosome 18. *Genomics.* 1995;25(2):591-4. Epub 1995/01/20. PubMed PMID: 7790000.
148. Cowley CM, Simrak D, Marsden MD, King IA, Arnemann J, Buxton RS. A YAC contig joining the desmocollin and desmoglein loci on human chromosome 18 and ordering of the desmocollin genes. *Genomics.* 1997;42(2):208-16. Epub 1997/06/01. doi: 10.1006/geno.1997.4718. PubMed PMID: 9192840.
149. Hunt DM, Sahota VK, Taylor K, Simrak D, Hornigold N, Arnemann J, Wolfe J, Buxton RS. Clustered cadherin genes: a sequence-ready contig for the desmosomal cadherin locus on human chromosome 18. *Genomics.* 1999;62(3):445-55. Epub 2000/01/25. doi: 10.1006/geno.1999.6036. PubMed PMID: 10644442.
150. Getsios S, Simpson CL, Kojima S, Harmon R, Sheu LJ, Dusek RL, Cornwell M, Green KJ. Desmoglein 1-dependent suppression of EGFR signaling promotes epidermal differentiation and

morphogenesis. *J Cell Biol.* 2009;185(7):1243-58. doi: 10.1083/jcb.200809044. PubMed PMID: 19546243; PMCID: PMC2712955.

151. Merritt AJ, Berika MY, Zhai W, Kirk SE, Ji B, Hardman MJ, Garrod DR. Suprabasal desmoglein 3 expression in the epidermis of transgenic mice results in hyperproliferation and abnormal differentiation. *Mol Cell Biol.* 2002;22(16):5846-58. Epub 2002/07/26. PubMed PMID: 12138195; PMCID: PMC133994.

152. Brennan D, Hu Y, Joubeh S, Choi YW, Whitaker-Menezes D, O'Brien T, Uitto J, Rodeck U, Mahoney MG. Suprabasal Dsg2 expression in transgenic mouse skin confers a hyperproliferative and apoptosis-resistant phenotype to keratinocytes. *J Cell Sci.* 2007;120(Pt 5):758-71. Epub 2007/02/08. doi: 10.1242/jcs.03392. PubMed PMID: 17284515.

153. Elias PM, Matsuyoshi N, Wu H, Lin C, Wang ZH, Brown BE, Stanley JR. Desmoglein isoform distribution affects stratum corneum structure and function. *J Cell Biol.* 2001;153(2):243-9. Epub 2001/04/20. PubMed PMID: 11309406; PMCID: PMC2169464.

154. Kowalczyk AP, Anderson JE, Borgwardt JE, Hashimoto T, Stanley JR, Green KJ. Pemphigus sera recognize conformationally sensitive epitopes in the amino-terminal region of desmoglein-1. *J Invest Dermatol.* 1995;105(2):147-52. Epub 1995/08/01. PubMed PMID: 7543545.

155. Mahoney MG, Wang Z, Rothenberger K, Koch PJ, Amagai M, Stanley JR. Explanations for the clinical and microscopic localization of lesions in pemphigus foliaceus and vulgaris. *J Clin Invest.* 1999;103(4):461-8. Epub 1999/02/18. doi: 10.1172/JCI5252. PubMed PMID: 10021453; PMCID: PMC408100.

156. Payne AS, Hanakawa Y, Amagai M, Stanley JR. Desmosomes and disease: pemphigus and bullous impetigo. *Curr Opin Cell Biol.* 2004;16(5):536-43. doi: 10.1016/j.ceb.2004.07.006. PubMed PMID: 15363804.

157. Amagai M, Matsuyoshi N, Wang ZH, Andl C, Stanley JR. Toxin in bullous impetigo and staphylococcal scalded-skin syndrome targets desmoglein 1. *Nat Med.* 2000;6(11):1275-7. Epub 2000/11/04. doi: 10.1038/81385. PubMed PMID: 11062541.

158. Has C, Jakob T, He Y, Kiritsi D, Hausser I, Bruckner-Tuderman L. Loss of desmoglein 1 associated with palmoplantar keratoderma, dermatitis and multiple allergies. *Br J Dermatol.* 2015;172(1):257-61. doi: 10.1111/bjd.13247. PubMed PMID: 25041099.

159. Has C, Technau-Hafsi K. Palmoplantar keratodermas: clinical and genetic aspects. *J Dtsch Dermatol Ges.* 2016;14(2):123-39; quiz 40. Epub 2016/01/29. doi: 10.1111/ddg.12930. PubMed PMID: 26819106.

160. Samuelov L, Sarig O, Harmon RM, Rapaport D, Ishida-Yamamoto A, Isakov O, Koetsier JL, Gat A, Goldberg I, Bergman R, Spiegel R, Eytan O, Geller S, Peleg S, Shomron N, Goh CS, Wilson NJ, Smith FJ, Pohler E, Simpson MA, McLean WH, Irvine AD, Horowitz M, McGrath JA, Green KJ, Sprecher E. Desmoglein 1 deficiency results in severe dermatitis, multiple allergies and metabolic wasting. *Nat Genet.* 2013;45(10):1244-8. doi: 10.1038/ng.2739. PubMed PMID: 23974871; PMCID: PMC3791825.

161. Cheng R, Yan M, Ni C, Zhang J, Li M, Yao Z. Report of Chinese family with severe dermatitis, multiple allergies and metabolic wasting syndrome caused by novel homozygous desmoglein-1 gene mutation. *J Dermatol*. 2016;43(10):1201-4. doi: 10.1111/1346-8138.13431. PubMed PMID: 27154412.
162. Kugelmann D, Radeva MY, Spindler V, Waschke J. Desmoglein 1 Deficiency Causes Lethal Skin Blistering. *J Invest Dermatol*. 2019. Epub 2019/01/21. doi: 10.1016/j.jid.2019.01.002. PubMed PMID: 30660666.
163. Harman KE, Seed PT, Gratian MJ, Bhogal BS, Challacombe SJ, Black MM. The severity of cutaneous and oral pemphigus is related to desmoglein 1 and 3 antibody levels. *Br J Dermatol*. 2001;144(4):775-80. Epub 2001/04/12. PubMed PMID: 11298536.
164. Sekiguchi M, Futei Y, Fujii Y, Iwasaki T, Nishikawa T, Amagai M. Dominant autoimmune epitopes recognized by pemphigus antibodies map to the N-terminal adhesive region of desmogleins. *J Immunol*. 2001;167(9):5439-48. Epub 2001/10/24. PubMed PMID: 11673563.
165. Kljuic A, Bauer RC, Christiano AM. Genomic organization of mouse desmocollin genes reveals evolutionary conservation. *DNA Seq*. 2004;15(2):148-52. Epub 2004/09/07. PubMed PMID: 15346771.
166. Collins JE, Legan PK, Kenny TP, MacGarvie J, Holton JL, Garrod DR. Cloning and sequence analysis of desmosomal glycoproteins 2 and 3 (desmocollins): cadherin-like desmosomal adhesion molecules with heterogeneous cytoplasmic domains. *J Cell Biol*. 1991;113(2):381-91. Epub 1991/04/01. PubMed PMID: 2010468; PMCID: PMC2288940.
167. Getsios S, Amargo EV, Dusek RL, Ishii K, Sheu L, Godsel LM, Green KJ. Coordinated expression of desmoglein 1 and desmocollin 1 regulates intercellular adhesion. *Differentiation*. 2004;72(8):419-33. Epub 2004/12/21. doi: 10.1111/j.1432-0436.2004.07208008.x. PubMed PMID: 15606501.
168. Chidgey M, Brakebusch C, Gustafsson E, Cruchley A, Hail C, Kirk S, Merritt A, North A, Tselepis C, Hewitt J, Byrne C, Fassler R, Garrod D. Mice lacking desmocollin 1 show epidermal fragility accompanied by barrier defects and abnormal differentiation. *J Cell Biol*. 2001;155(5):821-32. Epub 2001/11/21. doi: 10.1083/jcb.200105009. PubMed PMID: 11714727; PMCID: PMC2150874.
169. Hanakawa Y, Amagai M, Shirakata Y, Sayama K, Hashimoto K. Different effects of dominant negative mutants of desmocollin and desmoglein on the cell-cell adhesion of keratinocytes. *J Cell Sci*. 2000;113 (Pt 10):1803-11. Epub 2000/04/19. PubMed PMID: 10769211.
170. Iranzo P, Ishii N, Hashimoto T, Alsina-Gibert M. Nonclassical pemphigus with exclusively IgG anti-desmocollin 3-specific antibodies. *Australas J Dermatol*. 2019. Epub 2019/01/24. doi: 10.1111/ajd.12991. PubMed PMID: 30671942.
171. Ishii N, Teye K, Fukuda S, Uehara R, Hachiya T, Koga H, Tsuchisaka A, Numata S, Ohyama B, Tateishi C, Tsuruta D, Furumura M, Hattori S, Kawakami T, Ohata C, Hashimoto T. Anti-

desmocollin autoantibodies in nonclassical pemphigus. *Br J Dermatol.* 2015;173(1):59-68. Epub 2015/02/03. doi: 10.1111/bjd.13711. PubMed PMID: 25640111.

172. Ayub M, Basit S, Jelani M, Ur Rehman F, Iqbal M, Yasinzi M, Ahmad W. A homozygous nonsense mutation in the human desmocollin-3 (DSC3) gene underlies hereditary hypotrichosis and recurrent skin vesicles. *Am J Hum Genet.* 2009;85(4):515-20. Epub 2009/09/22. doi: 10.1016/j.ajhg.2009.08.015. PubMed PMID: 19765682; PMCID: PMC2756559.

173. Bolling MC, Mekkes JR, Goldschmidt WF, van Noesel CJ, Jonkman MF, Pas HH. Acquired palmoplantar keratoderma and immunobullous disease associated with antibodies to desmocollin 3. *Br J Dermatol.* 2007;157(1):168-73. Epub 2007/06/21. doi: 10.1111/j.1365-2133.2007.07920.x. PubMed PMID: 17578440.

174. Simpson MA, Mansour S, Ahnood D, Kalidas K, Patton MA, McKenna WJ, Behr ER, Crosby AH. Homozygous mutation of desmocollin-2 in arrhythmogenic right ventricular cardiomyopathy with mild palmoplantar keratoderma and woolly hair. *Cardiology.* 2009;113(1):28-34. Epub 2008/10/30. doi: 10.1159/000165696. PubMed PMID: 18957847.

175. Leung CL, Green KJ, Liem RK. Plakins: a family of versatile cytolinker proteins. *Trends Cell Biol.* 2002;12(1):37-45. Epub 2002/02/21. PubMed PMID: 11854008.

176. Bouameur JE, Favre B, Borradori L. Plakins, a versatile family of cytolinkers: roles in skin integrity and in human diseases. *J Invest Dermatol.* 2014;134(4):885-94. Epub 2013/12/20. doi: 10.1038/jid.2013.498. PubMed PMID: 24352042.

177. Green KJ, Stappenbeck TS, Parry DA, Virata ML. Structure of desmoplakin and its association with intermediate filaments. *J Dermatol.* 1992;19(11):765-9. Epub 1992/11/01. PubMed PMID: 1293163.

178. Kowalczyk AP, Hatzfeld M, Bornslaeger EA, Kopp DS, Borgwardt JE, Corcoran CM, Settler A, Green KJ. The head domain of plakophilin-1 binds to desmoplakin and enhances its recruitment to desmosomes. Implications for cutaneous disease. *The Journal of biological chemistry.* 1999;274(26):18145-8. Epub 1999/06/22. PubMed PMID: 10373410.

179. Stappenbeck TS, Green KJ. The desmoplakin carboxyl terminus coaligns with and specifically disrupts intermediate filament networks when expressed in cultured cells. *J Cell Biol.* 1992;116(5):1197-209. Epub 1992/03/01. PubMed PMID: 1740472; PMCID: PMC2289350.

180. Gallicano GI, Kouklis P, Bauer C, Yin M, Vasioukhin V, Degenstein L, Fuchs E. Desmoplakin is required early in development for assembly of desmosomes and cytoskeletal linkage. *J Cell Biol.* 1998;143(7):2009-22. Epub 1998/12/29. PubMed PMID: 9864371; PMCID: PMC2175222.

181. Vasioukhin V, Bowers E, Bauer C, Degenstein L, Fuchs E. Desmoplakin is essential in epidermal sheet formation. *Nat Cell Biol.* 2001;3(12):1076-85. Epub 2002/01/10. doi: 10.1038/ncb1201-1076. PubMed PMID: 11781569.

182. McAleer MA, Pohler E, Smith FJ, Wilson NJ, Cole C, MacGowan S, Koetsier JL, Godsel LM, Harmon RM, Gruber R, Crumrine D, Elias PM, McDermott M, Butler K, Broderick A, Sarig O,

Sprecher E, Green KJ, McLean WH, Irvine AD. Severe dermatitis, multiple allergies, and metabolic wasting syndrome caused by a novel mutation in the N-terminal plakin domain of desmoplakin. *J Allergy Clin Immunol*. 2015;136(5):1268-76. Epub 2015/06/16. doi: 10.1016/j.jaci.2015.05.002. PubMed PMID: 26073755; PMCID: PMC4649901.

183. Armstrong DK, McKenna KE, Purkis PE, Green KJ, Eady RA, Leigh IM, Hughes AE. Haploinsufficiency of desmoplakin causes a striate subtype of palmoplantar keratoderma. *Hum Mol Genet*. 1999;8(1):143-8. Epub 1999/01/15. PubMed PMID: 9887343.

184. Norgett EE, Hatsell SJ, Carvajal-Huerta L, Cabezas JC, Common J, Purkis PE, Whittock N, Leigh IM, Stevens HP, Kelsell DP. Recessive mutation in desmoplakin disrupts desmoplakin-intermediate filament interactions and causes dilated cardiomyopathy, woolly hair and keratoderma. *Hum Mol Genet*. 2000;9(18):2761-6. Epub 2000/11/07. PubMed PMID: 11063735.

185. Pigors M, Schwieger-Briel A, Cosgarea R, Diaconeasa A, Bruckner-Tuderman L, Fleck T, Has C. Desmoplakin mutations with palmoplantar keratoderma, woolly hair and cardiomyopathy. *Acta Derm Venereol*. 2015;95(3):337-40. Epub 2014/09/18. doi: 10.2340/00015555-1974. PubMed PMID: 25227139.

186. Gul IS, Hulpiau P, Saeys Y, van Roy F. Metazoan evolution of the armadillo repeat superfamily. *Cell Mol Life Sci*. 2017;74(3):525-41. Epub 2016/08/09. doi: 10.1007/s00018-016-2319-6. PubMed PMID: 27497926.

187. Choi HJ, Weis WI. Structure of the armadillo repeat domain of plakophilin 1. *J Mol Biol*. 2005;346(1):367-76. Epub 2005/01/25. doi: 10.1016/j.jmb.2004.11.048. PubMed PMID: 15663951.

188. Schmidt A, Jager S. Plakophilins--hard work in the desmosome, recreation in the nucleus? *Eur J Cell Biol*. 2005;84(2-3):189-204. Epub 2005/04/12. doi: 10.1016/j.ejcb.2004.12.020. PubMed PMID: 15819400.

189. Schwarz J, Ayim A, Schmidt A, Jager S, Koch S, Baumann R, Dunne AA, Moll R. Differential expression of desmosomal plakophilins in various types of carcinomas: correlation with cell type and differentiation. *Hum Pathol*. 2006;37(5):613-22. Epub 2006/05/02. doi: 10.1016/j.humpath.2006.01.013. PubMed PMID: 16647960.

190. Heid HW, Schmidt A, Zimbelmann R, Schafer S, Winter-Simanowski S, Stumpp S, Keith M, Figge U, Schnolzer M, Franke WW. Cell type-specific desmosomal plaque proteins of the plakoglobin family: plakophilin 1 (band 6 protein). *Differentiation*. 1994;58(2):113-31. Epub 1994/12/01. PubMed PMID: 7890138.

191. Bass-Zubek AE, Godsel LM, Delmar M, Green KJ. Plakophilins: multifunctional scaffolds for adhesion and signaling. *Curr Opin Cell Biol*. 2009;21(5):708-16. Epub 2009/08/14. doi: 10.1016/j.ceb.2009.07.002. PubMed PMID: 19674883; PMCID: PMC3091506.

192. Schmidt A, Langbein L, Rode M, Pratzel S, Zimbelmann R, Franke WW. Plakophilins 1a and 1b: widespread nuclear proteins recruited in specific epithelial cells as desmosomal plaque components. *Cell Tissue Res*. 1997;290(3):481-99. Epub 1998/02/07. PubMed PMID: 9369526.

193. Hatzfeld M, Haffner C, Schulze K, Vinzens U. The function of plakophilin 1 in desmosome assembly and actin filament organization. *J Cell Biol.* 2000;149(1):209-22. Epub 2000/04/04. PubMed PMID: 10747098; PMCID: PMC2175088.
194. McGrath JA, Hoeger PH, Christiano AM, McMillan JR, Mellerio JE, Ashton GH, Dopping-Hepenstal PJ, Lake BD, Leigh IM, Harper JI, Eady RA. Skin fragility and hypohidrotic ectodermal dysplasia resulting from ablation of plakophilin 1. *Br J Dermatol.* 1999;140(2):297-307. Epub 1999/05/08. PubMed PMID: 10233227.
195. Gurjar M, Raychaudhuri K, Mahadik S, Reddy D, Atak A, Shetty T, Rao K, Karkhanis MS, Gosavi P, Sehgal L, Gupta S, Dalal SN. Plakophilin3 increases desmosome assembly, size and stability by increasing expression of desmocollin2. *Biochem Biophys Res Commun.* 2018;495(1):768-74. Epub 2017/11/18. doi: 10.1016/j.bbrc.2017.11.085. PubMed PMID: 29146182.
196. Witcher LL, Collins R, Puttagunta S, Mechanic SE, Munson M, Gumbiner B, Cowin P. Desmosomal cadherin binding domains of plakoglobin. *The Journal of biological chemistry.* 1996;271(18):10904-9. Epub 1996/05/03. PubMed PMID: 8631907.
197. Chitaev NA, Leube RE, Troyanovsky RB, Eshkind LG, Franke WW, Troyanovsky SM. The binding of plakoglobin to desmosomal cadherins: patterns of binding sites and topogenic potential. *J Cell Biol.* 1996;133(2):359-69. Epub 1996/04/01. PubMed PMID: 8609168; PMCID: PMC2120792.
198. Pasdar M, Krzeminski KA, Nelson WJ. Regulation of desmosome assembly in MDCK epithelial cells: coordination of membrane core and cytoplasmic plaque domain assembly at the plasma membrane. *J Cell Biol.* 1991;113(3):645-55. Epub 1991/05/01. PubMed PMID: 1707884; PMCID: PMC2288966.
199. Bonne S, Gilbert B, Hatzfeld M, Chen X, Green KJ, van Roy F. Defining desmosomal plakophilin-3 interactions. *J Cell Biol.* 2003;161(2):403-16. Epub 2003/04/23. doi: 10.1083/jcb.200303036. PubMed PMID: 12707304; PMCID: PMC2172904.
200. Ruiz P, Brinkmann V, Ledermann B, Behrend M, Grund C, Thalhammer C, Vogel F, Birchmeier C, Gunthert U, Franke WW, Birchmeier W. Targeted mutation of plakoglobin in mice reveals essential functions of desmosomes in the embryonic heart. *J Cell Biol.* 1996;135(1):215-25. Epub 1996/10/01. PubMed PMID: 8858175; PMCID: PMC2121015.
201. Erken H, Yariz KO, Duman D, Kaya CT, Sayin T, Heper AO, Tekin M. Cardiomyopathy with alopecia and palmoplantar keratoderma (CAPK) is caused by a JUP mutation. *Br J Dermatol.* 2011;165(4):917-21. Epub 2011/06/15. doi: 10.1111/j.1365-2133.2011.10455.x. PubMed PMID: 21668431.
202. Cabral RM, Liu L, Hogan C, Dopping-Hepenstal PJ, Winik BC, Asial RA, Dobson R, Mein CA, Baselaga PA, Mellerio JE, Nanda A, Boente Mdel C, Kelsell DP, McGrath JA, South AP. Homozygous mutations in the 5' region of the JUP gene result in cutaneous disease but normal heart development in children. *J Invest Dermatol.* 2010;130(6):1543-50. Epub 2010/02/05. doi: 10.1038/jid.2010.7. PubMed PMID: 20130592.

203. Hanahan D, Weinberg RA. Hallmarks of cancer: the next generation. *Cell*. 2011;144(5):646-74. Epub 2011/03/08. doi: 10.1016/j.cell.2011.02.013. PubMed PMID: 21376230.
204. Livshits Z, Rao RB, Smith SW. An approach to chemotherapy-associated toxicity. *Emerg Med Clin North Am*. 2014;32(1):167-203. Epub 2013/11/28. doi: 10.1016/j.emc.2013.09.002. PubMed PMID: 24275174.
205. Pellegrini C, Maturo MG, Di Nardo L, Ciciarelli V, Gutierrez Garcia-Rodrigo C, Fagnoli MC. Understanding the Molecular Genetics of Basal Cell Carcinoma. *Int J Mol Sci*. 2017;18(11). Epub 2017/11/23. doi: 10.3390/ijms18112485. PubMed PMID: 29165358; PMCID: PMC5713451.
206. Pritchett EN, Doyle A, Shaver CM, Miller B, Abdelmalek M, Cusack CA, Malat GE, Chung CL. Nonmelanoma Skin Cancer in Nonwhite Organ Transplant Recipients. *JAMA Dermatol*. 2016;152(12):1348-53. Epub 2016/09/23. doi: 10.1001/jamadermatol.2016.3328. PubMed PMID: 27653769.
207. Hussein MR. Ultraviolet radiation and skin cancer: molecular mechanisms. *J Cutan Pathol*. 2005;32(3):191-205. Epub 2005/02/11. doi: 10.1111/j.0303-6987.2005.00281.x. PubMed PMID: 15701081.
208. Verkouteren JAC, Ramdas KHR, Wakkee M, Nijsten T. Epidemiology of basal cell carcinoma: scholarly review. *Br J Dermatol*. 2017;177(2):359-72. Epub 2017/02/22. doi: 10.1111/bjd.15321. PubMed PMID: 28220485.
209. Lomas A, Leonardi-Bee J, Bath-Hextall F. A systematic review of worldwide incidence of nonmelanoma skin cancer. *Br J Dermatol*. 2012;166(5):1069-80. Epub 2012/01/19. doi: 10.1111/j.1365-2133.2012.10830.x. PubMed PMID: 22251204.
210. Green AC, Olsen CM. Cutaneous squamous cell carcinoma: an epidemiological review. *Br J Dermatol*. 2017;177(2):373-81. Epub 2017/02/18. doi: 10.1111/bjd.15324. PubMed PMID: 28211039.
211. Greenburg G, Hay ED. Epithelia suspended in collagen gels can lose polarity and express characteristics of migrating mesenchymal cells. *J Cell Biol*. 1982;95(1):333-9. Epub 1982/10/01. PubMed PMID: 7142291; PMCID: PMC2112361.
212. Greenburg G, Hay ED. Cytodifferentiation and tissue phenotype change during transformation of embryonic lens epithelium to mesenchyme-like cells in vitro. *Dev Biol*. 1986;115(2):363-79. Epub 1986/06/01. PubMed PMID: 3519318.
213. Yan C, Grimm WA, Garner WL, Qin L, Travis T, Tan N, Han YP. Epithelial to mesenchymal transition in human skin wound healing is induced by tumor necrosis factor-alpha through bone morphogenic protein-2. *Am J Pathol*. 2010;176(5):2247-58. Epub 2010/03/23. doi: 10.2353/ajpath.2010.090048. PubMed PMID: 20304956; PMCID: PMC2861090.

214. Barriere G, Fici P, Gallerani G, Fabbri F, Rigaud M. Epithelial Mesenchymal Transition: a double-edged sword. *Clin Transl Med.* 2015;4:14. Epub 2015/05/02. doi: 10.1186/s40169-015-0055-4. PubMed PMID: 25932287; PMCID: PMC4409604.
215. Chaffer CL, San Juan BP, Lim E, Weinberg RA. EMT, cell plasticity and metastasis. *Cancer Metastasis Rev.* 2016;35(4):645-54. Epub 2016/11/24. doi: 10.1007/s10555-016-9648-7. PubMed PMID: 27878502.
216. Jolly MK, Ware KE, Gilja S, Somarelli JA, Levine H. EMT and MET: necessary or permissive for metastasis? *Mol Oncol.* 2017;11(7):755-69. Epub 2017/05/27. doi: 10.1002/1878-0261.12083. PubMed PMID: 28548345; PMCID: PMC5496498.
217. Xu J, Lamouille S, Derynck R. TGF-beta-induced epithelial to mesenchymal transition. *Cell Res.* 2009;19(2):156-72. Epub 2009/01/21. doi: 10.1038/cr.2009.5. PubMed PMID: 19153598; PMCID: PMC4720263.
218. Katsuno Y, Lamouille S, Derynck R. TGF-beta signaling and epithelial-mesenchymal transition in cancer progression. *Curr Opin Oncol.* 2013;25(1):76-84. Epub 2012/12/01. doi: 10.1097/CCO.0b013e32835b6371. PubMed PMID: 23197193.
219. Barrios-Rodiles M, Brown KR, Ozdamar B, Bose R, Liu Z, Donovan RS, Shinjo F, Liu Y, Dembowy J, Taylor IW, Luga V, Przulj N, Robinson M, Suzuki H, Hayashizaki Y, Jurisica I, Wrana JL. High-throughput mapping of a dynamic signaling network in mammalian cells. *Science.* 2005;307(5715):1621-5. Epub 2005/03/12. doi: 10.1126/science.1105776. PubMed PMID: 15761153.
220. Ozdamar B, Bose R, Barrios-Rodiles M, Wang HR, Zhang Y, Wrana JL. Regulation of the polarity protein Par6 by TGFbeta receptors controls epithelial cell plasticity. *Science.* 2005;307(5715):1603-9. Epub 2005/03/12. doi: 10.1126/science.1105718. PubMed PMID: 15761148.
221. Paul R, Ewing CM, Jarrard DF, Isaacs WB. The cadherin cell-cell adhesion pathway in prostate cancer progression. *Br J Urol.* 1997;79 Suppl 1:37-43. Epub 1997/03/01. PubMed PMID: 9088271.
222. Dunbier A, Guilford P. Hereditary diffuse gastric cancer. *Adv Cancer Res.* 2001;83:55-65. Epub 2001/10/23. PubMed PMID: 11665720.
223. Berx G, Van Roy F. The E-cadherin/catenin complex: an important gatekeeper in breast cancer tumorigenesis and malignant progression. *Breast Cancer Res.* 2001;3(5):289-93. Epub 2001/10/13. PubMed PMID: 11597316; PMCID: PMC138690.
224. Machado JC, Oliveira C, Carvalho R, Soares P, Berx G, Caldas C, Seruca R, Carneiro F, Sobrinho-Simoes M. E-cadherin gene (CDH1) promoter methylation as the second hit in sporadic diffuse gastric carcinoma. *Oncogene.* 2001;20(12):1525-8. Epub 2001/04/21. doi: 10.1038/sj.onc.1204234. PubMed PMID: 11313896.

225. Gravdal K, Halvorsen OJ, Haukaas SA, Akslen LA. A switch from E-cadherin to N-cadherin expression indicates epithelial to mesenchymal transition and is of strong and independent importance for the progress of prostate cancer. *Clin Cancer Res.* 2007;13(23):7003-11. Epub 2007/12/07. doi: 10.1158/1078-0432.CCR-07-1263. PubMed PMID: 18056176.
226. Chao YL, Shepard CR, Wells A. Breast carcinoma cells re-express E-cadherin during mesenchymal to epithelial reverting transition. *Mol Cancer.* 2010;9:179. Epub 2010/07/09. doi: 10.1186/1476-4598-9-179. PubMed PMID: 20609236; PMCID: PMC2907333.
227. Tabaries S, Dupuy F, Dong Z, Monast A, Annis MG, Spicer J, Ferri LE, Omeroglu A, Basik M, Amir E, Clemons M, Siegel PM. Claudin-2 promotes breast cancer liver metastasis by facilitating tumor cell interactions with hepatocytes. *Mol Cell Biol.* 2012;32(15):2979-91. Epub 2012/05/31. doi: 10.1128/MCB.00299-12. PubMed PMID: 22645303; PMCID: PMC3434516.
228. Martin TA, Mansel RE, Jiang WG. Loss of occludin leads to the progression of human breast cancer. *Int J Mol Med.* 2010;26(5):723-34. Epub 2010/09/30. PubMed PMID: 20878095.
229. Martin TA, Jordan N, Davies EL, Jiang WG. Metastasis to Bone in Human Cancer Is Associated with Loss of Occludin Expression. *Anticancer Res.* 2016;36(3):1287-93. Epub 2016/03/16. PubMed PMID: 26977027.
230. Ahmad R, Kumar B, Chen Z, Chen X, Muller D, Lele SM, Washington MK, Batra SK, Dhawan P, Singh AB. Loss of claudin-3 expression induces IL6/gp130/Stat3 signaling to promote colon cancer malignancy by hyperactivating Wnt/beta-catenin signaling. *Oncogene.* 2017;36(47):6592-604. Epub 2017/08/08. doi: 10.1038/onc.2017.259. PubMed PMID: 28783170.
231. Kahn M. Can we safely target the WNT pathway? *Nat Rev Drug Discov.* 2014;13(7):513-32. Epub 2014/07/02. doi: 10.1038/nrd4233. PubMed PMID: 24981364; PMCID: PMC4426976.
232. Duchartre Y, Kim YM, Kahn M. The Wnt signaling pathway in cancer. *Crit Rev Oncol Hematol.* 2016;99:141-9. Epub 2016/01/19. doi: 10.1016/j.critrevonc.2015.12.005. PubMed PMID: 26775730; PMCID: PMC5853106.
233. Clevers H, Nusse R. Wnt/beta-catenin signaling and disease. *Cell.* 2012;149(6):1192-205. Epub 2012/06/12. doi: 10.1016/j.cell.2012.05.012. PubMed PMID: 22682243.
234. Sebio A, Kahn M, Lenz HJ. The potential of targeting Wnt/beta-catenin in colon cancer. *Expert Opin Ther Targets.* 2014;18(6):611-5. Epub 2014/04/08. doi: 10.1517/14728222.2014.906580. PubMed PMID: 24702624.
235. Schatoff EM, Leach BI, Dow LE. Wnt Signaling and Colorectal Cancer. *Curr Colorectal Cancer Rep.* 2017;13(2):101-10. Epub 2017/04/18. doi: 10.1007/s11888-017-0354-9. PubMed PMID: 28413363; PMCID: PMC5391049.
236. Stockinger A, Eger A, Wolf J, Beug H, Foisner R. E-cadherin regulates cell growth by modulating proliferation-dependent beta-catenin transcriptional activity. *J Cell Biol.* 2001;154(6):1185-96. Epub 2001/09/21. doi: 10.1083/jcb.200104036. PubMed PMID: 11564756; PMCID: PMC2150811.

237. Shin SH, Lim DY, Reddy K, Malakhova M, Liu F, Wang T, Song M, Chen H, Bae KB, Ryu J, Liu K, Lee MH, Bode AM, Dong Z. A Small Molecule Inhibitor of the beta-Catenin-TCF4 Interaction Suppresses Colorectal Cancer Growth In Vitro and In Vivo. *EBioMedicine*. 2017;25:22-31. Epub 2017/10/17. doi: 10.1016/j.ebiom.2017.09.029. PubMed PMID: 29033371; PMCID: PMC5704052.
238. Piao HL, Yuan Y, Wang M, Sun Y, Liang H, Ma L. alpha-catenin acts as a tumour suppressor in E-cadherin-negative basal-like breast cancer by inhibiting NF-kappaB signalling. *Nat Cell Biol*. 2014;16(3):245-54. Epub 2014/02/11. doi: 10.1038/ncb2909. PubMed PMID: 24509793; PMCID: PMC3943677.
239. Raftopoulos I, Davaris P, Karatzas G, Karayannacos P, Kouraklis G. Level of alpha-catenin expression in colorectal cancer correlates with invasiveness, metastatic potential, and survival. *J Surg Oncol*. 1998;68(2):92-9. Epub 1998/06/12. PubMed PMID: 9624037.
240. Korinek V, Barker N, Morin PJ, van Wichen D, de Weger R, Kinzler KW, Vogelstein B, Clevers H. Constitutive transcriptional activation by a beta-catenin-Tcf complex in APC-/- colon carcinoma. *Science*. 1997;275(5307):1784-7. Epub 1997/03/21. PubMed PMID: 9065401.
241. Hiraki A, Shinohara M, Ikebe T, Nakamura S, Kurahara S, Garrod DR. Immunohistochemical staining of desmosomal components in oral squamous cell carcinomas and its association with tumour behaviour. *Br J Cancer*. 1996;73(12):1491-7. Epub 1996/06/01. PubMed PMID: 8664118; PMCID: PMC2074545.
242. Kurzen H, Munzing I, Hartschuh W. Expression of desmosomal proteins in squamous cell carcinomas of the skin. *J Cutan Pathol*. 2003;30(10):621-30. Epub 2004/01/28. PubMed PMID: 14744087.
243. Wang L, Liu T, Wang Y, Cao L, Nishioka M, Aguirre RL, Ishikawa A, Geng L, Okada N. Altered expression of desmocollin 3, desmoglein 3, and beta-catenin in oral squamous cell carcinoma: correlation with lymph node metastasis and cell proliferation. *Virchows Arch*. 2007;451(5):959-66. Epub 2007/09/12. doi: 10.1007/s00428-007-0485-5. PubMed PMID: 17846785.
244. Teh MT, Parkinson EK, Thurlow JK, Liu F, Fortune F, Wan H. A molecular study of desmosomes identifies a desmoglein isoform switch in head and neck squamous cell carcinoma. *J Oral Pathol Med*. 2011;40(1):67-76. Epub 2010/10/07. doi: 10.1111/j.1600-0714.2010.00951.x. PubMed PMID: 20923451.
245. Harada H, Iwatsuki K, Ohtsuka M, Han GW, Kaneko F. Abnormal desmoglein expression by squamous cell carcinoma cells. *Acta Derm Venereol*. 1996;76(6):417-20. Epub 1996/11/01. doi: 10.2340/0001555576417420. PubMed PMID: 8982400.
246. Tada H, Hatoko M, Tanaka A, Kuwahara M, Muramatsu T. Expression of desmoglein I and plakoglobin in skin carcinomas. *J Cutan Pathol*. 2000;27(1):24-9. Epub 2000/02/05. PubMed PMID: 10660128.
247. Xin Z, Yamaguchi A, Sakamoto K. Aberrant expression and altered cellular localization of desmosomal and hemidesmosomal proteins are associated with aggressive clinicopathological

features of oral squamous cell carcinoma. *Virchows Arch.* 2014;465(1):35-47. Epub 2014/05/23. doi: 10.1007/s00428-014-1594-6. PubMed PMID: 24849508.

248. Wong MP, Cheang M, Yorida E, Coldman A, Gilks CB, Huntsman D, Berean K. Loss of desmoglein 1 expression associated with worse prognosis in head and neck squamous cell carcinoma patients. *Pathology.* 2008;40(6):611-6. Epub 2008/08/30. doi: 10.1080/00313020802320614. PubMed PMID: 18752129.

249. De Bruin A, Muller E, Wurm S, Caldelari R, Wyder M, Wheelock MJ, Suter MM. Loss of invasiveness in squamous cell carcinoma cells overexpressing desmosomal cadherins. *Cell Adhes Commun.* 1999;7(1):13-28. Epub 1999/05/06. PubMed PMID: 10228732.

250. Chen J, O'Shea C, Fitzpatrick JE, Koster MI, Koch PJ. Loss of Desmocollin 3 in skin tumor development and progression. *Mol Carcinog.* 2012;51(7):535-45. Epub 2011/06/18. doi: 10.1002/mc.20818. PubMed PMID: 21681825; PMCID: PMC3178010.

251. Yang L, Chen Y, Cui T, Knosel T, Zhang Q, Albring KF, Huber O, Petersen I. Desmoplakin acts as a tumor suppressor by inhibition of the Wnt/beta-catenin signaling pathway in human lung cancer. *Carcinogenesis.* 2012;33(10):1863-70. Epub 2012/07/14. doi: 10.1093/carcin/bgs226. PubMed PMID: 22791817.

252. Yin T, Getsios S, Caldelari R, Kowalczyk AP, Muller EJ, Jones JC, Green KJ. Plakoglobin suppresses keratinocyte motility through both cell-cell adhesion-dependent and -independent mechanisms. *Proc Natl Acad Sci U S A.* 2005;102(15):5420-5. Epub 2005/04/05. doi: 10.1073/pnas.0501676102. PubMed PMID: 15805189; PMCID: PMC556221.

253. Fang WK, Chen B, Xu XE, Liao LD, Wu ZY, Wu JY, Shen J, Xu LY, Li EM. Altered expression and localization of desmoglein 3 in esophageal squamous cell carcinoma. *Acta Histochem.* 2014;116(5):803-9. Epub 2014/03/19. doi: 10.1016/j.acthis.2014.01.010. PubMed PMID: 24630396.

254. Brown L, Waseem A, Cruz IN, Szary J, Gunic E, Mannan T, Unadkat M, Yang M, Valderrama F, O'Toole EA, Wan H. Desmoglein 3 promotes cancer cell migration and invasion by regulating activator protein 1 and protein kinase C-dependent-Ezrin activation. *Oncogene.* 2014;33(18):2363-74. Epub 2013/06/12. doi: 10.1038/onc.2013.186. PubMed PMID: 23752190.

255. Brennan D, Mahoney MG. Increased expression of Dsg2 in malignant skin carcinomas: A tissue-microarray based study. *Cell Adh Migr.* 2009;3(2):148-54. Epub 2009/05/22. PubMed PMID: 19458482; PMCID: PMC2679873.

256. Brennan-Crispi DM, Overmiller AM, Tamayo-Orrego L, Marous MR, Sahu J, McGuinn KP, Cooper F, Georgiou IC, Frankfurter M, Salas-Alanis JC, Charron F, Millar SE, Mahoney MG, Riobo-Del Galdo NA. Overexpression of Desmoglein 2 in a Mouse Model of Gorlin Syndrome Enhances Spontaneous Basal Cell Carcinoma Formation through STAT3-Mediated Gli1 Expression. *J Invest Dermatol.* 2019;139(2):300-7. Epub 2018/10/07. doi: 10.1016/j.jid.2018.09.009. PubMed PMID: 30291846; PMCID: PMC6342634.

257. Cai F, Zhu Q, Miao Y, Shen S, Su X, Shi Y. Desmoglein-2 is overexpressed in non-small cell lung cancer tissues and its knockdown suppresses NSCLC growth by regulation of p27 and CDK2. *J Cancer Res Clin Oncol*. 2017;143(1):59-69. Epub 2016/09/16. doi: 10.1007/s00432-016-2250-0. PubMed PMID: 27629878.
258. Sahin U, Koslowski M, Dhaene K, Usener D, Brandenburg G, Seitz G, Huber C, Tureci O. Claudin-18 splice variant 2 is a pan-cancer target suitable for therapeutic antibody development. *Clin Cancer Res*. 2008;14(23):7624-34. Epub 2008/12/03. doi: 10.1158/1078-0432.CCR-08-1547. PubMed PMID: 19047087.
259. Micke P, Mattsson JS, Edlund K, Lohr M, Jirstrom K, Berglund A, Botling J, Rahnenfuehrer J, Marincevic M, Ponten F, Ekman S, Hengstler J, Woll S, Sahin U, Tureci O. Aberrantly activated claudin 6 and 18.2 as potential therapy targets in non-small-cell lung cancer. *Int J Cancer*. 2014;135(9):2206-14. Epub 2014/04/09. doi: 10.1002/ijc.28857. PubMed PMID: 24710653.
260. Wang M, Liu Y, Qian X, Wei N, Tang Y, Yang J. Downregulation of occludin affects the proliferation, apoptosis and metastatic properties of human lung carcinoma. *Oncol Rep*. 2018;40(1):454-62. Epub 2018/05/12. doi: 10.3892/or.2018.6408. PubMed PMID: 29750300.
261. Solimando AG, Brandl A, Mattenheimer K, Graf C, Ritz M, Ruckdeschel A, Stuhmer T, Mokhtari Z, Rudelius M, Dotterweich J, Bittrich M, Desantis V, Ebert R, Trerotoli P, Frassanito MA, Rosenwald A, Vacca A, Einsele H, Jakob F, Beilhack A. JAM-A as a prognostic factor and new therapeutic target in multiple myeloma. *Leukemia*. 2018;32(3):736-43. Epub 2017/10/25. doi: 10.1038/leu.2017.287. PubMed PMID: 29064484; PMCID: PMC5843918.
262. Magara K, Takasawa A, Osanai M, Ota M, Tagami Y, Ono Y, Takasawa K, Murata M, Hirohashi Y, Miyajima M, Yamada G, Hasegawa T, Sawada N. Elevated expression of JAM-A promotes neoplastic properties of lung adenocarcinoma. *Cancer Sci*. 2017;108(11):2306-14. Epub 2017/08/25. doi: 10.1111/cas.13385. PubMed PMID: 28837251; PMCID: PMC5666024.
263. McSherry EA, McGee SF, Jirstrom K, Doyle EM, Brennan DJ, Landberg G, Dervan PA, Hopkins AM, Gallagher WM. JAM-A expression positively correlates with poor prognosis in breast cancer patients. *Int J Cancer*. 2009;125(6):1343-51. Epub 2009/06/18. doi: 10.1002/ijc.24498. PubMed PMID: 19533747.
264. Zhang B, Chen X, Lin Y, Wang S, Bao Q. Occludin protein expression in human cervical cancer and its association with patient's clinical characteristics. *J Cancer Res Ther*. 2018;14(1):124-7. Epub 2018/03/09. doi: 10.4103/jcrt.JCRT_664_17. PubMed PMID: 29516973.
265. Huang JY, Xu YY, Sun Z, Wang ZN, Zhu Z, Song YX, Luo Y, Zhang X, Xu HM. Low junctional adhesion molecule A expression correlates with poor prognosis in gastric cancer. *J Surg Res*. 2014;192(2):494-502. Epub 2014/07/19. doi: 10.1016/j.jss.2014.06.025. PubMed PMID: 25033702.
266. Medici D, Hay ED, Goodenough DA. Cooperation between snail and LEF-1 transcription factors is essential for TGF-beta1-induced epithelial-mesenchymal transition. *Mol Biol Cell*. 2006;17(4):1871-9. Epub 2006/02/10. doi: 10.1091/mbc.e05-08-0767. PubMed PMID: 16467384; PMCID: PMC1415320.

267. Zhou YN, Xu CP, Chen Y, Han B, Yang SM, Fang DC. Alpha-catenin expression is decreased in patients with gastric carcinoma. *World J Gastroenterol.* 2005;11(22):3468-72. Epub 2005/06/11. PubMed PMID: 15948257; PMCID: PMC4316006.
268. Ding L, Ellis MJ, Li S, Larson DE, Chen K, Wallis JW, Harris CC, McLellan MD, Fulton RS, Fulton LL, Abbott RM, Hoog J, Dooling DJ, Koboldt DC, Schmidt H, Kalicki J, Zhang Q, Chen L, Lin L, Wendl MC, McMichael JF, Magrini VJ, Cook L, McGrath SD, Vickery TL, Appelbaum E, Deschryver K, Davies S, Guintoli T, Lin L, Crowder R, Tao Y, Snider JE, Smith SM, Dukes AF, Sanderson GE, Pohl CS, Delehaunty KD, Fronick CC, Pape KA, Reed JS, Robinson JS, Hodges JS, Schierding W, Dees ND, Shen D, Locke DP, Wiechert ME, Eldred JM, Peck JB, Oberkfell BJ, Lolofie JT, Du F, Hawkins AE, O'Laughlin MD, Bernard KE, Cunningham M, Elliott G, Mason MD, Thompson DM, Jr., Ivanovich JL, Goodfellow PJ, Perou CM, Weinstock GM, Aft R, Watson M, Ley TJ, Wilson RK, Mardis ER. Genome remodelling in a basal-like breast cancer metastasis and xenograft. *Nature.* 2010;464(7291):999-1005. Epub 2010/04/16. doi: 10.1038/nature08989. PubMed PMID: 20393555; PMCID: PMC2872544.
269. Thoreson MA, Reynolds AB. Altered expression of the catenin p120 in human cancer: implications for tumor progression. *Differentiation.* 2002;70(9-10):583-9. Epub 2002/12/21. doi: 10.1046/j.1432-0436.2002.700911.x. PubMed PMID: 12492499.
270. Dillon DA, D'Aquila T, Reynolds AB, Fearon ER, Rimm DL. The expression of p120ctn protein in breast cancer is independent of alpha- and beta-catenin and E-cadherin. *Am J Pathol.* 1998;152(1):75-82. Epub 1998/01/09. PubMed PMID: 9422525; PMCID: PMC1858125.
271. Shimazui T, Schalken JA, Girolodi LA, Jansen CF, Akaza H, Koiso K, Debruyne FM, Bringuier PP. Prognostic value of cadherin-associated molecules (alpha-, beta-, and gamma-catenins and p120cas) in bladder tumors. *Cancer Res.* 1996;56(18):4154-8. Epub 1996/09/15. PubMed PMID: 8797585.
272. Gold JS, Reynolds AB, Rimm DL. Loss of p120ctn in human colorectal cancer predicts metastasis and poor survival. *Cancer Lett.* 1998;132(1-2):193-201. Epub 1999/07/09. PubMed PMID: 10397474.
273. Skoudy A, Gomez S, Fabre M, Garcia de Herreros A. p120-catenin expression in human colorectal cancer. *Int J Cancer.* 1996;68(1):14-20. Epub 1996/09/27. doi: 10.1002/(SICI)1097-0215(19960927)68:1<14::AID-IJC3>3.0.CO;2-#. PubMed PMID: 8895533.
274. Chen YJ, Chang JT, Lee L, Wang HM, Liao CT, Chiu CC, Chen PJ, Cheng AJ. DSG3 is overexpressed in head neck cancer and is a potential molecular target for inhibition of oncogenesis. *Oncogene.* 2007;26(3):467-76. Epub 2006/08/01. doi: 10.1038/sj.onc.1209802. PubMed PMID: 16878157.
275. Huang CC, Lee TJ, Chang PH, Lee YS, Chuang CC, Jhang YJ, Chen YW, Chen CW, Tsai CN. Desmoglein 3 is overexpressed in inverted papilloma and squamous cell carcinoma of sinonasal cavity. *Laryngoscope.* 2010;120(1):26-9. Epub 2009/08/19. doi: 10.1002/lary.20151. PubMed PMID: 19688857.

276. Fukuoka J, Dracheva T, Shih JH, Hewitt SM, Fujii T, Kishor A, Mann F, Shilo K, Franks TJ, Travis WD, Jen J. Desmoglein 3 as a prognostic factor in lung cancer. *Hum Pathol.* 2007;38(2):276-83. Epub 2006/11/07. doi: 10.1016/j.humpath.2006.08.006. PubMed PMID: 17084439.
277. Khan K, Hardy R, Haq A, Ogunbiyi O, Morton D, Chidgey M. Desmocollin switching in colorectal cancer. *Br J Cancer.* 2006;95(10):1367-70. Epub 2006/11/08. doi: 10.1038/sj.bjc.6603453. PubMed PMID: 17088906; PMCID: PMC2360607.
278. Yashiro M, Nishioka N, Hirakawa K. Decreased expression of the adhesion molecule desmoglein-2 is associated with diffuse-type gastric carcinoma. *Eur J Cancer.* 2006;42(14):2397-403. Epub 2006/08/08. doi: 10.1016/j.ejca.2006.03.024. PubMed PMID: 16890424.
279. Biedermann K, Vogelsang H, Becker I, Plaschke S, Siewert JR, Hofler H, Keller G. Desmoglein 2 is expressed abnormally rather than mutated in familial and sporadic gastric cancer. *J Pathol.* 2005;207(2):199-206. Epub 2005/07/19. doi: 10.1002/path.1821. PubMed PMID: 16025435.
280. Oshiro MM, Kim CJ, Wozniak RJ, Junk DJ, Munoz-Rodriguez JL, Burr JA, Fitzgerald M, Pawar SC, Cress AE, Domann FE, Futscher BW. Epigenetic silencing of DSC3 is a common event in human breast cancer. *Breast Cancer Res.* 2005;7(5):R669-80. Epub 2005/09/20. doi: 10.1186/bcr1273. PubMed PMID: 16168112; PMCID: PMC1242132.
281. Klus GT, Rokaeus N, Bittner ML, Chen Y, Korz DM, Sukumar S, Schick A, Szallasi Z. Down-regulation of the desmosomal cadherin desmocollin 3 in human breast cancer. *Int J Oncol.* 2001;19(1):169-74. Epub 2001/06/16. PubMed PMID: 11408939.
282. Rieger-Christ KM, Ng L, Hanley RS, Durrani O, Ma H, Yee AS, Libertino JA, Summerhayes IC. Restoration of plakoglobin expression in bladder carcinoma cell lines suppresses cell migration and tumorigenic potential. *Br J Cancer.* 2005;92(12):2153-9. Epub 2005/06/09. doi: 10.1038/sj.bjc.6602651. PubMed PMID: 15942628; PMCID: PMC2361803.
283. Shiina H, Breault JE, Basset WW, Enokida H, Urakami S, Li LC, Okino ST, Deguchi M, Kaneuchi M, Terashima M, Yoneda T, Shigeno K, Carroll PR, Igawa M, Dahiya R. Functional Loss of the gamma-catenin gene through epigenetic and genetic pathways in human prostate cancer. *Cancer Res.* 2005;65(6):2130-8. Epub 2005/03/23. doi: 10.1158/0008-5472.CAN-04-3398. PubMed PMID: 15781623.
284. Winn RA, Heasley LE. Gamma-catenin expression is reduced or absent in a subset of human non-small cell lung cancers, and its re-expression inhibits cell growth. *Chest.* 2004;125(5 Suppl):122S-3S. Epub 2004/05/12. PubMed PMID: 15136458.
285. Redell MS, Tweardy DJ. Targeting transcription factors for cancer therapy. *Curr Pharm Des.* 2005;11(22):2873-87. Epub 2005/08/17. PubMed PMID: 16101443.
286. Ferone G, Mollo MR, Thomason HA, Antonini D, Zhou H, Ambrosio R, De Rosa L, Salvatore D, Getsios S, van Bokhoven H, Dixon J, Missero C. p63 control of desmosome gene expression and adhesion is compromised in AEC syndrome. *Hum Mol Genet.* 2013;22(3):531-43. Epub 2012/10/31. doi: 10.1093/hmg/dds464. PubMed PMID: 23108156; PMCID: PMC3542863.

287. Oshiro MM, Watts GS, Wozniak RJ, Junk DJ, Munoz-Rodriguez JL, Domann FE, Futscher BW. Mutant p53 and aberrant cytosine methylation cooperate to silence gene expression. *Oncogene*. 2003;22(23):3624-34. Epub 2003/06/06. doi: 10.1038/sj.onc.1206545. PubMed PMID: 12789271.
288. Cui T, Chen Y, Yang L, Knosel T, Huber O, Pacyna-Gengelbach M, Petersen I. The p53 target gene desmocollin 3 acts as a novel tumor suppressor through inhibiting EGFR/ERK pathway in human lung cancer. *Carcinogenesis*. 2012;33(12):2326-33. Epub 2012/09/04. doi: 10.1093/carcin/bgs273. PubMed PMID: 22941060.
289. Kume K, Haraguchi M, Hijioka H, Ishida T, Miyawaki A, Nakamura N, Ozawa M. The transcription factor Snail enhanced the degradation of E-cadherin and desmoglein 2 in oral squamous cell carcinoma cells. *Biochem Biophys Res Commun*. 2013;430(3):889-94. Epub 2012/12/25. doi: 10.1016/j.bbrc.2012.12.060. PubMed PMID: 23261431.
290. Kenchegowda D, Harvey SA, Swamynathan S, Lathrop KL, Swamynathan SK. Critical role of Klf5 in regulating gene expression during post-eyelid opening maturation of mouse corneas. *PloS one*. 2012;7(9):e44771. Epub 2012/10/02. doi: 10.1371/journal.pone.0044771. PubMed PMID: 23024760; PMCID: PMC3443110.
291. Owens P, Bazzi H, Engelking E, Han G, Christiano AM, Wang XJ. Smad4-dependent desmoglein-4 expression contributes to hair follicle integrity. *Dev Biol*. 2008;322(1):156-66. Epub 2008/08/12. doi: 10.1016/j.ydbio.2008.07.020. PubMed PMID: 18692037; PMCID: PMC2642977.
292. Wilanowski T, Caddy J, Ting SB, Hislop NR, Cerruti L, Auden A, Zhao LL, Asquith S, Ellis S, Sinclair R, Cunningham JM, Jane SM. Perturbed desmosomal cadherin expression in grainy head-like 1-null mice. *EMBO J*. 2008;27(6):886-97. Epub 2008/02/22. doi: 10.1038/emboj.2008.24. PubMed PMID: 18288204; PMCID: PMC2274933.
293. Mlacki M, Darido C, Jane SM, Wilanowski T. Loss of Grainy head-like 1 is associated with disruption of the epidermal barrier and squamous cell carcinoma of the skin. *PloS one*. 2014;9(2):e89247. Epub 2014/03/04. doi: 10.1371/journal.pone.0089247. PubMed PMID: 24586629; PMCID: PMC3930704.
294. Funakoshi S, Ezaki T, Kong J, Guo RJ, Lynch JP. Repression of the desmocollin 2 gene expression in human colon cancer cells is relieved by the homeodomain transcription factors Cdx1 and Cdx2. *Mol Cancer Res*. 2008;6(9):1478-90. Epub 2008/09/30. doi: 10.1158/1541-7786.MCR-07-2161. PubMed PMID: 18819935.
295. Chakravarthi BV, Nepal S, Varambally S. Genomic and Epigenomic Alterations in Cancer. *Am J Pathol*. 2016;186(7):1724-35. Epub 2016/06/25. doi: 10.1016/j.ajpath.2016.02.023. PubMed PMID: 27338107; PMCID: PMC4929396.
296. Pan J, Chen Y, Mo C, Wang D, Chen J, Mao X, Guo S, Zhuang J, Qiu S. Association of DSC3 mRNA down-regulation in prostate cancer with promoter hypermethylation and poor prognosis. *PloS one*. 2014;9(3):e92815. Epub 2014/03/26. doi: 10.1371/journal.pone.0092815. PubMed PMID: 24664224; PMCID: PMC3963953.

297. Wang Q, Peng D, Zhu S, Chen Z, Hu T, Soutto M, Saad R, Zhang S, Ei-Rifai W. Regulation of Desmocollin3 Expression by Promoter Hypermethylation is Associated with Advanced Esophageal Adenocarcinomas. *J Cancer*. 2014;5(6):457-64. Epub 2014/05/23. doi: 10.7150/jca.9145. PubMed PMID: 24847386; PMCID: PMC4026999.
298. Breault JE, Shiina H, Igawa M, Ribeiro-Filho LA, Deguchi M, Enokida H, Urakami S, Terashima M, Nakagawa M, Kane CJ, Carroll PR, Dahiya R. Methylation of the gamma-catenin gene is associated with poor prognosis of renal cell carcinoma. *Clin Cancer Res*. 2005;11(2 Pt 1):557-64. Epub 2005/02/11. PubMed PMID: 15701841.
299. Shafiei F, Rahnema F, Pawella L, Mitchell MD, Gluckman PD, Lobie PE. DNMT3A and DNMT3B mediate autocrine hGH repression of plakoglobin gene transcription and consequent phenotypic conversion of mammary carcinoma cells. *Oncogene*. 2008;27(18):2602-12. Epub 2007/11/14. doi: 10.1038/sj.onc.1210917. PubMed PMID: 17998942.
300. Oka D, Yamashita S, Tomioka T, Nakanishi Y, Kato H, Kaminishi M, Ushijima T. The presence of aberrant DNA methylation in noncancerous esophageal mucosae in association with smoking history: a target for risk diagnosis and prevention of esophageal cancers. *Cancer*. 2009;115(15):3412-26. Epub 2009/05/28. doi: 10.1002/cncr.24394. PubMed PMID: 19472401.
301. Ke XS, Qu Y, Rostad K, Li WC, Lin B, Halvorsen OJ, Haukaas SA, Jonassen I, Petersen K, Goldfinger N, Rotter V, Akslen LA, Oyan AM, Kalland KH. Genome-wide profiling of histone h3 lysine 4 and lysine 27 trimethylation reveals an epigenetic signature in prostate carcinogenesis. *PloS one*. 2009;4(3):e4687. Epub 2009/03/06. doi: 10.1371/journal.pone.0004687. PubMed PMID: 19262738; PMCID: PMC2650415.
302. Gould JJ, Kenney PA, Rieger-Christ KM, Silva Neto B, Wszolek MF, LaVoie A, Holway AH, Spurrier B, Austin J, Cammarata BK, Canes D, Libertino JA, Summerhayes IC. Identification of tumor and invasion suppressor gene modulators in bladder cancer by different classes of histone deacetylase inhibitors using reverse phase protein arrays. *J Urol*. 2010;183(6):2395-402. Epub 2010/04/21. doi: 10.1016/j.juro.2010.02.004. PubMed PMID: 20403623.
303. Asimaki A, Tandri H, Duffy ER, Winterfield JR, Mackey-Bojack S, Picken MM, Cooper LT, Wilber DJ, Marcus FI, Basso C, Thiene G, Tsatsopoulou A, Protonotarios N, Stevenson WG, McKenna WJ, Gautam S, Remick DG, Calkins H, Saffitz JE. Altered desmosomal proteins in granulomatous myocarditis and potential pathogenic links to arrhythmogenic right ventricular cardiomyopathy. *Circ Arrhythm Electrophysiol*. 2011;4(5):743-52. Epub 2011/08/24. doi: 10.1161/CIRCEP.111.964890. PubMed PMID: 21859801; PMCID: PMC3203520.
304. Wolf A, Rietscher K, Glass M, Huttelmaier S, Schutkowski M, Ihling C, Sinz A, Wingenfeld A, Mun A, Hatzfeld M. Insulin signaling via Akt2 switches plakophilin 1 function from stabilizing cell adhesion to promoting cell proliferation. *J Cell Sci*. 2013;126(Pt 8):1832-44. Epub 2013/02/28. doi: 10.1242/jcs.118992. PubMed PMID: 23444369.
305. Wallis S, Lloyd S, Wise I, Ireland G, Fleming TP, Garrod D. The alpha isoform of protein kinase C is involved in signaling the response of desmosomes to wounding in cultured epithelial

cells. *Mol Biol Cell*. 2000;11(3):1077-92. Epub 2000/03/11. doi: 10.1091/mbc.11.3.1077. PubMed PMID: 10712521; PMCID: PMC14832.

306. Tucker DK, Stahley SN, Kowalczyk AP. Plakophilin-1 protects keratinocytes from pemphigus vulgaris IgG by forming calcium-independent desmosomes. *J Invest Dermatol*. 2014;134(4):1033-43. Epub 2013/09/24. doi: 10.1038/jid.2013.401. PubMed PMID: 24056861; PMCID: PMC3961504.

307. Thomason HA, Cooper NH, Ansell DM, Chiu M, Merrit AJ, Hardman MJ, Garrod DR. Direct evidence that PKC α positively regulates wound re-epithelialization: correlation with changes in desmosomal adhesiveness. *J Pathol*. 2012;227(3):346-56. Epub 2012/03/13. doi: 10.1002/path.4016. PubMed PMID: 22407785.

308. Johnson JL, Koetsier JL, Sirico A, Agidi AT, Antonini D, Missero C, Green KJ. The desmosomal protein desmoglein 1 aids recovery of epidermal differentiation after acute UV light exposure. *J Invest Dermatol*. 2014;134(8):2154-62. Epub 2014/03/07. doi: 10.1038/jid.2014.124. PubMed PMID: 24594668; PMCID: PMC4102640.

309. Tokonzaba E, Chen J, Cheng X, Den Z, Ganeshan R, Muller EJ, Koch PJ. Plakoglobin as a regulator of desmocollin gene expression. *J Invest Dermatol*. 2013;133(12):2732-40. Epub 2013/05/09. doi: 10.1038/jid.2013.220. PubMed PMID: 23652796; PMCID: PMC3760975.

310. Mao X, Cho MJT, Ellebrecht CT, Mukherjee EM, Payne AS. Stat3 regulates desmoglein 3 transcription in epithelial keratinocytes. *JCI Insight*. 2017;2(9). Epub 2017/05/05. doi: 10.1172/jci.insight.92253. PubMed PMID: 28469076; PMCID: PMC5414550.

311. Lorch JH, Klessner J, Park JK, Getsios S, Wu YL, Stack MS, Green KJ. Epidermal growth factor receptor inhibition promotes desmosome assembly and strengthens intercellular adhesion in squamous cell carcinoma cells. *The Journal of biological chemistry*. 2004;279(35):37191-200. Epub 2004/06/19. doi: 10.1074/jbc.M405123200. PubMed PMID: 15205458.

312. Zuckerman JD, Lee WY, DelGaudio JM, Moore CE, Nava P, Nusrat A, Parkos CA. Pathophysiology of nasal polyposis: the role of desmosomal junctions. *Am J Rhinol*. 2008;22(6):589-97. Epub 2009/01/31. doi: 10.2500/ajr.2008.22.3235. PubMed PMID: 19178795.

313. Li G, Schaidler H, Satyamoorthy K, Hanakawa Y, Hashimoto K, Herlyn M. Downregulation of E-cadherin and Desmoglein 1 by autocrine hepatocyte growth factor during melanoma development. *Oncogene*. 2001;20(56):8125-35. Epub 2002/01/10. doi: 10.1038/sj.onc.1205034. PubMed PMID: 11781826.

314. Savagner P, Yamada KM, Thiery JP. The zinc-finger protein slug causes desmosome dissociation, an initial and necessary step for growth factor-induced epithelial-mesenchymal transition. *J Cell Biol*. 1997;137(6):1403-19. Epub 1997/06/16. PubMed PMID: 9182671; PMCID: PMC2132541.

315. Kampf C, Relova AJ, Sandler S, Roomans GM. Effects of TNF- α , IFN- γ and IL- β on normal human bronchial epithelial cells. *Eur Respir J*. 1999;14(1):84-91. Epub 1999/09/18. PubMed PMID: 10489833.

316. Godsel LM, Dubash AD, Bass-Zubek AE, Amargo EV, Klessner JL, Hobbs RP, Chen X, Green KJ. Plakophilin 2 couples actomyosin remodeling to desmosomal plaque assembly via RhoA. *Mol Biol Cell*. 2010;21(16):2844-59. Epub 2010/06/18. doi: 10.1091/mbc.E10-02-0131. PubMed PMID: 20554761; PMCID: PMC2921118.
317. Godsel LM, Hsieh SN, Amargo EV, Bass AE, Pascoe-McGillicuddy LT, Huen AC, Thorne ME, Gaudry CA, Park JK, Myung K, Goldman RD, Chew TL, Green KJ. Desmoplakin assembly dynamics in four dimensions: multiple phases differentially regulated by intermediate filaments and actin. *J Cell Biol*. 2005;171(6):1045-59. Epub 2005/12/21. doi: 10.1083/jcb.200510038. PubMed PMID: 16365169; PMCID: PMC2171300.
318. Bass-Zubek AE, Hobbs RP, Amargo EV, Garcia NJ, Hsieh SN, Chen X, Wahl JK, 3rd, Denning MF, Green KJ. Plakophilin 2: a critical scaffold for PKC alpha that regulates intercellular junction assembly. *J Cell Biol*. 2008;181(4):605-13. Epub 2008/05/14. doi: 10.1083/jcb.200712133. PubMed PMID: 18474624; PMCID: PMC2386101.
319. Roberts BJ, Johnson KE, McGuinn KP, Saowapa J, Svoboda RA, Mahoney MG, Johnson KR, Wahl JK, 3rd. Palmitoylation of plakophilin is required for desmosome assembly. *J Cell Sci*. 2014;127(Pt 17):3782-93. Epub 2014/07/09. doi: 10.1242/jcs.149849. PubMed PMID: 25002405; PMCID: PMC4150063.
320. Nekrasova OE, Amargo EV, Smith WO, Chen J, Kreitzer GE, Green KJ. Desmosomal cadherins utilize distinct kinesins for assembly into desmosomes. *J Cell Biol*. 2011;195(7):1185-203. Epub 2011/12/21. doi: 10.1083/jcb.201106057. PubMed PMID: 22184201; PMCID: PMC3246898.
321. Lewis JE, Jensen PJ, Wheelock MJ. Cadherin function is required for human keratinocytes to assemble desmosomes and stratify in response to calcium. *J Invest Dermatol*. 1994;102(6):870-7. Epub 1994/06/01. PubMed PMID: 8006450.
322. Lewis JE, Wahl JK, 3rd, Sass KM, Jensen PJ, Johnson KR, Wheelock MJ. Cross-talk between adherens junctions and desmosomes depends on plakoglobin. *J Cell Biol*. 1997;136(4):919-34. Epub 1997/02/24. PubMed PMID: 9049256; PMCID: PMC2132504.
323. Shafraz O, Rubsam M, Stahley SN, Caldara AL, Kowalczyk AP, Niessen CM, Sivasankar S. E-cadherin binds to desmoglein to facilitate desmosome assembly. *Elife*. 2018;7. Epub 2018/07/13. doi: 10.7554/eLife.37629. PubMed PMID: 29999492; PMCID: PMC6066328.
324. Resnik N, Sepcic K, Plemenitas A, Windoffer R, Leube R, Veranic P. Desmosome assembly and cell-cell adhesion are membrane raft-dependent processes. *The Journal of biological chemistry*. 2011;286(2):1499-507. doi: 10.1074/jbc.M110.189464. PubMed PMID: 21071449; PMCID: 3020758.
325. Singer SJ, Nicolson GL. The fluid mosaic model of the structure of cell membranes. *Science*. 1972;175(4023):720-31. Epub 1972/02/18. PubMed PMID: 4333397.

326. Rodriguez-Cuenca S, Pellegrinelli V, Campbell M, Oresic M, Vidal-Puig A. Sphingolipids and glycerophospholipids - The "ying and yang" of lipotoxicity in metabolic diseases. *Prog Lipid Res.* 2017;66:14-29. Epub 2017/01/21. doi: 10.1016/j.plipres.2017.01.002. PubMed PMID: 28104532.
327. Helenius A, Simons K. Solubilization of membranes by detergents. *Biochim Biophys Acta.* 1975;415(1):29-79. Epub 1975/03/25. PubMed PMID: 1091302.
328. Helenius A, Fries E, Garoff H, Simons K. Solubilization of the Semliki Forest virus membrane with sodium deoxycholate. *Biochim Biophys Acta.* 1976;436(2):319-34. Epub 1976/06/17. PubMed PMID: 1276219.
329. Simons K, Helenius A, Garoff H. Solubilization of the membrane proteins from Semliki Forest virus with Triton X100. *J Mol Biol.* 1973;80(1):119-33. Epub 1973/10/15. PubMed PMID: 4784893.
330. Stier A, Sackmann E. Spin labels as enzyme substrates. Heterogeneous lipid distribution in liver microsomal membranes. *Biochim Biophys Acta.* 1973;311(3):400-8. Epub 1973/07/06. PubMed PMID: 4354130.
331. Karnovsky MJ, Kleinfeld AM, Hoover RL, Klausner RD. The concept of lipid domains in membranes. *J Cell Biol.* 1982;94(1):1-6. Epub 1982/07/01. PubMed PMID: 6889603; PMCID: PMC2112185.
332. Simons K, Ikonen E. Functional rafts in cell membranes. *Nature.* 1997;387(6633):569-72. Epub 1997/06/05. doi: 10.1038/42408. PubMed PMID: 9177342.
333. Pike LJ. Rafts defined: a report on the Keystone Symposium on Lipid Rafts and Cell Function. *J Lipid Res.* 2006;47(7):1597-8. Epub 2006/04/29. doi: 10.1194/jlr.E600002-JLR200. PubMed PMID: 16645198.
334. Korn ED. Structure and Function of the Plasma Membrane : A biochemical perspective. *J Gen Physiol.* 1968;52(1):257-78. Epub 1968/07/01. PubMed PMID: 19873624; PMCID: PMC2225798.
335. Brown DA, London E. Structure and function of sphingolipid- and cholesterol-rich membrane rafts. *The Journal of biological chemistry.* 2000;275(23):17221-4. Epub 2000/04/20. doi: 10.1074/jbc.R000005200. PubMed PMID: 10770957.
336. Subczynski WK, Pasenkiewicz-Gierula M, Widomska J, Mainali L, Raguz M. High Cholesterol/Low Cholesterol: Effects in Biological Membranes: A Review. *Cell Biochem Biophys.* 2017;75(3-4):369-85. Epub 2017/04/19. doi: 10.1007/s12013-017-0792-7. PubMed PMID: 28417231; PMCID: PMC5645210.
337. Rog T, Pasenkiewicz-Gierula M. Cholesterol effects on the phospholipid condensation and packing in the bilayer: a molecular simulation study. *FEBS Lett.* 2001;502(1-2):68-71. Epub 2001/08/02. PubMed PMID: 11478950.

338. Rog T, Pasenkiewicz-Gierula M. Cholesterol effects on the phosphatidylcholine bilayer nonpolar region: a molecular simulation study. *Biophys J*. 2001;81(4):2190-202. Epub 2001/09/22. doi: 10.1016/S0006-3495(01)75867-5. PubMed PMID: 11566790; PMCID: PMC1301691.
339. Lingwood D, Simons K. Detergent resistance as a tool in membrane research. *Nat Protoc*. 2007;2(9):2159-65. doi: 10.1038/nprot.2007.294. PubMed PMID: 17853872.
340. Ahmed SN, Brown DA, London E. On the origin of sphingolipid/cholesterol-rich detergent-insoluble cell membranes: physiological concentrations of cholesterol and sphingolipid induce formation of a detergent-insoluble, liquid-ordered lipid phase in model membranes. *Biochemistry*. 1997;36(36):10944-53. Epub 1997/09/09. doi: 10.1021/bi971167g. PubMed PMID: 9283086.
341. Nezil FA, Bloom M. Combined influence of cholesterol and synthetic amphiphilic peptides upon bilayer thickness in model membranes. *Biophys J*. 1992;61(5):1176-83. Epub 1992/05/01. doi: 10.1016/S0006-3495(92)81926-4. PubMed PMID: 1600079; PMCID: PMC1260381.
342. Yuan C, Johnston LJ. Phase evolution in cholesterol/DPPC monolayers: atomic force microscopy and near field scanning optical microscopy studies. *J Microsc*. 2002;205(Pt 2):136-46. Epub 2002/03/07. PubMed PMID: 11879428.
343. Weiss TM, van der Wel PC, Killian JA, Koeppe RE, 2nd, Huang HW. Hydrophobic mismatch between helices and lipid bilayers. *Biophys J*. 2003;84(1):379-85. Epub 2003/01/14. doi: 10.1016/S0006-3495(03)74858-9. PubMed PMID: 12524291; PMCID: PMC1302619.
344. Kucerka N, Perlmutter JD, Pan J, Tristram-Nagle S, Katsaras J, Sachs JN. The effect of cholesterol on short- and long-chain monounsaturated lipid bilayers as determined by molecular dynamics simulations and X-ray scattering. *Biophys J*. 2008;95(6):2792-805. Epub 2008/06/03. doi: 10.1529/biophysj.107.122465. PubMed PMID: 18515383; PMCID: PMC2527263.
345. Pan J, Mills TT, Tristram-Nagle S, Nagle JF. Cholesterol perturbs lipid bilayers nonuniversally. *Phys Rev Lett*. 2008;100(19):198103. Epub 2008/06/04. doi: 10.1103/PhysRevLett.100.198103. PubMed PMID: 18518492; PMCID: PMC2695669.
346. Hung WC, Lee MT, Chen FY, Huang HW. The condensing effect of cholesterol in lipid bilayers. *Biophys J*. 2007;92(11):3960-7. Epub 2007/03/21. doi: 10.1529/biophysj.106.099234. PubMed PMID: 17369407; PMCID: PMC1868968.
347. de Meyer F, Smit B. Effect of cholesterol on the structure of a phospholipid bilayer. *Proc Natl Acad Sci U S A*. 2009;106(10):3654-8. Epub 2009/02/20. doi: 10.1073/pnas.0809959106. PubMed PMID: 19225105; PMCID: PMC2656135.
348. Dustin ML, Groves JT. Receptor signaling clusters in the immune synapse. *Annu Rev Biophys*. 2012;41:543-56. Epub 2012/03/13. doi: 10.1146/annurev-biophys-042910-155238. PubMed PMID: 22404679; PMCID: PMC4000727.
349. Huo H, Guo X, Hong S, Jiang M, Liu X, Liao K. Lipid rafts/caveolae are essential for insulin-like growth factor-1 receptor signaling during 3T3-L1 preadipocyte differentiation induction. *The*

Journal of biological chemistry. 2003;278(13):11561-9. Epub 2003/01/23. doi: 10.1074/jbc.M211785200. PubMed PMID: 12538586.

350. Hong S, Huo H, Xu J, Liao K. Insulin-like growth factor-1 receptor signaling in 3T3-L1 adipocyte differentiation requires lipid rafts but not caveolae. *Cell Death Differ*. 2004;11(7):714-23. Epub 2004/03/06. doi: 10.1038/sj.cdd.4401405. PubMed PMID: 15002041.

351. Panetta D, Biedi C, Repetto S, Cordera R, Maggi D. IGF-I regulates caveolin 1 and IRS1 interaction in caveolae. *Biochem Biophys Res Commun*. 2004;316(1):240-3. Epub 2004/03/09. doi: 10.1016/j.bbrc.2004.02.037. PubMed PMID: 15003536.

352. Langlet C, Bernard AM, Drevot P, He HT. Membrane rafts and signaling by the multichain immune recognition receptors. *Curr Opin Immunol*. 2000;12(3):250-5. Epub 2000/04/27. PubMed PMID: 10781401.

353. Drevot P, Langlet C, Guo XJ, Bernard AM, Colard O, Chauvin JP, Lasserre R, He HT. TCR signal initiation machinery is pre-assembled and activated in a subset of membrane rafts. *EMBO J*. 2002;21(8):1899-908. Epub 2002/04/16. doi: 10.1093/emboj/21.8.1899. PubMed PMID: 11953309; PMCID: PMC125369.

354. Janes PW, Ley SC, Magee AI, Kabouridis PS. The role of lipid rafts in T cell antigen receptor (TCR) signalling. *Semin Immunol*. 2000;12(1):23-34. Epub 2000/03/21. doi: 10.1006/smim.2000.0204. PubMed PMID: 10723795.

355. Tansey MG, Baloh RH, Milbrandt J, Johnson EM, Jr. GFRalpha-mediated localization of RET to lipid rafts is required for effective downstream signaling, differentiation, and neuronal survival. *Neuron*. 2000;25(3):611-23. Epub 2000/04/25. PubMed PMID: 10774729.

356. Roy S, Luetterforst R, Harding A, Apolloni A, Etheridge M, Stang E, Rolls B, Hancock JF, Parton RG. Dominant-negative caveolin inhibits H-Ras function by disrupting cholesterol-rich plasma membrane domains. *Nat Cell Biol*. 1999;1(2):98-105. Epub 1999/11/13. doi: 10.1038/10067. PubMed PMID: 10559881.

357. Tsui-Pierchala BA, Encinas M, Milbrandt J, Johnson EM, Jr. Lipid rafts in neuronal signaling and function. *Trends Neurosci*. 2002;25(8):412-7. Epub 2002/07/20. PubMed PMID: 12127758.

358. Bickel PE. Lipid rafts and insulin signaling. *Am J Physiol Endocrinol Metab*. 2002;282(1):E1-E10. Epub 2001/12/12. doi: 10.1152/ajpendo.2002.282.1.E1. PubMed PMID: 11739076.

359. Mollinedo F, Gajate C. Lipid rafts as major platforms for signaling regulation in cancer. *Adv Biol Regul*. 2015;57:130-46. Epub 2014/12/04. doi: 10.1016/j.jbior.2014.10.003. PubMed PMID: 25465296.

360. Simons K, Toomre D. Lipid rafts and signal transduction. *Nat Rev Mol Cell Biol*. 2000;1(1):31-9. Epub 2001/06/20. doi: 10.1038/35036052. PubMed PMID: 11413487.

361. van Meer G. Lipid traffic in animal cells. *Annu Rev Cell Biol*. 1989;5:247-75. Epub 1989/01/01. doi: 10.1146/annurev.cb.05.110189.001335. PubMed PMID: 2688705.

362. Cluett EB, Machamer CE. The envelope of vaccinia virus reveals an unusual phospholipid in Golgi complex membranes. *J Cell Sci.* 1996;109 (Pt 8):2121-31. Epub 1996/08/01. PubMed PMID: 8856508.
363. Coxey RA, Pentchev PG, Campbell G, Blanchette-Mackie EJ. Differential accumulation of cholesterol in Golgi compartments of normal and Niemann-Pick type C fibroblasts incubated with LDL: a cytochemical freeze-fracture study. *J Lipid Res.* 1993;34(7):1165-76. Epub 1993/07/01. PubMed PMID: 8371064.
364. Brugger B, Sandhoff R, Wegehingel S, Gorgas K, Malsam J, Helms JB, Lehmann WD, Nickel W, Wieland FT. Evidence for segregation of sphingomyelin and cholesterol during formation of COPI-coated vesicles. *J Cell Biol.* 2000;151(3):507-18. Epub 2000/11/04. PubMed PMID: 11062253; PMCID: PMC2185577.
365. Browman DT, Resek ME, Zajchowski LD, Robbins SM. Erlin-1 and erlin-2 are novel members of the prohibitin family of proteins that define lipid-raft-like domains of the ER. *J Cell Sci.* 2006;119(Pt 15):3149-60. Epub 2006/07/13. doi: 10.1242/jcs.03060. PubMed PMID: 16835267.
366. Hayashi T, Su TP. Sigma-1 receptors (sigma(1) binding sites) form raft-like microdomains and target lipid droplets on the endoplasmic reticulum: roles in endoplasmic reticulum lipid compartmentalization and export. *J Pharmacol Exp Ther.* 2003;306(2):718-25. Epub 2003/05/06. doi: 10.1124/jpet.103.051284. PubMed PMID: 12730355.
367. Kockx M, Dinnes DL, Huang KY, Sharpe LJ, Jessup W, Brown AJ, Kritharides L. Cholesterol accumulation inhibits ER to Golgi transport and protein secretion: studies of apolipoprotein E and VSVGt. *Biochem J.* 2012;447(1):51-60. Epub 2012/07/04. doi: 10.1042/BJ20111891. PubMed PMID: 22747346.
368. Griffiths G, Simons K. The trans Golgi network: sorting at the exit site of the Golgi complex. *Science.* 1986;234(4775):438-43. Epub 1986/10/24. PubMed PMID: 2945253.
369. Bretscher MS, Munro S. Cholesterol and the Golgi apparatus. *Science.* 1993;261(5126):1280-1. Epub 1993/09/03. PubMed PMID: 8362242.
370. Wang Y, Thiele C, Huttner WB. Cholesterol is required for the formation of regulated and constitutive secretory vesicles from the trans-Golgi network. *Traffic.* 2000;1(12):952-62. Epub 2001/02/24. PubMed PMID: 11208085.
371. de Jesus AJ, Allen TW. The determinants of hydrophobic mismatch response for transmembrane helices. *Biochim Biophys Acta.* 2013;1828(2):851-63. Epub 2012/09/22. doi: 10.1016/j.bbamem.2012.09.012. PubMed PMID: 22995244.
372. Palade GE. Blood capillaries of the heart and other organs. *Circulation.* 1961;24:368-88. Epub 1961/08/01. PubMed PMID: 13732173.

373. Yamada E. The fine structure of the gall bladder epithelium of the mouse. *J Biophys Biochem Cytol.* 1955;1(5):445-58. Epub 1955/09/25. PubMed PMID: 13263332; PMCID: PMC2229656.
374. Rothberg KG, Heuser JE, Donzell WC, Ying YS, Glenney JR, Anderson RG. Caveolin, a protein component of caveolae membrane coats. *Cell.* 1992;68(4):673-82. Epub 1992/02/21. PubMed PMID: 1739974.
375. Williams TM, Lisanti MP. The caveolin proteins. *Genome Biol.* 2004;5(3):214. Epub 2004/03/09. doi: 10.1186/gb-2004-5-3-214. PubMed PMID: 15003112; PMCID: PMC395759.
376. Sargiacomo M, Scherer PE, Tang Z, Kubler E, Song KS, Sanders MC, Lisanti MP. Oligomeric structure of caveolin: implications for caveolae membrane organization. *Proc Natl Acad Sci U S A.* 1995;92(20):9407-11. Epub 1995/09/26. PubMed PMID: 7568142; PMCID: PMC40994.
377. Monier S, Dietzen DJ, Hastings WR, Lublin DM, Kurzchalia TV. Oligomerization of VIP21-caveolin in vitro is stabilized by long chain fatty acylation or cholesterol. *FEBS Lett.* 1996;388(2-3):143-9. Epub 1996/06/17. PubMed PMID: 8690074.
378. Lajoie P, Kojic LD, Nim S, Li L, Dennis JW, Nabi IR. Caveolin-1 regulation of dynamin-dependent, raft-mediated endocytosis of cholera toxin-B sub-unit occurs independently of caveolae. *J Cell Mol Med.* 2009;13(9B):3218-25. Epub 2009/05/15. doi: 10.1111/j.1582-4934.2009.00732.x. PubMed PMID: 19438805; PMCID: PMC4516479.
379. Lamaze C, Dujeancourt A, Baba T, Lo CG, Benmerah A, Dautry-Varsat A. Interleukin 2 receptors and detergent-resistant membrane domains define a clathrin-independent endocytic pathway. *Mol Cell.* 2001;7(3):661-71. Epub 2001/07/21. PubMed PMID: 11463390.
380. Drochmans P, Freudenstein C, Wanson JC, Laurent L, Keenan TW, Stadler J, Leloup R, Franke WW. Structure and biochemical composition of desmosomes and tonofilaments isolated from calf muzzle epidermis. *J Cell Biol.* 1978;79(2 Pt 1):427-43. Epub 1978/11/01. PubMed PMID: 569157; PMCID: PMC2110254.
381. Morel E, Fouquet S, Strup-Perrot C, Pichol Thievend C, Petit C, Loew D, Faussat AM, Yvernault L, Pincon-Raymond M, Chambaz J, Rousset M, Thenet S, Clair C. The cellular prion protein PrP(c) is involved in the proliferation of epithelial cells and in the distribution of junction-associated proteins. *PloS one.* 2008;3(8):e3000. Epub 2008/08/21. doi: 10.1371/journal.pone.0003000. PubMed PMID: 18714380; PMCID: PMC2500194.
382. Stahley SN, Saito M, Faundez V, Koval M, Mattheyses AL, Kowalczyk AP. Desmosome assembly and disassembly are membrane raft-dependent. *PloS one.* 2014;9(1):e87809. doi: 10.1371/journal.pone.0087809. PubMed PMID: 24498201; PMCID: 3907498.
383. Roberts BJ, Svoboda RA, Overmiller AM, Lewis JD, Kowalczyk AP, Mahoney MG, Johnson KR, Wahl JK, 3rd. Palmitoylation of Desmoglein 2 Is a Regulator of Assembly Dynamics and Protein Turnover. *The Journal of biological chemistry.* 2016;291(48):24857-65. Epub 2016/10/21. doi: 10.1074/jbc.M116.739458. PubMed PMID: 27703000; PMCID: PMC5122758.

384. Overmiller AM, McGuinn KP, Roberts BJ, Cooper F, Brennan-Crispi DM, Deguchi T, Peltonen S, Wahl JK, 3rd, Mahoney MG. c-Src/Cav1-dependent activation of the EGFR by Dsg2. *Oncotarget*. 2016;7(25):37536-55. Epub 2016/10/23. doi: 10.18632/oncotarget.7675. PubMed PMID: 26918609; PMCID: PMC5122330.
385. Delva E, Jennings JM, Calkins CC, Kottke MD, Faundez V, Kowalczyk AP. Pemphigus vulgaris IgG-induced desmoglein-3 endocytosis and desmosomal disassembly are mediated by a clathrin- and dynamin-independent mechanism. *The Journal of biological chemistry*. 2008;283(26):18303-13. doi: 10.1074/jbc.M710046200. PubMed PMID: 18434319; PMCID: PMC2440613.
386. Overmiller AM, Pierluissi JA, Wermuth PJ, Sauma S, Martinez-Outschoorn U, Tuluc M, Luginbuhl A, Curry J, Harshyne LA, Wahl JK, 3rd, South AP, Mahoney MG. Desmoglein 2 modulates extracellular vesicle release from squamous cell carcinoma keratinocytes. *FASEB J*. 2017;31(8):3412-24. Epub 2017/04/26. doi: 10.1096/fj.201601138RR. PubMed PMID: 28438789; PMCID: PMC5503718.
387. Greaves J, Chamberlain LH. Palmitoylation-dependent protein sorting. *J Cell Biol*. 2007;176(3):249-54. Epub 2007/01/24. doi: 10.1083/jcb.200610151. PubMed PMID: 17242068; PMCID: PMC2063950.
388. Levental I, Lingwood D, Grzybek M, Coskun U, Simons K. Palmitoylation regulates raft affinity for the majority of integral raft proteins. *Proc Natl Acad Sci U S A*. 2010;107(51):22050-4. Epub 2010/12/07. doi: 10.1073/pnas.1016184107. PubMed PMID: 21131568; PMCID: PMC3009825.
389. Brennan D, Peltonen S, Dowling A, Medhat W, Green KJ, Wahl JK, 3rd, Del Galdo F, Mahoney MG. A role for caveolin-1 in desmoglein binding and desmosome dynamics. *Oncogene*. 2012;31(13):1636-48. doi: 10.1038/onc.2011.346. PubMed PMID: 21841821; PMCID: 3228894.
390. Garcia MA, Nelson WJ, Chavez N. Cell-Cell Junctions Organize Structural and Signaling Networks. *Cold Spring Harb Perspect Biol*. 2018;10(4). Epub 2017/06/11. doi: 10.1101/cshperspect.a029181. PubMed PMID: 28600395; PMCID: PMC5773398.
391. Amagai M, Stanley JR. Desmoglein as a target in skin disease and beyond. *J Invest Dermatol*. 2012;132(3 Pt 2):776-84. Epub 2011/12/23. doi: 10.1038/jid.2011.390. PubMed PMID: 22189787; PMCID: PMC3279627.
392. Hsu CK, Lin HH, Harn HI, Hughes MW, Tang MJ, Yang CC. Mechanical forces in skin disorders. *J Dermatol Sci*. 2018;90(3):232-40. Epub 2018/03/24. doi: 10.1016/j.jdermsci.2018.03.004. PubMed PMID: 29567352.
393. Harmon RM, Green KJ. Structural and functional diversity of desmosomes. *Cell Commun Adhes*. 2013;20(6):171-87. Epub 2013/11/12. doi: 10.3109/15419061.2013.855204. PubMed PMID: 24205984.

394. Al-Amoudi A, Diez DC, Betts MJ, Frangakis AS. The molecular architecture of cadherins in native epidermal desmosomes. *Nature*. 2007;450(7171):832-7. Epub 2007/12/08. doi: 10.1038/nature05994. PubMed PMID: 18064004.
395. Nekrasova O, Green KJ. Desmosome assembly and dynamics. *Trends Cell Biol*. 2013;23(11):537-46. Epub 2013/07/31. doi: 10.1016/j.tcb.2013.06.004. PubMed PMID: 23891292; PMCID: PMC3913269.
396. Troyanovsky S. Adherens junction assembly. *Subcell Biochem*. 2012;60:89-108. Epub 2012/06/08. doi: 10.1007/978-94-007-4186-7_5. PubMed PMID: 22674069; PMCID: PMC6002756.
397. Holthofer B, Windoffer R, Troyanovsky S, Leube RE. Structure and function of desmosomes. *Int Rev Cytol*. 2007;264:65-163. Epub 2007/10/30. doi: 10.1016/S0074-7696(07)64003-0. PubMed PMID: 17964922.
398. Quinlan RA, Schwarz N, Windoffer R, Richardson C, Hawkins T, Broussard JA, Green KJ, Leube RE. A rim-and-spoke hypothesis to explain the biomechanical roles for cytoplasmic intermediate filament networks. *J Cell Sci*. 2017;130(20):3437-45. Epub 2017/10/17. doi: 10.1242/jcs.202168. PubMed PMID: 29032358.
399. Jones JC, Kam CY, Harmon RM, Woychek AV, Hopkinson SB, Green KJ. Intermediate Filaments and the Plasma Membrane. *Cold Spring Harb Perspect Biol*. 2017;9(1). Epub 2017/01/05. doi: 10.1101/cshperspect.a025866. PubMed PMID: 28049646; PMCID: PMC5204322.
400. Al-Amoudi A, Castano-Diez D, Devos DP, Russell RB, Johnson GT, Frangakis AS. The three-dimensional molecular structure of the desmosomal plaque. *Proc Natl Acad Sci U S A*. 2011;108(16):6480-5. Epub 2011/04/06. doi: 10.1073/pnas.1019469108. PubMed PMID: 21464301; PMCID: PMC3081036.
401. Samuelov L, Sprecher E. Inherited desmosomal disorders. *Cell Tissue Res*. 2015;360(3):457-75. doi: 10.1007/s00441-014-2062-y. PubMed PMID: 25487406.
402. Brooke MA, Nitoiu D, Kelsell DP. Cell-cell connectivity: desmosomes and disease. *J Pathol*. 2012;226(2):158-71. Epub 2011/10/13. doi: 10.1002/path.3027. PubMed PMID: 21989576.
403. Stahley SN, Kowalczyk AP. Desmosomes in acquired disease. *Cell Tissue Res*. 2015;360(3):439-56. Epub 2015/03/22. doi: 10.1007/s00441-015-2155-2. PubMed PMID: 25795143; PMCID: PMC4456195.
404. Nava P, Laukoetter MG, Hopkins AM, Laur O, Gerner-Smidt K, Green KJ, Parkos CA, Nusrat A. Desmoglein-2: a novel regulator of apoptosis in the intestinal epithelium. *Mol Biol Cell*. 2007;18(11):4565-78. Epub 2007/09/07. doi: 10.1091/mbc.E07-05-0426. PubMed PMID: 17804817; PMCID: PMC2043542.
405. Pike LJ. Lipid rafts: heterogeneity on the high seas. *Biochem J*. 2004;378(Pt 2):281-92. Epub 2003/12/10. doi: 10.1042/BJ20031672. PubMed PMID: 14662007; PMCID: PMC1223991.

406. Simons K, Sampaio JL. Membrane organization and lipid rafts. *Cold Spring Harb Perspect Biol.* 2011;3(10):a004697. Epub 2011/06/02. doi: 10.1101/cshperspect.a004697. PubMed PMID: 21628426; PMCID: PMC3179338.
407. Lingwood D, Kaiser HJ, Levental I, Simons K. Lipid rafts as functional heterogeneity in cell membranes. *Biochem Soc Trans.* 2009;37(Pt 5):955-60. Epub 2009/09/17. doi: 10.1042/BST0370955. PubMed PMID: 19754431.
408. Honigsmann A, Pralle A. Compartmentalization of the Cell Membrane. *J Mol Biol.* 2016;428(24 Pt A):4739-48. Epub 2016/10/22. doi: 10.1016/j.jmb.2016.09.022. PubMed PMID: 27720722.
409. Levental I, Veatch SL. The Continuing Mystery of Lipid Rafts. *J Mol Biol.* 2016;428(24 Pt A):4749-64. doi: 10.1016/j.jmb.2016.08.022. PubMed PMID: 27575334; PMCID: PMC5124408.
410. Sezgin E, Levental I, Mayor S, Eggeling C. The mystery of membrane organization: composition, regulation and roles of lipid rafts. *Nat Rev Mol Cell Biol.* 2017. doi: 10.1038/nrm.2017.16. PubMed PMID: 28356571.
411. Santos AL, Preta G. Lipids in the cell: organisation regulates function. *Cell Mol Life Sci.* 2018;75(11):1909-27. Epub 2018/02/11. doi: 10.1007/s00018-018-2765-4. PubMed PMID: 29427074.
412. Diaz-Rohrer B, Levental KR, Levental I. Rafting through traffic: Membrane domains in cellular logistics. *Biochim Biophys Acta.* 2014;1838(12):3003-13. Epub 2014/08/19. doi: 10.1016/j.bbamem.2014.07.029. PubMed PMID: 25130318.
413. Charollais J, Van Der Goot FG. Palmitoylation of membrane proteins (Review). *Mol Membr Biol.* 2009;26(1):55-66. Epub 2008/12/17. doi: 10.1080/09687680802620369. PubMed PMID: 19085289.
414. Munday AD, Lopez JA. Posttranslational protein palmitoylation: promoting platelet purpose. *Arterioscler Thromb Vasc Biol.* 2007;27(7):1496-9. Epub 2007/06/22. doi: 10.1161/ATVBAHA.106.136226. PubMed PMID: 17581830.
415. Bornslaeger EA, Corcoran CM, Stappenbeck TS, Green KJ. Breaking the connection: displacement of the desmosomal plaque protein desmoplakin from cell-cell interfaces disrupts anchorage of intermediate filament bundles and alters intercellular junction assembly. *J Cell Biol.* 1996;134(4):985-1001. Epub 1996/08/01. PubMed PMID: 8769422; PMCID: PMC2120955.
416. Setzer SV, Calkins CC, Garner J, Summers S, Green KJ, Kowalczyk AP. Comparative analysis of armadillo family proteins in the regulation of a431 epithelial cell junction assembly, adhesion and migration. *J Invest Dermatol.* 2004;123(3):426-33. Epub 2004/08/12. doi: 10.1111/j.0022-202X.2004.23319.x. PubMed PMID: 15304078.
417. Wahl JK, 3rd. A role for plakophilin-1 in the initiation of desmosome assembly. *J Cell Biochem.* 2005;96(2):390-403. Epub 2005/07/01. doi: 10.1002/jcb.20514. PubMed PMID: 15988759.

418. Sobolik-Delmaire T, Reddy R, Pashaj A, Roberts BJ, Wahl JK, 3rd. Plakophilin-1 localizes to the nucleus and interacts with single-stranded DNA. *J Invest Dermatol.* 2010;130(11):2638-46. Epub 2010/07/09. doi: 10.1038/jid.2010.191. PubMed PMID: 20613778.
419. Lorent JH, Diaz-Rohrer B, Lin X, Spring K, Gorfe AA, Levental KR, Levental I. Structural determinants and functional consequences of protein affinity for membrane rafts. *Nat Commun.* 2017;8(1):1219. Epub 2017/11/02. doi: 10.1038/s41467-017-01328-3. PubMed PMID: 29089556; PMCID: PMC5663905.
420. Garcia-Garcia E, Brown EJ, Rosales C. Transmembrane mutations to FcγRIIA alter its association with lipid rafts: implications for receptor signaling. *J Immunol.* 2007;178(5):3048-58. PubMed PMID: 17312151.
421. Scheiffele P, Roth MG, Simons K. Interaction of influenza virus haemagglutinin with sphingolipid-cholesterol membrane domains via its transmembrane domain. *EMBO J.* 1997;16(18):5501-8. doi: 10.1093/emboj/16.18.5501. PubMed PMID: 9312009; PMCID: PMC1170182.
422. Diaz-Rohrer BB, Levental KR, Simons K, Levental I. Membrane raft association is a determinant of plasma membrane localization. *Proc Natl Acad Sci U S A.* 2014;111(23):8500-5. doi: 10.1073/pnas.1404582111. PubMed PMID: 24912166; PMCID: PMC4060687.
423. Saito M, Stahley SN, Caughman CY, Mao X, Tucker DK, Payne AS, Amagai M, Kowalczyk AP. Signaling dependent and independent mechanisms in pemphigus vulgaris blister formation. *PloS one.* 2012;7(12):e50696. Epub 2012/12/12. doi: 10.1371/journal.pone.0050696. PubMed PMID: 23226536; PMCID: PMC3513318.
424. Danescu S, Leppert J, Cosgarea R, Zurac S, Pop S, Baican A, Has C. Compound heterozygosity for dominant and recessive DSG1 mutations in a patient with atypical SAM syndrome (severe dermatitis, multiple allergies, metabolic wasting). *J Eur Acad Dermatol Venereol.* 2017;31(3):e144-e6. Epub 2016/09/16. doi: 10.1111/jdv.13967. PubMed PMID: 27632246.
425. Ishida-Yamamoto A, Kellsell D, Common J, Houseman MJ, Hashimoto M, Shibaki H, Asano K, Takahashi H, Hashimoto Y, Senshu T, Leigh IM, Iizuka H. A case of erythrokeratoderma variabilis without mutations in connexin 31. *Br J Dermatol.* 2000;143(6):1283-7. Epub 2000/12/21. PubMed PMID: 11122035.
426. Levental KR, Levental I. Isolation of giant plasma membrane vesicles for evaluation of plasma membrane structure and protein partitioning. *Methods Mol Biol.* 2015;1232:65-77. Epub 2014/10/22. doi: 10.1007/978-1-4939-1752-5_6. PubMed PMID: 25331128.
427. Levental KR, Levental I. Giant plasma membrane vesicles: models for understanding membrane organization. *Curr Top Membr.* 2015;75:25-57. Epub 2015/05/28. doi: 10.1016/bs.ctm.2015.03.009. PubMed PMID: 26015280.

428. Kim DE, Chivian D, Baker D. Protein structure prediction and analysis using the Robetta server. *Nucleic Acids Res.* 2004;32(Web Server issue):W526-31. Epub 2004/06/25. doi: 10.1093/nar/gkh468. PubMed PMID: 15215442; PMCID: PMC441606.
429. Lewis BA, Engelman DM. Lipid bilayer thickness varies linearly with acyl chain length in fluid phosphatidylcholine vesicles. *J Mol Biol.* 1983;166(2):211-7. Epub 1983/05/15. PubMed PMID: 6854644.
430. Niemela PS, Ollila S, Hyvonen MT, Karttunen M, Vattulainen I. Assessing the nature of lipid raft membranes. *PLoS Comput Biol.* 2007;3(2):e34. Epub 2007/02/27. doi: 10.1371/journal.pcbi.0030034. PubMed PMID: 17319738; PMCID: PMC1808021.
431. Lovgren ML, McAleer MA, Irvine AD, Wilson NJ, Tavadia S, Schwartz ME, Cole C, Sandilands A, Smith FJD, Zamiri M. Mutations in desmoglein 1 cause diverse inherited palmoplantar keratoderma phenotypes: implications for genetic screening. *Br J Dermatol.* 2017;176(5):1345-50. Epub 2016/11/02. doi: 10.1111/bjd.14973. PubMed PMID: 27534273; PMCID: PMC5485079.
432. Reddy T, Manrique S, Buyan A, Hall BA, Chetwynd A, Sansom MS. Primary and secondary dimer interfaces of the fibroblast growth factor receptor 3 transmembrane domain: characterization via multiscale molecular dynamics simulations. *Biochemistry.* 2014;53(2):323-32. doi: 10.1021/bi401576k. PubMed PMID: 24397339; PMCID: PMC4871223.
433. Parks GD, Lamb RA. Role of NH2-terminal positively charged residues in establishing membrane protein topology. *The Journal of biological chemistry.* 1993;268(25):19101-9. PubMed PMID: 8103052.
434. Schow EV, Freitas JA, Cheng P, Bernsel A, von Heijne G, White SH, Tobias DJ. Arginine in membranes: the connection between molecular dynamics simulations and translocon-mediated insertion experiments. *J Membr Biol.* 2011;239(1-2):35-48. Epub 2010/12/04. doi: 10.1007/s00232-010-9330-x. PubMed PMID: 21127848; PMCID: PMC3030942.
435. Marsh D. Energetics of hydrophobic matching in lipid-protein interactions. *Biophys J.* 2008;94(10):3996-4013. Epub 2008/02/01. doi: 10.1529/biophysj.107.121475. PubMed PMID: 18234817; PMCID: PMC2367201.
436. Genomes Project C, Auton A, Brooks LD, Durbin RM, Garrison EP, Kang HM, Korbel JO, Marchini JL, McCarthy S, McVean GA, Abecasis GR. A global reference for human genetic variation. *Nature.* 2015;526(7571):68-74. doi: 10.1038/nature15393. PubMed PMID: 26432245; PMCID: PMC4750478.
437. Sudmant PH, Rausch T, Gardner EJ, Handsaker RE, Abyzov A, Huddleston J, Zhang Y, Ye K, Jun G, Hsi-Yang Fritz M, Konkil MK, Malhotra A, Stutz AM, Shi X, Paolo Casale F, Chen J, Hormozdiari F, Dayama G, Chen K, Malig M, Chaisson MJ, Walter K, Meiers S, Kashin S, Garrison E, Auton A, Lam HY, Jasmine Mu X, Alkan C, Antaki D, Bae T, Cerveira E, Chines P, Chong Z, Clarke L, Dal E, Ding L, Emery S, Fan X, Gujral M, Kahveci F, Kidd JM, Kong Y, Lameijer EW, McCarthy S, Flicek P, Gibbs RA, Marth G, Mason CE, Menelaou A, Muzny DM, Nelson BJ, Noor A, Parrish NF, Pendleton M, Quitadamo A, Raeder B, Schadt EE, Romanovitch M, Schlattl A, Sebra R, Shabaln

AA, Untergasser A, Walker JA, Wang M, Yu F, Zhang C, Zhang J, Zheng-Bradley X, Zhou W, Zichner T, Sebat J, Batzer MA, McCarroll SA, Genomes Project C, Mills RE, Gerstein MB, Bashir A, Stegle O, Devine SE, Lee C, Eichler EE, Korbelt JO. An integrated map of structural variation in 2,504 human genomes. *Nature*. 2015;526(7571):75-81. doi: 10.1038/nature15394. PubMed PMID: 26432246; PMCID: PMC4617611.

438. Higasa K, Miyake N, Yoshimura J, Okamura K, Niihori T, Saitsu H, Doi K, Shimizu M, Nakabayashi K, Aoki Y, Tsurusaki Y, Morishita S, Kawaguchi T, Migita O, Nakayama K, Nakashima M, Mitsui J, Narahara M, Hayashi K, Funayama R, Yamaguchi D, Ishiura H, Ko WY, Hata K, Nagashima T, Yamada R, Matsubara Y, Umezawa A, Tsuji S, Matsumoto N, Matsuda F. Human genetic variation database, a reference database of genetic variations in the Japanese population. *J Hum Genet*. 2016;61(6):547-53. doi: 10.1038/jhg.2016.12. PubMed PMID: 26911352; PMCID: PMC4931044.

439. Nagasaki M, Yasuda J, Katsuoka F, Nariai N, Kojima K, Kawai Y, Yamaguchi-Kabata Y, Yokozawa J, Danjoh I, Saito S, Sato Y, Mimori T, Tsuda K, Saito R, Pan X, Nishikawa S, Ito S, Kuroki Y, Tanabe O, Fuse N, Kuriyama S, Kiyomoto H, Hozawa A, Minegishi N, Douglas Engel J, Kinoshita K, Kure S, Yaegashi N, To MJRPP, Yamamoto M. Rare variant discovery by deep whole-genome sequencing of 1,070 Japanese individuals. *Nat Commun*. 2015;6:8018. doi: 10.1038/ncomms9018. PubMed PMID: 26292667; PMCID: PMC4560751.

440. Wilson VG. Growth and differentiation of HaCaT keratinocytes. *Methods Mol Biol*. 2014;1195:33-41. doi: 10.1007/7651_2013_42. PubMed PMID: 24155234.

441. Tsunoda K, Ota T, Aoki M, Yamada T, Nagai T, Nakagawa T, Koyasu S, Nishikawa T, Amagai M. Induction of pemphigus phenotype by a mouse monoclonal antibody against the amino-terminal adhesive interface of desmoglein 3. *J Immunol*. 2003;170(4):2170-8. PubMed PMID: 12574390.

442. Sezgin E, Kaiser HJ, Baumgart T, Schwille P, Simons K, Levental I. Elucidating membrane structure and protein behavior using giant plasma membrane vesicles. *Nat Protoc*. 2012;7(6):1042-51. doi: 10.1038/nprot.2012.059. PubMed PMID: 22555243.

443. Levental I, Byfield FJ, Chowdhury P, Gai F, Baumgart T, Janmey PA. Cholesterol-dependent phase separation in cell-derived giant plasma-membrane vesicles. *Biochem J*. 2009;424(2):163-7. doi: 10.1042/BJ20091283. PubMed PMID: 19811449; PMCID: PMC3118457.

444. Levental I, Grzybek M, Simons K. Raft domains of variable properties and compositions in plasma membrane vesicles. *Proc Natl Acad Sci U S A*. 2011;108(28):11411-6. doi: 10.1073/pnas.1105996108. PubMed PMID: 21709267; PMCID: PMC3136254.

445. Percher A, Ramakrishnan S, Thinon E, Yuan X, Yount JS, Hang HC. Mass-tag labeling reveals site-specific and endogenous levels of protein S-fatty acylation. *Proc Natl Acad Sci U S A*. 2016;113(16):4302-7. doi: 10.1073/pnas.1602244113. PubMed PMID: 27044110; PMCID: PMC4843475.

446. Song CS, Rubin W, Rifkind AB, Kappas A. Plasma membranes of the rat liver. Isolation and enzymatic characterization of a fraction rich in bile canaliculi. *J Cell Biol.* 1969;41(1):124-32. Epub 1969/04/01. PubMed PMID: 4304740; PMCID: PMC2107735.
447. Tsukita S, Tsukita S. Isolation of cell-to-cell adherens junctions from rat liver. *J Cell Biol.* 1989;108(1):31-41. Epub 1989/01/01. PubMed PMID: 2463257; PMCID: PMC2115366.
448. Neville DM, Jr. The isolation of a cell membrane fraction from rat liver. *J Biophys Biochem Cytol.* 1960;8:413-22. Epub 1960/10/01. PubMed PMID: 13728607; PMCID: PMC2224936.
449. Forster F, Hegerl R. Structure determination in situ by averaging of tomograms. *Methods Cell Biol.* 2007;79:741-67. Epub 2007/03/01. doi: 10.1016/S0091-679X(06)79029-X. PubMed PMID: 17327182.
450. Kridin K. Pemphigus group: overview, epidemiology, mortality, and comorbidities. *Immunol Res.* 2018;66(2):255-70. Epub 2018/02/27. doi: 10.1007/s12026-018-8986-7. PubMed PMID: 29479654.
451. Amagai M, Tsunoda K, Zillikens D, Nagai T, Nishikawa T. The clinical phenotype of pemphigus is defined by the anti-desmoglein autoantibody profile. *J Am Acad Dermatol.* 1999;40(2 Pt 1):167-70. Epub 1999/02/20. PubMed PMID: 10025740.
452. Mortazavi H, Safi Y, Baharvand M, Rahmani S. Diagnostic Features of Common Oral Ulcerative Lesions: An Updated Decision Tree. *Int J Dent.* 2016;2016:7278925. Epub 2016/10/27. doi: 10.1155/2016/7278925. PubMed PMID: 27781066; PMCID: PMC5066016.
453. Yamashina Y, Miyagawa S, Kawatsu T, Iida T, Higashimine I, Shirai T, Kaneshige T. Polymorphisms of HLA class II genes in Japanese patients with pemphigus vulgaris. *Tissue Antigens.* 1998;52(1):74-7. Epub 1998/08/26. PubMed PMID: 9714477.
454. Loiseau P, Leclach L, Prost C, Lepage V, Busson M, Bastuji-Garin S, Roujeau JC, Charron D. HLA class II polymorphism contributes to specify desmoglein derived peptides in pemphigus vulgaris and pemphigus foliaceus. *J Autoimmun.* 2000;15(1):67-73. Epub 2000/08/11. doi: 10.1006/jaut.2000.0388. PubMed PMID: 10936030.
455. Khan SW, Iftikhar N, Ahmed TA, Bashir M. HLA- DR Alleles in Pakistani Patients of Pemphigus Vulgaris. *J Coll Physicians Surg Pak.* 2015;25(4):233-6. Epub 2015/04/23. doi: 10.2015/JCPSP.233236. PubMed PMID: 25899184.
456. Gonzalez-Escribano MF, Jimenez G, Walter K, Montes M, Perez-Bernal AM, Rodriguez MR, Conejo-Mir JS, Nunez-Roldan A. Distribution of HLA class II alleles among Spanish patients with pemphigus vulgaris. *Tissue Antigens.* 1998;52(3):275-8. Epub 1998/11/05. PubMed PMID: 9802608.
457. Carcassi C, Cottoni F, Floris L, Vacca A, Mulargia M, Arras M, Boero R, La Nasa G, Ledda A, Pizzati A, Cerimele D, Contu L. HLA haplotypes and class II molecular alleles in Sardinian and Italian patients with pemphigus vulgaris. *Tissue Antigens.* 1996;48(6):662-7. Epub 1996/12/01. PubMed PMID: 9008308.

458. Brochado MJ, Nascimento DF, Campos W, Deghaide NH, Donadi EA, Roselino AM. Differential HLA class I and class II associations in pemphigus foliaceus and pemphigus vulgaris patients from a prevalent Southeastern Brazilian region. *J Autoimmun.* 2016;72:19-24. Epub 2016/05/15. doi: 10.1016/j.jaut.2016.04.007. PubMed PMID: 27178774.
459. Gough SC, Simmonds MJ. The HLA Region and Autoimmune Disease: Associations and Mechanisms of Action. *Curr Genomics.* 2007;8(7):453-65. Epub 2007/11/01. doi: 10.2174/138920207783591690. PubMed PMID: 19412418; PMCID: PMC2647156.
460. Kridin K, Zelber-Sagi S, Bergman R. Pemphigus Vulgaris and Pemphigus Foliaceus: Differences in Epidemiology and Mortality. *Acta Derm Venereol.* 2017;97(9):1095-9. Epub 2017/05/26. doi: 10.2340/00015555-2706. PubMed PMID: 28536732.
461. Sarig O, Bercovici S, Zoller L, Goldberg I, Indelman M, Nahum S, Israeli S, Sagiv N, Martinez de Morentin H, Katz O, Baum S, Barzilai A, Trau H, Murrell DF, Bergman R, Hertl M, Rosenberg S, Nothen MM, Skorecki K, Schmidt E, Zillikens D, Darvasi A, Geiger D, Rosset S, Ibrahim SM, Sprecher E. Population-specific association between a polymorphic variant in ST18, encoding a pro-apoptotic molecule, and pemphigus vulgaris. *J Invest Dermatol.* 2012;132(7):1798-805. Epub 2012/03/23. doi: 10.1038/jid.2012.46. PubMed PMID: 22437316.
462. Ruocco V, De Angelis E, Lombardi ML. Drug-induced pemphigus. II. Pathomechanisms and experimental investigations. *Clin Dermatol.* 1993;11(4):507-13. Epub 1993/10/01. PubMed PMID: 8124640.
463. Feliciani C, Toto P, Amerio P, Pour SM, Coscione G, Shivji G, Wang B, Sauder DN. In vitro and in vivo expression of interleukin-1alpha and tumor necrosis factor-alpha mRNA in pemphigus vulgaris: interleukin-1alpha and tumor necrosis factor-alpha are involved in acantholysis. *J Invest Dermatol.* 2000;114(1):71-7. Epub 2000/01/05. doi: 10.1046/j.1523-1747.2000.00835.x. PubMed PMID: 10620118.
464. Newby CS, Barr RM, Greaves MW, Mallet AI. Cytokine release and cytotoxicity in human keratinocytes and fibroblasts induced by phenols and sodium dodecyl sulfate. *J Invest Dermatol.* 2000;115(2):292-8. Epub 2000/08/22. doi: 10.1046/j.1523-1747.2000.00056.x. PubMed PMID: 10951249.
465. De Dobbeleer G, Godfrine S, Gourdain JM, De Graef C, Heenen M. In vitro acantholysis induced by D-penicillamine, captopril, and piroxicam on dead de-epidermized dermis. *J Cutan Pathol.* 1992;19(3):181-6. Epub 1992/06/01. PubMed PMID: 1401343.
466. Yokel BK, Hood AF, Anhalt GJ. Induction of acantholysis in organ explant culture by penicillamine and captopril. *Arch Dermatol.* 1989;125(10):1367-70. Epub 1989/10/01. PubMed PMID: 2679399.
467. Ruocco V, de Luca M, Pisani M, de Angelis E, Vitale O, Astarita C. Pemphigus provoked by D(-)penicillamine. An experimental approach using in vitro tissue cultures. *Dermatologica.* 1982;164(4):236-48. Epub 1982/04/01. PubMed PMID: 7084544.

468. Bastuji-Garin S, Souissi R, Blum L, Turki H, Nouira R, Jomaa B, Zahaf A, Ben Osman A, Mokhtar I, Faza'a B, et al. Comparative epidemiology of pemphigus in Tunisia and France: unusual incidence of pemphigus foliaceus in young Tunisian women. *J Invest Dermatol*. 1995;104(2):302-5. Epub 1995/02/01. PubMed PMID: 7829889.
469. Yayli S, Harman M, Baskan EB, Karakas AA, Genc Y, Turk BG, Demirsoy EO, Gunasti S, Bilgili SG, Ilter N, Ferahbas A, Savk E, Afsar FS, Aytekin S, Kaya TI, Hayta SB, Ozgen Z, Gurel MS, Caliskan E, Balci DD, Gungor S, Kapicioglu Y, Ozuguz P, Aktan S, Dogramaci A, Kokcam I, Onsun N, Seckin D, Durdu M, Dursun R, Daye M, Dilek N, Karabacak E, Temel AB, Erdem C, Altun E, Gungor D, Kartal D, Akyol M, Koku Aksu EK, Uzun S. Epidemiology of Pemphigus in Turkey: One-year Prospective Study of 220 Cases. *Acta Dermatovenerol Croat*. 2017;25(3):181-8. Epub 2017/12/19. PubMed PMID: 29252169.
470. Lee YB, Lee JH, Lee SY, Kim JW, Yu DS, Han KD, Park YG. Incidence and death rate of pemphigus vulgaris and pemphigus foliaceus in Korea: A nationwide, population-based study (2006-2015). *J Dermatol*. 2018;45(12):1396-402. Epub 2018/10/16. doi: 10.1111/1346-8138.14667. PubMed PMID: 30320467.
471. Tavakolpour S, Darvishi M, Mirsafaei HS, Ghasemiadl M. Nucleoside/nucleotide analogues in the treatment of chronic hepatitis B infection during pregnancy: a systematic review. *Infect Dis (Lond)*. 2018;50(2):95-106. Epub 2017/10/13. doi: 10.1080/23744235.2017.1384957. PubMed PMID: 29020844.
472. Tavakolpour S, Rahimzadeh G. New Insights into the Management of Patients with Autoimmune Diseases or Inflammatory Disorders During Pregnancy. *Scand J Immunol*. 2016;84(3):146-9. Epub 2016/06/15. doi: 10.1111/sji.12453. PubMed PMID: 27300757.
473. Tamir A, Ophir J, Brenner S. Pemphigus vulgaris triggered by emotional stress. *Dermatology*. 1994;189(2):210. Epub 1994/01/01. doi: 10.1159/000246837. PubMed PMID: 8075459.
474. Wohl Y, Mashiah J, Kutz A, Hadj-Rabia S, Cohen AD. Pemphigus and depression comorbidity: a case control study. *Eur J Dermatol*. 2015;25(6):602-5. Epub 2015/11/11. doi: 10.1684/ejd.2015.2649. PubMed PMID: 26553704.
475. Stojanovich L, Marisavljevich D. Stress as a trigger of autoimmune disease. *Autoimmun Rev*. 2008;7(3):209-13. Epub 2008/01/15. doi: 10.1016/j.autrev.2007.11.007. PubMed PMID: 18190880.
476. Jang HW, Chun SH, Lee JM, Jeon J, Hashimoto T, Kim IH. Radiotherapy-induced pemphigus vulgaris. *J Dermatol*. 2014;41(9):851-2. Epub 2014/08/12. doi: 10.1111/1346-8138.12582. PubMed PMID: 25109377.
477. Ambay A, Stratman E. Ionizing radiation-induced pemphigus foliaceus. *J Am Acad Dermatol*. 2006;54(5 Suppl):251-2. Epub 2006/04/25. doi: 10.1016/j.jaad.2005.12.024. PubMed PMID: 16631963.

478. Badri T, Hammami H, Lachkham A, Benmously-Mlika R, Mokhtar I, Fenniche S. Radiotherapy-induced pemphigus vulgaris with autoantibodies targeting a 110 kDa epidermal antigen. *Int J Dermatol*. 2011;50(12):1475-9. Epub 2011/11/22. doi: 10.1111/j.1365-4632.2011.04889.x. PubMed PMID: 22097992.
479. Bertram F, Brocker EB, Zillikens D, Schmidt E. Prospective analysis of the incidence of autoimmune bullous disorders in Lower Franconia, Germany. *J Dtsch Dermatol Ges*. 2009;7(5):434-40. Epub 2009/01/28. doi: 10.1111/j.1610-0387.2008.06976.x. PubMed PMID: 19170813.
480. Tallab T, Joharji H, Bahamdan K, Karkashan E, Mourad M, Ibrahim K. The incidence of pemphigus in the southern region of Saudi Arabia. *Int J Dermatol*. 2001;40(9):570-2. Epub 2001/12/12. PubMed PMID: 11737450.
481. Serwin AB, Koper M, Flisiak I. Incidence of pemphigus vulgaris and pemphigus foliaceus in North-East Poland (Podlaskie Province) - a 15-year (2001-2015) bicentric retrospective study. *Int J Dermatol*. 2018;57(8):933-7. Epub 2018/06/07. doi: 10.1111/ijd.14078. PubMed PMID: 29873080.
482. Tsankov N, Vassileva S, Kamarashev J, Kazandjieva J, Kuzeva V. Epidemiology of pemphigus in Sofia, Bulgaria. A 16-year retrospective study (1980-1995). *Int J Dermatol*. 2000;39(2):104-8. Epub 2000/02/26. PubMed PMID: 10692058.
483. Langan SM, Smeeth L, Hubbard R, Fleming KM, Smith CJ, West J. Bullous pemphigoid and pemphigus vulgaris--incidence and mortality in the UK: population based cohort study. *BMJ*. 2008;337:a180. Epub 2008/07/11. doi: 10.1136/bmj.a180. PubMed PMID: 18614511; PMCID: PMC2483869.
484. Michailidou EZ, Belazi MA, Markopoulos AK, Tsatsos MI, Mourellou ON, Antoniadis DZ. Epidemiologic survey of pemphigus vulgaris with oral manifestations in northern Greece: retrospective study of 129 patients. *Int J Dermatol*. 2007;46(4):356-61. Epub 2007/04/20. doi: 10.1111/j.1365-4632.2006.03044.x. PubMed PMID: 17442072.
485. Pisanti S, Sharav Y, Kaufman E, Posner LN. Pemphigus vulgaris: incidence in Jews of different ethnic groups, according to age, sex, and initial lesion. *Oral Surg Oral Med Oral Pathol*. 1974;38(3):382-7. Epub 1974/09/01. PubMed PMID: 4528670.
486. Asilian A, Yoosefi A, Faghini G. Pemphigus vulgaris in Iran: epidemiology and clinical profile. *Skinmed*. 2006;5(2):69-71. Epub 2006/04/11. PubMed PMID: 16603836.
487. Murrell DF, Pena S, Joly P, Marinovic B, Hashimoto T, Diaz LA, Sinha AA, Payne AS, Daneshpazhooh M, Eming R, Jonkman MF, Mimouni D, Borradori L, Kim SC, Yamagami J, Lehman JS, Saleh MA, Culton DA, Czernik A, Zone JJ, Fivenson D, Ujiie H, Wozniak K, Akman-Karakas A, Bernard P, Korman NJ, Caux F, Drenovska K, Prost-Squarcioni C, Vassileva S, Feldman RJ, Cardones AR, Bauer J, Ioannides D, Jedlickova H, Palisson F, Patsatsi A, Uzun S, Yayli S, Zillikens D, Amagai M, Hertl M, Schmidt E, Aoki V, Grando SA, Shimizu H, Baum S, Cianchini G, Feliciani C, Iranzo P, Mascaro JM, Jr., Kowalewski C, Hall R, Groves R, Harman KE, Marinkovich MP, Maverakis E, Werth VP. Diagnosis and Management of Pemphigus: recommendations by an International Panel of

Experts. *J Am Acad Dermatol.* 2018. Epub 2018/02/14. doi: 10.1016/j.jaad.2018.02.021. PubMed PMID: 29438767.

488. Bastuji-Garin S, Sbidian E. How to validate outcome instruments for pemphigus. *J Invest Dermatol.* 2009;129(10):2328-30. Epub 2009/09/15. doi: 10.1038/jid.2009.228. PubMed PMID: 19749779.

489. Pfütze M, Niedermeier A, Hertl M, Eming R. Introducing a novel Autoimmune Bullous Skin Disorder Intensity Score (ABSIS) in pemphigus. *Eur J Dermatol.* 2007;17(1):4-11. Epub 2007/02/28. doi: 10.1684/ejd.2007.0090. PubMed PMID: 17324820.

490. Murrell DF, Dick S, Ahmed AR, Amagai M, Barnadas MA, Borradori L, Bystryń JC, Cianchini G, Diaz L, Fivenson D, Hall R, Harman KE, Hashimoto T, Hertl M, Hunzelmann N, Iranzo P, Joly P, Jonkman MF, Kitajima Y, Korman NJ, Martin LK, Mimouni D, Pandya AG, Payne AS, Rubenstein D, Shimizu H, Sinha AA, Sirois D, Zillikens D, Werth VP. Consensus statement on definitions of disease, end points, and therapeutic response for pemphigus. *J Am Acad Dermatol.* 2008;58(6):1043-6. Epub 2008/03/15. doi: 10.1016/j.jaad.2008.01.012. PubMed PMID: 18339444; PMCID: PMC2829665.

491. Rahbar Z, Daneshpazhooh M, Mirshams-Shahshahani M, Esmaili N, Heidari K, Aghazadeh N, Hejazi P, Ghajarzadeh M, Chams-Davatchi C. Pemphigus disease activity measurements: pemphigus disease area index, autoimmune bullous skin disorder intensity score, and pemphigus vulgaris activity score. *JAMA Dermatol.* 2014;150(3):266-72. Epub 2014/01/17. doi: 10.1001/jamadermatol.2013.8175. PubMed PMID: 24429657.

492. Ikeda S, Ogawa H. A nation-wide investigation for the revision of severity index of pemphigus (results of first and second investigation). Ministry of welfare and Health of Japan. 1997(Annual report of the intractable skin diseases study group (in Japanese)):115-8.

493. Ikeda S, Imamura S, Hashimoto I, Morioka S, Sakuma M, Ogawa H. History of the establishment and revision of diagnostic criteria, severity index and therapeutic guidelines for pemphigus in Japan. *Arch Dermatol Res.* 2003;295 Suppl 1:S12-6. Epub 2003/04/05. doi: 10.1007/s00403-002-0367-2. PubMed PMID: 12677427.

494. Agarwal M, Walia R, Kochhar AM, Chander R. Pemphigus Area and Activity Score (PAAS)-a novel clinical scoring method for monitoring of pemphigus vulgaris patients. *Int J Dermatol.* 1998;37(2):158-60. Epub 1998/05/16. PubMed PMID: 9542681.

495. Herbst A, Bystryń JC. Patterns of remission in pemphigus vulgaris. *J Am Acad Dermatol.* 2000;42(3):422-7. Epub 2000/02/25. PubMed PMID: 10688711.

496. Saraswat A, Bhushan K, India C. A new grading system for oral pemphigus. *Int J Dermatol.* 2003;42(5):413-4. Epub 2003/05/21. PubMed PMID: 12755987.

497. Mahajan VK, Sharma NL, Sharma RC, Garg G. Twelve-year clinico-therapeutic experience in pemphigus: a retrospective study of 54 cases. *Int J Dermatol.* 2005;44(10):821-7. Epub 2005/10/07. doi: 10.1111/j.1365-4632.2005.02218.x. PubMed PMID: 16207182.

498. Kumar B, Arora S, Kumaran MS, Jain R, Dogra S. Study of desmoglein 1 and 3 antibody levels in relation to disease severity in Indian patients with pemphigus. *Indian J Dermatol Venereol Leprol.* 2006;72(3):203-6. Epub 2006/06/13. PubMed PMID: 16766834.
499. Esmaili N, Chams-Davatchi C, Valikhani M, Farshidfar F, Parvaneh N, Tamizifar B. Treatment of pemphigus vulgaris with mycophenolate mofetil as a steroid-sparing agent. *Eur J Dermatol.* 2008;18(2):159-64. Epub 2008/04/22. doi: 10.1684/ejd.2008.0354. PubMed PMID: 18424375.
500. Chams-Davatchi C, Rahbar Z, Daneshpazhooh M, Mortazavizadeh SM, Akhyani M, Esmaili N, Balighi K. Pemphigus vulgaris activity score and assessment of convergent validity. *Acta Med Iran.* 2013;51(4):224-30. Epub 2013/05/22. PubMed PMID: 23690100.
501. Beutner EH, Jordon RE. Demonstration of Skin Antibodies in Sera of Pemphigus Vulgaris Patients by Indirect Immunofluorescent Staining. *Proc Soc Exp Biol Med.* 1964;117:505-10. Epub 1964/11/01. PubMed PMID: 14233481.
502. Diercks GF, Pas HH, Jonkman MF. Immunofluorescence of Autoimmune Bullous Diseases. *Surg Pathol Clin.* 2017;10(2):505-12. Epub 2017/05/10. doi: 10.1016/j.path.2017.01.011. PubMed PMID: 28477893.
503. Hrabovska Z, Jautova J, Hrabovsky V. A study of clinical, histopathological and direct immunofluorescence diagnosis in pemphigus group Utility of direct immunofluorescence. *Bratisl Lek Listy.* 2017;118(4):243-9. Epub 2017/05/05. doi: 10.4149/BLL_2017_048. PubMed PMID: 28471236.
504. Michel B, Ko CS. An organ culture model for the study of pemphigus acantholysis. *Br J Dermatol.* 1977;96(3):295-302. Epub 1977/03/01. PubMed PMID: 322692.
505. Creswell SN, Black MM, Bhogal B, Skeete MV. Correlation of circulating intercellular antibody titres in pemphigus with disease activity. *Clin Exp Dermatol.* 1981;6(5):477-83. Epub 1981/09/01. PubMed PMID: 7318238.
506. Amagai M, Komai A, Hashimoto T, Shirakata Y, Hashimoto K, Yamada T, Kitajima Y, Ohya K, Iwanami H, Nishikawa T. Usefulness of enzyme-linked immunosorbent assay using recombinant desmogleins 1 and 3 for serodiagnosis of pemphigus. *Br J Dermatol.* 1999;140(2):351-7. Epub 1999/05/08. PubMed PMID: 10233237.
507. Patsatsi A, Kyriakou A, Giannakou A, Pavlitou-Tsiontsi A, Lambropoulos A, Sotiriadis D. Clinical significance of anti-desmoglein-1 and -3 circulating autoantibodies in Pemphigus Patients Measured by Area Index and Intensity Score. *Acta Derm Venereol.* 2014;94(2):203-6. Epub 2013/09/03. doi: 10.2340/00015555-1666. PubMed PMID: 23995461.
508. Herrero-Gonzalez JE, Iranzo P, Benitez D, Lozano F, Herrero C, Mascaro JM, Jr. Correlation of immunological profile with phenotype and disease outcome in pemphigus. *Acta Derm Venereol.* 2010;90(4):401-5. Epub 2010/06/25. doi: 10.2340/00015555-0868. PubMed PMID: 20574606.

509. Sharma VK, Prasad HR, Khandpur S, Kumar A. Evaluation of desmoglein enzyme-linked immunosorbent assay (ELISA) in Indian patients with pemphigus vulgaris. *Int J Dermatol.* 2006;45(5):518-22. Epub 2006/05/17. doi: 10.1111/j.1365-4632.2006.02593.x. PubMed PMID: 16700783.
510. Zhao CY, Murrell DF. Outcome measures for autoimmune blistering diseases. *J Dermatol.* 2015;42(1):31-6. Epub 2015/01/07. doi: 10.1111/1346-8138.12711. PubMed PMID: 25558950.
511. Daneshpazhooh M, Zafarmand Sedigh V, Balighi K, Hosseini SH, Ramezani A, Kalantari MS, Ghandi N, Ghiasi M, Nikoo A, Chams-Davatchi C. Immunologic prediction of relapse in patients with pemphigus vulgaris (PV) in clinical remission. *J Am Acad Dermatol.* 2016;74(6):1160-5. Epub 2016/02/21. doi: 10.1016/j.jaad.2015.10.051. PubMed PMID: 26896293.
512. Bystryń JC, Steinman NM. The adjuvant therapy of pemphigus. An update. *Arch Dermatol.* 1996;132(2):203-12. Epub 1996/02/01. PubMed PMID: 8629830.
513. Bystryń JC. Adjuvant therapy of pemphigus. *Arch Dermatol.* 1984;120(7):941-51. Epub 1984/07/01. PubMed PMID: 6375579.
514. Risser J, Lewis K, Weinstock MA. Mortality of bullous skin disorders from 1979 through 2002 in the United States. *Arch Dermatol.* 2009;145(9):1005-8. Epub 2009/09/23. doi: 10.1001/archdermatol.2009.205. PubMed PMID: 19770439.
515. Wang M, Gao Y, Peng Y, Zhao J, Chen X, Zhu X. Yearly reduction of glucocorticoid dose by 50% as tapering schedule achieves complete remission for 124 pemphigus vulgaris patients. *J Dermatol.* 2016;43(3):325-8. Epub 2015/09/04. doi: 10.1111/1346-8138.13071. PubMed PMID: 26332949.
516. Oray M, Abu Samra K, Ebrahimiadib N, Meese H, Foster CS. Long-term side effects of glucocorticoids. *Expert Opin Drug Saf.* 2016;15(4):457-65. Epub 2016/01/21. doi: 10.1517/14740338.2016.1140743. PubMed PMID: 26789102.
517. Darjani A, Nickhah N, Hedayati Emami MH, Alizadeh N, Rafiei R, Eftekhari H, Gharaei Nejad K. Assessment of the Prevalence and Risk Factors Associated With Glucocorticoid-Induced Diabetes Mellitus in Pemphigus Vulgaris Patients. *Acta Med Iran.* 2017;55(6):375-80. Epub 2017/08/28. PubMed PMID: 28843238.
518. Wormser D, Chen DM, Brunetta PG, Sun D, Broder MS, Chang E, Reddy SR. Cumulative oral corticosteroid use increases risk of glucocorticoid-related adverse events in patients with newly diagnosed pemphigus. *J Am Acad Dermatol.* 2017;77(2):379-81. Epub 2017/07/18. doi: 10.1016/j.jaad.2017.04.1116. PubMed PMID: 28711092.
519. Chams-Davatchi C, Esmaili N, Daneshpazhooh M, Valikhani M, Balighi K, Hallaji Z, Barzegari M, Akhyani M, Ghodsi SZ, Seirafi H, Nazemi MJ, Mortazavi H, Mirshams-Shahshahani M. Randomized controlled open-label trial of four treatment regimens for pemphigus vulgaris. *J Am Acad Dermatol.* 2007;57(4):622-8. Epub 2007/06/23. doi: 10.1016/j.jaad.2007.05.024. PubMed PMID: 17583373.

520. Kakuta R, Yamagami J, Funakoshi T, Takahashi H, Ohyama M, Amagai M. Azathioprine monotherapy in autoimmune blistering diseases: A feasible option for mild to moderate cases. *J Dermatol.* 2018;45(3):334-9. Epub 2017/12/19. doi: 10.1111/1346-8138.14173. PubMed PMID: 29250862.
521. Beissert S, Werfel T, Frieling U, Bohm M, Sticherling M, Stadler R, Zillikens D, Rzany B, Hunzelmann N, Meurer M, Gollnick H, Ruzicka T, Pillekamp H, Junghans V, Bonsmann G, Luger TA. A comparison of oral methylprednisolone plus azathioprine or mycophenolate mofetil for the treatment of bullous pemphigoid. *Arch Dermatol.* 2007;143(12):1536-42. Epub 2007/12/19. doi: 10.1001/archderm.143.12.1536. PubMed PMID: 18087004.
522. Grillo-Lopez AJ. Rituximab: an insider's historical perspective. *Semin Oncol.* 2000;27(6 Suppl 12):9-16. Epub 2001/02/28. PubMed PMID: 11226006.
523. Salopek TG, Logsetty S, Tredget EE. Anti-CD20 chimeric monoclonal antibody (rituximab) for the treatment of recalcitrant, life-threatening pemphigus vulgaris with implications in the pathogenesis of the disorder. *J Am Acad Dermatol.* 2002;47(5):785-8. Epub 2002/10/26. PubMed PMID: 12399777.
524. Schmidt E, Goebeler M, Zillikens D. Rituximab in severe pemphigus. *Ann N Y Acad Sci.* 2009;1173:683-91. Epub 2009/09/18. doi: 10.1111/j.1749-6632.2009.04744.x. PubMed PMID: 19758216.
525. Joly P, Mouquet H, Roujeau JC, D'Incan M, Gilbert D, Jacquot S, Gougeon ML, Bedane C, Muller R, Dreno B, Doutre MS, Delaporte E, Pauwels C, Franck N, Caux F, Picard C, Tancrede-Bohin E, Bernard P, Tron F, Hertl M, Musette P. A single cycle of rituximab for the treatment of severe pemphigus. *N Engl J Med.* 2007;357(6):545-52. Epub 2007/08/10. doi: 10.1056/NEJMoa067752. PubMed PMID: 17687130.
526. Wang HH, Liu CW, Li YC, Huang YC. Efficacy of rituximab for pemphigus: a systematic review and meta-analysis of different regimens. *Acta Derm Venereol.* 2015;95(8):928-32. Epub 2015/04/18. doi: 10.2340/00015555-2116. PubMed PMID: 25881672.
527. Hashimoto T, Sugiura M, Kurihara S, Nishikawa T, Hatano H. Experimental acantholysis by complement-fixing intercellular antibodies. *Arch Dermatol Res.* 1982;273(1-2):129-35. Epub 1982/01/01. PubMed PMID: 7184469.
528. Hu CH, Michel B, Schiltz JR. Epidermal acantholysis induced in vitro by pemphigus autoantibody. An ultrastructural study. *Am J Pathol.* 1978;90(2):345-62. Epub 1978/02/01. PubMed PMID: 564142; PMCID: PMC2018159.
529. Jeffes EW, 3rd, Kaplan RP, Ahmed AR. Acantholysis produced in vitro with pemphigus serum: hydrocortisone inhibits acantholysis, while dapsone and 6-mercaptopurine do not inhibit acantholysis. *J Clin Immunol.* 1984;4(5):359-63. Epub 1984/09/01. PubMed PMID: 6541659.
530. Swanson DL, Dahl MV. Methylprednisolone inhibits pemphigus acantholysis in skin cultures. *J Invest Dermatol.* 1983;81(3):258-60. Epub 1983/09/01. PubMed PMID: 6886473.

531. van der Wier G, Pas HH, Jonkman MF. Experimental human cell and tissue models of pemphigus. *Dermatol Res Pract.* 2010;2010:143871. Epub 2010/06/30. doi: 10.1155/2010/143871. PubMed PMID: 20585596; PMCID: PMC2877615.
532. Schulze K, Galichet A, Sayar BS, Scothern A, Howald D, Zymann H, Siffert M, Zenhausem D, Bolli R, Koch PJ, Garrod D, Suter MM, Muller EJ. An adult passive transfer mouse model to study desmoglein 3 signaling in pemphigus vulgaris. *J Invest Dermatol.* 2012;132(2):346-55. Epub 2011/10/01. doi: 10.1038/jid.2011.299. PubMed PMID: 21956125; PMCID: PMC3258361.
533. Anhalt GJ, Labib RS, Voorhees JJ, Beals TF, Diaz LA. Induction of pemphigus in neonatal mice by passive transfer of IgG from patients with the disease. *N Engl J Med.* 1982;306(20):1189-96. Epub 1982/05/20. doi: 10.1056/NEJM198205203062001. PubMed PMID: 7040962.
534. Amagai M, Tsunoda K, Suzuki H, Nishifuji K, Koyasu S, Nishikawa T. Use of autoantigen-knockout mice in developing an active autoimmune disease model for pemphigus. *J Clin Invest.* 2000;105(5):625-31. Epub 2000/03/11. doi: 10.1172/JCI8748. PubMed PMID: 10712434; PMCID: PMC292455.
535. Zillikens D, Schmidt E, Reimer S, Chimanovitch I, Hardt-Weinelt K, Rose C, Brocker EB, Kock M, Boehncke WH. Antibodies to desmogleins 1 and 3, but not to BP180, induce blisters in human skin grafted onto SCID mice. *J Pathol.* 2001;193(1):117-24. Epub 2001/02/13. doi: 10.1002/1096-9896(2000)9999:9999<::AID-PATH742>3.0.CO;2-W. PubMed PMID: 11169524.
536. Schiltz JR, Michel B, Papay R. Pemphigus antibody interaction with human epidermal cells in culture. *J Clin Invest.* 1978;62(4):778-88. Epub 1978/10/01. doi: 10.1172/JCI109189. PubMed PMID: 701477; PMCID: PMC371829.
537. Denning MF, Guy SG, Ellerbroek SM, Norvell SM, Kowalczyk AP, Green KJ. The expression of desmoglein isoforms in cultured human keratinocytes is regulated by calcium, serum, and protein kinase C. *Exp Cell Res.* 1998;239(1):50-9. Epub 1998/03/25. doi: 10.1006/excr.1997.3890. PubMed PMID: 9511724.
538. Ishii K, Harada R, Matsuo I, Shirakata Y, Hashimoto K, Amagai M. In vitro keratinocyte dissociation assay for evaluation of the pathogenicity of anti-desmoglein 3 IgG autoantibodies in pemphigus vulgaris. *J Invest Dermatol.* 2005;124(5):939-46. Epub 2005/04/28. doi: 10.1111/j.0022-202X.2005.23714.x. PubMed PMID: 15854034.
539. Amagai M, Karpati S, Prussick R, Klaus-Kovtun V, Stanley JR. Autoantibodies against the amino-terminal cadherin-like binding domain of pemphigus vulgaris antigen are pathogenic. *J Clin Invest.* 1992;90(3):919-26. Epub 1992/09/01. doi: 10.1172/JCI115968. PubMed PMID: 1522242; PMCID: PMC329947.
540. Berkowitz P, Hu P, Liu Z, Diaz LA, Enghild JJ, Chua MP, Rubenstein DS. Desmosome signaling. Inhibition of p38MAPK prevents pemphigus vulgaris IgG-induced cytoskeleton reorganization. *The Journal of biological chemistry.* 2005;280(25):23778-84. Epub 2005/04/21. doi: 10.1074/jbc.M501365200. PubMed PMID: 15840580.

541. Berkowitz P, Hu P, Warren S, Liu Z, Diaz LA, Rubenstein DS. p38MAPK inhibition prevents disease in pemphigus vulgaris mice. *Proc Natl Acad Sci U S A*. 2006;103(34):12855-60. Epub 2006/08/16. doi: 10.1073/pnas.0602973103. PubMed PMID: 16908851; PMCID: PMC1568937.
542. Vielmuth F, Waschke J, Spindler V. Loss of Desmoglein Binding Is Not Sufficient for Keratinocyte Dissociation in Pemphigus. *J Invest Dermatol*. 2015;135(12):3068-77. Epub 2015/08/20. doi: 10.1038/jid.2015.324. PubMed PMID: 26288352.
543. Sanchez-Carpintero I, Espana A, Pelacho B, Lopez Moratalla N, Rubenstein DS, Diaz LA, Lopez-Zabalza MJ. In vivo blockade of pemphigus vulgaris acantholysis by inhibition of intracellular signal transduction cascades. *Br J Dermatol*. 2004;151(3):565-70. Epub 2004/09/21. doi: 10.1111/j.1365-2133.2004.06147.x. PubMed PMID: 15377341.
544. Spindler V, Waschke J. Role of Rho GTPases in desmosomal adhesion and pemphigus pathogenesis. *Ann Anat*. 2011;193(3):177-80. Epub 2011/03/29. doi: 10.1016/j.aanat.2011.02.003. PubMed PMID: 21441018.
545. Waschke J, Spindler V, Bruggeman P, Zillikens D, Schmidt G, Drenckhahn D. Inhibition of Rho A activity causes pemphigus skin blistering. *J Cell Biol*. 2006;175(5):721-7. Epub 2006/11/30. doi: 10.1083/jcb.200605125. PubMed PMID: 17130286; PMCID: PMC2064672.
546. Williamson L, Hunziker T, Suter MM, Muller EJ. Nuclear c-Myc: a molecular marker for early stage pemphigus vulgaris. *J Invest Dermatol*. 2007;127(6):1549-55. Epub 2007/02/23. doi: 10.1038/sj.jid.5700735. PubMed PMID: 17315040.
547. Williamson L, Raess NA, Caldelari R, Zakher A, de Bruin A, Posthaus H, Bolli R, Hunziker T, Suter MM, Muller EJ. Pemphigus vulgaris identifies plakoglobin as key suppressor of c-Myc in the skin. *EMBO J*. 2006;25(14):3298-309. Epub 2006/07/28. doi: 10.1038/sj.emboj.7601224. PubMed PMID: 16871158; PMCID: PMC1523185.
548. Jennings JM, Tucker DK, Kottke MD, Saito M, Delva E, Hanakawa Y, Amagai M, Kowalczyk AP. Desmosome disassembly in response to pemphigus vulgaris IgG occurs in distinct phases and can be reversed by expression of exogenous Dsg3. *J Invest Dermatol*. 2011;131(3):706-18. Epub 2010/12/17. doi: 10.1038/jid.2010.389. PubMed PMID: 21160493; PMCID: PMC3235416.
549. Calkins CC, Setzer SV, Jennings JM, Summers S, Tsunoda K, Amagai M, Kowalczyk AP. Desmoglein endocytosis and desmosome disassembly are coordinated responses to pemphigus autoantibodies. *The Journal of biological chemistry*. 2006;281(11):7623-34. Epub 2005/12/27. doi: 10.1074/jbc.M512447200. PubMed PMID: 16377623.
550. Stahley SN, Warren MF, Feldman RJ, Swerlick RA, Mattheyses AL, Kowalczyk AP. Super-Resolution Microscopy Reveals Altered Desmosomal Protein Organization in Tissue from Patients with Pemphigus Vulgaris. *J Invest Dermatol*. 2016;136(1):59-66. Epub 2016/01/15. doi: 10.1038/JID.2015.353. PubMed PMID: 26763424; PMCID: PMC4730957.
551. Hebert V, Boulard C, Houivet E, Duvert Lehembre S, Borradori L, Della Torre R, Feliciani C, Fania L, Zambruno G, Camaioni DB, Didona B, Marinovic B, Schmidt E, Schumacher N, Hunefeld C, Schanz S, Kern JS, Hofmann S, Bouyeure AC, Picard-Dahan C, Prost-Squarcioni C, Caux F, Alexandre

M, Ingen-Housz-Oro S, Bagot M, Tancrede-Bohin E, Bouaziz JD, Franck N, Vabres P, Labeille B, Richard MA, Delaporte E, Dupuy A, D'Incan M, Quereux G, Skowro F, Paul C, Livideanu CB, Beylot-Barry M, Doutre MS, Avenel-Audran M, Bedane C, Bernard P, Machet L, Maillard H, Jullien D, Debarbieux S, Sassolas B, Misery L, Abasq C, Dereure O, Lagoutte P, Ferranti V, Werth VP, Murrell DF, Hertl M, Benichou J, Joly P, French Study Group on Autoimmune Bullous Skin D, Autoimmune Bullous Skin Disease Task Force of the European Academy of D, Venereology. Large International Validation of ABSIS and PDAI Pemphigus Severity Scores. *J Invest Dermatol.* 2019;139(1):31-7. Epub 2018/10/12. doi: 10.1016/j.jid.2018.04.042. PubMed PMID: 30301637.

552. Spindler V, Endlich A, Hartlieb E, Vielmuth F, Schmidt E, Waschke J. The extent of desmoglein 3 depletion in pemphigus vulgaris is dependent on Ca(2+)-induced differentiation: a role in suprabasal epidermal skin splitting? *Am J Pathol.* 2011;179(4):1905-16. Epub 2011/08/26. doi: 10.1016/j.ajpath.2011.06.043. PubMed PMID: 21864491; PMCID: PMC3181381.

553. Rafei D, Muller R, Ishii N, Llamazares M, Hashimoto T, Hertl M, Eming R. IgG autoantibodies against desmocollin 3 in pemphigus sera induce loss of keratinocyte adhesion. *Am J Pathol.* 2011;178(2):718-23. Epub 2011/02/02. doi: 10.1016/j.ajpath.2010.10.016. PubMed PMID: 21281804; PMCID: PMC3069870.

554. Russo I, De Siena FP, Saponeri A, Alaibac M. Evaluation of anti-desmoglein-1 and anti-desmoglein-3 autoantibody titers in pemphigus patients at the time of the initial diagnosis and after clinical remission. *Medicine (Baltimore).* 2017;96(46):e8801. Epub 2017/11/18. doi: 10.1097/MD.00000000000008801. PubMed PMID: 29145342; PMCID: PMC5704887.

555. Mukaka MM. Statistics corner: A guide to appropriate use of correlation coefficient in medical research. *Malawi Med J.* 2012;24(3):69-71. Epub 2013/05/03. PubMed PMID: 23638278; PMCID: PMC3576830.

556. Hunt DM, Rickman L, Whittock NV, Eady RA, Simrak D, Dopping-Hepenstal PJ, Stevens HP, Armstrong DK, Hennies HC, Kuster W, Hughes AE, Arnemann J, Leigh IM, McGrath JA, Kelsell DP, Buxton RS. Spectrum of dominant mutations in the desmosomal cadherin desmoglein 1, causing the skin disease striate palmoplantar keratoderma. *Eur J Hum Genet.* 2001;9(3):197-203. doi: 10.1038/sj.ejhg.5200605. PubMed PMID: 11313759.

557. Rickman L, Simrak D, Stevens HP, Hunt DM, King IA, Bryant SP, Eady RA, Leigh IM, Arnemann J, Magee AI, Kelsell DP, Buxton RS. N-terminal deletion in a desmosomal cadherin causes the autosomal dominant skin disease striate palmoplantar keratoderma. *Hum Mol Genet.* 1999;8(6):971-6. PubMed PMID: 10332028.

558. Hammers CM, Stanley JR. Desmoglein-1, differentiation, and disease. *J Clin Invest.* 2013;123(4):1419-22. Epub 2013/03/26. doi: 10.1172/JCI69071. PubMed PMID: 23524961; PMCID: PMC3613937.

559. Harmon RM, Simpson CL, Johnson JL, Koetsier JL, Dubash AD, Najor NA, Sarig O, Sprecher E, Green KJ. Desmoglein-1/Erbin interaction suppresses ERK activation to support epidermal differentiation. *J Clin Invest.* 2013;123(4):1556-70. doi: 10.1172/JCI65220. PubMed PMID: 23524970; PMCID: PMC3613912.

560. Lacouture ME. Mechanisms of cutaneous toxicities to EGFR inhibitors. *Nat Rev Cancer*. 2006;6(10):803-12. doi: 10.1038/nrc1970. PubMed PMID: 16990857.
561. Nicholson RI, Gee JM, Harper ME. EGFR and cancer prognosis. *Eur J Cancer*. 2001;37 Suppl 4:S9-15. Epub 2001/10/13. PubMed PMID: 11597399.
562. Seshacharyulu P, Ponnusamy MP, Haridas D, Jain M, Ganti AK, Batra SK. Targeting the EGFR signaling pathway in cancer therapy. *Expert Opin Ther Targets*. 2012;16(1):15-31. Epub 2012/01/14. doi: 10.1517/14728222.2011.648617. PubMed PMID: 22239438; PMCID: PMC3291787.
563. Puri C, Tosoni D, Comai R, Rabellino A, Segat D, Caneva F, Luzzi P, Di Fiore PP, Tacchetti C. Relationships between EGFR signaling-competent and endocytosis-competent membrane microdomains. *Mol Biol Cell*. 2005;16(6):2704-18. Epub 2005/03/18. doi: 10.1091/mbc.E04-07-0596. PubMed PMID: 15772153; PMCID: PMC1142418.
564. Staubach S, Hanisch FG. Lipid rafts: signaling and sorting platforms of cells and their roles in cancer. *Expert Rev Proteomics*. 2011;8(2):263-77. Epub 2011/04/20. doi: 10.1586/epr.11.2. PubMed PMID: 21501018.
565. Balbis A, Posner BI. Compartmentalization of EGFR in cellular membranes: role of membrane rafts. *J Cell Biochem*. 2010;109(6):1103-8. Epub 2010/02/10. doi: 10.1002/jcb.22505. PubMed PMID: 20143338.
566. Ringerike T, Blystad FD, Levy FO, Madshus IH, Stang E. Cholesterol is important in control of EGF receptor kinase activity but EGF receptors are not concentrated in caveolae. *J Cell Sci*. 2002;115(Pt 6):1331-40. PubMed PMID: 11884532.
567. Irwin ME, Mueller KL, Bohin N, Ge Y, Boerner JL. Lipid raft localization of EGFR alters the response of cancer cells to the EGFR tyrosine kinase inhibitor gefitinib. *J Cell Physiol*. 2011;226(9):2316-28. doi: 10.1002/jcp.22570. PubMed PMID: 21660955; PMCID: PMC3103760.
568. Chen X, Resh MD. Cholesterol depletion from the plasma membrane triggers ligand-independent activation of the epidermal growth factor receptor. *The Journal of biological chemistry*. 2002;277(51):49631-7. doi: 10.1074/jbc.M208327200. PubMed PMID: 12397069.